

ไซโคลอาร์แทน ไตรเทอร์พีนอยด์ที่เป็นพิษต่อเซลล์จาก *Gardenia* spp.

นายธนศร นวลใย

วิทยานิพนธ์นี้เป็นส่วนหนึ่งของการศึกษาตามหลักสูตรปริญญาวิทยาศาสตรดุษฎีบัณฑิต

สาขาวิชาเคมี ภาควิชาเคมี

คณะวิทยาศาสตร์ จุฬาลงกรณ์มหาวิทยาลัย

ปีการศึกษา 2554

ลิขสิทธิ์ของจุฬาลงกรณ์มหาวิทยาลัย

บทคัดย่อและแฟ้มข้อมูลฉบับเต็มของวิทยานิพนธ์ตั้งแต่ปีการศึกษา 2554 ที่ให้บริการในคลังปัญญาจุฬาฯ (CUIR)

เป็นแฟ้มข้อมูลของนิสิตเจ้าของวิทยานิพนธ์ที่ส่งผ่านทางบัณฑิตวิทยาลัย

The abstract and full text of theses from the academic year 2011 in Chulalongkorn University Intellectual Repository (CUIR)

are the thesis authors' files submitted through the Graduate School.

CYTOTOXIC CYCLOARTANE TRITERPENOIDS FROM *Gardenia* spp.

Mr. Thanesuan Nuanyai

**A Thesis Submitted in Partial Fulfillment of the Requirements
for the Degree of Doctor of Philosophy Program in Chemistry**

Department of Chemistry

Faculty of Science

Chulalongkorn University

Academic Year 2011

Copyright of Chulalongkorn University

Thesis Title CYTOTOXIC CYCLOARTANE TRITERPENOIDS FROM
Gardenia spp.
By Mr. Thanesuan Nuanyai
Field of study Chemistry
Thesis Advisor Assistant Professor Khanitha Pudhom, Ph.D.
Thesis Co-advisor Associate Professor Tirayut Vilaivan, Ph.D.

Accepted by the Faculty of Science, Chulalongkorn University in Partial
Fulfillment of the Requirements for the Doctoral Degree

.....Dean of the Faculty of Science
(Professor Supot Hannongbua, Dr.rer.nat.)

THESIS COMMITTEE

.....Chairman
(Assistant Professor Warinthorn Chavasiri, Ph.D.)

.....Thesis Advisor
(Assistant Professor Khanitha Pudhom, Ph.D.)

.....Thesis Co-advisor
(Associate Professor Tirayut Vilaivan, Ph.D.)

.....Examiner
(Associate Professor Nongnuj Muangsin, Ph.D.)

.....Examiner
(Assistant Professor Preecha Phuwaprisirisan, Ph.D.)

.....External Examiner
(Professor Apichart Suksamrarn, Ph.D.)

ชเนศวร นวลใย: ไซโคลอาร์เทนไตรเทอร์พีนอยด์ที่เป็นพิษต่อเซลล์จาก *Gardenia* spp. (CYTOTOXIC CYCLOARTANE TRITERPENOIDS FROM *Gardenia* spp.)
 อ.ที่ปรึกษาวิทยานิพนธ์หลัก: ผศ.ดร.ขนิษฐา พุดหอม, อ.ที่ปรึกษาวิทยานิพนธ์ร่วม: รศ.ดร. ชีรยุทธ วิไลวัลย์, 208 หน้า.

การศึกษาไซโคลอาร์เทนไตรเทอร์พีนอยด์ของพืชสกุล *Gardenia* ห้าชนิดได้แก่ คำมอกหลวง (*G. sootepensis*) พุดป่า (*G. tubifera*) คำมอกน้อย (*G. obtusifolia*) พุดภูเก็ต (*G. thailandica*) และ พุดผา (*G. collinsae*) จากผลการศึกษาสามารถแยกสารได้จากส่วนยอดของต้นคำมอกหลวง (*G. sootepensis*) เป็นสารกลุ่ม 3,4-secocycloartane triterpenes ชนิดใหม่ 7 ชนิดคือ sootepins A-G และสารที่เคยมีรายงานมาก่อน 5 ชนิดคือ coronalolide, coronalolide methyl ester, tubiferolide methyl ester, secaubryenol, และ coronalolic acid สามารถแยกสารกลุ่มเดียวกันและเป็นสารชนิดใหม่ 4 ชนิดจากส่วนยางของพุดป่า (*G. tubifera*) คือ gardenoin A-D เช่นเดียวกับส่วนยอดของต้นคำมอกน้อย (*G. obtusifolia*) สามารถแยกสารที่ยังไม่เคยมีรายงานมาก่อน 4 ชนิดคือ gardenoins E-H และสารที่เคยมีรายงานมาก่อน 4 ชนิดคือ dikamakiartanes A, dikamakiartanes C, dikamakiartanes D, และ 5 α -cycloart-24-ene-3,16,23-trione จากการแยกสารจากยางของพุดภูเก็ต (*G. thailandica*) สามารถแยกสารชนิดใหม่ได้ 2 ชนิดคือ gardenoin I-J และ จากการแยกส่วนยอดของพุดผา (*G. collinsae*) สามารถแยกสารกลุ่ม dammarane triterpene ชนิดใหม่คือ 20*R*,24*R*-epoxy-3-oxo-dammarane-25 ζ ,26-diol และ C-24 epimer จากการนำสารทั้งหมดทดสอบการแสดงความเป็นพิษต่อเซลล์มะเร็งโดยใช้เซลล์มะเร็งทั้งหมด 5 ชนิดคือ มะเร็งเต้านม (BT474), มะเร็งปอด (CHAGO), มะเร็งตับ (Hep-G2), มะเร็งกระเพาะอาหาร (KATO-3), และมะเร็งลำไส้ (SW-620) ผลการทดสอบพบว่าสารที่มีหมู่ α -methylene- γ -butyrolactone จะแสดงความเป็นพิษต่อเซลล์มากกว่า และเมื่อศึกษาความสัมพันธ์ระหว่างโครงสร้างและความเป็นพิษกับเซลล์มะเร็งโดยเลือกใช้ sootepin A และ coronalolide เป็นสารตั้งต้น สำหรับเอสเทอร์ของ sootepin A ไม่แสดงความเป็นพิษต่อเซลล์มะเร็งเพิ่มขึ้น เช่นเดียวกับอนุพันธ์เอสเทอร์และเอไมด์ของ coronalolide และผลการศึกษาการปฏิริยาของหมู่ α -methylene- γ -butyrolactone กับนิวคลีโอโพลีบางชนิดพบว่าเป็นหมู่ที่มีความสำคัญกับการแสดงความเป็นพิษต่อเซลล์มะเร็ง และจากการศึกษากลไกการออกฤทธิ์กับเซลล์มะเร็งของ sootepin G กับ Hep-G2 พบว่า sootepin G แสดงผลการ apoptosis กับเซลล์มะเร็งได้

ภาควิชา.....เคมี..... ลายมือชื่อนิติ.....
 สาขาวิชา.....เคมี..... ลายมือชื่ออ.ที่ปรึกษาวิทยานิพนธ์หลัก.....
 ปีการศึกษา.....2554..... ลายมือชื่ออ.ที่ปรึกษาวิทยานิพนธ์ร่วม.....

##5073826523: MAJOR CHEMISTRY

KEYWORDS: CYCLOARTANE TRITERPENES/ *Gardenia* / SOOTEPIN /
GARDENOIN/ ANTICANCER

THANESUAN NUANYAI: CYTOTOXIC CYCLOARTANE
TRITERPENOIDS FROM *Gardenia* spp. ADVISOR: ASST. PROF.
KHANITHA PUDHOM, Ph.D., CO-ADVISOR: ASSOC. PROF. TIRAYUT
VILAIVAN, Ph.D., 208 pp.

In a phytochemical investigation of bioactive compounds from *Gardenia* spp., *G. sootepensis*, *G. tubifera*, *G. obtusifolia*, *G. thailandica* and *G. collinsae* were selected for isolation, purification and structure elucidation of their chemical constituents. The chromatographic separation of apical buds of *G. sootepensis* led to the isolation of seven new 3,4-*seco*-cycloartane triterpenes, sootepins A-G, along with five known compounds, coronalolide, coronalolide methyl ester, tubiferolide methyl ester, secoabryenol, and coronalolic acid. The same treatment with *G. tubifera* yielded three novel furano-3,4-*seco*-cycloartane triterpenes, gardenoins A-C, and a normal 3,4-*seco*-cycloartane triterpene, gardenoin D. Additionally, the apical buds of *G. obtusifolia* provided four new cycloartane triterpenes, gardenoins E-H, along with four known compounds, dikamakiartanes A, C, D, and 5 α -cycloart-24-ene-3,16,23-trione. The exudate of *G. thailandica* provided two additional new 3,4-*seco*-cycloartane triterpenoids, gardenoin I and J. Unlike other species, the isolation of *G. collinsae* buds yielded a new dammarane triterpenes and its C-24 epimer. Their structures were elucidated on the basis of spectroscopic methods (1D and 2D NMR, HREIMS, and X-ray diffraction analysis). All isolated compounds were tested for in vitro cytotoxic activity against human breast (BT474), lung (CHAGO), liver (Hep-G2), gastric (KATO-3), and colon (SW-620) cancer cell lines. Generally, the compounds possessing an exomethylene γ -lactone moiety showed broad cytotoxicity for all cell lines tested in 5-10 micromolar range, while the compounds without an α -methylene- γ -butyrolactone ring showed no significant activities. The structure activity relationship of isolated compounds, sootepin A and coronalolide. The ester derivatives of sootepin A at C-26 did not improve the cytotoxicity effect, while the amide and ester derivatives of coronalolide at C-3 are also result. Moreover, the reaction of α -methylene- γ -butyrolactone and some nucleophiles displayed these group was necessary for the cytotoxicity. Finally, the sootepin G showed the significant apoptotic with Hep-G2 cancer cell line.

Department:..... Chemistry..... Student's Signature.....

Field of Study:..... Chemistry..... Advisor's Signature.....

Academic Year:..... 2011..... Co-advisor's Signature.....

ACKNOWLEDGEMENTS

The author would like to express his sincere appreciation to his advisor, Assistant Professor Dr. Khanitha Pudhom, and co-advisor, Associate Professor Dr. Tirayut Vilaivan, Department of Chemistry, Faculty of Science, Chulalongkorn University, for excellent instruction, great valuable advice, kind guidance and support throughout this thesis.

Many thanks to the Chairperson: Assistant Professor Dr. Warinthorn Chavasiri, Department of Chemistry, Faculty of Science, Chulalongkorn University; the thesis examiners: Associate Professor Dr. Nongnuj Muangsin and Assistant Professor Preecha Phuwaprisirisan Department of Chemistry, Faculty of Science, Chulalongkorn University and Professor Dr. Apichart Suksamrarn Ramkhamhaeng University, for their invaluable discussion and suggestion.

I am grateful to Associate Professor Dr. Nongnuj Muangsin and Mr. Thapong Teerawatananond, Department of Chemistry, Faculty of Science, Chulalongkorn University and, who kindly performed the X-ray crystallographic analysis.

Sincere thanks are extended to the Institute of Biotechnology and Genetic Engineering, Chulalongkorn University, for tumor cell lines and facilitating use of the cytotoxicity assays throughout the entire study. The author also thanks Dr. Ruengrit Suppapan, Ms. Supichar Chokpaiboon and Mr. Chanin Sarigaputi for cytotoxic and apoptotic assays.

Special thanks to my friends in the Laboratory of Research Centre for Bioorganic Chemistry (RCBC), Department of Chemistry, Faculty of Science, Chulalongkorn University for their kindness and encouragement.

I wish to thank The 90th Anniversary of Chulalongkorn University Fund (Ratchadaphiseksomphot Endowment Fund) and Center of Excellence on Petrochemical and Materials Technology for granting in partial financial support to conduct this research.

Finally, I am deeply grateful to my family for their love and encouragement throughout my Ph.D. study.

CONTENTS

	Page
ABSTRACT IN THAI.....	iv
ABSTRACT IN ENGLISH.....	v
ACKNOWLEDGEMENTS.....	vi
CONTENTS.....	vii
LIST OF TABLES.....	viii
LIST OF FIGURES.....	x
LIST OF SCHEMES.....	xviii
LIST OF ABBREVIATIONS.....	xix
CHAPTER	
I INTRODUCTION.....	1
II CHEMICAL CONSITUENT FROM <i>Gardenia</i> spp.....	4
III STRUCTURE- ACTIVITY RELATIONSHIP OF CYCLOARTANE TRITERPENES DERIVATIVES.....	80
IV APOPTOTIC ACTIVATION OF HUMAN LIVER CANCER, HEP-G2, INDUCED BY SOOTEPIN G.....	102
V CONCLUSION.....	112
REFERENCES.....	117
APPENDIX.....	127
VITA.....	208

LIST OF TABLES

Table	Page
1. Details of plant materials.....	13
2. NMR data of compound 66 in CDCl ₃	26
3. NMR data of compound 67 in CDCl ₃	27
4. NMR data of compound 68 in CDCl ₃	28
5. NMR data of compound 69 in CDCl ₃	29
6. NMR data of compound 70 in CDCl ₃	30
7. ¹ H and ¹³ C NMR data (CDCl ₃) of coronalolide methyl ester and 10	31
8. ¹ H and ¹³ C NMR data (CDCl ₃) of coronalolide and compound 11	32
9. ¹ H and ¹³ C NMR data (CDCl ₃) of secaubryenol and compound 58	33
10. NMR data of compound 71 in CDCl ₃	37
11. NMR data of compound 72 in CDCl ₃	38
12. ¹ H and ¹³ C NMR data (CDCl ₃) of coronalolic acid and compound 12 ...	39
13. NMR data of compound 73 in CDCl ₃	45
14. NMR data of compound 74 in CDCl ₃	46
15. NMR data of compound 75 in C ₆ D ₆	47
16. NMR data of compound 76 in CDCl ₃	48
17. NMR data of compound 77 in CDCl ₃	55
18. NMR data of compound 78 in CDCl ₃	56
19. NMR data of compound 79 in acetone- <i>d</i> ₆	57
20. NMR data of compound 80 in CDCl ₃	58
21. ¹ H and ¹³ C NMR data (CDCl ₃) of 5 α -cycloart-24-ene-3,16,23-trione and compound 24	59
22. ¹ H and ¹³ C NMR data of dikamaliartane A and compound 61	61
23. ¹ H and ¹³ C NMR data of dikamaliartane C and compound 62	62
24. ¹ H and ¹³ C NMR data of Dikamaliartane D and compound 63	63
25. The NMR data of compound 81 in CDCl ₃	67

Table	Page
26. NMR data of compound 82 in CDCl ₃	68
27. NMR data of compound 83 in CDCl ₃	72
28. NMR data of compound 84 in CDCl ₃	73
29. NMR data of compound 85 in CDCl ₃	74
30. Cytotoxic data for α -methylene- γ -butyrolactone compounds.....	76
31. Cytotoxic data for 3,4- <i>seco</i> -cycloartane triterpenes.....	78
32. Cytotoxic data for cycloartane and dammarane triterpenes.....	79
33. Cytotoxic data for compounds 71 , and 157-171	99
34. Cytotoxic data for compounds 66 and 108-118	100
35. Some apoptotic-inducing natural compounds used in cancer chemotherapy.....	104

LIST OF FIGURES

Figure	Page
1. Isolated compounds from <i>G. sootepensis</i>	6
2. Isolated compounds from <i>Gardenia</i> spp.....	7
3. Isolated compounds from fruits of <i>G. sootepensis</i>	8
4. Isolated compounds from <i>G. obtusifolia</i>	8
5. Isolated compounds from <i>G. saxatilis</i>	9
6. Isolated compounds from <i>G. tubifera</i>	10
7. Isolated compounds from <i>G. thailandica</i>	11
8. Isolated compounds from <i>G. aubryi</i>	11
9. Isolated compounds from <i>G. gummifera</i> and <i>G. lucida</i>	12
10. Isolated compounds from <i>G. sootepensis</i> (Kampangpech province).....	18
11. Key HMBC (a) and NOE (b) correlations of compound 66	20
12. ORTEP drawing of 66 with atom labeling.....	20
13. Key HMBC (a) and NOE (b) correlations of compound 67	21
14. Key HMBC (a) and NOE (b) correlations of compound 68	22
15. Key HMBC (a) and NOE (b) correlations of compound 69	23
16. Key HMBC (a) and NOE (b) correlations of compound 70	23
17. Cycloartane triterpenes from apical buds of <i>G. sootepensis</i> (Kampangpech province).....	34
18. Key HMBC and NOE correlations of compound 71	35
19. Key HMBC (a) and NOE (b) correlations of compound 72	36
20. Cycloartane triterpenes from the exudate of <i>G. tubifera</i>	40
21. Key HMBC (a) and NOE (b) correlations of compound 73	41
22. Key HMBC (a) and NOE (b) correlations of compound 74	42
23. Key HMBC (a) and NOE (b) correlations of compound 75	43
24. Key HMBC (a) and NOE (b) correlations of compound 76	44
25. Cycloartane triterpenes from apical buds of <i>G. obtusifolia</i>	49
26. Key HMBC (a) and NOE (b) correlations of compound 77	51

Figure	Page
27. Key HMBC (a) and NOE (b) correlations of compound 78	51
28. Key HMBC (a) and NOE (b) correlations of compound 79	52
29. Key HMBC (a) and NOE (b) correlations of compound 80	53
30. Cycloartane triterpenes from <i>G. obtusifolia</i> exudates.....	64
31. Key HMBC (a) and NOE (b) correlations of compound 81	65
32. Key HMBC (a) and NOE (b) correlations of compound 82	66
33. Dammareane triterpenes from <i>G. collinsae</i> exudates.....	69
34. Key HMBC (a) and NOE (b) correlations of compound 83	70
35. Key HMBC (a) and NOE (b) correlations of compound 84	71
36. An α -methylene- γ -butyrolactone compounds from <i>Gardenia</i> spp.....	76
37. 3,4- <i>seco</i> -cycloartane triterpenes from <i>Gardenia</i> spp.....	77
38. cycloartane and dammarane triterpenes from <i>Gardenia</i> spp.....	78
39. Isolated cycloartanes from <i>G. obtusifolia</i> and modified compounds....	81
40. Skeleton of cycloartane-type triterpenes from the propolis.....	82
41. ¹ H-NMR (CDCl ₃) spectrum of crude reaction of tubiferolide methyl ester and 2-mercaptoethanol.....	95
42. ¹ H-NMR (CDCl ₃) spectrum of crude reaction of tubiferolide methyl ester and thiophenol.....	95
43. ¹ H-NMR (CDCl ₃) spectrum of crude reaction of tubiferolide methyl ester and ethanolamine.....	96
44. ¹ H-NMR (CDCl ₃) spectrum of crude reaction of tubiferolide methyl ester and pyrrolidine.....	96
45. ¹ H-NMR (CDCl ₃) spectrum of crude reaction of tubiferolide methyl ester and morpholine.....	97
46. The ester and amide derivatives of colonarolide.....	98
47. The ester derivatives of sootepin A.....	100
48. Extrinsic and intrinsic apoptosis pathway.....	103
49. Cell growth inhibition activity of sootepin G after treatment with the concentration of 4, 40, and 100 μ M for 48 h.....	109
50. Sootepin G caused G1 arrest induction in Hep-G2 cells.....	110

Figure	Page
51. Effects of sootepin G on Bcl-2, Bcl-xL, and β -actin degradation.....	111
52. Isolated compounds from five <i>Gardenia</i> spp.....	113
53. Ester and amide derivatives of colonarolide and sootepin A.....	115
54. ^1H NMR spectrum of compound 66 (CDCl_3 ; 400 MHz).....	128
55. ^{13}C NMR spectrum of compound 66 (CDCl_3 ; 100 MHz).....	128
56. ^1H - ^1H COSY spectrum of compound 66 (CDCl_3 ; 400 MHz).....	129
57. HSQC spectrum of compound 66 (CDCl_3 ; 400 MHz).....	129
58. HMBC spectrum of compound 66 (CDCl_3 ; 400 MHz).....	130
59. NOESY spectrum of compound 66 (CDCl_3 ; 400 MHz).....	130
60. ^1H NMR spectrum of compound 67 (CDCl_3 ; 400 MHz).....	131
61. ^{13}C NMR spectrum of compound 67 (CDCl_3 ; 100 MHz).....	131
62. ^1H - ^1H COSY spectrum of compound 67 (CDCl_3 ; 400 MHz).....	132
63. HSQC spectrum of compound 67 (CDCl_3 ; 400 MHz).....	132
64. HMBC spectrum of compound 67 (CDCl_3 ; 400 MHz).....	133
65. NOESY spectrum of compound 67 (CDCl_3 ; 400 MHz).....	133
66. ^1H NMR spectrum of compound 68 (CDCl_3 ; 400 MHz).....	134
67. ^{13}C NMR spectrum of compound 68 (CDCl_3 ; 100 MHz).....	134
68. ^1H - ^1H COSY spectrum of compound 68 (CDCl_3 ; 400 MHz).....	135
69. HSQC spectrum of compound 68 (CDCl_3 ; 400 MHz).....	135
70. HMBC spectrum of compound 68 (CDCl_3 ; 400 MHz).....	136
71. NOESY spectrum of compound 68 (CDCl_3 ; 400 MHz).....	136
72. ^1H NMR spectrum of compound 69 (CDCl_3 ; 400 MHz).....	137
73. ^{13}C NMR spectrum of compound 69 (CDCl_3 ; 100 MHz).....	137
74. ^1H - ^1H COSY spectrum of compound 69 (CDCl_3 ; 400 MHz).....	138
75. HSQC spectrum of compound 69 (CDCl_3 ; 400 MHz).....	138
76. HMBC spectrum of compound 69 (CDCl_3 ; 400 MHz).....	139
77. NOESY spectrum of compound 69 (CDCl_3 ; 400 MHz).....	139
78. ^1H NMR spectrum of compound 70 (CDCl_3 ; 400 MHz).....	140

Figure	Page
79. ^{13}C NMR spectrum of compound 70 (CDCl_3 ; 100 MHz).....	140
80. ^1H - ^1H COSY spectrum of compound 70 (CDCl_3 ; 400 MHz).....	141
81. HSQC spectrum of compound 70 (CDCl_3 ; 400 MHz).....	141
82. HMBC spectrum of compound 70 (CDCl_3 ; 400 MHz).....	142
83. NOESY spectrum of compound 70 (CDCl_3 ; 400 MHz).....	142
84. ^1H NMR spectrum of compound 71 (CDCl_3 ; 400 MHz).....	143
85. ^{13}C NMR spectrum of compound 71 (CDCl_3 ; 100 MHz).....	143
86. ^1H - ^1H COSY spectrum of compound 71 (CDCl_3 ; 400 MHz).....	144
87. HSQC spectrum of compound 71 (CDCl_3 ; 400 MHz).....	144
88. HMBC spectrum of compound 71 (CDCl_3 ; 400 MHz).....	145
89. NOESY spectrum of compound 71 (CDCl_3 ; 400 MHz).....	145
90. ^1H NMR spectrum of compound 72 (CDCl_3 ; 400 MHz).....	146
91. ^{13}C NMR spectrum of compound 72 (CDCl_3 ; 100 MHz).....	146
92. ^1H - ^1H COSY spectrum of compound 72 (CDCl_3 ; 400 MHz).....	147
93. HSQC spectrum of compound 72 (CDCl_3 ; 400 MHz).....	147
94. HMBC spectrum of compound 72 (CDCl_3 ; 400 MHz).....	148
95. NOESY spectrum of compound 72 (CDCl_3 ; 400 MHz).....	148
96. ^1H NMR spectrum of compound 73 (CDCl_3 ; 400 MHz).....	149
97. ^{13}C NMR spectrum of compound 73 (CDCl_3 ; 100 MHz).....	149
98. ^1H - ^1H COSY spectrum of compound 73 (CDCl_3 ; 400 MHz).....	150
99. HSQC spectrum of compound 73 (CDCl_3 ; 400 MHz).....	150
100. HMBC spectrum of compound 73 (CDCl_3 ; 400 MHz).....	151
101. NOESY spectrum of compound 73 (CDCl_3 ; 400 MHz).....	151
102. ^1H NMR spectrum of compound 74 (CDCl_3 ; 400 MHz).....	152
103. ^{13}C NMR spectrum of compound 74 (CDCl_3 ; 100 MHz).....	152
104. ^1H - ^1H COSY spectrum of compound 74 (CDCl_3 ; 400 MHz).....	153
105. HSQC spectrum of compound 74 (CDCl_3 ; 400 MHz).....	153
106. HMBC spectrum of compound 74 (CDCl_3 ; 400 MHz).....	154

Figure	Page
107. NOESY spectrum of compound 74 (CDCl ₃ ; 400 MHz).....	154
108. ¹ H NMR spectrum of compound 75 (C ₆ D ₆ ; 400 MHz).....	155
109. ¹³ C NMR spectrum of compound 75 (C ₆ D ₆ ; 100 MHz).....	155
110. ¹ H- ¹ H COSY spectrum of compound 75 (C ₆ D ₆ ; 400 MHz).....	156
111. HSQC spectrum of compound 75 (C ₆ D ₆ ; 400 MHz).....	156
112. HMBC spectrum of compound 75 (C ₆ D ₆ ; 400 MHz).....	157
113. NOESY spectrum of compound 75 (C ₆ D ₆ ; 400 MHz).....	157
114. ¹ H NMR spectrum of compound 76 (CDCl ₃ ; 400 MHz).....	158
115. ¹³ C NMR spectrum of compound 76 (CDCl ₃ ; 100 MHz).....	158
116. ¹ H- ¹ H COSY spectrum of compound 76 (CDCl ₃ ; 400 MHz).....	159
117. HSQC spectrum of compound 76 (CDCl ₃ ; 400 MHz).....	159
118. HMBC spectrum of compound 76 (CDCl ₃ ; 400 MHz).....	160
119. NOESY spectrum of compound 76 (CDCl ₃ ; 400 MHz).....	160
120. ¹ H NMR spectrum of compound 77 (CDCl ₃ ; 400 MHz).....	161
121. ¹³ C NMR spectrum of compound 77 (CDCl ₃ ; 100 MHz).....	161
122. ¹ H- ¹ H COSY spectrum of compound 77 (CDCl ₃ ; 400 MHz).....	162
123. HSQC spectrum of compound 77 (CDCl ₃ ; 400 MHz).....	162
124. HMBC spectrum of compound 77 (CDCl ₃ ; 400 MHz).....	163
125. 1D-NOE spectrum of compound 77 (CDCl ₃ ; 400 MHz).....	163
126. 1D-NOE spectrum of compound 77 (CDCl ₃ ; 400 MHz).....	164
127. 1D-NOE spectrum of compound 77 (CDCl ₃ ; 400 MHz).....	164
128. ¹ H NMR spectrum of compound 78 (CDCl ₃ ; 400 MHz).....	165
129. ¹³ C NMR spectrum of compound 78 (CDCl ₃ ; 100 MHz).....	165
130. ¹ H- ¹ H COSY spectrum of compound 78 (CDCl ₃ ; 400 MHz).....	166
131. HSQC spectrum of compound 78 (CDCl ₃ ; 400 MHz).....	166
132. HMBC spectrum of compound 78 (CDCl ₃ ; 400 MHz).....	167
133. 1D-NOE spectrum of compound 78 (CDCl ₃ ; 400 MHz).....	167
134. 1D-NOE spectrum of compound 78 (CDCl ₃ ; 400 MHz).....	168

Figure	Page
135. 1D-NOE spectrum of compound 78 (CDCl ₃ ; 400 MHz).....	168
136. ¹ H NMR spectrum of compound 79 (Acetone- <i>d</i> ₆ ; 400 MHz).....	169
137. ¹³ C NMR spectrum of compound 79 (CDCl ₃ ; 100 MHz).....	169
138. ¹ H- ¹ H COSY spectrum of compound 79 (Acetone- <i>d</i> ₆ ; 400 MHz).....	170
139. HSQC spectrum of compound 79 (Acetone- <i>d</i> ₆ ; 400 MHz).....	170
140. HMBC spectrum of compound 79 (Acetone- <i>d</i> ₆ ; 400 MHz).....	171
141. 1D-NOE spectrum of compound 79 (Acetone- <i>d</i> ₆ ; 400 MHz).....	171
142. 1D-NOE spectrum of compound 79 (Acetone- <i>d</i> ₆ ; 400 MHz).....	172
143. 1D-NOE spectrum of compound 79 (Acetone- <i>d</i> ₆ ; 400 MHz).....	172
144. ¹ H NMR spectrum of compound 80 (CDCl ₃ ; 400 MHz).....	173
145. ¹³ C NMR spectrum of compound 80 (CDCl ₃ ; 100 MHz).....	173
146. ¹ H- ¹ H COSY spectrum of compound 80 (CDCl ₃ ; 400 MHz).....	174
147. HSQC spectrum of compound 80 (CDCl ₃ ; 400 MHz).....	174
148. HMBC spectrum of compound 80 (CDCl ₃ ; 400 MHz).....	175
149. 1D-NOE spectrum of compound 80 (CDCl ₃ ; 400 MHz).....	175
150. 1D-NOE spectrum of compound 80 (CDCl ₃ ; 400 MHz).....	176
151. ¹ H NMR spectrum of compound 81 (CDCl ₃ ; 400 MHz).....	176
152. ¹³ C NMR spectrum of compound 81 (CDCl ₃ ; 100 MHz).....	177
153. ¹ H- ¹ H COSY spectrum of compound 81 (CDCl ₃ ; 400 MHz).....	177
154. HSQC spectrum of compound 81 (CDCl ₃ ; 400 MHz).....	178
155. HMBC spectrum of compound 81 (CDCl ₃ ; 400 MHz).....	178
156. NOESY spectrum of compound 81 (CDCl ₃ ; 400 MHz).....	179
157. ¹ H NMR spectrum of compound 82 (CDCl ₃ ; 400 MHz).....	179
158. ¹³ C NMR spectrum of compound 82 (CDCl ₃ ; 100 MHz).....	180
159. ¹ H- ¹ H COSY spectrum of compound 82 (CDCl ₃ ; 400 MHz).....	180
160. HSQC spectrum of compound 82 (CDCl ₃ ; 400 MHz).....	181
161. HMBC spectrum of compound 82 (CDCl ₃ ; 400 MHz).....	181
162. NOESY spectrum of compound 82 (CDCl ₃ ; 400 MHz).....	182

Figure	Page
163. ¹ H NMR spectrum of compound 83 (CDCl ₃ ; 400 MHz).....	182
164. ¹³ C NMR spectrum of compound 83 (CDCl ₃ ; 100 MHz).....	183
165. ¹ H- ¹ H COSY spectrum of compound 83 (CDCl ₃ ; 400 MHz).....	183
166. HSQC spectrum of compound 83 (CDCl ₃ ; 400 MHz).....	184
167. HMBC spectrum of compound 83 (CDCl ₃ ; 400 MHz).....	184
168. NOESY spectrum of compound 83 (CDCl ₃ ; 400 MHz).....	185
169. ¹ H NMR spectrum of compound 84 (CDCl ₃ ; 400 MHz).....	185
170. ¹³ C NMR spectrum of compound 84 (CDCl ₃ ; 100 MHz).....	186
171. ¹ H- ¹ H COSY spectrum of compound 84 (CDCl ₃ ; 400 MHz).....	186
172. HSQC spectrum of compound 84 (CDCl ₃ ; 400 MHz).....	187
173. HMBC spectrum of compound 84 (CDCl ₃ ; 400 MHz).....	187
174. NOESY spectrum of compound 84 (CDCl ₃ ; 400 MHz).....	188
175. ¹ H NMR spectrum of compound 10 (CDCl ₃ ; 400 MHz).....	188
176. ¹³ C NMR spectrum of compound 10 (CDCl ₃ ; 100 MHz).....	189
177. ¹ H NMR spectrum of compound 11 (CDCl ₃ ; 400 MHz).....	189
178. ¹³ C NMR spectrum of compound 11 (CDCl ₃ ; 100 MHz).....	190
179. ¹ H NMR spectrum of compound 12 (CDCl ₃ ; 400 MHz).....	190
180. ¹³ C NMR spectrum of compound 12 (CDCl ₃ ; 100 MHz).....	191
181. ¹ H NMR spectrum of compound 24 (CDCl ₃ ; 400 MHz).....	191
182. ¹³ C NMR spectrum of compound 24 (CDCl ₃ ; 100 MHz).....	192
183. ¹ H NMR spectrum of compound 41 (CDCl ₃ ; 400 MHz).....	192
184. ¹³ C NMR spectrum of compound 41 (CDCl ₃ ; 100 MHz).....	193
185. ¹ H NMR spectrum of compound 58 (CDCl ₃ ; 400 MHz).....	193
186. ¹³ C NMR spectrum of compound 58 (CDCl ₃ ; 100 MHz).....	194
187. ¹ H NMR spectrum of compound 61 (Acetone- <i>d</i> ₆ ; 400 MHz).....	194
188. ¹³ C NMR spectrum of compound 61 (Acetone- <i>d</i> ₆ ; 100 MHz).....	195
189. ¹ H NMR spectrum of compound 62 (CDCl ₃ ; 400 MHz).....	195
190. ¹ H NMR spectrum of compound 63 (CDCl ₃ ; 400 MHz).....	196
191. ¹³ C NMR spectrum of compound 63 (CDCl ₃ ; 100 MHz).....	196

Figure	Page
192. ¹ H NMR spectrum of compound 85 (CDCl ₃ ; 400 MHz).....	197
193. ¹³ C NMR spectrum of compound 85 (CDCl ₃ ; 100 MHz).....	197
194. ¹ H-NMR spectrum of reaction of coronalolide and adenosine 5'- monophosphate disodium salt hydrate in DMSO- <i>d</i> ₆ :D ₂ O (5:1); A at room temperature (24 h.), B at 40°C (72 h).....	198
195. ¹ H-NMR spectrum of reaction of coronalolide and cytidine 5'- monophosphate disodium salt hydrate in DMSO- <i>d</i> ₆ :D ₂ O (5:1); A at room temperature (24 h.), B at 40°C (72 h).....	199
196. ¹ H-NMR spectrum of reaction of coronalolide and guanosine 5'- monophosphate disodium salt hydrate in DMSO- <i>d</i> ₆ :D ₂ O (5:1); A at room temperature (24 h.), B at 40°C (72 h).....	200
197. ¹ H-NMR spectrum of reaction of coronalolide and uridine 5'- monophosphate disodium salt hydrate in DMSO- <i>d</i> ₆ :D ₂ O (5:1); A at room temperature (24 h.), B at 40°C (72 h).....	201
198. ¹ H-NMR (DMSO- <i>d</i> ₆) spectrum of reaction of coronalolide and cysteine at room temperature (72 h.).....	201
199. ¹ H-NMR (DMSO- <i>d</i> ₆) spectrum of reaction of coronalolide and cysteine methyl ester HCl at room temperature (72 h.).....	202
200. <i>Gardenia sootepensis</i> (Rubiaceae).....	203
201. <i>Gardenia tubifera</i> (Rubiaceae).....	204
202. <i>Gardenia obtusifolia</i> (Rubiaceae).....	205
203. <i>Gardenia thailandica</i> (Rubiaceae).....	206
204. <i>Gardenia collinsae</i> (Rubiaceae).....	207

LIST OF SCHEMES

Scheme	Page
1. Propose reaction of coronalolide (11) and adenosine 5'-monophosphate disodium salt hydrate.....	94

LIST OF ABBREVIATIONS

<i>J</i>	Coupling constant
δ	Chemical shift
δ_{H}	Chemical shift of proton
δ_{C}	Chemical shift of carbon
s	Singlet (for NMR spectra)
d	Doublet (for NMR spectra)
dd	Doublet of doublet (for NMR spectra)
ddd	Doublet of doublet of doublet (for NMR spectra)
dddd	Doublet of doublet of doublet of doublet (for NMR spectra)
t	Triplet (for NMR spectra)
m	Multiplet (for NMR spectra)
q	Quartet (for NMR spectra)
brs	Broad singlet (for NMR spectra)
brd	Broad doublet (for NMR spectra)
qC	Quaternary carbon
calcd.	Calculated
^1H NMR	Proton nuclear magnetic resonance
^{13}C NMR	Carbon-13 nuclear magnetic resonance
2D NMR	Two dimensional nuclear magnetic resonance
^1H - ^1H COSY	Homonuclear (proton-proton) correlation spectroscopy
NOESY	Nuclear overhauser effect spectroscopy
HSQC	Heteronuclear single quantum coherence
HMBC	Heteronuclear multiple bond correlation
ORTEP	Oak ridge thermal ellipsoid plot
HPLC	High performance liquid chromatography
HRESIMS	High resolution electrospray ionization mass spectrometry
ESIMS	Electrospray ionization mass spectrometry
CC	Column chromatography
TLC	Thin layer chromatography

MIC	Minimum inhibitory concentration
IC ₅₀	Half maximal inhibitory concentration
CDCl ₃	Deuterated chloroform
MeOH	Methanol
EtOH	Ethanol
CHCl ₃	Chloroform
CH ₂ Cl ₂	Dichloromethane
EtOAc	Ethyl acetate
DMSO	Dimethylsulfoxide
KBr	Potassium bromide
(NH ₄) ₆ Mo ₇ O ₂₄	Ammonium molybdate
H ₂ SO ₄	Sulfuric acid
SiO ₂	Silicon dioxide
g	Gram (s)
mg	Milligram (s)
mL	Milliliter (s)
μg	Microgram (s)
μL	Microliter (s)
μM	Micromolar
mM	Millimolar
L	Liter (s)
M	Molar
min	Minute
h	Hour
rpm	Round per minute
m	Meter (s)
mm	Millimeter (s)
cm	Centimeter (s)
nm	Nanometer
Hz	Hertz
MHz	Megahertz

cm^{-1}	Reciprocal centimeter (unit of wave number)
ppm	part per million
NMR	Nuclear magnetic resonance
MS	Mass spectrometry
IR	Infrared
UV	Ultraviolet
m.p.	Melting point
α	Alpha
β	Beta
m/z	Mass to charge ratio
$[\text{M}+\text{H}]^+$	Protonated molecule
$[\text{M}+\text{Na}]^+$	Pseudomolecular ion
$[\alpha]_{\text{D}}^{20}$	Specific rotation at 20 °C and sodium D line (589 nm)
λ_{max}	Wavelength of maximum absorption
c	Concentration
ϵ	Molar extinction coefficient
Å	Angstrom
°C	Degree celcius
deg.	Degree
sp.	Species
No.	Number
ATCC	American type culture collection
UCLA	University of California, Los Angeles
ESBL	Extended-spectrum beta-lactamase
BT-474	Breast ductal carcinoma
CHAGO	Undifferentiated lung carcinoma
KATO-3	Gastric carcinoma
SW-620	Colon adenocarcinoma
CH-Liver	Liver cell line

CHAPTER I

INTRODUCTION

With estimated 7.6 million deaths reported in 2005, cancer is the second leading cause of death amongst the world's population. Each year, several billion dollars are invested in cancer research in an attempt to understand the disease processes involved and to try to discover possible therapies to combat this debilitating disease. The potential market for immune drugs is huge and is a rapidly growing area in the biopharmaceutical arena.

During the past 5 decades of research in anti-cancer drug discovery, about 100 products have been provided for clinical treatment of malignancy. Significant progress has been made in the chemotherapeutic management of hematologic malignancies, however, more than 50% of patients with tissue tumors either felt to respond or die from the disease [1]. Hence, the discovery of novel anti-cancer therapeutic agents remains critically important.

Terrestrial plants have been used as medicines in Egypt, China, India and Greece from ancient time and an impressive number of modern drugs have been developed from them. The isolation of the vinca alkaloids, vinblastine and vincristine from the Madagascar periwinkle, *Catharanthus roseus* (Apocynaceae) introduced a new area of the use of plant material as anticancer agents. They were the first agents to advance into clinical use for the treatment of cancer. Vinblastine and vincristine are primarily used in combination with other cancer chemotherapeutic drugs for the treatment of a variety of cancers, including leukemias, lymphomas, advanced testicular cancer, breast and lung cancers and Kaposi's sarcoma [2].

The discovery of paclitaxel (Taxol®) from the bark of the Pacific Yew, *Taxus brevifolia* (Taxaceae), is another evidence of the success in natural product drug discovery. Various parts of *Taxus brevifolia* and other *Taxus* species (e.g. *T. canadensis*, *T. baccata*) have been used by several native American Tribes for the

treatment of some non-cancerous cases [2], while *T. baccata* was reported to use in the Indian Ayurvedic medicine for the treatment of cancer. The structure of paclitaxel was elucidated in 1971 and was clinically introduced to the US market in the early 1990s [3, 4]. Paclitaxel is significantly active against ovarian cancer, advanced breast cancer, small and non-small cell lung cancer. Camptothecin, isolated from the Chinese ornamental tree *Camptotheca acuminata* (Nyssaceae), was advanced to clinical trials by NCI in the 1970s but was dropped because of severe bladder toxicity. Later, topotecan and irinotecan, semi-synthetic derivatives of camptothecin, are developed and used for the treatment of ovarian and small cell lung cancers, and colorectal cancers, respectively [4, 5]. Epipodophyllotoxin is an isomer of podophyllotoxin which was isolated as the active anti-tumor agent from the roots of *Podophyllum* species, *P. peltatum* and *P. emodi* (Berberidaceae) [6]. Etoposide and teniposide are two semi-synthetic derivatives of epipodophyllotoxin and are used in the treatment of lymphomas and bronchial and testicular cancers [2].

However, the vast majority of the deaths occur after medical intervention with anticancer therapy, both conventional chemotherapy and novel targeted therapy, it can be concluded that these patients die from drug resistant cancers. A growing number of studies have revealed that mechanisms underlying the development of drug resistance in cancer cells are manifold and complex and very likely are dependent on cell and microenvironment context. In view of these facts, it is important to document the mechanisms of drug resistance and understand which are the dominant resistance pathways in a particular tumor type that could provide potential therapeutic targets in a clinical setting [7].

For these reasons, the finding of new drugs from medicinal plants might be one of the ways to obtain effective candidates for treating a variety of diseases in humans and animals. Plants belonging to the genus *Gardenia* have proved to be a rich source of triterpenoids, especially cycloarane triterpenes, some of which displayed interesting biological activities including cytotoxic and anti-HIV-1 effects [8-10].

Gardenia, a large genus centered in the Old World tropics. At least 10 species occur in Thailand, growing in diverse vegetation types such as lowland

evergreen, montane and deciduous forests; some occupy specialized habitats (e.g. *G. saxatilis*, confined to rocky areas). *Gardenia* is a popular ornamental shrub found worldwide. Fruits of *G. jasminoides* Ellis (Rubiaceae) (Chinese herbal name is Zhi Zi) has been used for the remedy for hepatic pain due to cirrhosis, abdominal pain due to dysentery, anti-phlogistics, diuretic, laxative, choleric, and homeostatic purposes in the treatment of trauma by external application. In the theory of traditional Chinese medicine, *Gardenia* is belong to bitter and cold and enters the heart, lung and triple burner meridians. Recent reports indicate that *Gardenia* herb also has mild antiangiogenic properties and sedative effect [12]. The primary active components of *G. jasminoids* fruits are iridoid glycosides (mainly geniposide and gardenoside), chlorogenic acid, and ursolic acid. Moreover, previous investigations on the plants in this genus have led to the isolation of an array of structurally diverse cycloartanes with a wide range of biological activities, particularly cytotoxic and anti-human immunodeficiency virus or HIV effects.

Therefore, the objectives of this research are summarized as follow;

1. To extract, isolate and purify cycloartane triterpenes from the five *Gardenia* spp., the apical buds of *G. sootepensis*, *G. obtusifolia*, and *G. collinsae*, as well as, the exudate of *G. tubifera* and *G. thailandica*
2. To elucidate structures of isolated cycloartane triterpenes by spectroscopic techniques
3. To evaluate anticancer activity of isolated cycloartane triterpenes
4. To synthesize the analogs of selected cycloartane triterpenes and study their structure-activity relationships
5. To study the action mechanism of selected cycloartane triterpene derivatives on anticancer activity

CHAPTER II

CHEMICAL CONSITUENTS FROM *GARDENIA* SPP.

2.1 Introduction

The *Gardenia* spp. is widely used for herb in traditional medicines. The significant biological activities and important ethnomedical applications of several *Gardenia* species including insomnia (*G. erubescens*) [13], birth control (*G. jasminoides*) [14], antiplasmodial (*G. saxatilis*) [15], asthma (*G. ternifolia*) [16], as a febrifuge and astringent (*G. lutea*) [17], antiviral (*G. gummifera*) [18], reverse transcriptase inhibition and HIV-1-reverse transcriptase (*G. coronaria*) [8] activities have been reported. The major constituents of *Gardenia* fruits are iridoid glycosides such as geniposide, gardenoside, gardoside, shanzhiside, scandoside methyl ester, methyl deacetyl asperulosidate geniposidic acid, 1-*O*-acetylgeniposide and genipin-1- β -gentiobioside. Moreover, the previous investigation of this genus has led to the isolation of a number of cycloartane-type triterpenes with a wide range of biological activities, particularly anti-HIV and cytotoxicity [8-10, 22-23].

2.1.1 Botanical Characteristic of *Gardenia* spp.

Kingdom: Plantae

Subkingdom: Tracheobionta

Superdivision: Spermatophyta

Division: Magnoliophyta

Class: Magnoliopsida

Subclass: Asteridae

Order: Gentiales

Family: Rubiaceae

Genus: *Gardenia* Ellis

2.1.1.1 Botanical Characteristic of *Gardenia sootepensis* Hutch.

G. sootepensis (Kham-mok-luang) is native to Thailand where it is found as a canopy species in dry dipterocarp forest that persists without

fire disturbance [19]. A small extensively branched tree that grows to 9 m tall. The leaves are arranged in opposite pairs along the branches, are oval in shape, and are covered with hairs. The light green leaves have conspicuous venation with the secondary veins running almost perpendicular from the midvein to the outer leaf margin. Solitary star-shaped flowers are borne in the leaf axils and are white when they first open then mature to a dark, golden yellow. The calyx forms a sheath around the base of the long tubular flower, which has five widely spreading petal lobes that are narrow at the base and widen towards the tips. The anthers (pollen producing structures) are inserted into the floral tube and barely extend beyond it. The round fruit contains many seeds that are immersed in a fleshy pulp [11].

2.1.1.2 Botanical Characteristic of *Gardenia tubifera* Wall.

G. tubifera was found in undisturbed to slightly disturbed (open) mixed dipterocarp and swamp forests up to 500 m altitude. Usually on alluvial sites along rivers and streams on sandy soils. In secondary forests usually present as a pre-disturbance remnant. Sub-canopy tree up to 29 m tall and 36 cm diameter at breast height. Stipules about 5 mm long, triangular. Leaves opposite, simple, pinnate-veined, glabrous. Flowers ca. 52 mm diameter, white-yellow-orange, with up to 150 mm long corolla tube, flowers placed solitary at twig tips. Fruits ca. 42 mm diameter, pale green, dehiscent berry/capsule filled with many seeds in orange pulp [11].

2.1.1.3 Botanical Characteristic of *Gardenia obtusifolia* Roxb.

Deciduous treelet 2.5 m tall, basal diameter 6 cm; bark thin, nearly smooth to sparsely cracked and slightly roughened, grey; branchlets dark grey; calyx light green; corolla buds pale light green; mature corolla tube light green, turning cream; lobes initially white, rapidly becoming light orange on both sides; anthers tan; stigma/style pale light green; fragrant; old fruits light brown; leaves very immature; blades green above, light green below; old leaves dry, on the ground [24].

2.1.1.4 Botanical Characteristic of *Gardenia thailandica* Trivang.

A medium-size extensively branched tree that grows to 5-10 m tall. The leaves are arranged in opposite pairs along the branches, are oval in shape, wide 5-10 cm, long 14-38 cm, and are covered with hairs. The light green leaves have conspicuous venation with the secondary veins running almost

perpendicular from the midvein to the outer leaf margin. Solitary star-shaped flowers are borne in the leaf axils and are white when they first open then mature to a dark, golden yellow. The calyx forms a sheath around the base of the long tubular flower, which has five widely spreading petal lobes that are narrow at the base and widen towards the tips. The anthers (pollen producing structures) are inserted into the floral tube and barely extend beyond it. The round fruit contains many seeds that are immersed in a fleshy pulp [24].

2.1.1.5 Botanical Characteristic of *Gardenia collinsae* Craib

Deciduous tree 7 m, dbh 14 cm; bark thin, outer bark thin, very finely roughened, sparsely lenticellate, brown; flaking and exposing greenish inner bark; calyx & corolla buds green; mature corolla: base of tube light green, tube other-wise & both sides of lobes bright white; anthers cream; stigma pale light orangish; fragrant; leaves new; blades bright green above, light green underneath [24].

2.2 Literature Review

In 1991, Liang and co-workers identified two pigments, a brick-red and a light-yellow pigment (**1-2**) from flowers of *G. sootepensis* along with seven known compounds, β -sitosterol (**3**), palmitic acid (**4**), heneicosane (**5**), pentacosanol (**6**), heptacosanol (**7**), nonacosane (**8**), and triacontane (**9**) (Figure 1).

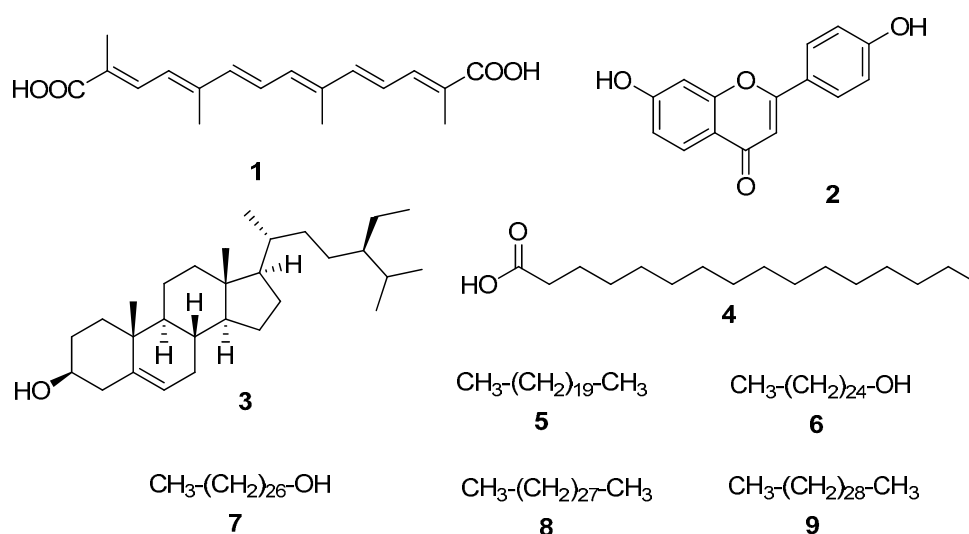


Figure 1. Isolated compounds from *G. sootepensis*.

In 1997, Silva and co-workers isolated the leaf and twig extracts of *G. coronaria* and *G. sootepensis* [8]. Coronololide methyl ester (**10**), coronololide (**11**), and coronalolic acid (**12**) were isolated from the leaves and stems of *G. coronaria*, and **12** was also isolated from the leaves of *G. sootepensis*. All compounds showed broad cytotoxic activity against a panel of human cancer cell lines.

In 1998, Rukachaisirikul and co-workers studied the chemical constituents of *G. sootepensis* twigs [26]. A new sesquiterpene with a guaiane skeleton named sootepdienone (**13**) and four known compounds, 4-hydroxy-3-methoxybenzoic acid (**14**), 4-hydroxy-3,5-dimethoxybenzoic acid (**15**), 5,7,4'-trihydroxy-6-methoxy flavone (**16**), and 5,7,3'-trihydroxy-6,4',5'-trimethoxyflavone (**17**) were isolated.

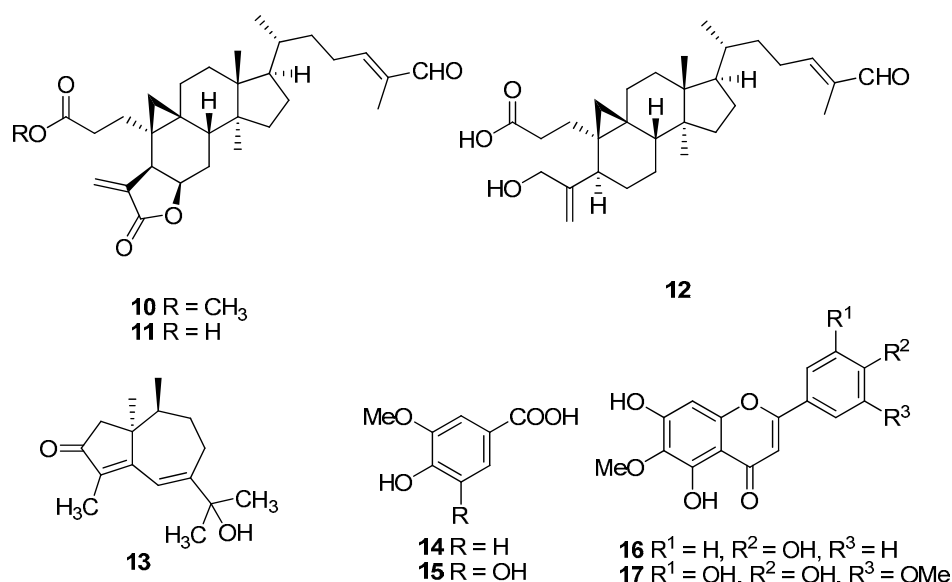


Figure 2. Isolated compounds from *Gardenia* spp.

In 1999, Wang and co-workers investigated the fruits of *G. sootepensis* collected in China [27]. Seven compounds were isolated, *D*-mannitol (**18**), β -sitosterol (**3**), deacetylasperulosidic acid methyl ester (**19**), geniposidic acid (**20**), geniposide (**21**), and scandoside methyl ester (**22**).

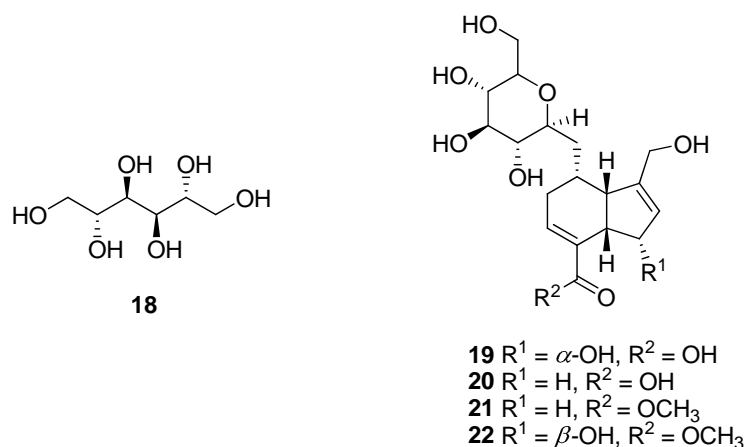


Figure 3. Isolated compounds from fruits of *G. sootepensis*.

In 2002, Tuchinda and co-workers determined the chemical constituents of leaves and twigs of *G. obtusifolia* [9]. Three novel compounds, 5 α -Cycloart-24-ene-3,23-dione (**23**), 5 α -cycloart-24-ene-3,16,23-trione (**24**) and methyl 3,4-*seco*-cycloart-4(28),24-diene-29-hydroxy-23-oxo-3-oate (**25**) were isolated, together with five known flavones 5,7,4'-trihydroxy-3,8-dimethoxyflavone (**26**), 5,7,4'-trihydroxy-3,8,3'-tri-methoxyflavone (**27**), 5,7,4'-trihydroxy-3,6,8-trimethoxyflavone (**28**), 5,4'-dihydroxy-3,6,7,8-tetramethoxyflavone (**29**) and 5,3'-dihydroxy-3,6,7,8,4'-pentamethoxyflavone (**30**). Compounds **25**–**29** showed significant cytotoxic activities on several human cancer cell lines, especially **29** and its diacetate.

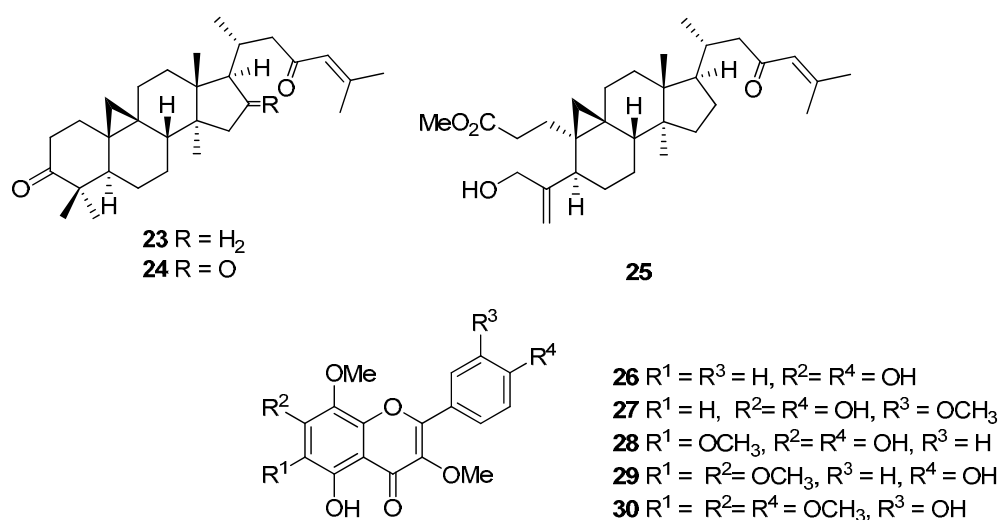


Figure 4. Isolated compounds from *G. obtusifolia*.

In 2003, Suksamran and co-workers described the isolation of ten triterpenoids from twigs of *G. saxatilis*, lupenone (**31**), lupeol (**32**), betulinic acid (**33**), oleanolic acid (**34**), ursolic acid (**35**), winchic acid (27-*O*-feruloyloxybetulinic acid) (**36**), messagenic acids A (**37**) and B (**38**), (27-*O*-*p*-(*E*)-coumaroyloxyoleanolic acid) (**39**) and 27-*O*-*p*-(*E*)-coumaroyloxyursolic acid (**40**) [15]. Compounds **37**- **40** exhibited antiplasmodial activity with the IC₅₀ values of 1.5, 3.8 and 2.9 $\mu\text{g/mL}$, respectively.

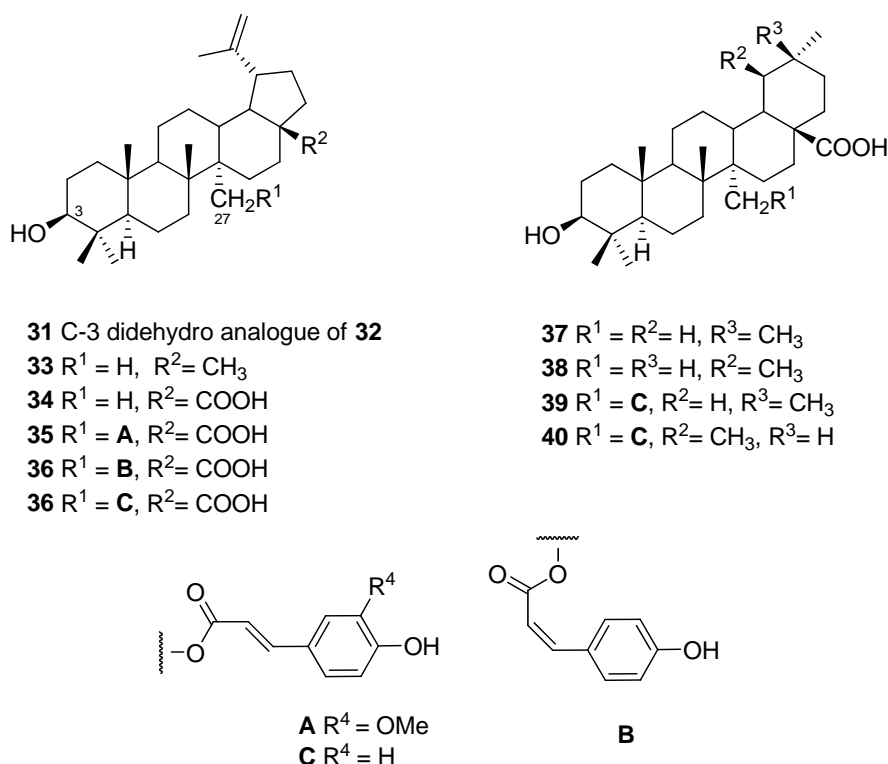
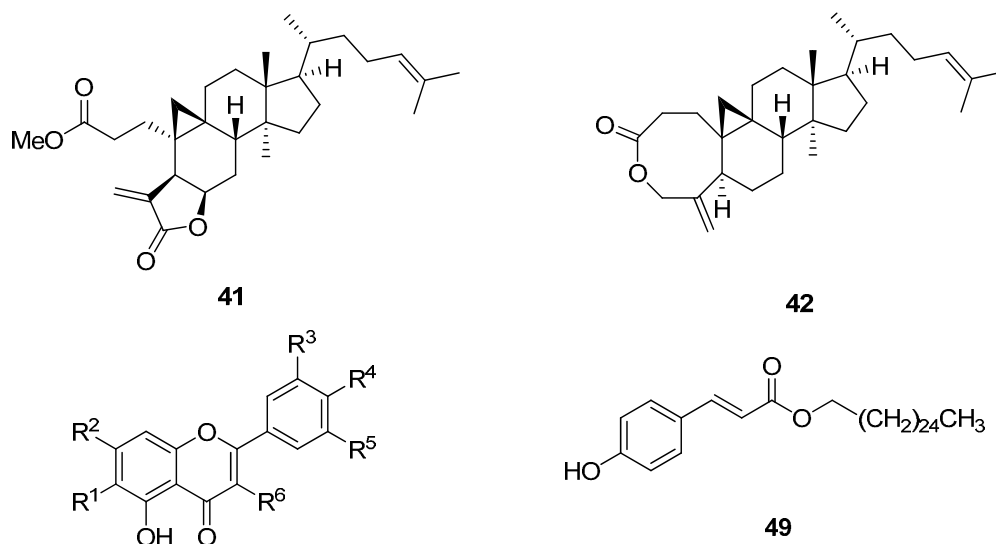


Figure 5. Isolated compounds from *G. saxatilis*.

In 2004, Reutrakul and co-workers investigated the hexane and chloroform extracts of the leaves and twigs of *G. tubifera* [15]. Eleven compounds, tubiferolide methyl ester (**41**), tubiferaoctanolide (**42**), coronalolide (**11**), coronalolide methyl ester (**10**), 5,3',5'-trihydroxy-7,4'-dimethoxy-flavone (**43**), 5,3',5'-trihydroxy-3,6,7,4'-tetramethoxyflavone (**44**), 5,7,4'-trihydroxy-6-methoxyflavone (**45**), 5,7,3'-trihydroxy-6,4',5'-trimethoxyflavone (**46**), 5,3'-dihydroxy-7,4',5'-trimethoxyflavone (**47**), 5,3'-dihydroxy-6,7,4',5'-tetramethoxyflavone (**48**), and hexacosyl 4'-hydroxy-trans-cinnamate (**49**) were obtained. Compounds **11**, **45**, **47** and **48** showed significant

cytotoxicity against only in P-388 cell line. Compound **41** was cytotoxic against P-388, KB, Col-2 and Lu-1, while **10** was active in P-388 and BCA-1.



43 R¹ = R⁶ = H, R⁴ = OMe, R³ = R⁵ = OH

44 R¹ = R² = R⁴ = OMe, R³ = R⁵ = OH

45 R¹ = OMe, R² = R⁴ = OH, R³ = R⁵ = R⁶ = H

46 R¹ = R⁴ = R⁵ = OMe, R² = R³ = OH, R⁶ = H

47 R¹ = R⁶ = H, R² = R⁴ = R⁵ = OMe, R³ = OH

48 R¹ = R² = R⁴ = R⁵ = OMe, R³ = OH, R⁶ = H

Figure 6. Isolated compounds from *G. tubifera*.

In 2004, Tuchinda and co-workers reported the isolation and identification of compounds from leaves and twigs of *G. thailandica* [10]. Four cycloartane triterpenes, thailandiol (**50**), gardenolic acid A (**51**), quadrangularic acid E (**52**) and 3 β -hydroxy-5 α -cycloart-24(31)-en-28-oic acid (**53**), and four flavones, 5-hydroxy-7,2',3',4',5',6'-hexamethoxyflavone (**54**), 5,7-dihydroxy-2',3',4',5',6'-pentamethoxyflavone (**55**), 5-hydroxy-7,2',3',4',5'-pentamethoxyflavone (**56**) and 5,7-dihydroxy-2',3',4',5'-tetramethoxyflavone (**57**) were isolated.

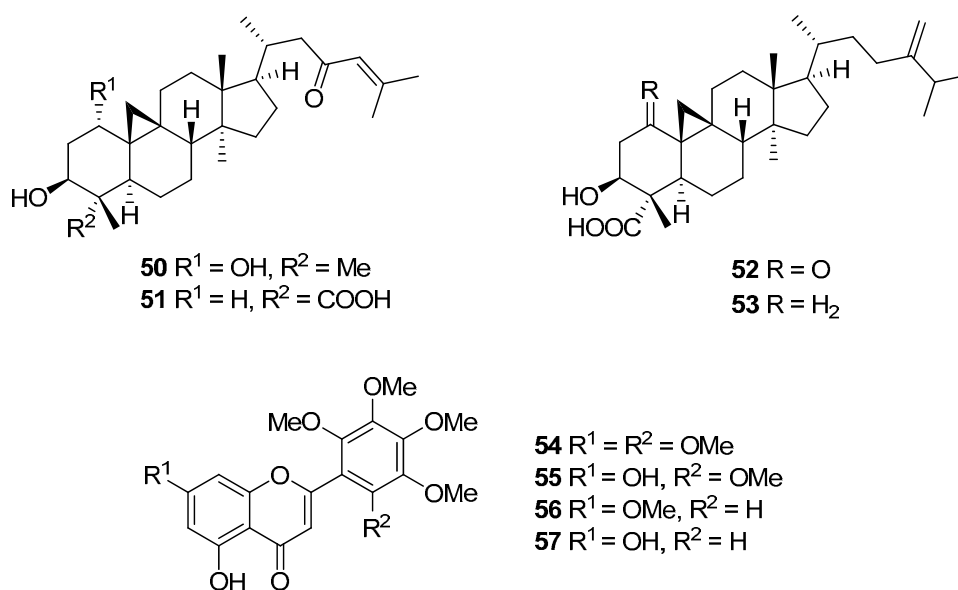


Figure 7. Isolated compounds from *G. thailandica*.

In 2006, Grougnet and co-workers reported the isolation of three new 3,4-*seco*-cycloartanes, secaubryenol (**58**), secaubrytriol (**59**), and secaubrylide (**60**) from an exudate collected on the aerial parts of *G. aubryi* [22]. Only compound **60** bearing an exomethylene γ -lactone ring system was found to be very weakly cytotoxic by IC_{50} value ranging from 21-52 μM against cell lines tested.

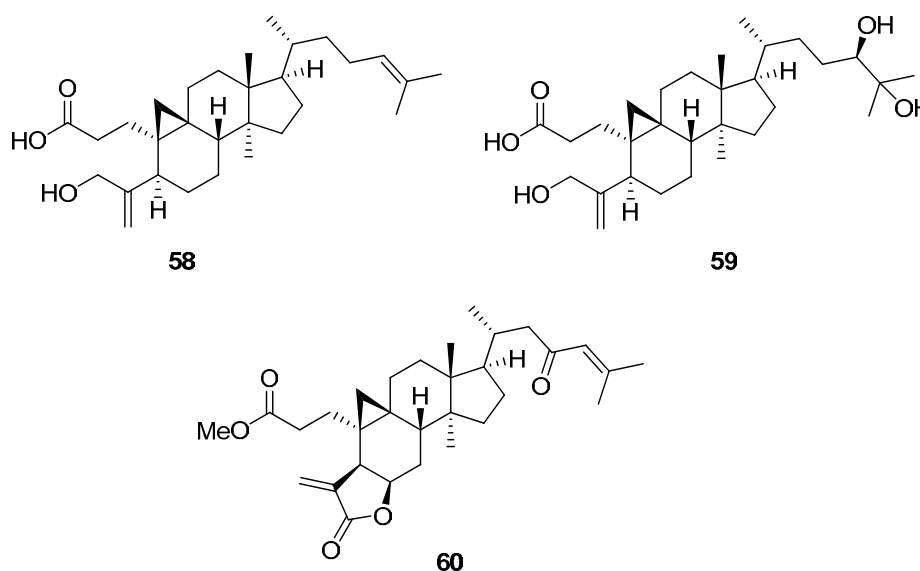


Figure 8. Isolated compounds from *G. aubryi*.

In 2009, Kunert and co-workers investigated the constituents of dikamali gum, the resin of *G. gummifera* and *G. lucida* [29]. Five new cycloartane triterpenes, dikamaliartanes A and C-F (**61-65**), together with secaubryenol (**58**), were obtained. Their antibacterial activity was evaluated, but all of them did not show any significant activity.

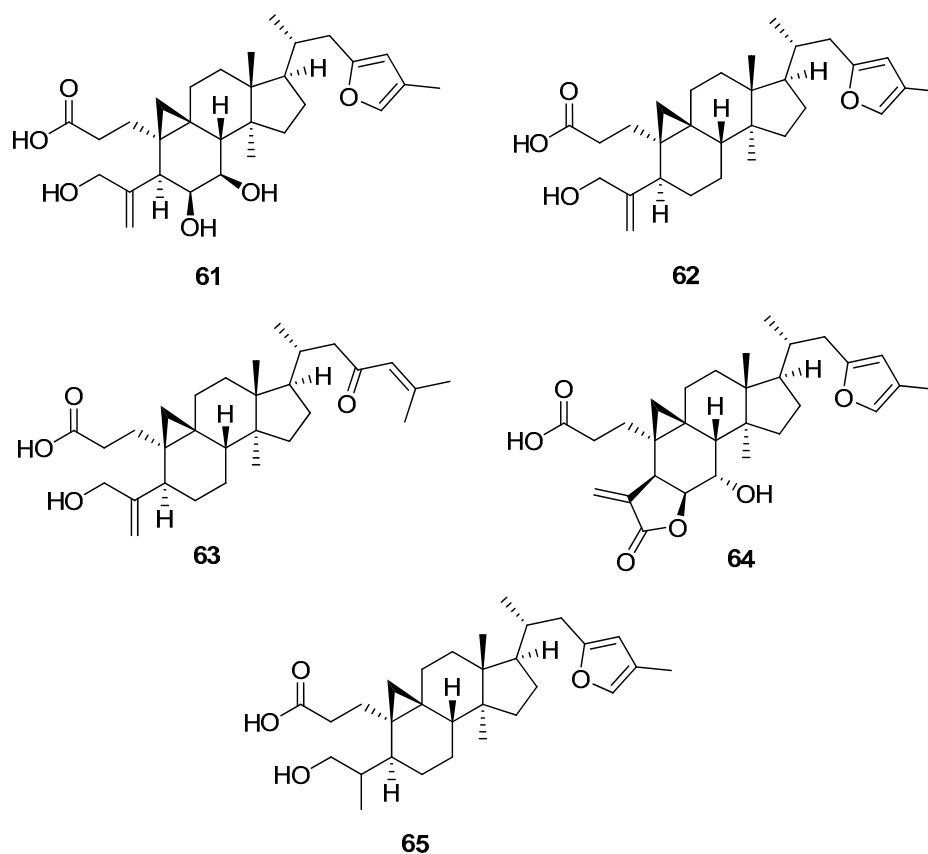


Figure 9. Isolated compounds from *G. gummifera* and *G. lucida*.

2.3 Experiments

2.3.1 Plant materials

Plant materials used in this study were collected from various areas of Thailand and their voucher specimens have been deposited at the Forest Herbarium, Royal Forest Department, Bangkok, Thailand as follows;

Table 1. Details of plant materials.

<i>Gardenia</i> spp.	Deposit no.	Parts	Collecting place	Collecting time
<i>G. sootepensis</i>	156377	apical buds	Kamphaeng-phet	November 2008
	162604	apical buds	Khon-kaen	December 2009
<i>G. tubifera</i>	159044	exudate	Bangkok	June 2009
<i>G. obtusifolia</i>	162605	apical buds	Khon-kaen	December 2009
<i>G. thailandica</i>	159039	exudate	Bangkok	July 2009
<i>G. collinsae</i>	159041	apical buds	Nakhon-sawan	February 2010

2.3.2 General Experimental Procedures

2.3.2.1 Nuclear magnetic resonance spectrometer (NMR)

NMR spectra were recorded in CDCl₃, acetone-*d*₆, and C₆D₆ on a Bruker AV400 and Varian Mercury 400 plus spectrometer at 400 MHz for ¹H NMR and 100 MHz for ¹³C NMR using TMS (tetramethylsilane) as internal standard.

2.3.2.2 Mass spectrometer (MS)

HRESIMS spectra were obtained with a Bruker micrOTOF.

2.3.2.3 Ultraviolet-visible spectrophotometer (UV-vis)

UV data were recorded on a CARY 50 Probe UV-visible spectrophotometer.

2.3.2.4 Fourier transforms infrared spectrophotometer (FT-IR)

FT-IR spectra were recorded on a Perkin-Elmer Model 1760X Fourier Transform Infrared Spectrophotometer. Solid samples were formally examined by incorporating the sample with potassium bromide (KBr) to form a pellet.

2.3.2.5 Optical rotation

Optical rotations were measured on a Perkin-Elmer 341 polarimeter at 589 nm.

2.3.2.6 Melting point

Melting points were recorded on a Fisher-Johns melting point apparatus.

2.3.2.7 X-ray crystallography

The crystal structure was solved by direct methods and using the SHELXS97 program. Crystallographic data, excluding structure factors, have been deposited at the Cambridge Crystallographic Data Centre.

2.3.3 Chemicals

2.3.3.1 Solvent

All commercial grade solvents, used in this research such as hexane, dichloromethane (CH₂Cl₂), ethyl acetate (EtOAc), acetone and methanol (MeOH), were purified by distillation prior to use.

2.3.3.2 Other chemicals

Merck's silica gel 60 No. 7734 and No. 9385 were used as adsorbents for open column chromatography. Merck's thin layer chromatography (TLC) aluminum, silica gel 60 F₂₅₄ pre-coated, 20x20 cm, layer thickness 0.2 mm were used for TLC analysis. Detection was visualized under ultraviolet light at wavelengths of 254 nm and dipped with (NH₄)₆Mo₇O₂₄ in 5% H₂SO₄ solution.

2.3.4 Extraction and Isolation

2.3.4.1 Fresh apical buds of *G. sootepensis* (Kamphaeng-phet province)

The fresh apical buds of *G. sootepensis* (93.11 g) were extracted with MeOH (500 mL × 2, each 2 days) at room temperature. After removing the solvent in vacuo, the combined MeOH crude extract was suspended in H₂O (250 mL), then partitioned with EtOAc (200 mL × 3), to afford an EtOAc crude extract (43.47 g). The extract was chromatographed on a silica gel column eluted with a gradient of hexane-CH₂Cl₂ (from 1:0 to 0:1) to yield seven fractions (I-VII). Fraction IV (3.27 g) was subjected to silica gel column chromatography (CC) and eluted with a gradient system of EtOAc-hexane to give 11 subfractions (IVa-IVk). Subfractions IVf and IVi were combined and then subjected to CC over silica gel using a mixture of EtOAc-hexane (1:3) to afford **68** (21 mg), **66** (125 mg), and **70** (24 mg). Subfraction IVk was separated on a silica gel column (EtOAc-hexane, 1:2) to yield **10** (450 mg). Fraction V was rechromatographed on a silica gel column using EtOAc-hexane (1:3) to furnish **70** (170 mg), **41** (170 mg), and a second crop of **10** (1.75 g). Fraction VI was separated into four fractions (VIa-VId) by CC over silica gel (EtOAc-hexane,

1:1), and VI_d was further purified by a silica gel column eluting with acetone-hexane (1:2) to yield **11** (14 mg) and **67** (30 mg). Fraction VII was subjected to silica gel CC eluted with a gradient system of acetone-hexane (from 1:9 to 1:4) to give 13 fractions (VII_a-VII_m). VII_c was further purified by preparative TLC (acetone-benzene, 1:9) to yield **69** (23 mg). VII_i afforded secauryenol **58** (48 mg) after recrystallization from acetone-hexane.

2.3.4.2 Fresh apical buds of *G. sootepensis* (Khon-kaen province)

EtOAc crude extract (160 g) of *G. sootepensis* apical buds (1 Kg) collected from Khonkaen province was obtained by the same manner with 2.3.4.1. It was further chromatographed on a silica gel column eluted with a gradient of hexane-EtOAc (from 1:0 to 0:1) to yield eight fractions (I-VIII). Fraction II was separated on a silica gel column (acetone-hexane, 1:9) to yield **75** (45 mg), tubiferolide methyl ester (**70**, 2.3 g), sootepin A (**67**, 4.5 g), sootepin C (**66**, 730 mg), and coronalolide methyl ester (**69**, 7.5 g). Fraction V (37.9 g) was subjected to silica gel CC and eluted with a gradient system of Acetone-hexane to give ten subfractions (Va-Vj). Subfraction V_b was separated by silica gel CC with acetone-hexane (2:8) to yield coronalolic acid (**76**, 550 mg). Subfractions V_e was subjected to CC over silica gel using a mixture of acetone-CH₂Cl₂ (5:95) to afford **77** (30 mg).

2.3.4.3 Exudate of *G. tubifera*

The dried exudate (5.74 g) of *G. tubifera* was dissolved in a 1:1 mixture of CH₂Cl₂ and MeOH (10 mL). This solution was subsequently subjected to passage over a silica gel column eluted with a gradient system of hexane-EtOAc (from 1:0 to 3:2) to yield 12 fractions (I-XII). Precipitation from fraction V (3.27 g) led to the isolation of the pure compound **78** (26.9 mg) after filtration. Fraction IX (2.3 g) was rechromatographed on a silica gel column using a gradient system of acetone-hexane (from 1:4 to 3:7) to give **79** (24.2 mg). Fraction X (1.18 g) was further purified using a silica gel column eluting with acetone-hexane (1:3) to afford **80** (52.1 mg). Fraction XII (2.0 g) was subjected to silica gel CC eluted with a gradient system of acetone-hexane (from 1:2 to 1:1) to yield **81** (56.7 mg) and **74** (61.8 mg).

2.3.4.4 Fresh apical buds of *G. obtusifolia*

EtOAc crude extract (80 g) of *G. sootepensis* apical buds (400 g) collected from Khonkaen province was obtained by the same manner with 2.3.4.1. The extract was fractionated by silica gel flash CC, eluted with a gradient system of hexane-EtOAc and EtOAc-MeOH to yield 13 fractions (I-XIII). Fraction V was subjected to silica gel CC and eluted with a gradient system of acetone-hexane (from 1:9 to 1:4) to afford **82** (53.9 mg), **83** (17.4 mg), **84** (37.8 mg) and **85** (10.5 mg). Fraction VI was separated on a silica gel column using acetone-hexane mixtures (from 1:9 to 3:7) to give secaubryenol (**74**, 22.6 mg). Fraction IX was separated into 14 fractions (IXa-IXn) by CC over silica gel eluted with the mixtures of acetone-hexane (from 1:4 to 1:1), and it was found that subfractions IXh and IXn provided the pure compounds **86** (10 mg) and **87** (55 mg), respectively. Subfraction IXk was further purified by silica gel CC, eluted with 1:99 MeOH-CH₂Cl₂, to yield **88** (70 mg). Fraction XI was then applied to a silica gel column and eluted with MeOH-CH₂Cl₂ (from 3:97 to 8:92) to afford **89** (748.5 mg).

2.3.4.5 Exudate of *G. thailandica*

Solution of *G. thailandica* (10 g) in a 1:1 mixture of CH₂Cl₂ and MeOH (20 mL) was subsequently subjected to passage over a silica gel column eluted with a gradient system of acetone-hexane (from 1:4 to 1:0) to yield 11 fractions (I-XI). Fraction III (453.7 mg) was subjected to silica gel CC using a mixture of acetone-hexane (1:4) as an eluent to afford **68** (53 mg). Fraction V was further purified using a silica gel column eluted with acetone-hexane (1:4) to give **87** (9.0 mg). Fraction VI was rechromatographed on a silica gel column, eluting with acetone-hexane (1:2) to afford **74** (255.6 mg) and **76** (29.2 mg), while fraction VII was separated by CC eluting with acetone-hexane (1:3) to yield **88** (10.0 mg).

3.4.6 Fresh apical buds of *G. collinsae*

EtOAc crude extract (11 g) of *G. collinsae* apical buds (53 g) collected from Nakornsawan province was obtained by the same manner with 2.3.4.1. The EtOAc extract was fractionated by a silica gel column eluted with a gradient

system of EtOAc-hexane to yield 25 pooled fractions (I–XXV). Fractions IX and X were combined together and then recrystallized with a 1:4 mixture of acetone-hexane to give **89** (950 mg). Fraction XXI afforded **90** (35.2 mg) after precipitation and filtration. Fraction XXII was rechromatographed on a silica gel column, eluting with MeOH–CH₂Cl₂ (2:98) system to afford nine subfractions (XXIIa–XXIIi). Subfraction XXII d was further purified by CC on silica gel with a mixture of acetone-hexane (1:3) to yield **91** (8.0 mg).

2.3.5 Cytotoxic activity

Cytotoxicity assay was carried out at the institute of Biotechnology and Genetic Engineering, Chulalongkorn University. All isolated compounds were tested for their cytotoxic activity towards five human cancer cell lines including HEP-G2 (hepatocarcinoma), SW-620 (colon adenocarcinoma), CHAGO (undifferentiated lung carcinoma), KATO-3 (gastric carcinoma) and BT-474 (breast ductal carcinoma) cancer cell lines. Herein, the *in vitro* cytotoxicity was determined by using MTT (3-(4,5-dimethylthiazol-2-yl)-2,5-diphenyltrazolium bromide) colorimetric method. In principle, the viable cell number/well was directly proportional to the production of formazan, which could be measured spectrophotometrically.

The human cancer cell line was harvested from exponential-phase maintenance cultures (T-25 cm² flask), counted by trypan blue exclusion, seed cells in a 96-well culture plates at a density of 1×10^5 cells/well in 200 μ L of culture medium without compounds to be tested. Cells were cultured in a 5% CO₂ incubator at 37 °C, 100% relative humidity for 24 h. Culture medium containing the sample was dispensed into the appropriate wells (control cells group, N = 3; each sample treatment group, N = 3). Peripheral wells of each plate (lacking cells) were utilized for sample blank (N = 3) and medium/DMSO blank (N = 3) for “background” determination. Culture plates were then incubated for 72 h prior to the addition of tetrazolium reagent. MTT stock solution (5 mg/mL in PBS) was sterilized by filtering through 0.45 μ L filter units. MTT working solution was prepared just prior to culture application by dilution of MTT stock 1:5 (v/v) in pre-warmed standard culture

medium. The freshly prepared MTT reagent (10 μL) was added into each well and mixed gently for 1 minute on an orbital shaker. The cells were further incubated for 4 h at 37 $^{\circ}\text{C}$ in a 5% CO_2 incubator. After incubation, the formazan produced in the cells captured as dark crystals in the bottom of the wells. All of the culture medium supernatant was removed from wells and 150 μL of DMSO was added to dissolve the resulting formazan. Samples in the culture plate were mixed for 5 minutes on an orbital shaker. Subsequently, 25 μL of 0.1M glycine (pH 10.5) was added and the culture plate was shaken for 5 minutes. Following formazan solubilization, the absorbance was measured using a microplate reader at 540 nm (single wavelength, calibration factor = 1.00).

2.4 Results and Discussion

2.4.1 Isolation and characterization of cycloartane triterpenes from apical buds of *G. sootepensis* (Kamphaeng-phet province)

The MeOH extract of fresh apical buds of *G. sootepensis* was partitioned between EtOAc and water to afford an EtOAc extract, which was subjected to silica gel CC using EtOAc-hexane mixtures of increasing polarity as eluent. Further purification by repeated normal column chromatography and preparative thin-layer chromatography gave five new 3,4-*seco*-cycloartanes (**66-70**) and four known compounds coronalolide methyl ester (**10**), tubiferolide methyl ester (**41**), coronalolide (**11**), and secaubryenol (**58**). The structures of new compounds were elucidated by extensive spectral methods including 1D, 2D NMR, and HRESIMS, as well as by single-crystal x-ray diffraction analysis (if any).

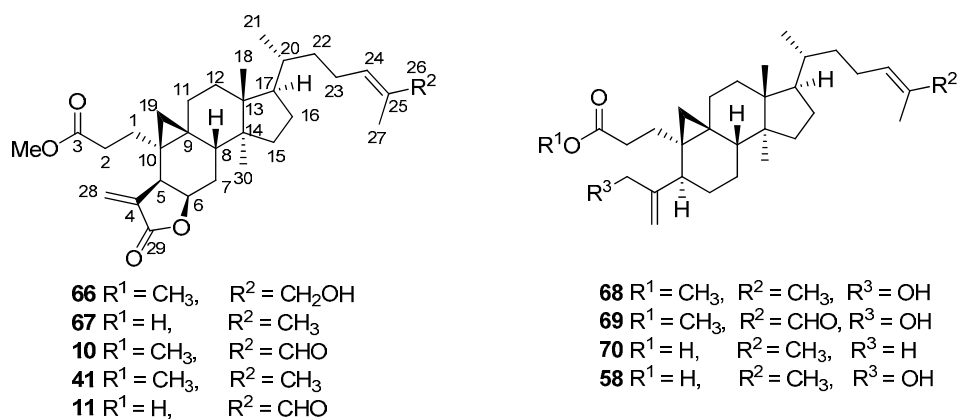


Figure 10. Isolated compounds from *G. sootepensis* (Kamphangpech province).

Sootepin A (**66**) was obtained as colorless crystals, m.p. 143–144 °C, $[\alpha]_D^{25} +173.0$ (c 0.1, MeOH), UV (MeOH) v_{\max} ($\log \epsilon$) 210 (3.84), and IR (KBr) v_{\max} 3566, 3503, 2952, 1755, 1733, 1459, 1378, 1266, 1145, 1002 cm^{-1} . Its molecular formula was determined as $\text{C}_{31}\text{H}_{46}\text{O}_5$ from the HRESIMS ion at m/z 499.3427 $[\text{M} + \text{H}]^+$, indicating nine degrees of unsaturation. The ^1H NMR spectrum displayed a pair of doublets at δ_H 0.16 and 0.41 ($J = 4.8$ Hz), characteristic of the C-19 methylene protons of the cyclopropane ring of a cycloartane triterpene, an olefinic proton, one vinylic methyl group, two tertiary methyl groups, one secondary methyl group, and one methoxy methyl. A pair of doublets at δ_H 5.73 and 6.33 ($J = 1.6$ Hz) were ascribed to H-28a and H-28b in the exocyclic methylene γ -lactone ring, and signals of the β - and γ -methine protons of the lactone ring appeared at δ_H 3.23 (H-5) and 4.74 (H-6), respectively. In addition, the lactonization of C-4 onto C-6 was confirmed by the HMBC correlations observed from H-6 to C-29 (δ_C 170.8) (Figure 11). The ^{13}C and HSQC spectra revealed the presence of 31 nonequivalent carbons including two carbonyl carbons, four sp^2 carbons (two quaternary C, one CH, and one CH_2), and 26 sp^3 carbons (four quaternary C, five CH, 13 CH_2 , four CH_3 , and one $-\text{OCH}_3$). These ^1H and ^{13}C spectra were closely related to those previously reported for tubiferolide methyl ester (**41**) [23], except for the marked differences in chemical shift values corresponding to the side chain at C-26. In the ^1H NMR spectrum of **66**, the signal attributable to an oxygen-bearing methylene at δ_H 3.99 replaced those corresponding to the methyl signal of **41** at δ_H 1.68. The relative stereochemistry of **66** was assigned on the basis of a NOESY experiment (Figure 11). Observation of a strong NOESY cross-peak between H-5 and H-6 permitted the assignment of a relative 5,6-*cis*-configuration. Additionally, the compound exhibited NOEs between H-8 and H₃-18, H-8 and H-19b, H-6 and H₃-30, H-17 and H₃-30, and H-17 and H₃-21. These were in good agreement with the relative configurations at C-5, C-6, C-8, C-9, C-10, C-13, C-14, and C-17 long-established for the cycloartane core. Finally, the relative configuration of compound **66** was confirmed by X-ray diffraction analysis as shown in Figure 12.

X-ray Crystallographic Analysis of Sootepin A (66) Crystal data: colorless crystal; $C_{31}H_{46}O_5$, $M_r = 498.68$, triclinic, $P1$, $a = 7.3556(2)$ Å, $b = 7.4296(2)$ Å, $c = 14.2899(4)$ Å, $\alpha = 81.7620(10)^\circ$, $\beta = 82.9370(10)^\circ$, $\gamma = 65.0020(10)^\circ$, $Z = 1$, and $V = 698.77(3)$ Å³, Mo K α radiation, $\lambda = 0.71073$ Å. The intensity data were collected at 293 K to a maximum 2θ value of 50.92° . Of the 7425 reflections collected, 4618 were unique, 329 parameters ($R_{\text{int}} = 0.0232$). The crystal structure was solved by direct methods and using the SHELXS97 program. Refinements were made by full-matrix least-squares on all F^2 data using SHELXL97 to final R values [$I > 2\sigma(I)$] of $R_1 = 0.0454$, $wR_2 = 0.1219$ and goodness of fit on $F^2 = 1.010$. All non-hydrogen atoms were anisotropically refined. All hydrogen atoms were added at calculated positions and refined using a rigid model. Crystallographic data, excluding structure factors, have been deposited at the Cambridge Crystallographic Data Centre under the deposition number CCDC 730211. Copies can be obtained, free of charge, on application to CCDC, 12 Union Road, Cambridge, CB2 1EZ, UK (fax: +44-0-1223-226033, e-mail: deposit@ccdc.cam.ac.uk).

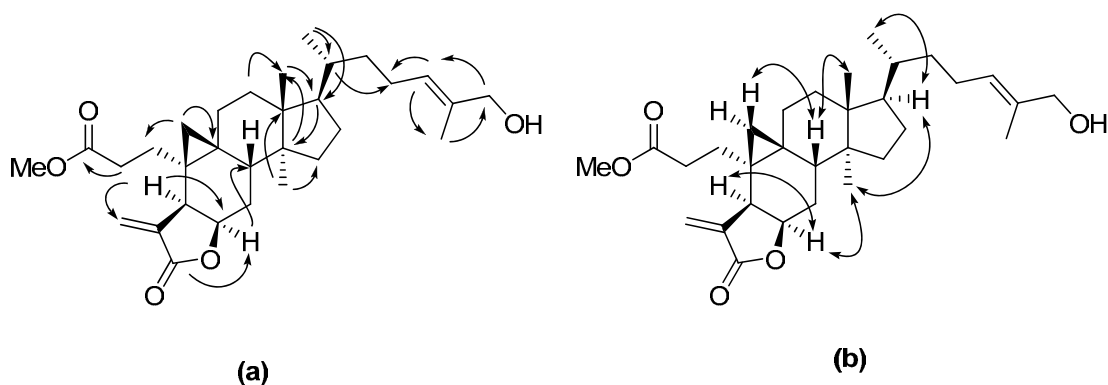


Figure 11. Key HMBC (a) and NOE (b) correlations of compound **66**.

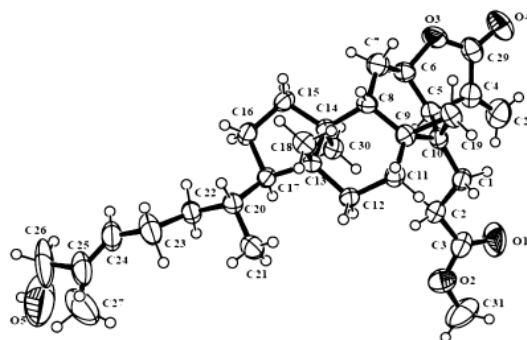


Figure 12. ORTEP drawing of **66** with atom labeling.

Sootepin B (**67**) was isolated as a light yellow, amorphous solid, m.p. 132–133 °C, $[\alpha]_D^{25} +167.0$ (c 0.15, MeOH), UV (MeOH) λ_{\max} (log ϵ) 213 (4.11), IR (KBr) ν_{\max} 3530, 3424, 2942, 1744, 1708, 1450, 1377, 1279 cm^{-1} . It had the molecular formula $\text{C}_{30}\text{H}_{44}\text{O}_4$, as established by HRESIMS (m/z 469.3315 $[\text{M} + \text{H}]^+$). In the ^1H NMR spectrum, typical signals for a cyclopropane methylene proton appeared as two doublets at δ_H 0.16 and 0.43 ($J = 5.2$ Hz), and its NMR data were almost the same those of tubiferolide methyl ester (**41**), except for the absence of a methoxy group at C-3 in **41**. The relative configuration of **67** was assigned to be the same as that of **66** and **41** by comparing their NMR data and NOESY correlations of H-5/H-6, H-6/H₃-30, H-8/H₃-18, H-8/H-19b, and H-17/H₃-21.

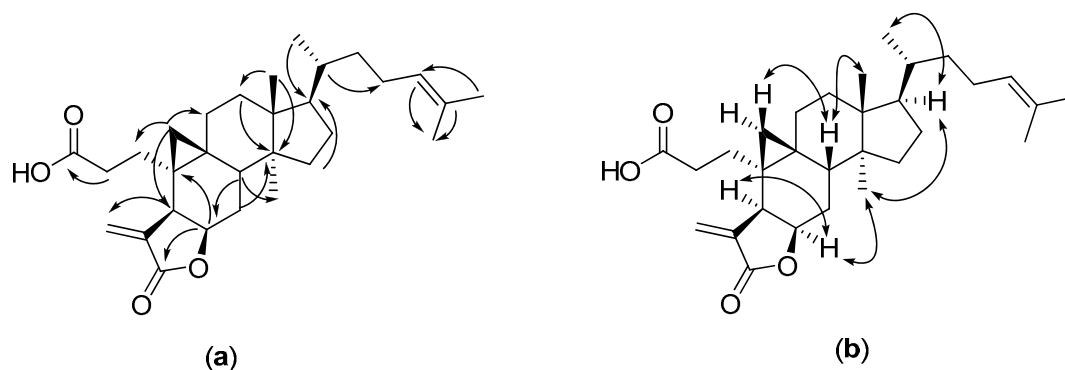


Figure 13. Key HMBC (a) and NOE (b) correlations of compound **67**.

Sootepin C (**68**), obtained as a colorless oil, $[\alpha]_D^{25} +173.0$ (c 0.1, MeOH), UV (MeOH) λ_{\max} (log ϵ) 207 (3.46), IR (KBr) ν_{\max} 3436, 2934, 1742, 1450, 1370, 1266, 1159 cm^{-1} . It had a molecular formula of $\text{C}_{31}\text{H}_{50}\text{O}_3$ as determined by HRESIMS (m/z 471.3840 $[\text{M} + \text{H}]^+$), suggesting seven degrees of unsaturation. The ^1H NMR spectrum also showed typical signals associated with a 3,4-*seco*-cycloartane triterpene, including two tertiary methyl singlets at δ_H 0.92 and 0.96, one secondary methyl doublet at δ_H 0.88 ($J = 6.4$ Hz), and a characteristic pair of doublets at δ_H 0.46 and 0.71 ($J = 4.3$ Hz), assigned to the C-19 methylene protons in the cyclopropane ring. Allylic coupling observed in the COSY spectrum between a two-proton broad singlet at δ_H 4.13 accounting for a primary alcoholic group and two broad singlets of a terminal alkene at δ_H 5.07 and 5.09 was suggestive of the structure of a 29-hydroxy-3,4-*seco*-cycloartane. Both ^1H and ^{13}C NMR data of **68** were virtually identical to

those previously reported for secaubryenol (**58**)⁵, with the only difference being the appearance of a three-proton singlet of a methoxy group at δ_H 3.64. Consequently, the structure of this derivative was established as **68**. The same NOESY correlations of H-8/H₃-18, H-8/H-19b, H-17/H₃-21, and H-17/H₃-30 as for **58** gave evidence for the relative configuration of **68** at C-5, C-8, C-9, C-10, C-13, C-14, C-17, and C-20 (Figure 14).

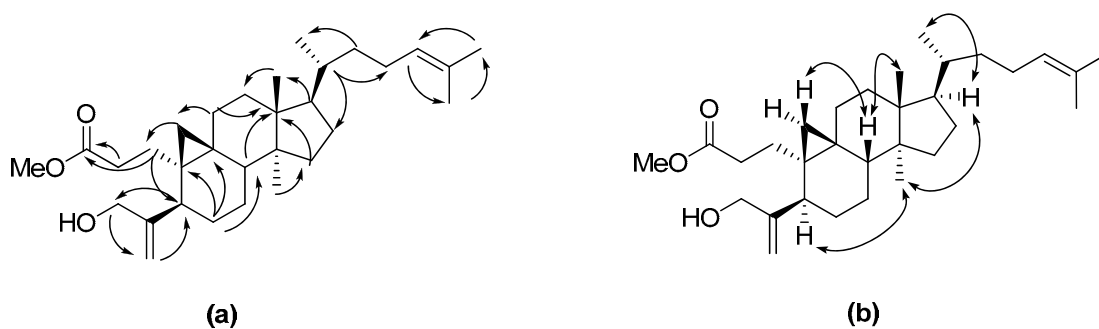


Figure 14. Key HMBC (a) and NOE (b) correlations of compound **68**.

Sootepin D (**69**) was obtained as a colorless oil, $[\alpha]_D^{25} +58.0$ (c 0.1, MeOH), UV (MeOH) λ_{\max} (log ϵ) 231 (4.08), IR (KBr) ν_{\max} 3428, 2938, 2868, 1724, 1683, 1450, 1372, 1164, 1062 cm^{-1} , and its molecular formula $\text{C}_{31}\text{H}_{48}\text{O}_4$ was deduced from the HRESIMS (m/z 485.3628 $[\text{M} + \text{H}]^+$), 14 mass units more than that of **68**. Comparison of the ^1H and ^{13}C NMR spectra of **69** with those of **68** revealed them to be very similar, with the only difference being the appearance of a singlet due to an aldehyde group at δ_H 9.39 in the ^1H NMR spectrum, coupled in the HSQC spectrum to a newly appearing aldehyde carbonyl carbon at δ_C 195.5, while a vinylic methyl signal at δ_H 1.68 and at δ_C 17.6 had disappeared. The relative configuration of **69** was assigned to be the same as that of **68** on the basis of NOESY correlations H-8/H₃-18, H-8/H-19b, H-17/H₃-21, and H-17/H₃-30. Thus, the structure of this new compound was established as **69**.

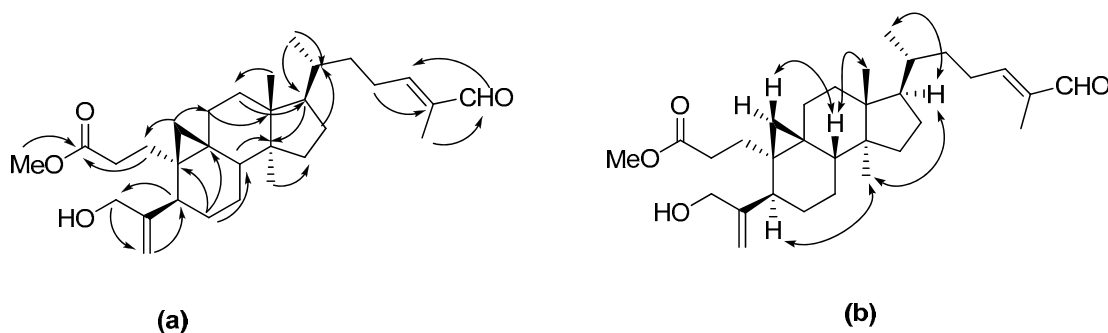


Figure 15. Key HMBC (a) and NOE (b) correlations of compound **69**.

Sootepin E (**70**) was isolated as a colorless gum, $[\alpha]_D^{25} +97.0$ (c 0.1, MeOH), UV (MeOH) λ_{\max} (log ϵ) 208 (3.77), IR (KBr) ν_{\max} 3443, 2936, 1708, 1457, 1370, 1300, 1209 cm^{-1} . Its molecular formula, $\text{C}_{30}\text{H}_{48}\text{O}_2$, was determined on the basis of HRESIMS at m/z 441.3731 $[\text{M} + \text{H}]^+$. The ^1H and ^{13}C NMR data of **70** were also similar to those of **68**. The NMR spectrum showed the presence of an additional vinylic methyl at δ_H 1.68 and at δ_C 19.7, while the signals of oxygen-bearing methylene (C-29) at δ_H 4.13 and at δ_C 64.7 as for **68** had disappeared. This indicated that the OH-29 in **68** was replaced by H-29. There was no three-proton singlet characteristic of a methoxy group observed. Thus, the structure of this derivative was depicted as **5**. The relative configuration of **70** was established to be the same as that of **68** and **69** on the basis of the NOESY correlations.

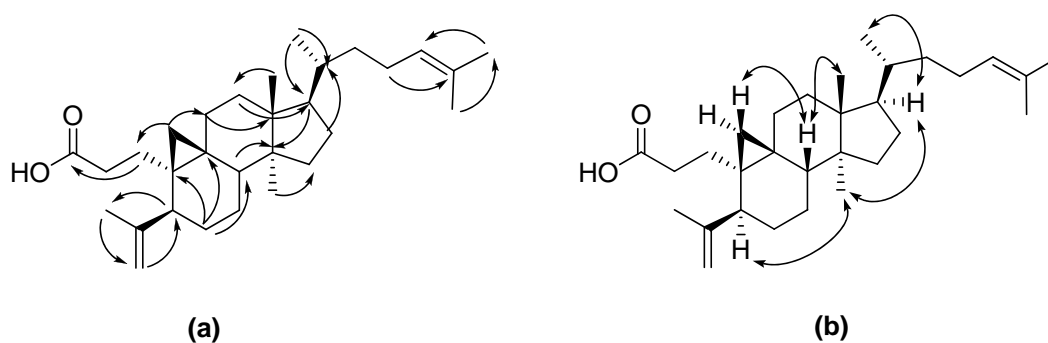


Figure 16. Key HMBC (a) and NOE (b) correlations of compound **70**.

The ^1H NMR spectrum of compound **10** in CDCl_3 (Table 7) displayed; a pair of doublets at δ_H 0.17 and 0.40 (1H each, d, $J = 5.2$ Hz), an aldehyde

proton at δ_H 9.37 (1H, s), a pair of doublet at δ_H 5.72 and 6.31 (1H each, d, J = 1.8 Hz), an olefinic proton at δ_H 6.47 (1H, t, J = 7.5 Hz), an oxygenated methine proton at δ_H 4.73 (1H, dd, J = 8.3, 6.0 Hz), a methyl ester proton at δ_H 3.67 (3H, s), four methyl protons at δ_H 0.90, 0.92, 1.73 (3H each s), and 0.91 (3H, m). Based on the spectroscopic data above, compound **10** was identified to be a coronalolide methyl ester. The structure of this compound was finally confirmed by comparison of the spectral data with those previously reported (Table 7) by Silva and co-workers in 1999 [8].

The ^1H NMR spectrum of compound **11** in CDCl_3 (Table 8) displayed; a pair of doublets at δ_H 0.19 and 0.43 (1H each, d, J = 5.3 Hz), a pair of broad singlet at δ_H 5.74 and 6.33 (1H each, br s), an olefinic proton at δ_H 6.49 (1H, t, J = 7.2 Hz), an oxygenated methine proton at δ_H 4.75 (1H, dd, J = 8.1, 7.5 Hz), and four methyl protons at δ_H 0.91, 0.94 \times 2, and 1.75 (3H each br s). Based on the spectroscopic data above, compound **11** was identified to be a coronalolide. The structure of this compound was finally confirmed by comparison of the spectral data with those previously reported (Table 8) by Silva and co-workers in 1999 [8].

The ^1H NMR spectrum of compound **41** in CDCl_3 (Table 9) displayed; a pair of doublets at δ_H 0.16 and 0.42 (1H each, d, J = 5.3 Hz). A pair of doublet at δ_H 5.73 (1H, d, J = 2.0 Hz) and 6.33 (1H, d, J = 2.3 Hz), an olefinic proton at δ_H 5.09 (1H, br t, J = 6.9 Hz), an oxygenated methine proton at δ_H 4.75 (1H, dd, J = 7.9, 6.7 Hz), a methyl ester proton at δ_H 3.69 (3H, s), four tertiary methyl protons at δ_H 0.90, 0.93, 1.60, and 1.68 (3H each s), and a secondary methyl proton at δ_H 0.89 (3H, d, J = 6.6 Hz). Based on the spectroscopic data above, compound **70** was identified to be a tubiferolide methyl ester. The structure of this compound was finally confirmed by comparison of the spectral data with those previously reported (Table 9) by Reutrakul and co-workers in 2004 [23].

The ^1H NMR spectrum of compound **58** in CDCl_3 (Table 9) displayed; a pair of doublets at δ_H 0.48 and 0.73 (1H each, J = 4.2 Hz), a multiplet proton at δ_H 5.10 (2H, m), an olefinic proton at δ_H 5.08 (1H, m), an oxygenated methylene proton at δ_H 4.14 (2H, br s), four tertiary methyl protons at δ_H 0.92, 0.96, 1.60, and 1.68 (3H each s), and a secondary methyl proton at δ_H 0.88 (3H, d, J = 6.3

Hz). Based on the spectroscopic data above, compound **58** was identified to be a secaubryenol. The structure of this compound was finally confirmed by comparison of the spectral data (Table 9) with those previously reported by Grougnet and co-workers in 2006 [22].

Table 2. NMR data of compound **66** in CDCl₃.

Position	¹ H	¹³ C	HMBC
1	2.24 (1H, m), 1.61 (1H, m)	30.9	C-2, C-3, C-5, C-9, C-10
2	2.48 (2H, m)	31.2	C-1, C-3, C-10
3		173.5	
4		139.1	
5	3.23 (1H, br d, <i>J</i> = 8.0 Hz)	39.0	C-1, C-4, C-6, C-28, C-29
6	4.74 (1H, dd, <i>J</i> = 7.1, 7.3 Hz)	74.5	C-4, C-8, C-10, C-29
7	1.61 (1H, m), 1.78 (1H, m)	27.2	C-6, C-8, C-14
8	2.12 (1H, m)	38.3	C-6, C-7, C-10, C-13, C-14, C-15
9		25.1	
10		28.2	
11	1.78 (1H, m), 1.65 (1H, m)	26.5	C-8, C-9, C-12, C-13, C-14, C-19
12	1.66 (2H, m)	33.0	C-9, C-11, C-12, C-13, C-18
13		45.7	
14		48.6	
15	1.32 (2H, m)	34.8	C-13, C-20, C-30
16	1.32 (1H, m), 1.93 (1H, m)	27.7	C-13, C-14, C-15, C-20
17	1.61 (1H, m)	51.4	C-14, C-21, C-23
18	0.90 (3H, s)	15.9	C-12, C-13, C-14, C-18
19	0.16 (1H, d, <i>J</i> = 4.8 Hz) 0.41 (1H, d, <i>J</i> = 5.0 Hz)	23.0	38.3, 30.9, 28.2, 26.5, 25.1
20	1.06 (1H, m)	35.9	C-23
21	0.83 (3H, m)	18.4	C-17, C-22
22	1.53 (1H, m), 1.23 (1H, m)	35.9	C-17, C-21, C-22, C-23
23	2.12 (1H, m), 1.91 (1H, m)	24.5	C-22, C-24, C-25
24	5.38 (1H, br t, <i>J</i> = 6.5 Hz)	126.8	C-23, C-27
25		134.4	
26	3.99 (2H, s)	69.0	C-24, C-25, C-27
27	1.66 (3H, s)	13.6	C-24, C-25, C-26
28	5.73 (1H, d, <i>J</i> = 1.6 Hz) 6.33 (1H, d, <i>J</i> = 1.6 Hz)	123.1	C-4, C-16, C-22, C-29
29		170.8	
30	0.88 (3H, s)	20.1	C-8, C-13, C-14, C-15
OMe	3.68 (3H, s)	51.8	C-3

Table 3. NMR data of compound **67** in CDCl₃.

Position	¹ H	¹³ C	HMBC
1	2.26 (1H, m), 1.59 (1H, m)	31.0	C-2, C-10
2	2.53 (1H, m), 2.46 (1H, m)	31.2	C-1, C-3, C-10
3		178.6	
4		139.1	
5	3.23 (1H, d, <i>J</i> = 8.3 Hz)	39.0	C-4, C-6, C-10, C-19, C-24, C-28
6	4.74 (1H, dd, <i>J</i> = 7.8, 6.9 Hz)	74.6	C-10, C-29
7	1.80 (1H, m), 1.54 (1H, m)	27.2	C-5, C-6, C-8, C-14
8	2.13 (1H, br t, <i>J</i> = 5.5 Hz)	38.3	C-6, C-9, C-12, C-14, C-30
9		25.1	
10		28.1	
11	1.80 (1H, m), 1.54 (1H, m)	26.6	C-8, C-10, C-12, C-13
12	1.59 (2H, m)	33.0	C-13, C-14
13		45.7	
14		48.6	
15	1.33 (2H, m)	34.8	C-13
16	1.91 (1H, m), 1.33 (1H, m)	27.7	C-14
17	1.59 (1H, m)	51.4	C-13, C-14
18	0.92 (3H, br s)	15.8	C-12, C-13, C-14, C-17
19	0.43 (1H, d, <i>J</i> = 5.2 Hz) 0.16 (1H, d, <i>J</i> = 5.2 Hz)	23.0	C-1, C-5, C-8, C-11
20	1.42 (1H, m)	35.9	C-13
21	0.88 (3H, d, <i>J</i> = 6.5 Hz)	18.4	C-17
22	1.42 (1H, m)	36.3	
23	2.02 (1H, m), 1.83 (1H, m)	24.9	C-20, C-24, C-25
24	5.08 (1H, t, <i>J</i> = 6.8 Hz)	125.0	C-23, C-27
25		131.1	
26	1.67 (3H, br s)	25.7	C-24, C-25, C-27
27	1.59 (3H, br s)	17.7	C-24, C-25, C-26
28	6.33 (1H, d, <i>J</i> = 2.0 Hz) 5.72 (1H, d, <i>J</i> = 2.0 Hz)	123.2	C-3, C-5, C-10, C-29
29		170.9	
30	0.90 (3H, br s)	20.1	C-8, C-13, C-14

Table 4. NMR data of compound **68** in CDCl₃.

Position	¹ H	¹³ C	HMBC
1	2.10 (1H, m), 1.38 (1H, m)	28.9	C-2, C-3, C-5, C-9, C-11, C-19
2	2.50 (1H, m), 2.28 (1H, m)	31.6	C-1, C-3, C-5, C-11, C-19
3		174.6	
4		152.5	
5	2.50 (1H, m)	42.1	C-4, C-6, C-7, C-28, C-29
6	1.68 (1H, m), 1.05 (1H, m)	29.0	C-5, C-7, C-8, C-9, C-14
7	1.68 (1H, m), 1.27 (1H, m)	25.3	C-5, C-8, C-9
8	1.52 (1H, m)	47.9	C-9, C-13, C-14, C-15, C-19, C-30
9		21.8	
10		27.4	
11	2.12 (1H, m), 1.55 (1H, m)	26.9	C-9, C-10, C-13, C-14, C-19
12	1.68 (2H, m)	33.0	C-9, C-13, C-17, C-18
13		45.1	
14		48.8	
15	1.27 (2H, m)	35.7	C-13, C-17
16	1.28 (2H, m)	25.1	C-13, C-17, C-20
17	1.60 (1H, m)	52.2	C-13, C-14
18	0.98 (3H, br s)	18.2	C-12, C-13, C-14, C-17
19	0.71 (1H, d, <i>J</i> = 4.3 Hz) 0.46 (1H, d, <i>J</i> = 4.3 Hz)	30.2	C-1, C-5, C-8, C-9, C-11
20	1.68 (1H, m)	35.8	C-13, C-14, C-17, C-18, C-22, C-23
21	0.88 (3H, d, <i>J</i> = 6.4 Hz)	18.2	C-17, C-20, C-22
22	1.52 (1H, m), 1.03 (1H, m)	36.3	C-20, C-23
23	2.03 (1H, m), 1.86 (1H, m)	24.9	C-17, C-22, C-24, C-25
24	5.10 (1H, m)	125.2	C-23, C-27
25		130.9	
26	1.68 (3H, m)	25.7	C-23, C-24, C-25
27	1.60 (3H, m)	17.6	C-23, C-24, C-25
28	5.09 (1H, br s) 5.07 (1H, br s)	110.4	C-5, C-29
29	4.13 (2H, br s)	64.7	C-4, C-28
30	0.92 (3H, br s)	19.3	C-8, C-13, C-14
OMe	3.64 (3H, s)	51.6	C-3

Table 5. NMR data of compound **69** in CDCl₃.

Position	¹ H	¹³ C	HMBC
1	1.68 (1H, m), 1.36 (1H, m)	28.9	C-2, C-3, C-15, C-19
2	2.51 (1H, m), 2.28 (1H, m)	31.6	C-1, C-3, C-19
3		174.5	
4		152.4	
5	2.50 (1H, m)	42.1	C-4, C-6, C-7, C-28, C-29
6	2.14 (1H, m), 1.00 (1H, m)	28.9	C-5, C-7, C-8, C-9
7	1.33 (1H, m), 1.08 (1H, m)	25.3	C-5, C-8, C-9
8	1.53 (1H, m)	47.9	C-9, C-13, C-14, C-15, C-19, C-30
9		21.8	
10		28.3	
11	2.12 (1H, m), 1.21 (1H, m)	26.9	C-9, C-12, C-13, C-14, C-19
12	1.66 (2H, m)	33.0	C-9, C-13, C-17, C-18
13		45.1	
14		48.9	
15	1.30 (2H, m)	35.6	C-13, C-17
16	1.92 (1H, m), 1.30 (1H, m)	28.1	C-13, C-17, C-15
17	1.66 (1H, m)	52.1	C-13, C-14
18	0.97 (3H, s)	18.0	C-12, C-13, C-14, C-17
19	0.72 (1H, d, <i>J</i> = 4.3 Hz) 0.48 (1H, d, <i>J</i> = 4.3 Hz)	30.2	C-5, C-6, C-8, C-9
20	1.49 (1H, m)	36.0	C-13, C-14, C-17, C-18
21	0.93 (3H, br s)	18.0	C-17, C-20
22	1.58 (1H, m), 1.21 (1H, m)	34.7	C-20
23	2.40 (1H, m), 2.27 (1H, m)	26.0	C-17, C-24, C-25
24	6.49 (1H, t, <i>J</i> = 7.0 Hz)	155.6	C-23, C-27
25		139.1	
26	9.39 (1H, s)	195.5	C-24, C-25, C-27
27	1.75 (3H, s)	9.2	C-24, C-25, C-26
28	5.10 (2H, br s)	110.5	C-5, C-29
29	4.13 (2H, br s)	64.7	C-4, C-28
30	0.93 (3H, s)	19.4	C-13, C-14
OMe	3.64 (3H, s)	51.6	C-3

Table 6. NMR data of compound **70** in CDCl₃.

Position	¹ H	¹³ C	HMBC
1	2.06 (1H, m), 1.37 (1H, m)	28.8	C-2, C-3, C-5, C-9, C-19
2	2.54 (1H, m), 2.30 (1H, m)	31.3	C-1, C-3, C-10
3		179.7	
4		149.5	
5	2.42 (1H, m)	45.9	C-4, C-6, C-7, 19.7, C-28, C-29
6	1.47 (1H, m), 1.08 (1H, m)	27.7	C-5, C-7, C-8, C-9, C-10
7	1.35 (1H, m), 1.08 (1H, m)	25.0	C-5, C-9, C-10
8	1.60 (1H, m)	47.7	C-9, C-10, C-11, C-14
9		21.4	
10		27.0	
11	2.09 (1H, m), 1.26 (1H, m)	26.9	C-9, C-10, C-12, C-13, C-19
12	1.65 (2H, m)	33.0	C-9, C-11, C-14, C-17, C-18
13		45.1	
14		48.9	
15	1.37 (1H, m), 1.28 (1H, m)	35.9	C-8, C-13, C-14, C-16, C-17, C-30
16	1.89 (1H, m), 1.28 (1H, m)	28.1	C-8, C-13, C-14, C-15, C-17, C-30
17	1.60 (1H, m)	52.2	C-14
18	0.95 (3H, br s)	18.0	C-12, C-13, C-14, C-17
19	0.73 (1H, d, <i>J</i> = 4.1 Hz) 0.40 (1H, d, <i>J</i> = 4.1 Hz)	30.0	C-1, C-5, C-8, C-9, C-10, C-11
20	1.28 (1H, m)	35.6	C-17
21	0.88 (3H, d, <i>J</i> = 6.3 Hz)	18.2	C-17, C-20, C-22, C-23
22	1.48 (1H, m), 1.05 (1H, m)	36.3	C-23
23	2.05 (1H, m), 1.89 (1H, m)	24.9	C-20, C-22, C-24, C-25
24	5.10 (1H, t, <i>J</i> = 7.1 Hz)	125.2	C-23, C-27
25		130.9	
26	1.68 (3H, br s)	25.7	C-24, C-25, C-27
27	1.60 (3H, br s)	17.6	C-24, C-25, C-26
28	4.81 (1H, br s) 4.73 (1H, br s)	111.5	C-5, C-29
29	1.68 (3H, br s)	19.7	C-4, C-5, C-27, C-28
30	1.68 (3H, br s)	19.3	C-8, C-13, C-14, C-15

Table 7. ^1H and ^{13}C NMR data (CDCl_3) of coronalolide methyl ester and **10**.

Position	Coronalolide methyl ester		Compound 10	
	^1H	^{13}C	^1H	^{13}C
1	2.25 (1H, m), 1.61 (1H, m)	30.8	2.23 (1H, m), 1.58 (1H, m)	30.9
2	2.55 (1H, m), 2.45 (1H, m)	31.1	2.50 (1H, m), 2.41 (1H, m)	31.2
3		173.3		173.4
4		139.0		139.1
5	3.23 (1H, br d, $J = 8.0$ Hz)	38.9	3.23 (1H, br d, $J = 8.3$ Hz)	39.0
6	4.74 (1H, td, $J = 8.0, 6.5$ Hz)	74.3	4.73 (1H, dd, $J = 8.3, 6.0$ Hz)	74.4
7	1.77 (1H, m), 1.55 (1H, m)	27.1	1.73 (1H, m), 1.52 (1H, m)	27.2
8	2.12 (1H, t, $J = 5.5$ Hz)	38.2	2.10 (1H, t, $J = 5.7$ Hz)	38.3
9		25.0		25.1
10		28.1		28.2
11	1.6-1.7 (2H, m)	26.4	1.5-1.6 (1H, m)	26.5
12	1.6-1.7 (2H, m)	32.9	1.67 (1H, m), 1.60 (1H, m)	33.0
13		45.7		45.7
14		48.6		48.7
15	1.37 (2H, m)	34.7	1.33 (2H, m)	34.7
16	1.95 (1H, m), 1.37 (1H, m)	27.7	1.93 (1H, m), 1.33 (1H, m)	27.8
17	1.65 (1H, m)	51.2	1.62 (1H, m)	51.3
18	0.95 (3H, s)	15.9	0.92 (3H, m)	16.0
19	0.43 (1H, d, $J = 5.5$ Hz) 0.19 (1H, d, $J = 5.5$ Hz)	23.1	0.40 (1H, d, $J = 5.2$ Hz) 0.17 (1H, d, $J = 5.2$ Hz)	23.2
20	1.48 (1H, m)	35.9	1.48 (1H, m)	36.0
21	0.94 (3H, m)	18.2	0.91 (3H, m)	18.2
22	1.63 (1H, m), 1.24 (1H, m)	34.7	1.60 (1H, m), 1.22 (1H, m)	34.8
23	2.43 (1H, m), 2.32 (1H, m)	25.9	2.33 (1H, m), 2.28 (1H, m)	26.0
24	6.49 (1H, tq, $J = 6.5, 1.5$ Hz)	155.2	6.47 (1H, t, $J = 7.5$ Hz)	155.3
25		139.0		139.1
26	9.40 (1H, s)	195.2	9.37 (1H, s)	195.4
27	1.76 (3H, br s)	9.1	1.73 (3H, br s)	9.2
28	6.34 (1H, d, $J = 2.5$ Hz) 5.75 (1H, d, $J = 2.3$ Hz)	123.0	6.31 (1H, d, $J = 1.9$ Hz) 5.72 (1H, d, $J = 1.8$ Hz)	123.1
29		170.6		170.7
30	0.92 (3H, s)	20.0	0.90 (3H, s)	20.1
OMe	3.69 (3H, s)	51.7	3.67 (3H, s)	51.8

Table 8. ^1H and ^{13}C NMR data (CDCl_3) of coronalolide and compound **11**.

Position	Coronalolide		Compound 11	
	^1H	^{13}C	^1H	^{13}C
1		30.7		30.7
2		31.2		31.1
3		178.1		178.1
4		139.1		139.1
5	3.25 (1H, br d, $J = 8.4$ Hz)	39.0	3.23 (1H, d, $J = 8.1$ Hz)	39.0
6	4.77 (1H, td, $J = 8.4, 6.7$ Hz)	74.4	4.75 (1H, dd, $J = 8.1, 7.5$ Hz)	74.5
7		27.2		27.2
8		38.2		38.3
9		25.1		25.1
10		28.1		28.1
11		26.5		26.5
12		33.0		33.0
13		45.7		45.7
14		48.6		48.6
15		34.8		34.7
16		27.8		27.8
17		51.4		51.4
18	0.95 (3H, s)	16.0	0.94 (3H, br s)	16.0
19	0.44 (1H, d, $J = 5.4$ Hz) 0.19 (1H, d, $J = 5.4$ Hz)	23.2	0.43 (1H, d, $J = 5.2$ Hz) 0.19 (1H, d, $J = 5.2$ Hz)	23.2
20		36.0		36.0
21	0.94 (3H, d, $J = 6.5$ Hz)	18.2	0.94 (3H, br s)	18.3
22		34.8		34.8
23		26.0		26.1
24	6.51 (1H, bt, $J = 6.2$ Hz)	155.4	6.49 (1H, t, $J = 7.2$ Hz)	155.4
25		139.1		139.1
26	9.40 (1H, s)	195.5	9.39 (1H, s)	195.5
27	1.76 (3H, br s)	9.2	1.75 (3H, s)	9.2
28	6.35 (1H, d, $J = 2.2$ Hz) 5.75 (1H, d, $J = 2.0$ Hz)	123.1	6.33 (1H, br s) 5.74 (1H, br s)	123.2
29		170.7		170.7
30	0.92 (3H, s)	20.1	0.91 (3H, s)	20.1

Table 9. ^1H and ^{13}C NMR data (CDCl_3) of secaubryenol and compound **58**.

Position	Secaubryenol		Compound 58	
	^1H	^{13}C	^1H	^{13}C
1	2.12 (1H, m), 1.36 (1H, m)	28.7	2.13 (1H, m), 1.37 (1H, m)	28.7
2	2.51 (1H, m), 2.30 (1H, m)	31.5	2.52 (1H, m), 2.32 (1H, m)	31.6
3		179.1		179.6
4		152.1		152.1
5	2.51 (1H, m)	41.9	2.50 (1H, m)	42.0
6	1.69 (1H, m), 0.99 (1H, m)	28.9	1.68 (1H, m), 1.02 (1H, m)	28.9
7	1.28 (1H, m), 1.07 (1H, m)	25.2	1.28 (1H, m), 1.08 (1H, m)	25.2
8	1.55 (1H, m)	47.9	1.55 (1H, m)	47.9
9		21.8		21.8
10		27.3		27.3
11	2.10 (1H, m), 1.22 (1H, m)	26.9	2.07 (2H, m)	27.0
12	1.65 (2H, m)	32.9	1.65 (2H, m)	33.0
13		45.0		45.1
14		48.8		48.8
15	1.29 (2H, m)	35.6	1.28 (2H, m)	35.7
16	1.91 (1H, m), 1.30 (1H, m)	28.1	1.90 (1H, m), 1.33 (1H, m)	28.1
17	1.60 (1H, m)	52.2	1.50 (1H, m)	52.2
18	0.97 (3H, s)	18.1	0.96 (3H, s)	18.2
19	0.73 (1H, d, $J = 4.5$ Hz) 0.49 (1H, d, $J = 4.5$ Hz)	30.2	0.73 (1H, d, $J = 4.2$ Hz) 0.48 (1H, d, $J = 4.2$ Hz)	30.3
20	1.40 (1H, m)	35.8	1.39 (1H, m)	35.9
21	0.88 (3H, s)	18.2	0.88 (3H, d, $J = 6.3$ Hz)	18.2
22	1.40 (1H, m), 1.05 (1H, m)	36.2	1.44 (1H, m), 1.08 (1H, m)	36.3
23	2.03 (1H, m), 1.86 (1H, m)	24.9	2.03 (1H, m), 1.85 (1H, m)	24.9
24	5.10 (1H, m)	125.2	5.08 (1H, m)	125.2
25		130.9		130.9
26	1.70 (3H, s)	25.7	1.68 (3H, s)	25.7
27	1.62 (3H, s)	17.6	1.60 (3H, s)	17.6
28	5.10 (2H, m)	110.6	5.10 (2H, m)	110.6
29	4.07 (2H, br s)	64.6	4.14 (2H, br s)	64.6
30	0.93 (3H, s)	19.3	0.92 (3H, s)	19.4

2.4.2 Isolation and characterization of cycloartane triterpenes from apical buds of *G. sootepensis* (Khon-kaen province)

The MeOH extract of fresh apical buds of *G. sootepensis* was partitioned between EtOAc and water to afford an EtOAc extract, which was subjected to silica gel column chromatography using EtOAc-hexane mixtures of increasing polarity as eluent. Further purification by repeated normal column chromatography gave two new 3,4-*seco*-cycloartanes (**71-72**) and four known compounds, sootepin C (**68**), sootepin A (**66**), coronalolide methyl ester (**10**), and coronalolic acid (**12**). All structures of the known compounds were determined by comparison of their NMR spectroscopic data with those in the literature.

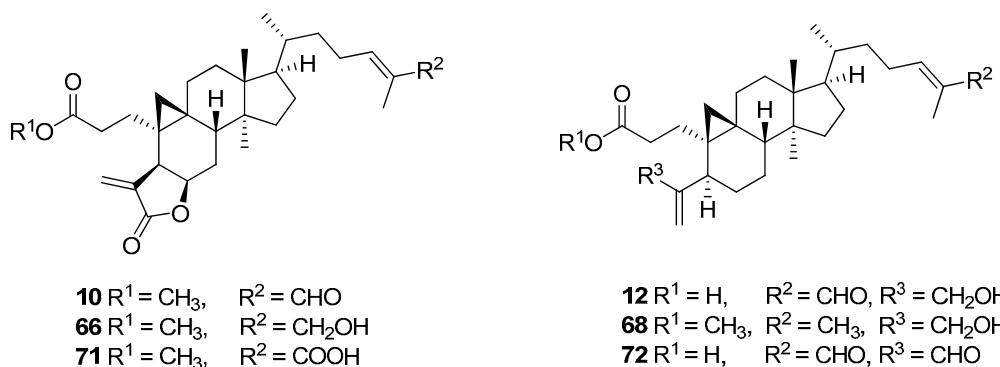


Figure 17. Cycloartane triterpenes from apical buds of *G. sootepensis* (Kampangpech province).

Sootepin F (**71**) was obtained as a white amorphous solid, $[\alpha]_D^{27} +87.0$ (c 0.2, MeOH), UV (MeOH) λ_{\max} (log ϵ) 240 (3.00). Its molecular formula was determined as C₃₁H₄₅O₆ from the HRESIMS ion at m/z 535.2975 [M+Na]⁺ (Calcd. 535.3036). The ¹³C and HSQC experiment revealed the presence of 31 nonequivalent carbons including three carbonyl carbon (δ_C 170.8, 173.0 and 173.5), four sp² carbons [two quaternary C (δ_C 126.7 and 139.1), one CH (δ_C 145.7), and one CH₂ (δ_C 123.2)], a sp³ oxygenated methine (δ_C 74.5), a methoxy carbon (δ_C 51.9), ten sp³ methylene (δ_C 23.0, 25.9, 26.5, 27.2, 27.7, 31.0, 31.2, 33.0, 34.7, and 34.8), four sp³ methine carbon (δ_C 36.0, 38.3, 39.0 and 51.3), four sp³ quaternary carbon (δ_C 25.1, 28.2, 45.7, and 48.7), and four methyl carbons (δ_C 12.0, 15.9, 18.3, and 20.1). The ¹H NMR spectrum (Table 10) showed a pair of doublets at δ_H 0.17 and 0.42 ($J =$

5.1 Hz), characteristic of the C-19 methylene protons of cyclopropane ring of a cycloartane triterpene. A pair of doublets at δ_H 5.74 and 6.33 ($J = 1.5$ Hz) was ascribed to H-28a and H-28b in the exocyclic methylene γ -lactone ring, and signals of the β - and γ -methine protons of the lactone ring appeared at δ_H 3.23 (H-5) and 4.74 (H-6), respectively. The above data suggested that **71** is a 3,4-*seco*-cycloartane triterpenoid. The NMR data of **71** were almost the same as those of coronalolide methyl ester (**10**), except for the absence of an aldehyde group at C-26 in coronalolide methyl ester, and instead of carboxylic acid group in **71**. This was confirmed by the HMBC correlation of the methyl carbon at δ_H 1.83 to the carbonyl carbon at δ_C 173.0, suggesting that **71** has the carboxylic acid group at C-26.

The relative stereochemistry of **71** was elucidated by NOESY experiment (Figure 18). Observation of a strong NOESY cross-peak between H-5 and H-6 permitted the assignment of a relative 5,6-*cis*-configuration. Consistent with this, the cross-peaks between H-8 and H₃-18, H-8 and H-19b, H-6 and H₃-30, H-17 and H₃-30, and H-17 and H₃-21. There were in good agreement with the relative configurations at C-5, C-6, C-8, C-9, C-10, C-13, C-14, and C-17 long-established for the cycloartane core.

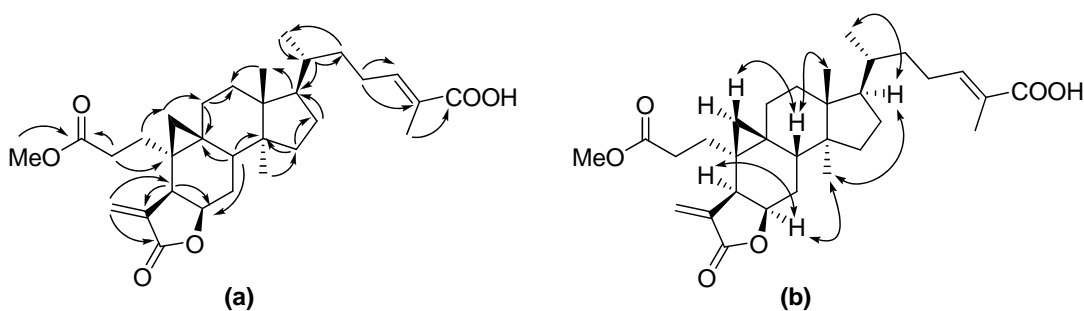


Figure 18. Key HMBC (a) and NOE (b) correlations of compound **71**.

Sootepin G (**72**) was isolated as colorless oil, $[\alpha]_D^{25} +54.0$ (c 0.2, MeOH), UV (MeOH) λ_{\max} (log ϵ) 245 (2.98). The molecular formula of **72** was determined to be C₃₀H₄₄O₄ from the HRESIMS and NMR data. The ¹³C NMR and HSQC spectra displayed three carbonyl compound (δ_C 179.4, 195.3, and 195.6), four sp² carbons [two quaternary C (δ_C 139.1 and 153.8), one CH (δ_C 155.7), and one CH₂

(δ_C 135.3)], eleven sp^3 methylenes carbons (δ_C 25.1, 26.1, 27.9, 28.1, 28.5, 29.0, 29.8, 31.5, 32.9, 34.7, and 36.0), four sp^3 methine carbon (δ_C 33.9, 35.7, 48.1, and 52.2), four sp^3 quaternary carbon (δ_C 22.6, 26.8, 45.1, and 48.8), and four methyl carbons (δ_C 9.2, 18.0, 18.3, and 19.4). The 1H NMR of **72** showed the two singlet aldehyde proton at δ_H 9.38 and 9.51, the HMBC correlation between δ_H 9.38 with C-24 and C-27, and δ_H 9.51 with C-5 and C-28, suggesting that the aldehyde group are attached at C-26 and C-29, respectively. Additionally, the NMR data of **72** closely related to coronalolic acid (**12**), except for the presence of an aldehyde group at C-26 in **72**. Thus, the structure of this derivative was depicted as **72**. The same NOESY correlations of H-5/H₃-30, H-8/H₃-18, H-8/H-19b, H-17/H₃-21, and H-17/H₃-30 as for coronalolic acid gave evidence for the relative configuration of **72** at C-5, C-8, C-9, C-10, C-13, C-14, C-17, and C-20 (Figure 19).

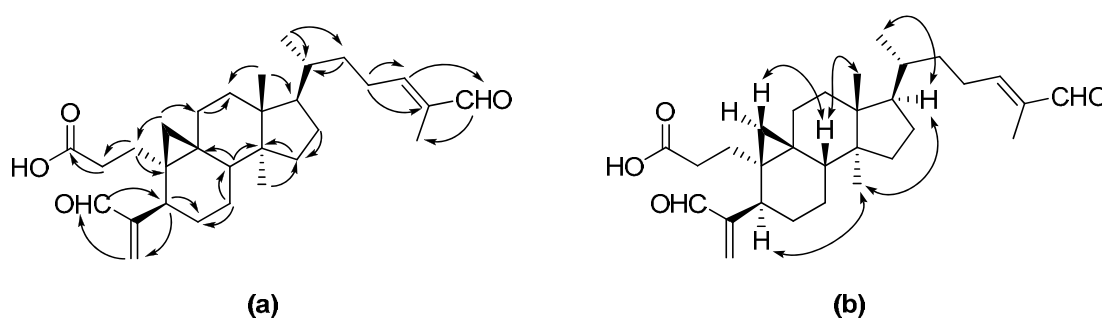


Figure 19. Key HMBC (a) and NOE (b) correlations of compound **72**.

The 1H NMR spectrum of compound **12** in $CDCl_3$ (Table 12) displayed; a pair of doublets at δ_H 0.48 and 0.72 (1H each, d, $J = 4.1$ Hz), an aldehyde proton at δ_H 9.38 (1H, s), a pair of broad singlet at δ_H 5.10 and 5.08 (1H each, br s), an olefinic proton at δ_H 6.49 (1H, t, $J = 7.3$ Hz), an oxygenated methylene proton at δ_H 4.13 (2H, br s), three tertiary methyl protons at δ_H 0.93, 0.96, and 1.74 (3H each, s), and a secondary methyl proton at δ_H 0.92 (3H, br s). Based on the spectroscopic data above, compound **12** was identified to be a coronalolic acid. The structure of this compound was finally confirmed by comparison of the spectral data with those previously reported by Silva and co-workers in 1999 [8].

Table 10. NMR data of compound **71** in CDCl₃.

Position	¹ H	¹³ C	HMBC
1	2.28 (1H, m), 1.60 (1H, m)	31.0	C-2, C-3, C-5, C-10, C-19
2	2.49 (1H, m), 2.42 (1H, m)	31.2	C-3, C-10
3		173.5	
4		139.1	
5	3.23 (1H, d, <i>J</i> = 8.3 Hz)	39.0	C-1, C-4, C-6, C-10, C-19, C-28, C-29
6	4.74 (1H, dd, <i>J</i> = 14.5, 7.7 Hz)	74.5	C-8, C-10, C-29
7	1.76 (1H, m), 1.51 (1H, m)	27.2	C-5, C-6, C-9, C-10
8	2.11 (1H, m)	38.3	C-6, C-9, C-11, C-14, C-30
9		25.1	
10		28.2	
11	1.66 (2H, m)	26.5	C-8, C-9, C-10, C-12, C-13
12	1.61 (2H, m)	33.0	C-18
13		45.7	
14		48.7	
15	1.34 (2H, m)	34.8	C-13, C-14, C-16, C-17, C-30
16	1.92 (1H, m), 1.33 (1H, m)	27.7	C-13, C-14, C-15, C-17
17	1.60 (1H, m)	51.3	C-18
18	0.93 (3H, m)	15.9	C-12, C-13, C-14, C-17
19	0.42 (1H, d, <i>J</i> = 5.1 Hz) 0.17 (1H, d, <i>J</i> = 5.1 Hz)	23.0	C-1, C-5, C-9, C-10, C-11
20	1.44 (1H, m)	36.0	C-17, C-23
21	0.94 (3H, m)	18.3	C-22
22	1.56 (1H, m), 1.17 (1H, m)	34.7	C-21, C-23, C-24
23	2.24 (1H, m), 2.10 (1H, m)	25.9	C-24, C-25
24	6.89 (1H, t, <i>J</i> = 7.1 Hz)	145.7	C-22, C-23, C-25, C-26, C-27
25		126.7	
26		173.0	
27	1.83 (3H, s)	12.0	C-24, C-25, C-26
28	6.33 (1H, d, <i>J</i> = 1.5 Hz) 5.74 (1H, d, <i>J</i> = 1.5 Hz)	123.2	C-4, C-5, C-29
29		170.8	
30	0.89 (3H, m)	20.1	C-13, C-14
OMe	3.69 (3H, s)	51.9	C-3

Table 11. NMR data of compound **72** in CDCl₃.

Position	¹ H	¹³ C	HMBC
1	1.90 (1H, m), 1.43 (1H, m)	28.5	C-2, C-3, C-15, C-9
2	2.59 (1H, m), 2.25 (1H, m)	31.5	C-3
3		179.4	
4		153.8	
5	2.99 (1H, m)	33.9	C-4, C-6, C-19, C-28, C-29
6	1.66 (1H, m), 0.78 (1H, m)	29.0	C-5, C-7, C-8, C-9, C-10
7	1.30 (1H, m), 1.13 (1H, m)	25.1	C-5, C-10
8	1.52 (1H, dd, <i>J</i> = 4.0 Hz)	48.1	C-6, C-7, C-19, C-14, C-30
9		22.6	
10		26.8	
11	1.25 (2H, m)	27.9	C-8, C-9, C-18
12	1.66 (2H, m)	32.9	C-9, C-13, C-14, C-18
13		45.1	
14		48.8	
15	1.30 (2H, m)	36.0	C-14, C-30
16	1.90 (1H, m), 1.30 (1H, m)	28.1	C-15
17	1.66 (1H, m)	52.2	C-13, C-14
18	0.97 (3H, s)	18.3	C-17
19	0.75 (1H, d, <i>J</i> = 3.9 Hz) 0.49 (1H, d, <i>J</i> = 3.9 Hz)	29.8	C-1, C-5, C-8, C-9, C-10
20	1.30 (1H, m)	35.7	
21	0.91 (3H, m)	18.0	C-17, C-20, C-22
22	1.60 (1H, m), 1.23 (1H, m)	34.7	C-20
23	2.39 (1H, m), 2.27 (1H, m)	26.1	C-22, C-24, C-25
24	6.47 (1H, m)	155.7	C-23, C-27
25		139.1	
26	9.38 (1H, s)	195.6	C-24, C-25, C-27
27	1.74 (3H, s)	9.2	
28	6.47 (1H, br s) 6.06 (1H, br s)	135.3	C-4, C-5, C-29
29	9.51 (1H, s)	195.3	C-4, C-5, C-28
30	0.97 (3H, s)	19.4	C-13, C-14

Table 12. ^1H and ^{13}C NMR data (CDCl_3) of coronalolic acid and compound **12**.

Position	coronalolic acid		Compound 12	
	^1H	^{13}C	^1H	^{13}C
1		28.1		28.1
2		30.3		30.3
3		179.3		179.1
4		152.1		152.1
5		41.9		41.9
6		28.7		28.7
7		25.2		25.2
8		47.9		47.9
9		21.8		21.8
10		27.4		27.3
11		26.9		26.9
12		33.0		33.0
13		45.1		45.1
14		48.9		48.8
15		35.6		35.6
16		28.1		28.1
17		52.1		52.1
18	0.98 (3H, s)	18.1	0.96 (3H, s)	18.2
19	0.74 (1H, d, $J = 5.0$ Hz) 0.50 (1H, d, $J = 5.0$ Hz)	30.3	0.72 (1H, d, $J = 4.1$ Hz) 0.48 (1H, d, $J = 4.1$ Hz)	30.3
20		36.0		35.9
21	0.93 (3H, d, $J = 6.5$ Hz)	18.2	0.92 (3H, br s)	18.2
22		34.7		34.7
23		26.1		26.1
24	6.51 (1H, br t, $J = 6.8$ Hz)	155.7	6.49 (1H, t, $J = 7.3$ Hz)	155.8
25		139.2		139.1
26	9.40 (1H, s)	196.0	9.38 (1H, s)	195.6
27	1.78 (3H, br s)	9.2	1.74 (3H, s)	9.2
28	5.11 (1H, s) 5.09 (1H, s)	110.6	5.10 (1H, br s) 5.08 (1H, br s)	110.6
29	4.12 (3H, br s)	64.7	4.13 (2H, br s)	64.7
30	0.94 (3H, s)	19.4	0.93 (3H, s)	19.4

2.4.3 Isolation and characterization of cycloartane triterpenes from *G. tubifera* exudate

The exudate collected on the aerial parts of *G. tubifera* was dissolved in a 1:1 mixture of CH₂Cl₂ and MeOH, which was then subjected to silica gel CC using EtOAc-hexane mixtures of increasing polarity as eluent. Further purification by repeated normal CC gave four new 3,4-*seco*-cycloartane triterpenes (**73-76**) and the known compound secaubryenol (**58**).

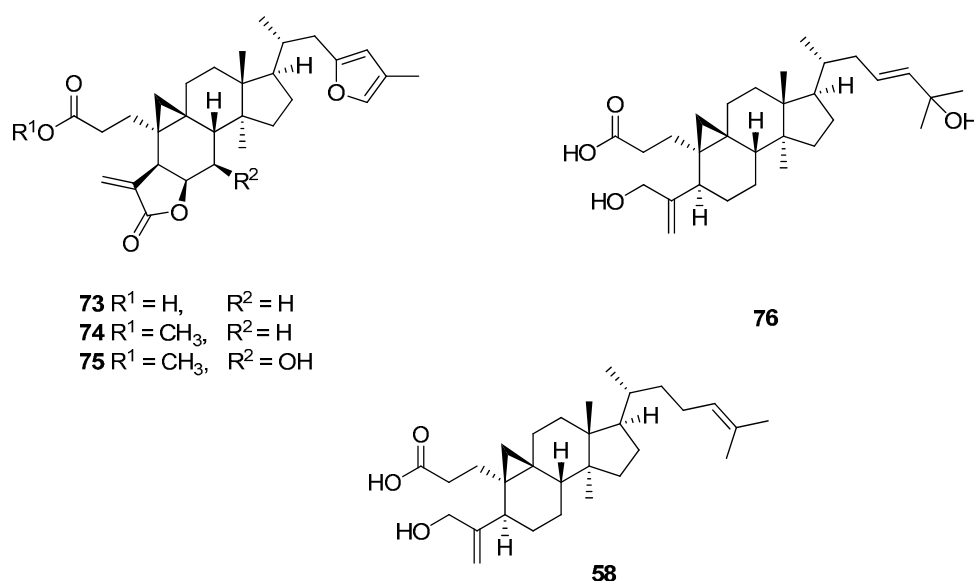


Figure 20. Cycloartane triterpenes from the exudate of *G. tubifera*.

Gardenoin A (**73**) was obtained as a white amorphous solid m.p. 92–93 °C; $[\alpha]_D^{20} +111$ (*c* 0.1, MeOH); UV (MeOH) λ_{\max} (log ϵ) 215 (4.07) nm; IR (KBr) ν_{\max} 3350, 2918, 2851, 1732, 1457, 1379, 1270, 1178, 992 cm⁻¹. Its molecular formula was determined as C₃₀H₄₀O₅ from the HRESIMS ion at *m/z* 503.2771 [M + Na]⁺ (calcd 503.2773), which indicated 11 degrees of unsaturation. The IR spectrum showed absorption bands for hydroxy (3350 cm⁻¹) and carbonyl (1732 cm⁻¹) groups. Analysis of ¹³C and HSQC spectra revealed the presence of 30 nonequivalent carbons including two carbonyl carbons (δ_C 177.9 and 170.7), two *sp*² oxygenated carbons [one quaternary C (δ_C 155.2) and one CH (δ_C 137.4)], four *sp*² carbons [two quaternary C (δ_C 139.1 and 120.4), one CH (δ_C 109.1), and one CH₂ (δ_C 123.2)], one

sp^3 oxygenated methine (δ_C 74.4), nine sp^3 methylenes (δ_C 35.0, 34.8, 32.8, 31.0, 30.7, 27.8, 27.2, 26.5, and 23.0), four sp^3 methines (δ_C 51.3, 39.0, 38.3, and 36.3), four quaternary carbons (δ_C 48.7, 45.8, 28.1, and 25.1), and four methyl carbons (δ_C 20.1, 18.8, 15.9, and 9.8). The ^1H NMR spectrum (Table 13) displayed a pair of doublets at δ_H 0.18 and 0.44 ($J = 5.3$ Hz), characteristic of the C-19 methylene protons of the cyclopropane ring of a cycloartane triterpene. A pair of doublets at δ_H 5.74 and 6.34 ($J = 1.6$ Hz) was ascribed to H-28a and H-28b in the exocyclic methylene γ -lactone ring, and signals of the β - and γ -methine protons of the lactone ring appeared at δ_H 3.24 (H-5) and 4.76 (H-6), respectively. An observed HMBC correlation from H-6 to C-29 (δ_C 170.7) (Figure 21) was used to confirm the lactonization of C-4 to C-6. These data suggested that **73** is a 3,4-*seco*-cycloartane triterpenoid. Additionally, the NMR spectra indicated the presence of a disubstituted furan ring (δ_H 5.86 and 7.06; δ_C 155.2, 137.4, 120.4, and 109.1). On the basis of HMBC data, the cross-peak observed from Me-27 to C-25 and C-24 and from H2-22 to C-23 and C-24 allowed H₂C-22 and Me-27 to be connected to C-23 and C-25 of the furan ring, respectively. These results, together with the lack of coupling between the two hydrogen atoms of the furan at δ_H 5.86 and 7.06, demonstrated that the furan ring is 2,4-disubstituted. The above data were closely related to those previously reported for dikamaliartane E [29], with the only difference being the absence of the hydroxy group at C-7 in dikamaliartane E.

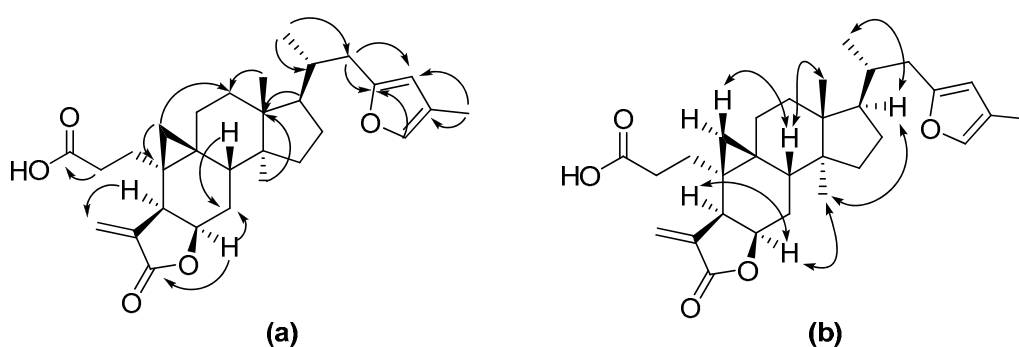


Figure 21. Key HMBC (a) and NOE (b) correlations of compound **73**.

The relative stereochemistry of **73** was elucidated by NOESY experiment (Figure 21). The 5,6-*cis*-configuration has been found to be exclusively β in all known 3,4-*seco*-cycloartanes. Consistent with this, for compound **73**, the cross-

peaks in the NOESY spectrum from H-5 to H-6, H-6 to Me-30, Me-30 to H-17, and H-17 to Me-21 indicated an α -orientation of these protons. Additionally, NOESY correlations of H-8 with H-19 β and Me-18, and Me-18 with H-20, suggested that H-8, Me-18, and H-20 are in a β -orientation. These were in good agreement with the relative configurations at C-5, C-6, C-8, C-9, C-10, C-13, C-14, C-17, and C-20, long-established for the cycloartane core.

Gardenoin B (**74**) was isolated as a white amorphous solid m.p. 82–83 °C; $[\alpha]_D^{20} +41$ (*c* 0.1, MeOH); UV (MeOH) λ_{\max} ($\log \epsilon$) 210 (3.12) nm; IR (KBr) ν_{\max} 2918, 2850, 1762, 1737, 1464, 1437, 1298, 1278, 1172, 942 cm^{-1} with the molecular formula $\text{C}_{31}\text{H}_{42}\text{O}_5$ as determined by the HRESIMS ion at m/z 517.2929 [$\text{M} + \text{Na}$] $^+$ (calcd 517.2930). In the ^1H NMR spectrum, the typical signals for a cyclopropane methylene proton appeared as two doublets at δ_H 0.16 and 0.42 ($J = 5.3$ Hz), and its NMR data were almost the same those of **73**, except for the presence of a methoxy group at C-3 in **74**. This was confirmed by the HMBC correlation of the singlet methoxy protons at δ_H 3.69 to the carbonyl carbon at δ_C 173.5, suggesting that **74** is the methyl ester derivative of **73**. The relative configuration was determined to be the same as **73** from the NOESY spectrum.

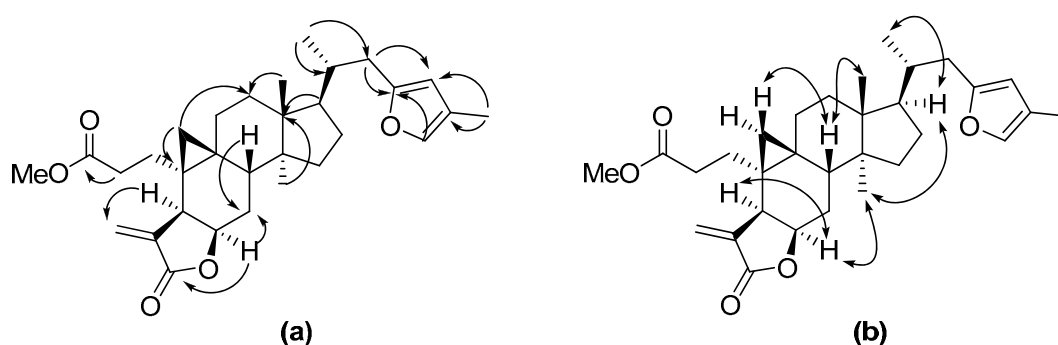


Figure 22. Key HMBC (a) and NOE (b) correlations of compound **74**.

Gardenoin C (**75**) was isolated as a white amorphous solid, m.p. 98–100 °C; $[\alpha]_D^{20} +134$ (*c* 0.1, MeOH); UV (MeOH) λ_{\max} ($\log \epsilon$) 210 (4.04) nm; IR (KBr) ν_{\max} 3456, 2934, 2875, 1712, 1654, 1458, 1376, 1272, 1143, 941 cm^{-1} with an evaluated molecular formula of $\text{C}_{31}\text{H}_{42}\text{O}_6$ by the HRESIMS ion at m/z 533.2878 [$\text{M} + \text{Na}$] $^+$ (calcd 533.2879). Comparison of the ^1H and ^{13}C NMR spectra of **75** with those

of **74** revealed these to be very similar. Significant differences appeared only in the resonances corresponding to position C-7. The replacement in **74** of the two multiplets (δ_H 0.16 and 0.42) in **74** by a double doublet at δ_H 3.44 ($J = 3.8, 4.9$ Hz), coupled in the HSQC spectrum to a newly appearing oxymethine resonance at δ_C 69.1, indicated the occurrence of a hydroxy group at C-7. This was also confirmed by the HMBC correlations (Figure 23) of H-7/C-5, H-7/C-8, and H-8/C-7. The similar NOESY correlations between **75** (Figure 23) and **73** (Figure 21) were indicative of the same stereochemistry of the core skeleton of **75** as compared to **73**. The key NOE cross-peak for **75** between H-7 and H-6 and between H-7 and Me-30 confirmed the α -orientation of H-7.

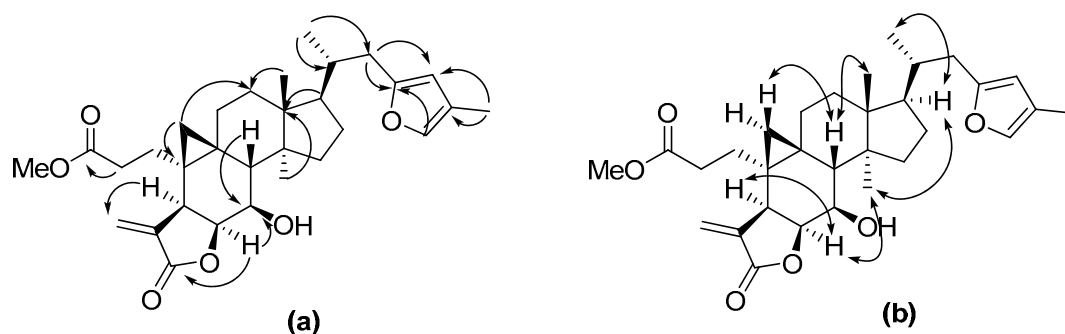


Figure 23. Key HMBC (a) and NOE (b) correlations of compound **75**.

Gardenoin D (**76**) was isolated as a white, amorphous solid, m.p. 91–92 °C; $[\alpha]_D^{20} +113$ (c 0.1, MeOH); UV (MeOH) λ_{\max} ($\log \epsilon$) 210 (4.02) nm; IR (KBr) ν_{\max} 3449, 2939, 2871, 1709, 1647, 1457, 1377, 1278, 1169, 1025, 899 cm^{-1} and its molecular formula was deduced as $\text{C}_{30}\text{H}_{48}\text{O}_4$ from the HRESIMS data (m/z 495.3452 $[\text{M} + \text{Na}]^+$, calcd 495.3450), suggesting seven degrees of unsaturation. The ^1H NMR spectrum displayed the typical signals associated with a 3,4-*seco*-cycloartane triterpene, including a characteristic pair of doublets at δ_H 0.47 and 0.71 ($J = 3.9$ Hz), attributable to the C-19 methylene protons in the cyclopropane ring, two tertiary methyl singlets at δ_H 0.91 and 0.96, and one secondary methyl doublet at δ_H 0.85 ($J = 6.3$ Hz). Allylic coupling observed in the COSY spectrum between a two-proton broad singlet at δ_H 4.12, accounting for a primary alcoholic group and a two-proton broad singlet of a terminal alkene at δ_H 5.08, was suggestive of the structure of

a 29-hydroxy-3,4-*seco*-cycloartane. Both ^1H and ^{13}C NMR signals of **76** were very similar to those of *secaubrytriol*, with the marked differences being the appearance of a two-proton broad singlet due to a disubstituted alkene moiety between C-23 and C-24 at δ_{H} 5.59, coupled to the carbon resonances at δ_{C} 139.2 and 125.6 in the HSQC spectrum, and the absence of a hydroxy group attached to C-24 in *secaubrytriol*. Furthermore, the NMR signals attributable to the side chain of **76** closely resembled those previously described for *cucurbita-5,23(E)-diene-3 β ,7 β ,25-triol*, giving evidence for a (3*E*)-2-hydroxy-2-methylhept-3-en-6-yl unit attached at C-17. Therefore, the structure of **76** was established as shown. The same NOESY correlations of H-8/Me-18, H-8/H-19 β , H-17/Me-21, H-17/Me-30, and H-20/Me-18 as for *secaubryenol* (**58**) allowed the relative stereochemistry of **76** to be depicted as shown.

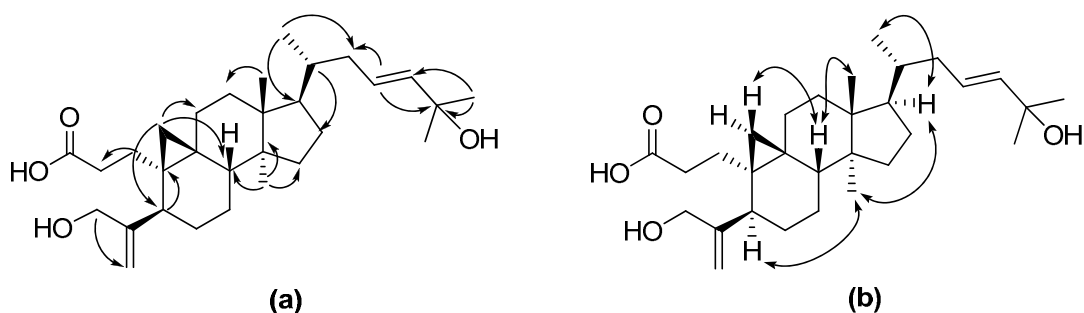


Figure 24. Key HMBC (a) and NOE (b) correlations of compound **76**.

Table 13. NMR data of compound **73** in CDCl₃.

Position	¹ H	¹³ C	HMBC
1	2.26 (1H, m), 1.61 (1H, m)	30.7	C-3, C-10
2	2.56 (1H, m), 2.46 (1H, m)	31.0	C-1, C-3
3		177.9	
4		139.1	
5	3.24 (1H, d, <i>J</i> = 8.1 Hz)	39.0	C-1, C-4, C-6, C-19, C-28, C-29
6	4.76 (1H, d, <i>J</i> = 7.8, 7.6 Hz)	74.4	C-5, C-29
7	1.81 (1H, m), 1.54 (1H, m)	27.2	C-5, C-6, C-9, C-14
8	2.24 (1H, m)	38.3	C-9, C-16
9		25.1	
10		28.1	
11	1.79 (1H, m), 1.55 (1H, m)	26.5	C-8, C-9
12	1.61 (2H, m)	32.8	C-8, C-13, C-14
13		45.8	
14		48.7	
15	1.37 (2H, m)	34.8	C-8, C-13, C-14
16	1.98 (1H, m), 1.37 (1H, m)	27.8	C-14
17	1.61 (1H, m)	51.3	C-14
18	0.96 (3H, s)	15.9	C-12, C-13, C-14, C-17
19	0.44 (1H, d, <i>J</i> = 5.3 Hz) 0.18 (1H, d, <i>J</i> = 5.3 Hz)	23.0	C-1, C-5, C-9, C-10
20	1.77 (1H, m)	36.3	C-22
21	0.86 (3H, d, <i>J</i> = 6.3 Hz)	18.8	C-17, C-20, C-22
22	2.15 (1H, m), 2.00 (1H, m)	35.0	C-17, C-20, C-21, C-23, C-24
23		155.2	
24	5.86 (1H, s)	109.1	C-23, C-25, C-26
25		120.4	
26	7.06 (1H, s)	137.4	C-23, C-24, C-25
27	1.99 (3H, s)	9.8	C-24, C-25, C-26
28	6.34 (1H, br s) 5.74 (1H, br s)	123.2	C-4, C-5, C-29
29		170.7	
30	0.91 (3H, s)	20.1	C-8, C-13, C-14, C-15

Table 14. NMR data of compound **74** in CDCl₃.

Position	¹ H	¹³ C	HMBC
1	2.04 (1H, m), 1.60 (1H, m)	30.9	
2	2.50 (1H, m), 2.46 (1H, m)	31.2	C-3, C-9, C-10
3		173.5	
4		139.1	
5	3.23 (1H, d, <i>J</i> = 8.3 Hz)	39.0	C-1, C-4, C-6, C-7, C-29
6	4.75 (1H, dd, <i>J</i> = 6.9, 8.0 Hz)	74.4	C-7, C-29
7	1.75 (1H, m), 1.54 (1H, m)	27.2	C-5, C-6, C-9
8	2.15 (1H, t, <i>J</i> = 5.5 Hz)	38.3	C-6, C-7, C-13, C-14, C-30
9		25.0	
10		28.2	
11	1.78 (1H, m), 1.54 (1H, m)	26.5	
12	1.60 (2H, m)	32.8	
13		45.8	
14		48.7	
15	1.36 (2H, m)	34.8	
16	2.04 (1H, m), 1.42 (1H, m)	27.8	
17	1.60 (1H, m)	51.3	C-13
18	0.95 (3H, s)	15.8	C-12, C-13, C-14, C-17
19	0.42 (1H, d, <i>J</i> = 5.3 Hz) 0.16 (1H, d, <i>J</i> = 5.3 Hz)	22.9	C-5, C-7, C-8, C-12
20	1.80 (1H, m)	36.3	
21	0.86 (3H, d, <i>J</i> = 6.5 Hz)	18.8	C-17, C-20, C-22
22	2.70 (1H, dd, <i>J</i> = 2.6, 14.6 Hz) 2.25 (1H, m)	35.0	C-20, C-21, C-23, C-24
23		155.2	
24	5.85 (1H, s)	109.0	C-23, C-25, C-26
25		120.3	
26	7.06 (1H, s)	137.3	C-23, C-24, C-25
27	1.98 (3H, s)	9.8	C-24, C-25, C-26
28	6.33 (1H, d, <i>J</i> = 1.8 Hz) 5.73 (1H, d, <i>J</i> = 1.8 Hz)	123.2	C-4, C-5, C-29
29		170.7	
30	0.91 (3H, s)	20.1	C-8, C-13, C-14, C-22
OMe	3.69 (3H, s)	51.8	C-3

Table 15. NMR data of compound **75** in C₆D₆.

Position	¹ H	¹³ C	HMBC
1	1.94 (1H, m), 1.26 (1H, m)	31.5	C-5, C-9, C-10
2	2.13 (2H, m)	35.2	C-1, C-3, C-10
3		173.0	
4		140.1	
5	2.60 (1H, d, <i>J</i> = 8.8 Hz)	39.6	C-6, C-4, C-10
6	4.18 (1H, dd, <i>J</i> = 3.5, 8.8 Hz)	77.1	C-10, C-29
7	3.44 (1H, dd, <i>J</i> = 3.8, 4.9 Hz)	69.1	C-5, C-8, C-9
8	2.01 (1H, d, <i>J</i> = 6.2 Hz)	46.0	C-10, C-14, C-15, C-30
9		24.7	
10		28.3	
11	1.42 (1H, m), 1.26 (1H, m)	26.8	C-8, C-9, C-12, C-13
12	1.42 (2H, m)	32.6	C-13
13		46.2	
14		47.6	
15	1.40 (2H, m)	36.4	C-12, C-13
16	1.40 (2H, m)	28.4	C-12, C-13
17	1.39 (1H, m)	51.2	C-13, C-16
18	0.71 (3H, s)	16.4	C-13, C-14, C-17, C-20
19	0.89 (1H, m) -0.08 (1H, d, <i>J</i> = 4.7 Hz)	25.9	C-5, C-9, C-10, C-12, C-13
20	1.72 (1H, m)	36.7	C-17, C-22
21	0.89 (3H, m)	19.0	C-17, C-20, C-22
22	2.72 (1H, dd, <i>J</i> = 14.6, 2.4 Hz) 2.22 (1H, m)	35.5	C-17, C-20, C-23
23		155.6	
24	5.84 (1H, s)	109.5	C-23, C-25, C-26
25		120.6	
26	7.01 (1H, s)	138.0	C-23, C-24, C-25
27	1.85 (3H, s)	9.9	C-24, C-25, C-26
28	6.18 (1H, d, <i>J</i> = 1.9 Hz) 5.17 (1H, d, <i>J</i> = 1.9 Hz)	120.3	C-4, C-5, C-29
29		170.2	
30	0.71 (3H, s)	20.1	C-13, C-14
OMe	3.39 (3H, s)	51.3	C-3

Table 16. NMR data of compound **76** in CDCl₃.

Position	¹ H	¹³ C	HMBC
1	2.13 (1H, m), 1.35 (1H, m)	28.7	C-2, C-10
2	2.50 (1H, m), 2.30 (1H, m)	31.5	C-1, C-10
3		179.0	
4		152.1	
5	2.50 (1H, m)	41.9	C-4, C-6, C-10, C-29
6	1.67 (1H, m), 0.93 (1H, m)	28.9	
7	1.30 (1H, m)	25.2	C-5
8	1.52 (1H, m)	47.9	C-14, C-15
9		21.8	
10		27.3	
11	2.10 (1H, m), 1.25 (1H, m)	26.9	C-9, C-10, C-12
12	1.67 (2H, m)	32.8	C-13, C-14
13		45.1	
14		48.8	
15	1.31 (2H, m)	35.7	
16	1.91 (2H, m)	28.0	C-13, C-15
17	1.57 (1H, m)	51.9	C-13, C-15, C-18
18	0.96 (3H, s)	18.2	C-12, C-13, C-14, C-17
19	0.71 (1H, d, <i>J</i> = 3.9 Hz) 0.47 (1H, d, <i>J</i> = 3.9 Hz)	30.2	C-1, C-5, C-9, C-10, C-11
20	1.34 (1H, m)	36.3	C-16
21	0.85 (3H, d, <i>J</i> = 6.3 Hz)	18.2	C-20, C-22
22	2.17 (1H, m), 1.73 (1H, m)	39.0	
23	5.59 (1H, br s)	125.6	C-22, C-25
24	5.59 (1H, br s)	139.2	C-25
25		70.9	
26	1.31 (3H, br s)	29.8	C-24, C-25
27	1.31 (3H, br s)	29.8	C-24, C-25
28	5.08 (2H, br s)	110.6	C-4, C-5, C-29
29	4.12 (2H, br s)	64.6	C-4, C-28
30	0.91 (3H, s)	19.3	C-8, C-13, C-14, C-15

2.4.4 Isolation and characterization of cycloartane triterpenes from apical buds of *G. obtusifolia*

The MeOH extract of fresh apical buds of *G. obtusifolia* was partitioned between EtOAc and water to afford an EtOAc extract, which was subjected to silica gel column chromatography using EtOAc-hexane mixtures of increasing polarity as eluent. Further purification by repeated normal column chromatography and preparative thin-layer chromatography gave four new cycloartane triterpenes (**77-80**), together with five known compounds, dikamaliartanes A (**61**), C (**62**) and D (**63**), 5 α -cycloart-24-ene-3,16,23-trione (**24**) and secaubryenol (**58**).

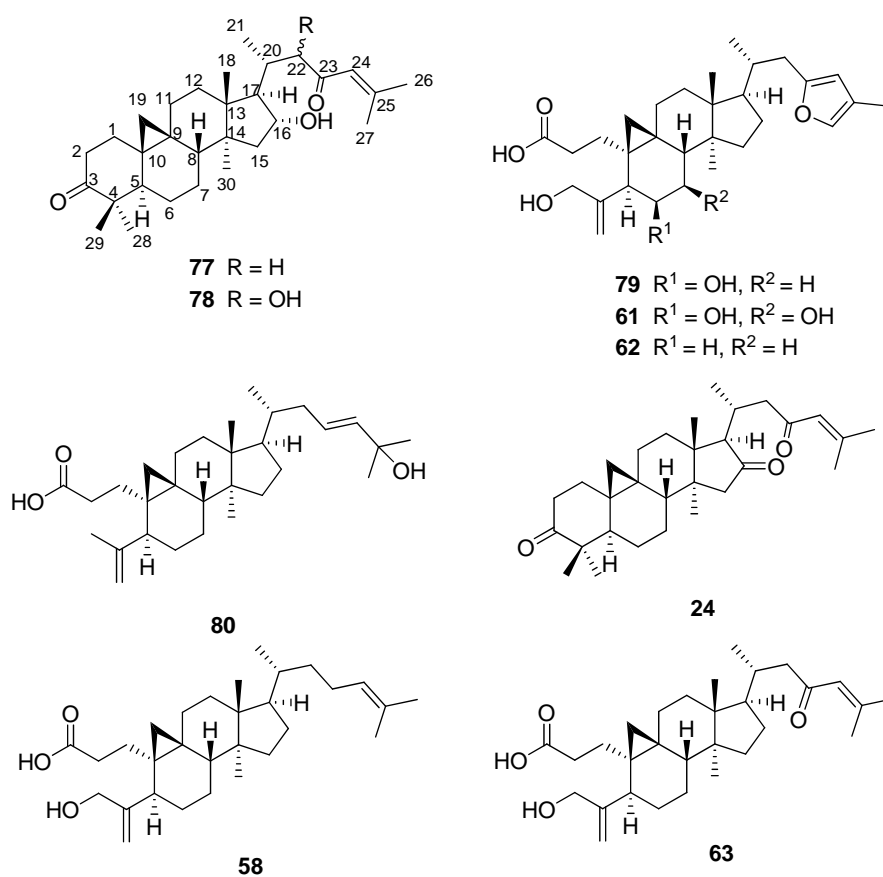


Figure 25. Cycloartane triterpenes from apical buds of *G. obtusifolia*

Gardenoin E (**77**) was obtained as a white, amorphous solid, $[\alpha]_D^{25}$ -19.0 (*c* 0.1, MeOH); UV (MeOH) λ_{\max} ($\log \epsilon$) 305.1 (3.18); IR (KBr) 3439, 2939, 1712, 1617, 1443, 1378, 1117, 1035 cm^{-1} . Its molecular formula was established as $\text{C}_{30}\text{H}_{46}\text{O}_3$ by the high resolution-electrospray ionization-mass spectrum (HR-ESI-MS) ion at m/z 477.3341 $[\text{M}+\text{Na}]^+$ (Calcd 477.3345), indicating eight degrees of unsaturation. The IR absorption bands at 3439 and 1712 cm^{-1} implied the presence of hydroxyl and carbonyl functionalities. The ^1H -NMR spectrum (Table 17) displayed a pair of doublets at δ_H 0.58 and 0.79 ($J = 4.1$ Hz), characteristic of the C-19 methylene protons of cyclopropane ring of a cycloartane triterpene. The ^{13}C -NMR and heteronuclear single quantum coherence (HSQC) data revealed the presence of 30 nonequivalent carbons including two ketone carbonyls, six tertiary methyls, one secondary methyl, nine methylenes, six methines (one oxygenated and one olefinic) and six quaternary carbons (one olefinic). These NMR data indicated that three of the eight units of unsaturation come from one carbon-carbon double bond and two carbonyls. Therefore, the remaining five degrees required **77** to comprise a pentacyclic core. The above NMR data strongly suggested that **77** was a normal cycloartanone-type triterpenoid. The existence of two geminal vinylmethyls connected to a carbonyl group was corroborated by heteronuclear multiple bond connectivity (HMBC) correlations from olefinic proton at δ_H 6.11 (H-24) to a carbonyl (δ_C 202.6, C-23), Me-26 and Me-27. The NMR data of **1** were similar to those of 5α -cycloart-24-ene-3,16,23-trione (**24**) [9], except for the presence of a hydroxyl group at C-16 instead of a ketone carbonyl in **24**. This was verified by HMBC correlations of H-16 to C-14, C-17 and C-20, and by ^1H - ^1H correlation spectroscopy (COSY) correlations of H-16/H₂-15 and H-16/H-17 (Figure 26). Observed nuclear Overhauser effect spectroscopy (NOE) correlations of Me-28/H-5, H-5/H-7a, H-7a/Me-30 and Me-30/H-17 indicated an α -orientation of these protons, while the correlations of H-8/Me-18 and H-16/Me-18 suggested that H-16 is a β -orientation (Figure 26). Additionally, the obvious 1D NOE correlation of H-17 and Me-21 together with chemical shift comparison of the side chain unit (C-20 to C-27) with those of **24** determined the configuration of Me-21 to be in an α -orientation [9]. The structure of **77** was thus assigned as shown.

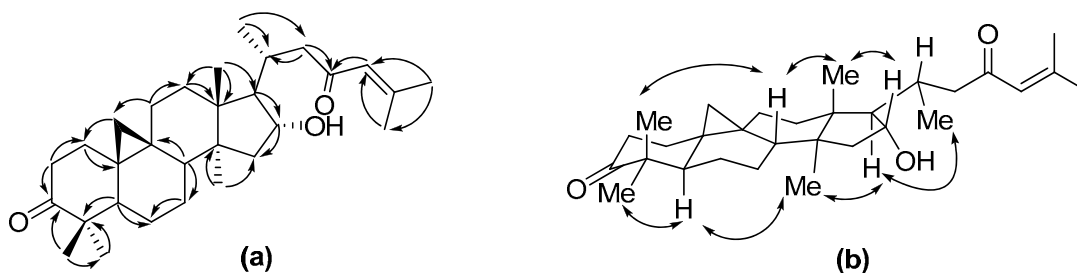


Figure 26. Key HMBC (a) and NOE (b) correlations of compound **77**.

Gardenoin F (**78**) was obtained as a white amorphous solid, $[\alpha]_D^{25} - 21.0$ (c 0.1, MeOH); UV (MeOH) λ_{\max} ($\log \epsilon$) 433.9 (2.56), 238 (3.90); IR (KBr) 3443, 2935, 1704, 1614, 1452, 1398, 1108, 1063 cm^{-1} and its molecular formula $\text{C}_{30}\text{H}_{46}\text{O}_4$ was deduced from the HR-ESI-MS ion at m/z 493.3289 $[\text{M}+\text{Na}]^+$ (Calcd 493.3294), 16 mass units more than **77**. Comparison of the ^1H and ^{13}C -NMR spectra of **78** with those of **77** revealed them to be very similar, with the only difference being the appearance of a singlet due to an oxymethine proton at δ_H 4.44 in the ^1H -NMR spectrum, coupled in the HSQC spectrum to a newly appearing an oxygenated methine carbon at δ_C 78.7, while a methylene signal at δ_H 2.83 (dd, $J = 4.0, 15.0$ Hz) and 2.41 (dd, $J = 7.0, 15.0$ Hz), and at δ_C 50.4 had disappeared. The relative configuration of **78** was assigned to be the same as that of **77** on the basis of the nuclear Overhauser effect (NOE) correlations.

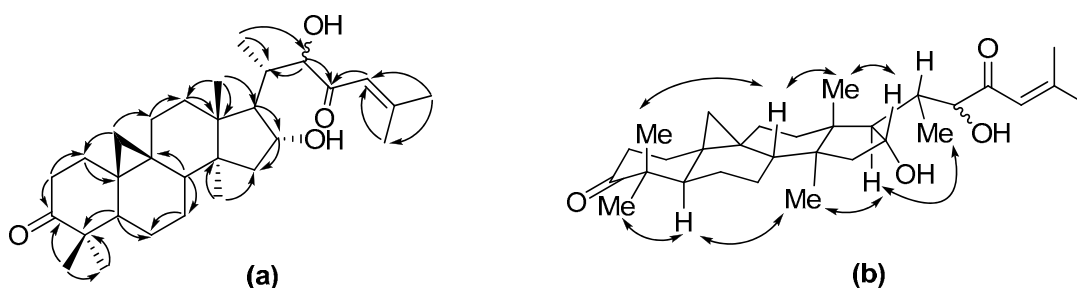


Figure 27. Key HMBC (a) and NOE (b) correlations of compound **78**.

Gardenoin G (**79**), a white amorphous solid, $[\alpha]_D^{25} + 45.0$ (c 0.1, MeOH); UV (MeOH) λ_{\max} ($\log \epsilon$) 275.1 (3.01); IR (KBr) 3426, 2939, 1708, 1456, 1378, 1045, 1026 cm^{-1} had the molecular formula of $\text{C}_{30}\text{H}_{44}\text{O}_5$ as established by HR-

ESI-MS (m/z 507.3087 $[M+Na]^+$, Calcd 507.3086). The 1H -NMR spectrum (Table 19) also displayed the characteristic signals for cyclopropane methylene protons of a cycloartane triterpene as two doublets at δ_H 0.42 and 1.11 ($J = 3.0$ Hz), and two broad singlets of a terminal alkene at δ_H 5.08 and 5.14.

These data suggested that **79** is a 3,4-*seco*-cycloartane triterpenoid. Additionally, the NMR spectra indicated the presence of a 2,4-disubstituted furan ring (δ_H 5.80 and 7.02; δ_C 108.4 CH, 119.7 C, 136.9 CH, 154.8 C) in side chain. Extensive analysis of 1D- and 2D-NMR spectra revealed that the structure of **79** was virtually identical to that of dikamaliartane A (**61**) [29], except for the presence of one more methylene group (δ_H 1.31 m, 1.97 m; δ_C 27.6) in place of the oxygenated methine at C-7 position in **61**. This was confirmed by HMBC correlations from H-6 and H-8 to C-7 (Figure 27). The relative stereochemistry of **79** was established to be the same as that of **61** on the basis of NOE correlations of H-5/H-6, H-6/Me-30, H-17/Me-30 and H-8/Me-18. The configuration at C-20 was assumed to be the same as that of **61** and **62** because the carbon signals due to C-20-C-27 of **79** were superimposable with those previously reported [29].

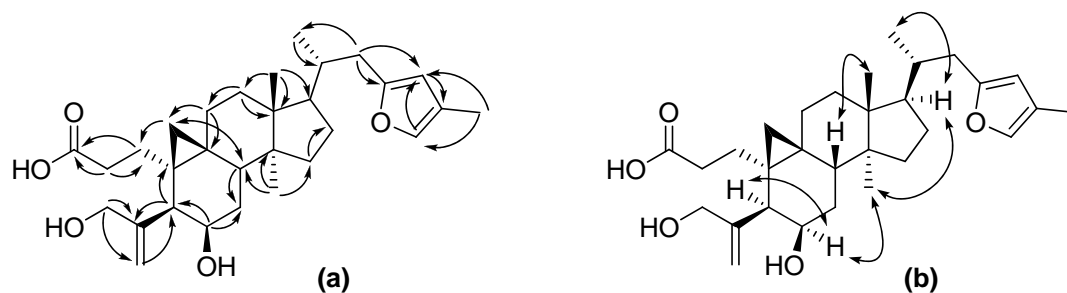


Figure 28. Key HMBC (a) and NOE (b) correlations of compound **79**.

Gardenoin H (**80**), colorless gum, $[\alpha]_D^{25} +22.0$ ($c = 0.1$, MeOH); UV (MeOH) λ_{max} ($\log \epsilon$) 232.0 (3.17); IR (KBr) 3426, 2921, 1708, 1460, 1372, 1273, 1155 cm^{-1} had the molecular formula of $C_{30}H_{48}O_3$ as determined by HR-ESI-MS (m/z 479.3496 $[M+Na]^+$, Calcd 479.3501). The 1H -NMR spectrum also showed typical signals associated with a 3,4-*seco*-cycloartane triterpene, including a characteristic pair of doublets at δ_H 0.40 and 0.73 (d, $J = 4.3$ Hz), attributable to the C-19 methylene protons in the cyclopropane ring, and two singlets of an exomethylene moiety at δ_H

4.71 and 4.73. A two proton broad singlet at δ_H 5.60, showing HMBC correlations to C-24, C-25 and C-26 (Figure 28), was identified as a disubstituted alkene moiety between C-23 and C-24. The ^1H - and ^{13}C -NMR of **80** were very similar to those previously reported of gardenoin D(**63**) [29], with the marked difference being the appearance of an additional three-proton singlet of a vinylic methyl at δ_H 1.69 and δ_C 19.7, replacing the oxygenated methylene signals at C-29 in gardenoin D (**63**). The relative configuration of **80** was deduced to be the same as that of gardenoin D (**63**) on the basis of the NOESY correlations.

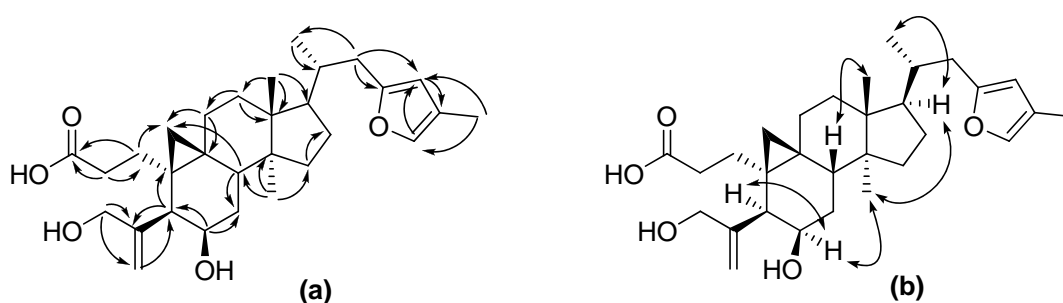


Figure 29. Key HMBC (a) and NOE (b) correlations of compound **80**.

The ^1H NMR spectrum of compound **24** in CDCl_3 (Table 21) displayed; a pair of doublets at δ_H 0.64 and 0.84 (1H each, $J = 54.2$ Hz), an olefinic proton at δ_H 6.10 (1H, br s), six tertiary methyl protons at δ_H 1.05, 1.09, 1.10, 1.18, 1.87, and 2.13 (3H each s), and a secondary methyl proton at δ_H 0.97 (3H, d, $J = 9.8$ Hz). Based on the spectroscopic data above, compound **24** was identified to be a α -cycloart-24-ene-3,16,23-trione. The structure of this compound was finally confirmed by comparison of the spectral data with those previously reported by Tuchinda and co-worker in 2002 [9].

The ^1H NMR spectrum of compound **61** in acetone- d_6 (Table 22) displayed; a signal at δ_H 0.58 and 1.71 (1H each, m), a pair of singlet proton at δ_H 5.21 and 5.26 (1H each, s), disubstituted furan ring at δ_H 5.92 and 7.14 (1H, each, s), an oxygenated methylene proton at δ_H 4.08, and 4.26 (1H, d, $J = 13.2$ Hz), two oxygenated methine proton at δ_H 3.62 (1H, br s), and 3.89 (1H, br d, $J = 11.4$ Hz) three tertiary methyl protons at δ_H 1.10, 1.11, and 1.95 (3H each s), and a secondary methyl proton at δ_H 0.88 (3H, d, $J = 6.4$ Hz). Based on the spectroscopic data above,

compound **61** was identified to be a dikamaliaratane A. The structure of this compound was finally confirmed by comparison of the spectral data (Table 22) with those previously reported by Kunert and co-worker in 2010 [29].

The ^1H NMR spectrum of compound **62** in CDCl_3 (Table 23) displayed; a pair of doublets at δ_H 0.43 and 0.91 (1H each, d, $J = 4.3$ Hz), a pair of singlet proton at δ_H 5.10 and 5.14 (1H each, s), disubstituted furan ring at δ_H 5.86 and 7.06 (1H, each, s), an oxygenated methylene proton at δ_H 4.14 (2H, br s), three tertiary methyl protons at δ_H 1.00, 1.01, and 1.99 (3H each s), and a secondary methyl proton at δ_H 0.86 (3H, d, $J = 6.5$ Hz). Based on the spectroscopic data above, compound **62** was identified to be a dikamaliaratane C. The structure of this compound was finally confirmed by comparison of the spectral data (Table 23) with those previously reported by Kunert and co-worker in 2010 [29].

The ^1H NMR spectrum of compound **63** in CDCl_3 (Table 24) displayed; a pair of doublets at δ_H 0.48 and 0.73 (1H each, $J = 4.2$ Hz), a pair of broad singlet proton at δ_H 5.08 and 5.10 (1H each, br s). Moreover, the ^1H NMR signal displayed; an olefinic proton at δ_H 6.06 (1H, s), an oxygenated methylene proton at δ_H 4.12 (2H, br s), four tertiary methyl protons at δ_H 0.93, 1.01, 1.86, and 2.14 (3H each s), and a secondary methyl proton at δ_H 0.88 (3H, d, $J = 6.2$ Hz). Based on the spectroscopic data above, compound **63** was identified to be a dikamaliaratane D. The structure of this compound was finally confirmed by comparison of the spectral data (Table 24) with those previously reported by Kunert and co-worker in 2010 [29].

Table 17. NMR data of compound **77** in CDCl₃.

Position	¹ H	¹³ C	HMBC
1	1.87 (1H, m), 1.22 (1H, m)	33.3	C-2, C-9
2	2.70 (1H, m), 2.31 (1H, m)	37.4	C-1, C-3
3		216.4	
4		50.2	
5	1.72 (1H, m)	48.4	C-4, C-6, C-7, C-8
6	1.57 (1H, m), 0.92 (1H, m)	21.4	C-7
7	1.36 (1H, m), 1.18 (1H, m)	26.7	C-6, C-8
8	1.53 (1H, m)	47.5	C-7, C-9
9		20.4	
10		26.1	
11	2.11 (1H, m), 1.17 (1H, m)	26.0	C-12, C-19
12	1.72 (2H, m)	32.5	C-13
13		47.2	
14		47.5	
15	1.88 (1H, m), 1.43 (1H, m)	47.9	C-14, C-30
16	4.00 (1H, m)	77.5	C-15, C-22
17	1.74 (1H, m)	61.2	C-13, C-16, C-18
18	1.05 (3H, s)	19.1	C-12, C-13, C-22
19	0.79 (1H, d, <i>J</i> = 4.1 Hz) 0.58 (1H, d, <i>J</i> = 4.1 Hz)	29.9	C-1, C-9, C-10, C-11
20	2.16 (1H, m)	32.0	C-22
21	0.97 (3H, d, <i>J</i> = 6.7 Hz)	19.9	C-17, C-20, C-22
22	2.83 (1H, dd, <i>J</i> = 4.0, 15.0 Hz) 2.41 (1H, dd, <i>J</i> = 7.4, 15.0 Hz)	50.4	C-20, C-21, C-23
23		202.6	
24	6.11 (1H, br s)	125.1	C-23, C-25
25		155.7	
26	2.16 (3H, s)	20.8	C-24, C-25, C-27
27	1.90 (3H, s)	27.8	C-24, C-25, C-26
28	1.05 (3H, s)	22.2	C-3, C-4, C-29
29	1.10 (3H, s)	20.8	C-3, C-4, C-28
30	1.15 (3H, s)	20.1	C-14

Table 18. NMR data of compound **78** in CDCl₃.

Position	¹ H	¹³ C	HMBC
1	1.86 (1H, m), 1.55 (1H, m)	33.3	C-2, C-5, C-10, C-19
2	2.70 (1H, m), 2.31 (1H, m)	37.4	C-1, C-3
3		216.5	
4		50.2	
5	1.74 (1H, m)	48.4	C-4, C-7
6	1.59 (1H, m), 0.99 (1H, m)	20.8	C-5, C-7, C-8
7	1.39 (1H, m), 1.19 (1H, m)	26.7	C-6, C-8
8	1.50 (1H, m)	48.1	C-14
9		20.4	
10		26.1	
11	2.12 (1H, m), 1.19 (1H, m)	26.0	C-9, C-12
12	1.86 (2H, m)	32.7	C-13, C-18
13		47.0	
14		47.7	
15	1.85 (1H, m), 1.52 (1H, m)	46.1	C-16, C-17, C-30
16	4.25 (1H, dd, <i>J</i> = 5.7, 8.2 Hz)	76.5	C-14, C-17, C-20
17	2.07 (1H, m)	59.3	C-14, C-20
18	1.08 (3H, s)	19.8	C-12, C-17
19	0.79 (1H, d, <i>J</i> = 4.0 Hz) 0.57 (1H, d, <i>J</i> = 4.0 Hz)	29.9	C-1, C-8, C-9, C-10
20	2.10 (1H, m)	36.4	C-17
21	0.68 (3H, d, <i>J</i> = 5.8 Hz)	12.7	C-17, C-20, C-22
22	4.44 (1H, d, <i>J</i> = 4.2 Hz)	78.7	C-20, C-21, C-23
23		200.2	
24	6.16 (1H, s)	118.8	C-23, C-26, C-27
25		160.2	
26	2.23 (3H, s)	21.5	C-23, C-24, C-25, C-27
27	1.99 (3H, s)	28.2	C-23, C-24, C-25, C-26
28	1.04 (3H, s)	22.2	C-3, C-4, C-29
29	1.09 (3H, s)	21.4	C-3, C-4, C-28
30	1.17 (3H, s)	20.0	C-14

Table 19. NMR data of compound **79** in acetone-*d*₆.

Position	¹ H	¹³ C	HMBC
1	2.11 (1H, m), 1.30 (1H, m)	30.7	C-3, C-19
2	2.32 (2H, m)	31.3	C-1, C-3
3		173.5	
4		149.7	
5	2.55 (1H, m)	45.8	C-4, C-6, C-10, C-19, C-28
6	3.96 (1H, br s)	67.4	C-5, C-7, C-10
7	1.97 (1H, m), 1.31 (1H, m)	27.6	C-8
8	2.07 (1H, m)	38.8	C-6, C-9, C-19
9		20.7	
10		24.8	
11	2.20 (1H, m), 1.08 (1H, m)	25.9	C-8, C-9, C-19
12	1.59 (2H, m)	32.5	C-11, C-13, C-18
13		44.9	
14		47.9	
15	1.25 (2H, m)	35.3	C-16, C-30
16	1.89 (1H, m), 1.17 (1H, m)	29.3	
17	1.60 (1H, m)	51.9	C-13, C-18
18	0.97 (3H, s)	18.0	C-12, C-13, C-14, C-17
19	1.11 (1H, d, <i>J</i> = 3.0 Hz) 0.42 (1H, d, <i>J</i> = 3.0 Hz)	32.1	C-1, C-5, C-8
20	1.64 (1H, m)	35.8	
21	0.75 (1H, d, <i>J</i> = 6.0 Hz)	17.6	C-17, C-20
22	2.60 (1H, m), 2.16 (1H, m)	34.2	C-21, C-23, C-24
23		154.8	
24	5.80 (1H, br s)	108.4	C-23, C-25, C-26, C-27
25		119.7	
26	7.02 (1H, br s)	136.9	C-23, C-24
27	1.83 (3H, s)	8.4	C-24, C-25, C-26
28	5.14 (1H, br s) 5.08 (1H, br s)	113.6	C-4, C-5, C-29
29	4.14 (1H, d, <i>J</i> = 13.0 Hz) 3.94 (1H, d, <i>J</i> = 13.0 Hz)	63.5	C-4, C-5, C-28
30	0.91 (3H, s)	18.8	C-13, C-14, C-15

Table 20. NMR data of compound **80** in CDCl₃.

Position	¹ H	¹³ C	HMBC
1	2.07 (1H, m), 1.35 (1H, m)	28.8	C-9, C-19
2	2.53 (1H, m), 2.31 (1H, m)	31.3	C-1, C-3
3		179.1	
4		149.4	
5	2.42 (1H, m)	45.9	C-6
6	1.51 (1H, m), 1.08 (1H, m)	27.7	C-8, C-30
7	1.31 (1H, m), 1.08 (1H, m)	25.0	C-8, C-30
8	1.57 (1H, m)	47.7	C-10
9		21.4	
10		27.0	
11	2.06 (1H, m), 1.31 (1H, m)	27.0	C-19
12	1.64 (2H, m)	32.9	C-10, C-13, C-18
13		45.1	
14		49.0	
15	1.31 (2H, m)	35.6	C-14, C-16
16	1.91 (2H, m)	28.0	C-13
17	1.59 (1H, m)	52.0	C-13, C-20
18	0.98 (3H, s)	18.1	C-12, C-13, C-17
19	0.73 (1H, d, <i>J</i> = 4.3 Hz) 0.40 (1H, d, <i>J</i> = 4.3 Hz)	29.7	C-8, C-9, C-10
20	1.46 (1H, m)	36.4	
21	0.86 (3H, d, <i>J</i> = 6.4 Hz)	18.3	C-17, C-22
22	2.19 (1H, m), 1.75 (1H, m)	39.0	C-20, C-23
23	5.60 (1H, br s)	125.7	C-22, C-25
24	5.60 (1H, br s)	139.3	C-22, C-25
25		70.9	
26	1.31 (3H, br s)	29.9	C-24, C-25, C-27
27	1.31 (3H, br s)	29.8	
28	4.81 (1H, br s) 4.73 (1H, br s)	111.6	C-5, C-30
29	1.69 (3H, s)	19.7	C-4, C-5, C-28
30	0.92 (3H, s)	19.3	C-13, C-14, C-15

Table 21. ^1H and ^{13}C NMR data (CDCl_3) of 5α -cycloart-24-ene-3,16,23-trione and compound **24**.

Position	5α -cycloart-24-ene-3,16,23-trione		Compound 24	
	^1H	^{13}C	^1H	^{13}C
1	1.89 (1H, obsc.) 1.56 (1H, obsc.)	33.1	1.88 (1H, m) 1.56 (1H, m)	33.1
2	2.72 (1H, ddd, $J = 14, 14, 6.3$ Hz), 2.32 (1H, obsc.)	37.3	2.71 (1H, m) 2.33 (1H, m)	37.3
3		215.9		216.2
4		50.2		50.2
5	1.75 (1H, dd, $J = 12.2, 4.3$ Hz)	48.3	1.75 (1H, m)	48.3
6	1.62 (1H, obsc.) 0.97 (1H, dddd, $J = 12.6, 12.6, 12.6, 2.6$ Hz)	21.3	1.61 (1H, m) 0.97 (1H, m)	21.3
7	1.37 (1H, obsc.), 1.21 (1H, m)	26.2	1.36 (1H, m), 1.21 (1H, m)	26.2
8	1.69 (1H, obsc.)	47.3	1.68 (1H, m)	47.3
9		20.4		20.4
10		26.5		26.4
11	2.16 (1H, obsc.), 1.28 (1H, m)	26.2	2.16 (1H, m), 1.27 (1H, m)	26.2
12	1.85 (2H, obsc.)	31.3	1.85 (2H, m)	31.2
13		42.1		42.1
14		45.3		45.3
15	2.07 (1H, d, $J = 18.5$ Hz) 2.01 (1H, d, $J = 18.5$ Hz)	50.9	2.06 (1H, m), 2.01 (1H, m)	50.9
16		219.2		219.4
17	2.30 (1H, obsc.)	60.9	2.30 (1H, m)	60.9
18	1.20 (3H, s)	19.0	1.18 (3H, s)	19.0
19	0.86 (1H, br d, $J = 4.4$ Hz) 0.65 (1H, d, $J = 4.4$ Hz)	30.0	0.84 (1H, d, $J = 4.2$ Hz) 0.64 (1H, d, $J = 4.2$ Hz)	30.1
20	2.33 (1H, obsc.)	27.4	2.32 (1H, m)	27.4
21	0.99 (3H, d, $J = 5.7$ Hz)	20.2	0.97 (3H, d, $J = 9.8$ Hz)	20.2
22	3.20 (1H, m) 2.34 (1H, obsc.)	50.0	3.19 (1H, m) 2.33 (1H, m)	50.0
23		200.7		200.8
24	6.11 (1H, m)	124.4	6.10 (1H, br s)	124.4
25		154.2		154.4
26	2.14 (3H, d, $J = 1.0$ Hz)	20.7	2.13 (3H, s)	20.7

Table 21. (Cont.) The ^1H and ^{13}C NMR data of 5α -cycloart-24-ene-3,16,23-trione and compound **24**

Position	5α -cycloart-24-ene-3,16,23-trione		Compound 24	
	^1H	^{13}C	^1H	^{13}C
27	1.88 (3H, d, $J = 1.3$ Hz)	27.6	1.87 (3H, s)	27.7
28	1.06 (3H, s)	22.2	1.05 (3H, s)	22.1
29	1.11 (3H, s)	20.6	1.10 (3H, s)	20.6
30	1.10 (3H, s)	19.7	1.09 (3H, s)	19.7

Table 22. ^1H and ^{13}C NMR data of dikamaliartane A and compound **61**.

Position	Dikamaliartane A ^a		Compound 61 ^b	
	^1H	^{13}C	^1H	^{13}C
1	2.60 (1H, m), 1.74 (1H, m)	31.1		31.2
2	2.92 (1H, m) 2.67 (1H, t, $J = 15.0$ Hz)	33.0		32.8
3		176.3		174.4
4		151.0		149.0
5	3.25 (1H, s)	47.2		
6	4.45 (1H, s)	74.3	3.89 (1H, br s)	73.5
7	3.96 (1H, d, $J = 11.4$ Hz)	72.6	3.62 (1H, br d, $J = 11.4$ Hz)	71.9
8	2.60 (1H, m)	46.9		45.9
9		21.6		21.0
10		26.4		25.5
11	2.47 (1H, m), 1.31 (1H, m)	27.0		26.2
12	1.64 (2H, m)	33.3		32.8
13		46.4		46.1
14		48.6		47.9
15	2.13 (1H, q, $J = 10.2$ Hz) 1.85 (1H, m)	39.1		38.4
16	2.09 (1H, m) 1.40 (1H, q, $J = 10.2$ Hz)	29.3		28.7
17	1.65 (1H, m)	52.3		51.8
18	1.17 (3H, s)	19.1	1.10 (3H, s)	18.2
19	1.75 (1H, s), 0.72 (1H, s)	32.7	1.71 (1H, m), 0.58 (1H, br s)	31.9
20	1.83 (1H, m)	36.8		36.3
21	0.99 (3H, d, $J = 6.6$ Hz)	18.9	0.88 (3H, d, $J = 6.4$ Hz)	18.5
22	2.82 (1H, d, $J = 15.0$ Hz) 2.31 (1H, dd, $J = 15.0$ Hz)	35.4		34.8
23		156.0		155.3
24	6.30 (1H, s)	109.6	5.92 (1H, s)	109.0
25		120.8		120.2
26	7.31 (1H, s)	138.0	7.14 (1H, s)	137.4
27	1.99 (3H, s)	9.9	1.95 (3H, s)	9.1
28	5.71 (1H, s), 5.53 (1H, s)	113.2	5.26 (1H, s), 5.21 (1H, s)	113.9
29	4.82 (1H, d, $J = 13.8$ Hz) 4.58 (1H, d, $J = 13.8$ Hz)	64.8	4.26 (1H, d, $J = 13.2$ Hz) 4.08 (1H, d, $J = 13.2$ Hz)	64.0
30	1.30 (3H, s)	19.4	1.11 (3H, s)	18.6

^a recorded in Pyridine- d_5 , ^b recorded in Acetone- d_6

Table 23. ^1H and ^{13}C NMR data of dikamaliartane C and compound **62**.

Position	Dikamaliartane C ^a		Compound 62 ^b
	^1H	^{13}C	^1H
1	2.55 (1H, m), 1.71 (1H, m)	30.1	
2	2.95 (1H, m), 2.60 (1H, m)	32.8	
3		176.4	
4		155.0	
5	2.77 (1H, m)	42.8	
6	1.75 (1H, m), 1.12 (1H, m)	29.4	
7	1.22 (1H, m), 1.07 (1H, m)	25.7	
8	1.53 (1H, t, $J = 7.2$ Hz, 1H)	48.2	
9		22.1	
10		28.1	
11	2.23 (1H, m), 1.28 (1H, m)	27.3	
12	1.55 (2H, m)	33.4	
13		45.4	
14		49.2	
15	1.29 (2H, m)	36.0	
16	1.98 (1H, m), 1.36 (1H, m)	28.4	
17	1.60 (1H, m)	52.6	
18	0.98 (3H, s)	18.5	1.01 (3H, s)
19	0.79 (1H, d, $J = 3.6$ Hz) 0.47 (1H, d, $J = 3.6$ Hz)	30.6	0.91 (1H, d, $J = 4.3$ Hz) 0.43 (1H, d, $J = 4.3$ Hz)
20	1.81 (1H, m)	36.2	
21	0.94 (3H, m)	18.5	0.86 (3H, d, $J = 6.5$ Hz)
22	2.78 (1H, m) 2.29 (1H, dd, $J = 15.0, 9.6$ Hz)	36.7	
23		25.4	
24	6.04 (1H, s)	125.8	5.86 (1H, s)
25		130.9	
26	7.34 (1H, s)	17.7	7.06 (1H, s)
27	1.98 (3H, s)	25.8	1.99 (3H, s)
28	5.62 (1H, s) 5.30 (1H, s)	109.2	5.14 (1H, s) 5.10 (1H, s)
29	4.53 (2H, s)	64.0	4.14 (2H, s)
30	0.92 (3H, s)	19.6	1.00 (3H, s)

^a recorded in Pyridine-*d*₅, ^b recorded in CDCl₃

Table 24. ^1H and ^{13}C NMR data of Dikamaliaratane D and compound **63**.

Position	Dikamaliaratane D ^a		Compound 63 ^b	
	^1H	^{13}C	^1H	^{13}C
1	2.56 (1H, m), 1.72 (1H, m)	30.0		28.8
2	2.96 (1H, t, $J = 11.4$ Hz) 2.63 (1H, m)	32.9		31.6
3		n.d.		178.9
4		155.0		152.3
5	2.79 (1H, dd, $J = 12.0, 4.8$ Hz)	42.8		41.9
6	1.76 (1H, m), 1.13 (1H, m)	29.4		28.9
7	1.23 (1H, m), 1.10 (1H, m)	25.7		25.3
8	1.55 (1H, m)	48.1		47.9
9		22.0		21.8
10		28.2		27.5
11	2.25 (1H, m), 1.29 (1H, m)	27.2		27.0
12	1.58 (2H, m)	33.2		32.9
13		45.5		45.2
14		49.3		49.0
15	1.30 (2H, m)	35.9		35.6
16	1.89 (1H, m), 1.32 (1H, m)	28.5		28.3
17	1.66 (1H, m)	52.7		52.5
18	1.02 (3H, s)	18.4	1.01 (3H, s)	18.2
19	0.79 (1H, d, $J = 3.6$ Hz) 0.48 (1H, d, $J = 3.6$ Hz)	30.6	0.73 (1H, d, $J = 4.2$ Hz) 0.48 (1H, d, $J = 4.2$ Hz)	30.3
20	2.20 (1H, m)	33.7		33.5
21	1.03 (3H, d, $J = 6.6$ Hz)	19.6	0.88 (3H, d, $J = 6.2$ Hz)	19.3
22	2.60 (1H, m), 2.21 (1H, m)	35.4		35.5
23		200.8		201.7
24	6.20 (1H, s)	125.0	6.06 (1H, br s)	124.4
25		154.0		154.8
26	2.25 (3H, s)	20.6	2.14 (3H, s)	20.7
27	1.78 (3H, s)	27.3	1.86 (3H, s)	27.7
28	5.63 (1H, s) 5.31 (1H, s)	109.2	5.10 (1H, s) 5.08 (1H, s)	110.7
29	4.54 (2H, s)	64.0	4.12 (2H, br s)	64.8
30	0.95 (3H, s)	19.6	0.93 (3H, s)	19.4

^a recorded in Pyridine-*d*₅, ^b recorded in CDCl₃

2.4.5 Isolation and characterization of cycloartane triterpenes from *G. thailandica* exudate

The exudate collected from the aerial parts of *G. thailandica* was dissolved in a 1:1 mixture of CH₂Cl₂ and MeOH, which was then subjected to silica gel column chromatography using acetone–hexane mixtures of increasing polarity as eluent. Further purification by repeated normal phase column chromatography gave two new 3,4-*seco*-cycloartane triterpenes (**81** and **82**) and three known compounds, sootepin E (**70**), coronalolic acid (**12**), and secaubryenol (**58**). The structures of **12**, **58**, and **70** were determined by comparison of their NMR spectroscopic data with those in the literature.

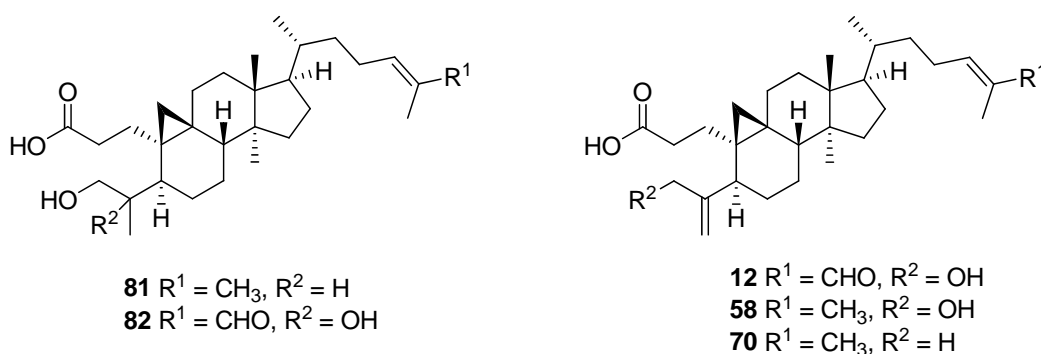


Figure 30. Cycloartane triterpenes from *G. obtusifolia* exudate

Compound **81** was obtained as colorless gum, $[\alpha]_{25}^D +29.0$ (*c* 0.1, MeOH); UV (MeOH) λ_{\max} (log ϵ) 329.9 (2.37), 275.1 (2.49) nm; IR (KBr) 3443, 2934, 1704, 1600, 1452, 1370, 1108, 1046 cm⁻¹. Its molecular formula was established as C₃₀H₅₀O₃ by the HRESIMS ion at *m/z* 481.3655 [M+Na]⁺ (calcd 481.3658), indicating six degrees of unsaturation. The IR absorption bands at 3443 and 1704 cm⁻¹ implied the presence of hydroxyl and carbonyl functionalities. The 1D NMR data (Table 25) indicated that two of the six units of unsaturation came from one carbon–carbon double bond and a carboxylic acid group. Therefore, the remaining degrees of unsaturation required **81** to have a tetracyclic core. Analysis of the ¹³C NMR and HSQC spectra revealed the presence of 30 nonequivalent carbons including one carboxylic carbonyl, six methyls (four tertiary and two secondary), 12 methylenes (one oxygenated), six methines (one olefinic) and five quaternary carbons

(one olefinic). The ^1H NMR spectrum (Table 25) displayed typical signals associated with a 3,4-*seco*-cycloartane triterpenoid including two tertiary methyl singlets at δ_H 0.91 and 0.95, one secondary methyl doublet at 0.81 (d, $J = 7.0$ Hz), and a pair of doublets at δ_H 0.39 and 0.61 ($J = 4.2$ Hz), characteristic of the C-19 methylene protons of a cyclopropane ring of a cycloartane triterpene. Both ^1H and ^{13}C NMR signals of **81** were very similar to those of secaubryenol (**58**) [22], with the marked difference being the appearance of a three-proton doublet at δ_H 0.81 due to an additional secondary methyl (C-28) and a methine (C-4) proton at δ_H 2.15 instead of signals observed for a terminal alkene moiety in **58**. This was confirmed by HMBC correlations of H₃-28 to C-4, C-29, and by ^1H - ^1H COSY correlations of H₂-29/H-4 and H-4/H₃-28 (Figure 30). The relative configuration of **81** was established to be the same as secaubryenol on the basis of NOE correlations. Observed NOESY correlations of H-5/Me-30, Me-30/H-17 and H-17/Me-21 indicated an α -orientation of these protons, while the correlations of H-8/Me-18, H-8/H₂-19 and Me-18/H-20 suggested that they were β -oriented (Figure 31). Thus, **81** was determined as a new 29-hydroxy-3,4-*seco*-cycloartane and given the name as gadenoin I.

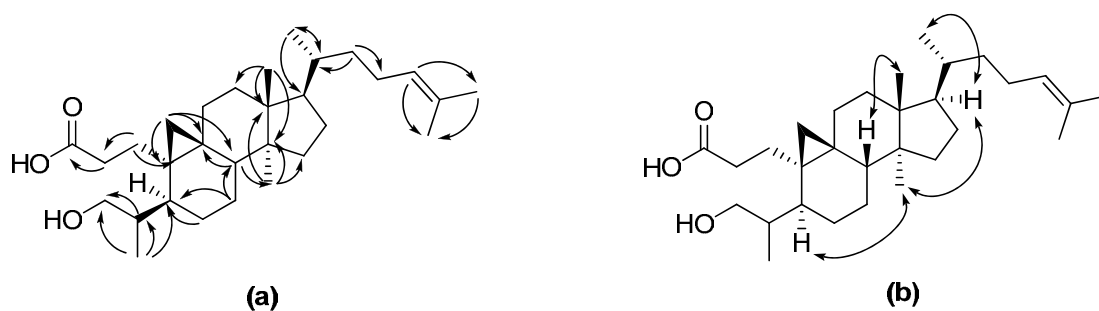


Figure 31. Key HMBC (a) and NOE (b) correlations of compound **81**.

Compound **82** was obtained as colorless needles, m.p. 110–111 °C; $[\alpha]_{25}^D +32.0$ (c 0.1, MeOH); UV (MeOH) λ_{\max} ($\log \epsilon$) 231.1 (3.62), 227 (3.64) nm; IR (KBr) 3439, 2939, 1712, 1617, 1443, 1378, 1117, 1034 cm^{-1} , and its molecular formula $\text{C}_{30}\text{H}_{48}\text{O}_5$ was deduced from the HRESIMS ion at m/z 511.3403 $[\text{M}+\text{Na}]^+$ (calcd 511.3399). Obvious in the ^1H NMR spectrum were a cyclopropane methylene (C-19) at δ_H 0.54 and 0.56, a pair of broad singlets, five methyls due to four tertiary and one secondary methyls, and an aldehyde δ_H 9.38. Comparison of the ^1H and ^{13}C

NMR spectra of **82** with those of **81** revealed them to be very similar, except for the presence of an aldehyde group (δ_H 9.38, δ_C 195.6), and the absence of a vinylic methyl in **81**. Additionally, one more significant difference between **81** and **82** was found at the side chain connected to C-5 according to the appearance of an oxygenated quaternary carbon at δ_C 78.3 (C-4) instead of a methine carbon in **82**. This was clarified by no vicinal ^1H - ^1H COSY correlations observed for H₂-29 through H₃-28 which indicated the quaternary center adjacent to them. The full assignment and connectivity were determined by ^1H - ^1H COSY and HMBC correlations as shown in Figure 31. The relative configuration of **82** was deduced to be the same as that of **81** on the basis of the NOESY correlations. Thus, the structure of **82** was as indicated and it was named gardenoin J.

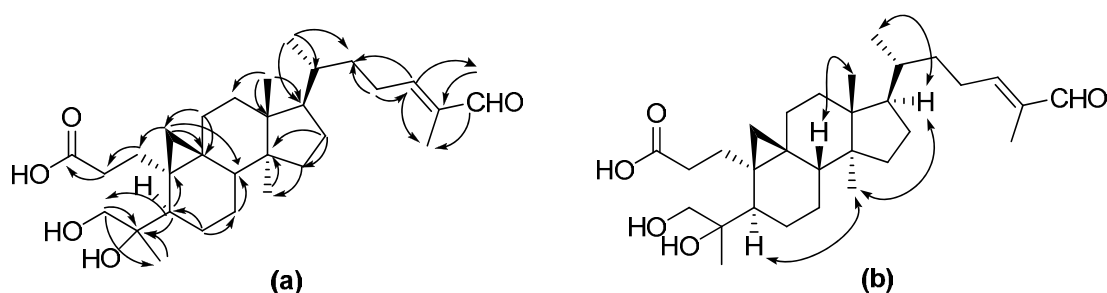


Figure 32. Key HMBC (a) and NOE (b) correlations of compound **82**.

Table 25. NMR data of compound **81** in CDCl₃.

Position	¹ H	¹³ C	HMBC
1	1.34 (2H, m)	27.9	C-2, C-3, C-5
2	2.49 (1H, m), 2.32 (1H, m)	31.8	C-1, C-3
3		179.2	
4	2.15 (1H, m)	36.6	C-29
5	1.94 (1H, m)	35.3	C-10, C-19, C-28
6	1.28 (1H, m), 1.01 (1H, m)	25.2	C-5, C-8
7	1.28 (2H, m)	25.0	C-5, C-8
8	1.42 (1H, m)	48.4	C-9, C-14, C-19, C-30
9		21.3	
10		27.2	
11	2.11 (1H, m), 1.17 (1H, m)	27.0	C-1, C-9, C-12, C-19
12	1.65 (2H, m)	33.1	C-8, C-11, C-13, C-18
13		45.0	
14		48.9	
15	1.39 (2H, m)	35.9	C-16
16	1.28 (2H, m)	28.1	C-15, C-20
17	1.58 (1H, m)	52.3	C-13
18	0.95 (3H, s)	18.3	C-12, C-13, C-14, C-17
19	0.61 (1H, d, <i>J</i> = 4.2 Hz) 0.39 (1H, d, <i>J</i> = 4.2 Hz)	30.3	C-5, C-8, C-19, C-10
20	1.28 (1H, m)	35.8	C-21, C-22
21	0.88 (1H, d, <i>J</i> = 6.3 Hz)	18.2	C-17, C-20
22	1.42 (1H, m), 1.03 (1H, m)	36.3	C-20, C-23
23	2.04 (1H, m), 1.86 (1H, m)	24.9	
24	5.10 (1H, t, <i>J</i> = 6.9 Hz)	125.2	C-25, C-26, C-27
25		130.9	
26	1.68 (3H, s)	25.7	C-24, C-25, C-27
27	1.60 (3H, s)	17.6	C-24, C-25, C-26
28	0.81 (3H, d, <i>J</i> = 7.0 Hz)	11.8	C-4, C-5, C-29
29	3.48 (2H, d, <i>J</i> = 7.1 Hz)	66.7	C-4, C-28
30	0.91 (3H, s)	19.4	C-13, C-14, C-15

Table 26. NMR data of compound **82** in CDCl₃.

Position	¹ H	¹³ C	HMBC
1	2.51 (1H, m), 1.37 (1H, m)	29.9	C-3, C-9, C-19
2	2.68 (1H, m), 2.28 (1H, m)	31.9	C-1, C-3
3		178.7	
4		78.3	
5	2.08 (1H, m)	42.9	C-4, C-7, C-10, C-19, C-29
6	2.06 (1H, m), 1.79 (1H, m)	24.8	C-5, C-7, C-8
7	1.27 (2H, m)	25.8	C-8, C-9
8	1.29 (1H, m)	48.7	C-6, C-19, C-30
9		23.5	
10		29.7	
11	2.12 (1H, m), 1.14 (1H, m)	26.5	C-8, C-9, C-13, C-19
12	1.65 (2H, m)	33.1	C-8, C-9
13		44.9	
14		47.9	
15	1.30 (2H, m)	35.9	C-8, C-13, C-30
16	1.91 (1H, m), 1.27 (1H, m)	28.2	C-13, C-15, C-30
17	1.60 (1H, m)	52.2	C-15, C-16
18	0.94 (3H, s)	18.6	C-12, C-13, C-17
19	0.56 (1H, br s) 0.54 (1H, br s)	31.1	C-5, C-8, C-9, C-11
20	1.42 (1H, m)	35.9	
21	0.91 (3H, m)	18.0	C-17, C-20, C-22
22	1.60 (1H, m), 1.22 (1H, m)	34.7	C-20
23	2.40 (1H, m), 2.27 (1H, m)	26.1	C-22, C-24
24	6.50 (1H, t, <i>J</i> = 7.1 Hz)	155.8	C-22, C-23, C-26, C-27
25		139.1	
26	9.38 (1H, s)	195.6	C-24, C-25, C-27
27	1.74 (3H, s)	9.2	C-24, C-25, C-26
28	1.22 (3H, s)	24.4	C-4, C-29
29	3.88 (1H, d, <i>J</i> = 11.0 Hz) 3.46 (1H, d, <i>J</i> = 11.0 Hz)	67.6	C-4, C-5, C-28
30	0.90 (3H, s)	19.5	C-13, C-14, C-15

2.4.6 Isolation and characterization of dammarane triterpenes from *G. collinsae* exudate

The MeOH-soluble fraction of the fresh apical buds of *G. collinsae* was partitioned between EtOAc and H₂O to afford an EtOAc extract, which was then subjected to silica gel column chromatography using EtOAc-hexane mixtures of increasing polarity as eluent. Further purification by repeated normal-phase column chromatography yielded a new dammarane-type triterpene (**83**) and its C-24 epimer (**84**), along with (20*R*,24*R*)-ocotillone (**85**) (Figure 33).

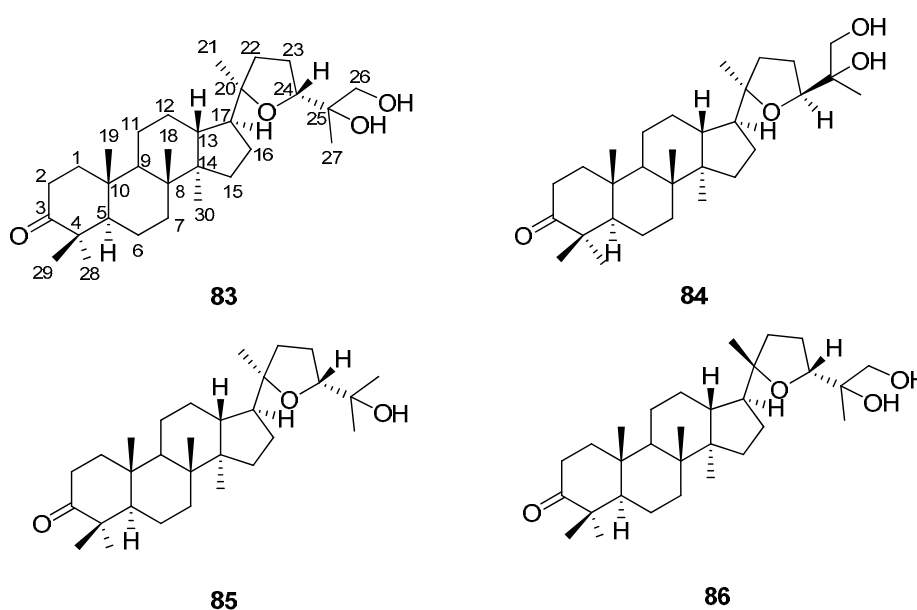


Figure 33. Dammarane triterpenes from *G. collinsae* exudate

Compound **83**, a white amorphous powder, had the molecular formula C₃₀H₅₀O₄ as established by the HRESIMS ion at m/z 497.3609 [M+Na]⁺ (calcd 497.3607). Its IR spectrum showed absorption bands at 1710 and 3466 (broad) cm⁻¹, which indicated the presence of carbonyl and hydroxyl groups. Inspection of the ¹³C NMR and HSQC spectra revealed the presence of 30 nonequivalent carbons consisting of one ketone carbonyl, seven tertiary methyls, 11 methylenes (one oxygenated), five methines (one oxygenated) and six quaternary carbons (two oxygenated). The ¹H NMR spectrum of **83** (Table 28) displayed seven singlet signals of tertiary methyls at δ_H 0.87, 0.93, 0.99, 1.01, 1.03, 1.08 and 1.16, associating with

dammarane-type triterpenoid. The planar structure of **83** was elucidated on the basis of 2D NMR (^1H - ^1H COSY, HSQC and HMBC) spectroscopic data (Figure 31). The tetrahydrofuran ring was evident from a key HMBC correlation from an oxygenated methine proton at δ_{H} 3.82 (H-24) to C-20. An oxygenated methylene group (δ_{H} 3.37 and 3.67; δ_{C} 71.3) was located as C-26 which was addressed by HMBC correlations from H-26 to C-24 and C-25. Detailed analyses of the NMR spectroscopic data of **83** as described above led to the establishment of the same planar structure as 20*S*,24*R*-epoxy-3-oxo-dammarane-25 ξ ,26-diol (**86**) [32]. The NMR data of **83** were also similar to those of **86**, with the marked difference being the ^{13}C resonances of Me-21 (δ_{C} 22.5 for **86**) and oxygenated carbons of the tetrahydrofuran unit [δ_{C} 86.4 qC (C-20), 82.7 CH (C-24) for **86**]. These results implied that compounds **83** and **86** are diastereomers differing from each other by the relative configurations of the C-20 and C-24 chiral centers. Comparison of the ^{13}C NMR data of **83** with those of (20*R*,24*R*)-ocotillone (**85**) and 20*S*,24*R*-epoxy-3-oxo-dammarane-25 ξ ,26-diol (**86**) at C-20 and C-24 (Table 28) indicated that compound **83** should have the 20*R*,24*R* configuration. Furthermore, this was also supported by the lack of NOESY correlation between Me-21 and H-24 (Figure 34). Thus, compound **83** was determined to be a new dammarane triterpene, 20*R*,24*R*-epoxy-3-oxo-dammarane-25 ξ ,26-diol.

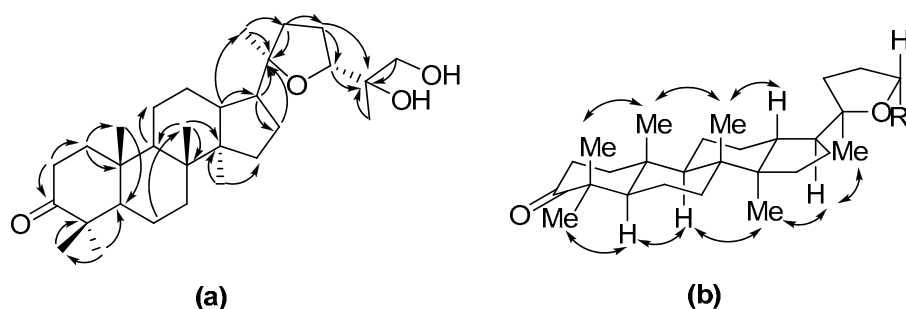


Figure 34. Key HMBC (a) and NOE (b) correlations of compound **83**.

Compound **84** was obtained as colorless gum, and it had the same molecular formula and gross structure as compound **83** by HRESIMS and interpretation of its 2D NMR spectroscopic data. The NMR spectra of **84** (Table 29) were very similar to those of **83**. The only marked difference was the intense NOESY

correlation between H-24 and Me-21 (Figure 32) observed in **84**, but lacked in **83**. This supported that compound **84** should have the $20R,24S$ configuration.

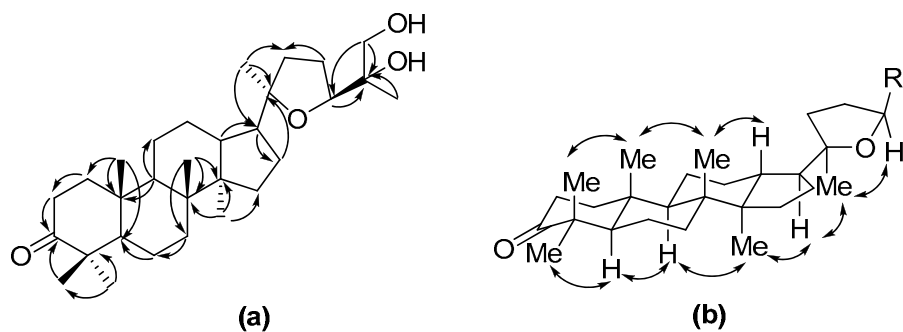


Figure 35. Key HMBC (a) and NOE (b) correlations of compound **84**.

Compound **85** was determined to be $(20R,24R)$ -ocotillone by means of the comparison with the reported spectral data [30] and [31].

Table 27. NMR data of compound **83** in CDCl₃.

Position	¹ H	¹³ C	HMBC
1	1.91 (1H, m), 1.45 (1H, m)	39.9	C-5, C-10, C-19
2	2.46 (2H, m)	34.1	C-1, C-3, C-10
3		218.0	
4		47.4	
5	1.36 (1H, m)	55.3	
6	1.55 (1H, m), 1.45 (1H, m)	19.6	C-10
7	1.56 (1H, m), 1.30 (1H, m)	34.5	
8		40.2	
9	1.41 (1H, m)	49.9	C-10, C-11
10		36.8	
11	1.52 (1H, m), 1.25 (1H, m)	22.1	
12	1.75 (1H, m), 1.33 (1H, m)	25.7	
13	1.61 (1H, m)	43.1	C-14, C-21
14		50.0	
15	1.47 (1H, m), 1.10 (1H, m)	31.3	
16	1.80 (2H, m)	26.1	C-20
17	1.85 (1H, m)	50.0	C-16, C-20, C-22
18	0.99 (3H, s)	15.1	C-7, C-8, C-9
19	0.93 (3H, s)	16.0	C-5, C-8, C-9, C-10
20		87.8	
21	1.16 (3H, s)	26.7	C-17, C-20
22	1.78 (1H, m), 1.68 (1H, m)	34.4	C-20, C-23
23	2.08 (1H, m), 1.81 (1H, m)	26.2	C-22, C-24, C-25
24	3.82 (1H, dd, <i>J</i> = 4.9, 10.4 Hz)	86.3	C-21, C-25
25		70.6	
26	3.67 (1H, t, <i>J</i> = 10.8 Hz) 3.37 (1H, d, <i>J</i> = 10.8 Hz)	71.3	C-21, C-24, C-25
27	1.01 (3H, s)	20.0	C-24, C-26
28	1.08 (3H, s)	27.0	C-4, C-5, C-29
29	1.03 (3H, s)	21.0	C-4, C-5, C-28
30	0.87 (3H, s)	16.2	C-14, C-15
26-OH	3.21 (1H, br d, <i>J</i> = 10.6 Hz)		

Table 28. NMR data of compound **84** in CDCl₃.

Position	¹ H	¹³ C	HMBC
1	1.91 (1H, m), 1.44 (1H, m)	39.9	C-2, C-10, C-19
2	2.46 (2H, m)	34.1	C-1, C-3, C-10
3		218.1	
4		47.4	
5	1.37 (1H, m)	55.3	
6	1.55 (1H, m), 1.46 (1H, m)	19.7	C-5, C-10
7	1.56 (1H, m), 1.31 (1H, m)	34.6	C-5, C-6
8		40.3	
9	1.42 (1H, m)	49.7	C-10, C-11
10		36.9	
11	1.51 (1H, m), 1.24 (1H, m)	22.3	
12	1.76 (1H, m), 1.29 (1H, m)	25.8	
13	1.64 (1H, m)	43.0	C-14, C-16
14		50.0	
15	1.46 (1H, m), 1.09 (1H, m)	31.4	C-30
16	1.82 (2H, m)	27.1	C-20
17	1.86 (1H, m)	50.1	C-20, C-22, C-23
18	0.99 (3H, s)	15.2	C-7, C-8, C-17
19	0.93 (3H, s)	16.1	C-1, C-5, C-9, C-10
20		86.8	
21	1.16 (3H, s)	26.7	C-17, C-20, C-22
22	1.88 (1H, m), 1.70 (1H, m)	34.7	C-20, C-23
23	1.81 (1H, m), 1.23 (1H, m)	27.1	C-22
24	3.83 (1H, dd, <i>J</i> = 4.7, 10.2 Hz)	86.3	C-23, C-25
25		72.5	
26	3.73 (1H, d, <i>J</i> = 11.0 Hz) 3.39 (1H, t, <i>J</i> = 11.0 Hz)	67.5	C-24, C-25
27	1.11 (3H, s)	21.4	C-24, C-25, C-26
28	1.07 (3H, s)	26.9	C-3, C-4, C-5, C-29
29	1.04 (3H, s)	21.0	C-3, C-4, C-5, C-28
30	0.87 (3H, s)	16.3	C-8, C-13, C-14, C-15

Table 29. NMR data of compound **85** in CDCl₃.

Position	¹ H	¹³ C	HMBC
1	1.93 (1H, m), 1.47 (1H, m)	39.9	
2	2.47 (2H, m)	34.1	
3		218.1	
4		47.4	
5	1.37 (1H, m)	55.3	
6	1.56 (1H, m), 1.46 (1H, m)	19.7	
7	1.56 (1H, m), 1.31 (1H, m)	34.6	
8		40.3	
9	1.42 (1H, m)	49.8	
10		36.9	
11	1.52 (1H, m), 1.26 (1H, m)	22.3	
12	1.77 (1H, m), 1.32 (1H, m)	25.8	
13	1.68 (1H, m)	43.0	
14		50.0	
15	1.46 (1H, m), 1.09 (1H, m)	31.4	
16	1.84 (2H, m)	27.0	
17	1.88 (1H, m)	50.2	
18	1.01 (3H, s)	15.2	C-7, C-8, C-9
19	0.94 (3H, s)	16.1	C-1, C-9, C-10
20		86.5	
21	1.15 (3H, s)	27.2	
22	1.88 (1H, m), 1.68 (1H, m)	34.8	
23	1.79 (1H, m), 1.32 (1H, m)	26.4	
24	3.63 (1H, m)	86.4	
25		70.2	
26	1.11 (3H, s)	24.1	C-24, C-25, C-27
27	1.19 (3H, s)	27.8	C-24, C-25, C-26
28	1.08 (3H, s)	26.7	C-3, C-4, C-5, C-29
29	1.04 (3H, s)	21.0	C-3, C-4, C-5, C-28
30	0.88 (3H, s)	16.3	C-8, C-13, C-14, C-15

2.4.7 Cytotoxic activity of isolated compounds

All isolated compounds were tested for *in vitro* cytotoxic activity against five human cancer cell lines; breast (BT474), lung (CHAGO), liver (Hep-G2), gastric (KATO-3), and colon (SW-620) cancer cell lines. Based on their structures, the compounds could be classified into four groups including 3,4-*seco*-cycloartanes with an exomethylene γ -lactone moiety, normal 3,4-*seco*-cycloartanes, normal cycloartanes and dammaranes. Thus, their cytotoxicity was individually presented in Tables 31-33.

As shown in Table 31, most compounds in the series of 3,4-*seco*-cycloartanes possessing an exomethylene γ -lactone displayed broad cytotoxicity against all cell lines tested. Surprisingly, only compound **73** bearing a furan ring in side chain did not show activity at all. However, when IC₅₀ values of **73** was compared to those of **74** and **75**, it revealed that the methyl ester at C-1 is required for activity of this group.

For fourteen normal 3,4-*seco*-cycloartanes, only compounds **70** and **72** showed toxicity against all cell lines tested with IC₅₀ values ranging from 3.97 to 13.77 μ M as shown in Table 32. It was noticed that the presence of a primary alcohol (-CH₂OH) in place of a methyl and an aldehyde at C-26 and C-29 caused a significant loss of activity. Moreover, the nucleophiles adduct of tubiferolide methyl ester led to the complete loss of activity as observed in **81** and **82**.

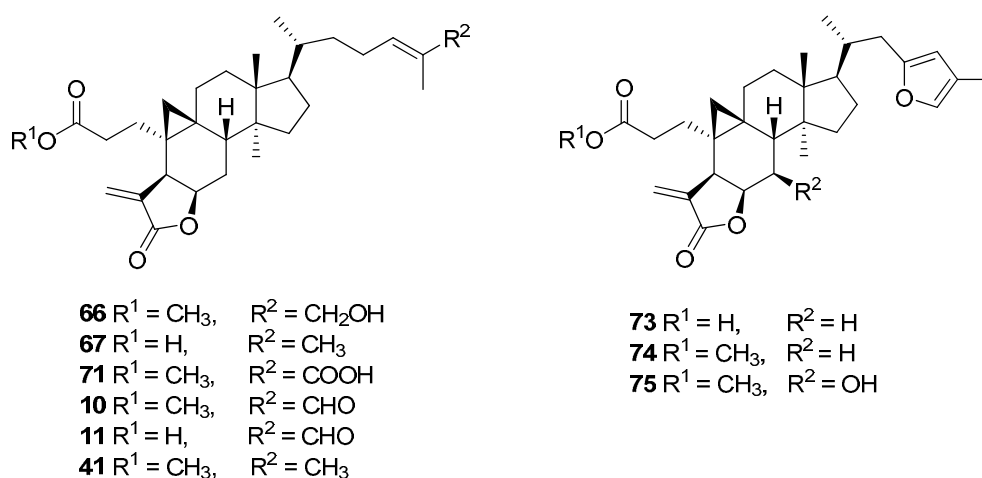


Figure 36. An α -methylene- γ -butyrolactone compounds from *Gardenia* spp.

Table 30. Cytotoxic data for α -methylene- γ -butyrolactone compounds

Compound	IC ₅₀ (μ M)*				
	BT474	KATO-3	CHAGO	SW-620	Hep-G2
10	I	17.4	I	12.46	13.69
11	13.65	12.12	11.23	10.32	13.28
41	11.04	10.15	8.45	11.97	7.06
66	11.80	4.21	7.96	3.61	5.82
67	10.63	7.85	11.18	11.88	12.50
71	I	18.59	10.12	13.19	14.34
73	I	I	I	I	I
74	I	12.30	3.31	I	9.42
75	I	12.69	8.69	4.90	5.42
Doxorubicin	16.41	10.02	7.32	I	6.18

*I: inactive, IC₅₀ > 20 μ M

Only three normal cycloartanes (**24**, **77** and **78**) were isolated and their cytotoxic data are shown in Table 33. There was no apparent significant or only a slight cytotoxicity on cell lines tested by these normal cycloartanes. This suggested that 3,4-*seco*-cycloartanes were more potent than normal ones. For the last group, dammarane triterpenes, similar results were obtained. Only compound **85** displayed moderate activity on CHAGO and SW-620 with the same IC_{50} value of 6.25 μ M.

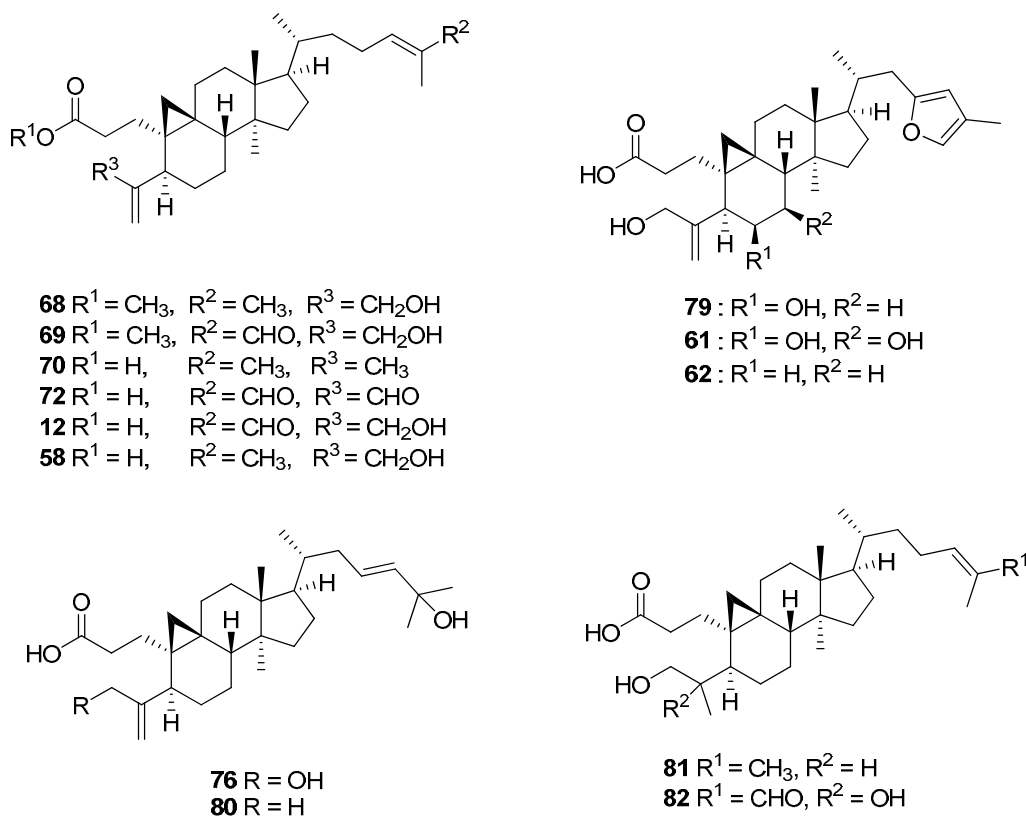


Figure 34. 3,4-*seco*-cycloartane triterpenes from *Gardenia* spp.

Table 31. Cytotoxic data for 3,4-*seco*-cycloartane triterpenes

Compound	IC ₅₀ (μ M)*				
	BT474	KATO-3	CHAGO	SW-620	Hep-G2
12	I	I	I	I	I
58	I	I	I	I	I
61	I	I	I	I	I
62	I	I	I	I	I
63	I	I	I	I	I
68	I	16.55	I	I	7.41
69	I	15.16	I	I	I
70	13.77	4.33	11.80	9.58	7.13
72	13.12	9.41	12.14	11.65	3.97
76	I	I	I	I	I
79	I	I	I	I	I
80	I	I	I	I	I
81	I	I	I	I	I
82	I	I	I	I	I
Doxorubicin	16.41	10.02	7.32	I	6.18

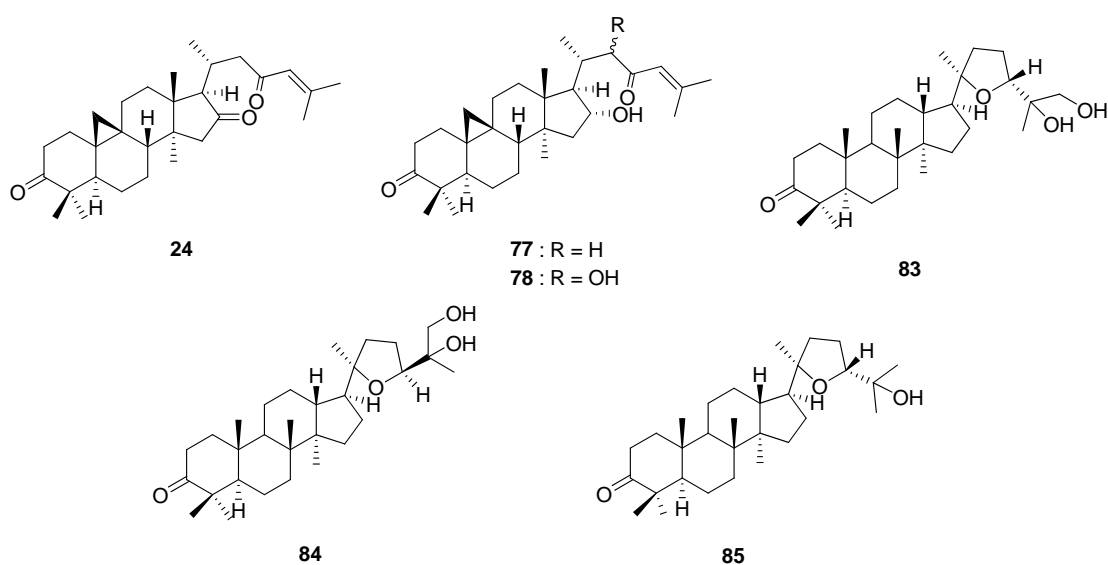
* I : inactive, IC₅₀ > 20 μ M**Figure 38.** cycloartane and dammarane triterpenes from *Gardenia* spp.

Table 32. Cytotoxic data for cycloartane and dammarane triterpenes

Compound	IC ₅₀ μM*				
	BT474	KATO-3	CHAGO	SW-620	Hep-G2
24	I	I	I	I	I
77	I	I	I	I	I
78	I	15.38	11.71	11.86	I
83	I	I	I	I	I
84	I	I	I	I	I
85	I	I	6.25	6.25	I
Doxorubicin	16.41	10.02	7.32	I	6.18

*I : inactive, IC₅₀ > 20 μM

2.5 Conclusion

Nineteen new compounds, sootepins A-G (**61-72**), gardenoins A-J (**73-82**), 20*R*,24*R*-epoxy-3-oxo-dammarane-25ξ,26-diol (**83**), and 20*R*,24*S*-epoxy-3-oxo-dammarane-25ξ,26-diol (**84**), together with ten known compounds, coronalolide methyl ester (**10**), tubiferolide methyl ester (**41**), coronalolide (**11**), secaubryenol (**58**), coronalolic acid (**12**), α-cycloart-24-ene-3,16,23-trione (**24**), dikamaliaratane D (**63**), dikamaliaratane C (**62**), dikamaliaratane A (**61**), and (20*R*,24*R*)-ocotillone (**85**) were isolated from five *Gardenia* plants. All compounds were tested for their cytotoxic activity against five human cancer cell lines. Among isolated triterpenes, 3,4-*seco*-cycloartanes possessing an exomethylene γ-lactone displayed the most potent activity and provided the broad cytotoxic activity against all cell lines tested. In addition, the presence of an α-methylene moiety at C-29 were also required for cytotoxicity in a series of normal 3,4-*seco*-cycloartanes.

CHAPTER III

STRUCTURE-ACTIVITY RELATIONSHIPS OF 3,4-*seco*-CYCLOARTANE DERIVATIVES

3.1 Introduction

Years of cumulative research can result in the development of a clinically useful drug, providing either a cure for a particular disease or symptomatic relief from a physiological disorder. A lead compound with a desired pharmacological activity may have associated with undesirable side effects, characteristics that limit its bioavailability, or structural features which adversely influence its metabolism and excretion from the body. Bioisosterism represents one approach used by the medicinal chemists [33].

One of the major areas that organic chemists can contribute to the development of new therapeutic agents is the study of the structure-activity relationships (SAR) of lead compounds. Analog synthesis of potential natural products will not only extend the resources from natural metabolites to an almost unlimited degree, but also help identify functional groups or structure features that are responsible for specific interactions of the drug molecule with receptors in the body, thus allowing the design of analogs with improved activity. In addition, the availability of synthetic drug analogs is often critical in cell biology studies, especially with appropriate techniques such as radioactive, fluorescent, and photo affinity labeling [90].

Triterpenes are a large and diverse class of organic compounds, produced by a variety of plants. The biological activities of triterpenes are very interesting such as cancer chemopreventive, anti-ucler, antidiabetic, angiogenesis inhibitor, anti HIV effect, and so on. Ring 3,4-*seco*-cycloartane type triterpenes have been mainly found in plants belonging to the genus *Gardenia* from family Rubiaceae. Many of them have been found to exhibit cytotoxic activities toward various cancer cell lines. In the

previous chapter, we described the isolation and characterization of a number of these triterpenes from the apical buds and exudate of Thai *Gardenia* species that exhibit cytotoxicity against five human cancer cell lines. Since 3,4-*seco*-cycloartanes with an exomehtylene γ -lactone showed the most promising activity, its analogs were designed and synthesized to gain more information about the structure-activity relationships of this compound series. Coronalolide (**11**) and sootepin A (**66**) obtained from *G. sootepensis* were used as starting materials for the modification at 3-position and 26-position, respectively.

3.2 Literature Review

In 2002 Tuchinda and co-worker studied the cytotoxic activity of isolated cycloartane triterpenes from leaves and twigs of *G. obtusifolia* and their modified derivatives. Naturally occurring compounds **23** and **24** showed no toxicity ($IC_{50} > 20 \mu M$) toward all cancer cell lines tested, leukemia (P-388), nasopharyngeal (KB), colon (Col-2), breast (BCA-1), lung (Lu-1), and rat glioma (ASK), while the modified compounds **87-91** showed broad cytotoxicity [9].

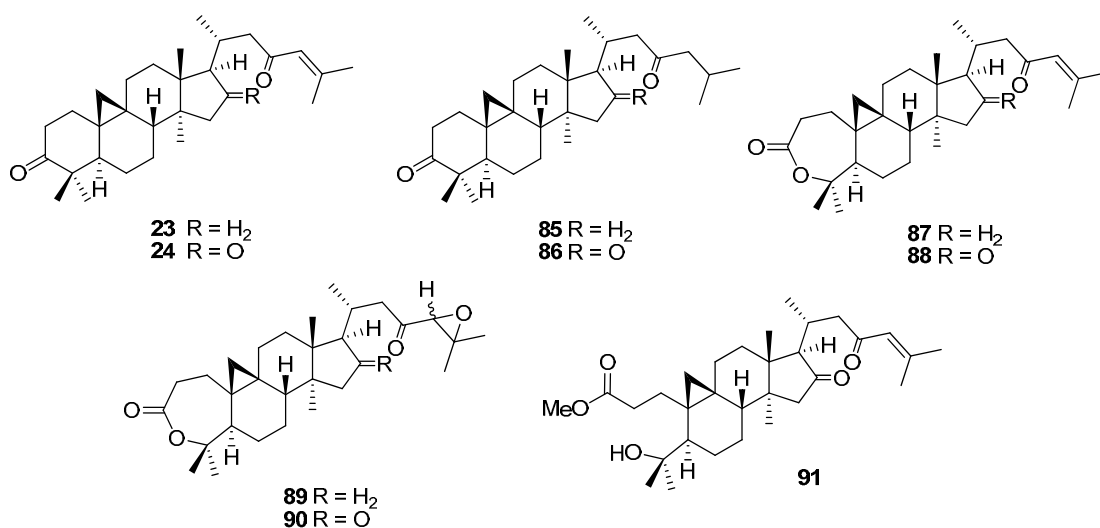


Figure 39. Isolated cycloartanes from *G. obtusifolia* and modified compounds.

In 2009 Feng and co-worker studied structure-activity relationships of cycloartane triterpenes isolated from the propolis. All compounds were test *in vitro*

against six different cancer cell lines; three murine cancer cell lines (colon 26-L5 carcinoma, B16-BL6 melanoma, and Lewis lung carcinoma) and three human cancer cell lines (lung A549 adenocarcinoma, cervix HeLa adenocarcinoma and HT-1080 fibrosarcoma). The results showed the functionality at C-3 position in cycloartane skeleton affected their cytotoxic effect, and the potency of activity was in the order of α -OH > =O > β -OH. The hydroxylation at C-23 or C-27 led to the enhancement of cytotoxicity, but the loss of activity was observed by hydroxylation at C-22 or C-28. Moreover, it was found the elongated conjugation between C-22 and C-26 in the side chain significantly increased the activity [35].

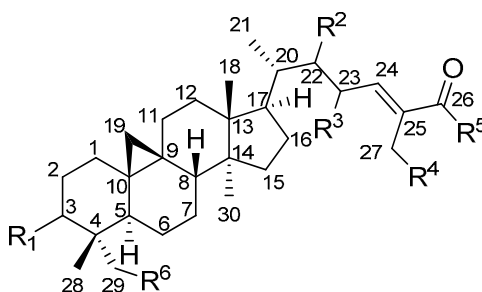


Figure 40. Skeleton of cycloartane-type triterpenes from the propolis

3.3 Experiments

3.3.1 General Experimental Procedures

3.3.2.1 Nuclear magnetic resonance spectrometer (NMR)

The NMR spectra were recorded in CDCl₃, D₂O, and DMSO-*d*₆ using a Bruker AV400 and Varian Mercury 400 plus spectrometer at 400 MHz for ¹H NMR and 100 MHz for ¹³C NMR using TMS (tetramethylsilane) as internal standard.

3.3.2.2 Mass spectrometer (MS)

HRESIMS spectra were obtained with a Bruker micrOTOF.

3.3.2 Chemicals

3.3.2.1 Solvent and chemicals

Reagents and solvents used below were obtained from commercial sources and when required were purified. Three starting materials,

sootepin A (**66**), corolanolide (**11**), and tubiferolide methyl ester (**41**) were isolated from *G. sootepensis*.

3.3.2.2 Chromatography

Merck's silica gel 60 No. 9385 was used as adsorbent for open column chromatography. Merck's thin layer chromatography (TLC) aluminum and glass sheets, silica gel 60 F₂₅₄ precoated, 20x20 cm, layer thickness 0.2 mm were used for TLC analysis. Detection was visualized under ultraviolet light at wavelengths of 254 nm and dipped with (NH₄)₆Mo₇O₂₄ in 5% H₂SO₄ solution.

3.3.3 Cytotoxic activity

Cytotoxicity test was carried out by the same manner with 2.3.5.

3.3.4. Reaction of cyloartane triterpene with some nucleophiles

3.3.4.1. Reaction of coronalolide (**11**) with nucleotides

A 5.0 mg of coronalolide (0.01 mmol) and nucleobase 5'-monophosphate disodium salt hydrate (0.01 mmol) were dissolved in 600 μ L of mixture of dimethyl sulfoxide-*d*₆ and D₂O (5:1) in a NMR sample tube. The solution was sealed with a parafilm. This solution was monitored by ¹H NMR and kept at room temperature for 24 h. Then, the solution was kept under the 40°C for 72 h and monitored by ¹H NMR.

3.3.4.2. Reaction of coronalolide (**11**) with sulfur compounds

A 0.01 mmol of coronalolide (5.0 mg) and 0.01 mmol of sulfur derivative (cysteine or cysteine methyl ester HCl) were dissolved in 500 μ L of dimethylsulfoxide-*d*₆ in a NMR sample tube. The solution was sealed with a parafilm. It was further monitored by ¹H NMR and kept at room temperature for 72 h.

3.3.4.3. Reaction of tubiferolide methyl ester (**41**) with sulfur and amine derivatives

A 0.04 mmol of tubiferolide methyl ester (20.0 mg), 0.04 mmol of sulfur or amine derivatives (2-mercaptoethanol, ethanolamine, pyrrolidine, morpholine, or thiophenol), ethanol (0.5 mL) and CH₂Cl₂ (2 mL) were mixed together

at room temperature for 24 h. The solvent was then removed under reduced pressure and the reaction was analyzed by ^1H NMR.

3.3.5. Synthesis of cycloartane triterpene derivatives

General procedure 1: Synthesis of compounds **157**, **160-166**, and **171-172**

Coronalolide (**11**) (50.0 mg, 0.10 mmol), alcohol or amine (0.16 mmol), DCC (25.0 mg, 0.12 mmol), HOBT (17.0 mg, 0.13 mmol), triethylamine (100 μL , 0.60 mmol), and CH_2Cl_2 (3.0 mL) were combined and stirred for overnight. The solution was precipitated with cold CH_3CN , filtrated, and evaporated *in vacuo*. The residue was then purified by column chromatography over silica gel using ethyl acetate-hexane or acetone-hexane mixtures as eluent.

Compound 92: Compound **92** (30.3 mg, 54% yield) was obtained from coronalolide (**11**) and phenol, ^1H NMR (400 MHz, CDCl_3); δ_{H} 9.42 (s, 1H), 7.41 (t, $J = 7.7$ Hz, 2H), 7.28 (m, 1H), 7.92 (d, $J = 7.7$, 2H), 6.51 (t, $J = 7.2$, 1H), 6.38 (br s, 1H), 5.81 (br s, 1H), 4.80 (dd, $J = 14.4$, 7.4 Hz, 1H), 3.33 (d, $J = 8.2$, 1H), 2.84-1.90 (m, 11H), 1.86-1.20 (m, 15H), 0.97 (m, 9H), 0.49 (d, $J = 5.2$ Hz, 1H), 0.27 (d, $J = 5.2$ Hz, 1H); ^{13}C NMR (100 MHz, CDCl_3); δ_{C} 195.3, 171.5, 170.6, 155.2, 150.5, 139.2 \times 2, 129.5 \times 2, 126.0, 123.2, 121.4 \times 2, 74.4, 51.4, 48.6, 45.7, 39.1, 38.3, 36.0, 34.8, 34.7, 33.0, 31.6, 30.9, 28.2, 27.8, 27.2, 26.6, 26.0, 25.2, 24.9, 23.4, 20.1, 18.2, 9.1; HRESIMS m/z $[\text{M}+\text{Na}]^+$ calcd for $\text{C}_{36}\text{H}_{46}\text{O}_5\text{Na}$, 581.3243, found 581.3234.

Compound 95: Compound **95** (14.0 mg, 21% yield) was obtained from coronalolide (**11**) and *L*-phenylalanine methyl ester HCl; ^1H NMR (400 MHz, CDCl_3); δ_{H} 9.39 (s, 1H), 7.27 (m, 3H), 7.07 (d, $J = 7.2$ Hz, 2H), 6.49 (t, $J = 7.1$ Hz, 1H), 5.92 (d, $J = 7.4$ Hz, 1H), 5.73 (br s, 1H), 4.88 (dd, $J = 13.2$, 6.0 Hz, 1H), 4.71 (dd, $J = 14.3$, 7.3 Hz, 1H), 3.74 (s, 3H), 3.22 (m, 1H), 2.42-1.80 (m, 10H), 1.78-1.20 (m, 16H), 0.92 (m, 9H), 0.40 (d, $J = 5.0$ Hz, 1H), 0.16 (d, $J = 5.0$ Hz, 1H); ^{13}C NMR (100 MHz, CDCl_3) δ_{C} 195.4, 172.2, 171.7, 170.8, 155.3, 139.2, 139.1, 135.8, 129.2 \times 2, 128.6 \times 2, 127.2, 123.3, 74.5, 53.0, 52.5, 51.4, 48.6, 45.8, 39.0, 38.3, 37.8, 36.0, 34.8, 34.7, 33.9, 33.0, 31.3, 28.4, 27.8, 27.3, 26.6, 26.0, 25.1, 23.4, 20.1, 18.3,

16.0, 9.2; HRESIMS m/z $[M+Na]^+$ calcd for $C_{40}H_{53}NO_6Na$, 666.3771, found 666.3811.

Compound 96: Compound **96** (12.2 mg, 22% yield) was obtained from coronalolide (**11**) and benzylamine; 1H NMR (400 MHz, $CDCl_3$) δ_H 9.39 (s, 1H), 7.29 (m, 5H) 6.49 (t, $J = 7.0$ Hz, 1H), 6.33 (s, 1H), 5.86 (s, 1H), 5.78 (s, 1H), 4.71 (dd, $J = 14.6, 7.8$ Hz, 1H), 4.44 (m, 2H), 2.44-1.26 (m, 24H), 3.26 (d, $J = 8.2$ Hz, 1H), 0.94-0.90 (m, 9H), 0.41 (d, $J = 5.0$ Hz, 1H), 0.19 (d, $J = 5.0$ Hz, 1H) : ^{13}C NMR (100 MHz, $CDCl_3$) δ_C 195.4, 171.9, 170.8, 155.3, 139.2 \times 2, 138.1, 128.8 \times 2, 128.0 \times 2, 127.7, 123.3, 74.5, 51.4, 48.7, 45.8, 43.8, 39.2, 38.4, 36.0, 34.8, 34.8, 33.6, 33.0, 31.6, 28.5, 27.8, 27.3, 26.6, 26.0, 25.1, 23.3, 20.2, 18.3, 16.0, 9.2; HRESIMS m/z $[M+H]^+$ calcd for $C_{37}H_{50}NO_4$, 572.3740, found 572.3755.

Compound 97: Compound **97** (10.0 mg, 16% yield) was obtained from coronalolide (**11**) and decylamine; 1H NMR (400 MHz, $CDCl_3$); δ_H 9.39 (s, 1 H), 6.48 (t, $J = 7.2$ Hz, 1H), 6.33 (s, 1H), 5.78 (s, 1H), 5.48 (m, 1H), 4.73 (q, $J=7.4, 7.6$ Hz, 1H), 3.24 (m, 3H), 2.41-1.25 (m, 40H) 0.94-0.86 (m, 12H), 0.41 (d, $J = 5.1$ Hz, 1H), 0.19 (d, $J = 5.1$ Hz, 1H): ^{13}C NMR (100 MHz, $CDCl_3$) δ_C 195.4, 172.0, 170.8, 155.2, 139.3, 139.2, 123.3, 74.6, 51.5, 48.7, 45.8, 39.7, 39.2, 38.4, 36.1, 34.8, 34.8, 33.7, 33.0, 31.9, 31.6, 29.6, 29.5 \times 2, 29.3 \times 2, 28.5, 27.8, 27.4, 26.9, 26.6, 26.0, 25.2, 23.4, 22.7, 20.2, 18.3, 16.0, 14.1, 9.2; HRESIMS m/z $[M+H]^+$ calcd for $C_{40}H_{64}NO_4$, 622.4835, found 622.4812.

Compound 98: Compound **98** (11.0 mg, 19% yield) was obtained from coronalolide (**11**) and heptylamine; 1H NMR (400 MHz, $CDCl_3$); δ_H 9.40 (s, 1 H), 6.49 (t, $J = 6.5$ Hz, 1H), 6.34 (s, 1H), 5.79 (s, 1H), 5.45 (m, 1H), 4.74 (q, $J = 6.5, 6.4$ Hz, 1H), 3.25 (m, 3H), 2.41-1.30 (m, 34H), 0.95-0.88 (m, 12H), 0.42 (d, $J = 4.0$ Hz, 1H), 0.20 (d, $J = 4.0$ Hz, 1H) : ^{13}C NMR (100 MHz, $CDCl_3$); δ_C 195.3, 172.0, 170.8, 155.2, 139.3, 139.2, 123.3, 74.6, 51.5, 48.8, 45.8, 39.8, 39.3, 38.4, 36.1, 34.95, 34.8, 33.7, 33.1, 31.7, 31.6, 29.7, 28.9, 28.5, 27.8, 27.4, 26.9, 26.6, 26.1, 25.2, 23.4, 22.6, 20.2, 18.3, 16.1, 14.1, 9.2; HRESIMS m/z $[M+H]^+$ calcd for $C_{37}H_{58}NO_4$, 580.4366, found 580.4298.

Compound 99: Compound **99** (10.0 mg, 19% yield) was obtained from coronalolide (**11**) and *n*-butylamine; ^1H NMR (400 MHz, CDCl_3); δ_{H} 9.40 (s, 1H), 6.49 (t, $J = 6.9$ Hz, 1H), 6.33 (br s, 1H), 5.79 (br s, 1H), 4.74 (m, 1H), 3.26 (m, 3H), 2.47-1.67 (m, 14H), 1.66-1.16 (m, 17H), 0.97-0.89 (m, 9H), 0.41 (d, $J = 3.6$ Hz, 1H), 0.19 (d, $J = 3.6$ Hz, 1H); ^{13}C NMR (100 MHz, CDCl_3) δ_{C} 195.3, 172.0, 170.8, 155.2, 139.3, 139.2, 123.3, 74.6, 51.5, 48.7, 45.8, 39.4, 39.3, 38.4, 36.1, 34.9, 34.8, 33.7, 33.0, 31.7, 31.6, 28.5, 27.8, 27.4, 26.6, 26.1, 25.2, 23.4, 20.2, 20.1, 18.3, 16.0, 13.7, 9.2; HRESIMS m/z $[\text{M}+\text{H}]^+$ calcd for $\text{C}_{34}\text{H}_{52}\text{NO}_4$, 538.3896, found 538.3844.

Compound 100: Compound **100** (12.0 mg, 22% yield) was obtained from coronalolide (**11**) and *sec*-butylamine; ^1H NMR (400 MHz, CDCl_3); δ_{C} 9.39 (s, 1H), 6.48 (t, $J = 6.8$ Hz, 1H), 6.33 (br s, 1H), 5.78 (br s, 1H), 5.52 (m, 1H), 4.73 (dd, $J = 14.6, 7.8$ Hz, 1H), 3.27 (d, $J = 7.8$ Hz, 1H), 3.07 (t, $J = 6.0$ Hz, 2H), 2.39-1.44 (m, 25 H), 0.92 (m, 15H), 0.48 (d, $J = 5.4$ Hz, 1H), 0.18 (d, $J = 5.4$ Hz, 1H); ^{13}C NMR (100 MHz, CDCl_3) δ_{C} ; 195.4, 172.1, 170.8, 155.3, 139.3, 139.2, 123.3, 74.6, 51.5, 48.7, 47.0, 45.8, 39.2, 38.4, 36.1, 34.8, 34.8, 33.7, 33.0, 31.7, 29.7, 28.5, 27.8, 27.3, 26.6, 26.1, 25.2, 23.4, 20.2, 20.2, 20.1, 18.3, 16.0, 9.2; HRESIMS m/z $[\text{M}+\text{H}]^+$ calcd for $\text{C}_{34}\text{H}_{52}\text{NO}_4$, 538.3896, found 538.3842.

Compound 101: Compound **101** (14.0 mg, 16% yield) was obtained from coronalolide (**11**) and *tert*-butylamine; ^1H NMR (400 MHz, CDCl_3); δ_{H} 9.40 (s, 1H), 6.49 (t, $J = 7.4$ Hz, 1H), 6.34 (br s, 1H), 5.80 (br s, 1H), 5.30 (br s, 1H), 5.26 (br s, 1H), 4.74 (dd, $J = 14.7, 7.6$ Hz, 1H), 3.27 (d, $J = 9.0$ Hz, 1H), 2.41 (m, 1H), 2.35-1.87 (m, 7 H), 1.82-1.45 (m, 12H), 1.41-1.18 (m, 12 H), 0.94 (m, 9H), 0.41 (d, $J = 5.1$ Hz, 1H), 0.19 (d, $J = 5.1$ Hz, 1H); ^{13}C NMR (100 MHz, CDCl_3); δ_{C} 195.3, 171.4, 170.8, 155.2, 139.24, 139.20, 123.3, 74.5, 51.5, 51.4, 48.7, 45.8, 39.3, 38.4, 36.1, 34.9, 34.8, 34.5, 33.0, 31.7, 29.7, 28.8 \times 3, 28.6, 27.8, 27.4, 26.6, 25.2, 23.4, 20.2, 18.3, 16.0, 9.2; HRESIMS m/z $[\text{M}+\text{H}]^+$ calcd for $\text{C}_{34}\text{H}_{52}\text{NO}_4$, 538.3896, found 538.3850.

Compound 106: Compound **106** (12.3 mg, 23% yield) was obtained from coronalolide (**11**) and pyrrolidine; ^1H NMR (400 MHz, CDCl_3); δ_{H} 9.38 (s, 1H), 6.48 (t, $J = 7.2$ Hz, 1H), 6.31 (s, 1H), 5.79 (s, 1H), 4.75 (dd, $J = 12.5, 6.3$

Hz, 1H), 3.45 (s, 4H), 3.30 (d, $J = 7.7$ Hz, 1H), 2.47-1.19 (m, 28H), 0.94 (m, 9H), 0.39 (d, $J = 5.0$ Hz, 1H), 0.20 (d, $J = 5.0$ Hz, 1H): ^{13}C NMR (100 MHz, CDCl_3) δ_{C} 195.4, 171.1, 170.9, 155.3, 139.3, 139.2, 123.2, 74.6, 51.5, 48.7, 46.8, 46.0, 45.8, 39.2, 38.5, 36.1, 34.9, 34.8, 33.0, 31.8, 31.0, 28.6, 27.8, 27.4, 26.6, 26.1, 25.2, 24.4, 24.4, 23.6, 20.2, 18.3, 16.1, 9.2; HRESIMS m/z $[\text{M}+\text{H}]^+$ calcd for $\text{C}_{34}\text{H}_{50}\text{NO}_4$, 536.3740, found 536.3725.

Compound 107: Compound **107** (12.0 mg, 22% yield) was obtained from coronalolide (**11**) and piperidine; ^1H NMR (400 MHz, CDCl_3) δ_{H} 9.40 (s, 1H), 6.49 (t, $J = 7.2$ Hz, 1H), 6.33 (s, 1H), 5.78 (s, 1H), 4.76 (dd, $J = 14.3, 7.3$ Hz, 1H), 3.56 (m, 2H), 3.41 (m, 2H), 3.30 (d, $J = 8.0$ Hz, 1H), 2.49-1.22 (m, 30H), 0.95 (m, 9H), 0.41 (d, $J = 5.1$ Hz, 1H), 0.22 (d, $J = 5.1$ Hz, 1H) : ^{13}C NMR (100 MHz, CDCl_3) δ_{C} 195.4, 170.9, 170.5, 155.3, 139.3, 139.2, 123.2, 74.6, 51.5, 48.7, 46.8, 45.8, 42.8, 39.3, 38.5, 36.1, 34.9, 34.8, 33.0, 31.6, 30.4, 28.6, 27.8, 27.4, 26.7, 26.6, 26.0, 25.5, 25.2, 24.5, 23.6, 20.2, 18.3, 16.1, 9.2; HRESIMS m/z $[\text{M}+\text{H}]^+$ calcd for $\text{C}_{35}\text{H}_{52}\text{NO}_4$, 550.3896, found 550.3903.

General procedure 2: Synthesis of compounds **93-94** and **102-105**

Coronalolide (**11**) (50.0 mg, 0.10 mmol), *N*-Hydroxysuccinimide (17.4 mg, 0.15 mmol), EDC·HCl (31.5 mg, 0.15 mmol), and CH_2Cl_2 (2.00 mL) were combined and stirred. A solution of amine (0.15 mmol), K_2CO_3 (100 mg, 0.80 mmol) and water (2.0 mL) were added over a period of 20 min. The mixture was stirred for 3 h at room temperature. The solution was quenched by the addition of 1N HCl. The organic layer was extract with EtOAc (2 \times), NaHCO_3 , brine, dried with MgSO_4 , filtrated, and the solvent was evaporated *in vacuo*. The residue was then purified by column chromatography over silica gel using ethyl acetate-hexane or acetone-hexane mixture as the eluent.

Compound 93: Compound **93** (17.5 mg, 30% yield) was obtained from coronalolide (**11**) and *N*-hydroxysuccinimide; ^1H NMR (400 MHz, CDCl_3); δ_{H} 9.40 (s, 1H), 6.49 (t, $J = 6.8$ Hz, 1H), 6.35 (br s, 1H), 5.75 (br s, 1H), 4.77 (m, 1H), 3.26 (d, $J = 7.7$ Hz, 1H), 2.93-2.67 (m, 6H), 2.47-2.24 (m, 2H), 2.16-1.87 (m, 2H),

1.85-1.43 (m, 14H), 1.41-1.16 (m, 4H), 0.95 (m, 9H), 0.47 (d, $J = 5.0$ Hz, 1H), 0.27 (d, $J = 5.0$ Hz, 1H): ^{13}C NMR (100 MHz, CDCl_3) δ_{C} 195.3, 170.5, 169.0, 168.2, 155.2, 139.2, 139.1, 123.2, 74.4, 51.5, 48.6, 45.7, 39.1, 39.2, 38.2, 36.0, 34.9, 34.8, 33.0, 30.8, 28.4, 28.1, 27.8, 27.2, 26.6, 26.0, 25.6 \times 2, 25.3, 23.8, 20.1, 18.3, 16.2, 9.2; HRESIMS m/z $[\text{M}+\text{H}]^+$ calcd for $\text{C}_{34}\text{H}_{46}\text{NO}_7$, 580.3274, found 580.3336.

Compound 94: Compound **94** (21.0 mg, 41% yield) was obtained from coronalolide (**11**) and *L*-phenylalanine; ^1H NMR (400 MHz, CDCl_3) ; δ_{H} 9.39 (s, 1H), 7.16 (br s, 5H), 6.48 (t, $J = 6.9$ Hz, 1H), 6.17 (br s, 1H), 5.56 (br s, 1H), 4.57 (br s, 2H), 3.22-2.89 (m, 4H), 2.41-1.25 (m, 23H), 0.92-0.79 (m, 9H), 0.25 (br s, 1H), -0.06 (br s, 1H) : ^{13}C NMR (100 MHz, CDCl_3) δ_{C} 195.3, 173.8, 171.2 \times 2, 155.3, 139.2 \times 2, 137.5, 129.1 \times 2, 128.5 \times 2, 126.8, 123.4, 74.8, 51.4, 50.7, 48.6, 45.7, 39.0, 38.3, 37.4, 36.1, 34.8, 33.3, 32.9, 31.5, 30.8, 28.2, 27.8, 27.2, 26.4, 26.1, 25.0, 23.4, 20.1, 18.3, 15.9, 9.2; HRESIMS m/z $[\text{M}+\text{H}]^+$ calcd for $\text{C}_{39}\text{H}_{52}\text{NO}_6$, 630.3795, found 630.3805.

Compound 102: Compound **102** (21.0 mg, 19% yield) was obtained from coronalolide (**11**) and diethylamine; ^1H NMR (400 MHz, CDCl_3) ; δ_{H} 9.40 (s, 1H), 6.49 (t, $J = 7.0$ Hz, 1H), 6.34 (s, 1H), 5.80 (s, 1H), 4.76 (dd, $J = 14.4, 7.4$ Hz, 1H), 3.40-3.29 (m, 5H), 2.46-1.10 (m, 30H), 0.95-0.93 (m, 9H), 0.42 (d, $J = 4.96$ Hz, 1H), 0.21 (d, $J = 4.96$ Hz, 1H): ^{13}C NMR (100 MHz, CDCl_3) δ_{C} 195.3, 171.3, 170.8, 155.2, 139.3, 139.2, 123.2, 74.5, 51.5, 48.8, 45.8, 42.2, 40.3, 39.4, 38.5, 36.1, 34.9, 34.8, 33.0, 31.6, 30.2, 28.7, 27.8, 27.4, 26.7, 26.1, 25.1, 23.4, 20.2, 18.3, 16.0, 14.5, 13.1, 9.2; HRESIMS m/z $[\text{M}+\text{H}]^+$ calcd for $\text{C}_{34}\text{H}_{52}\text{NO}_4$, 538.3896, found 538.3886.

Compound 103: Compound **103** (10.2 mg, 17% yield) was accomplished from coronalolide (**11**) and 3-bromopropylamine HCl; ^1H NMR (400 MHz, CDCl_3) δ_{H} 9.40 (s, 1 H), 6.49 (t, $J = 6.7$ Hz, 1H), 6.34 (s, 1H), 5.78 (s, 1H), 5.74 (s, 1H), 4.75 (dd, $J = 13.7, 6.5$ Hz, 1H), 3.43 (m, 4H), 3.27 (d, $J = 8.0$ Hz, 1H), 2.41-1.26 (m, 26H), 0.95-0.93 (m, 9H), 0.42 (d, $J = 4.0$ Hz, 1H), 0.20 (d, $J = 4.0$ Hz, 1H): ^{13}C NMR (100 MHz, CDCl_3) δ_{C} 195.3, 172.3, 170.7, 155.2, 139.2, 139.2, 123.2, 74.5, 51.4, 48.7, 45.8, 39.2, 38.4, 38.3, 36.0, 34.8, 34.8, 33.5, 33.0, 32.1, 31.5, 30.8,

28.5, 27.8, 27.3, 26.6, 26.0, 25.1, 23.3, 20.2, 18.3, 16.0, 9.2 ; HRESIMS m/z $[M+H]^+$ calcd for $C_{33}H_{49}^{79}BrNO_4$, 602.2845, found 602.2855.

Compound 104: Compound **104** (15.0 mg, 27% yield) was obtained from coronalolide (**11**) and 3-methoxypropylamine; 1H NMR (400 MHz, $CDCl_3$) δ_H 9.40 (s, 1H), 6.49 (t, $J = 6.9$ Hz, 1H), 6.33 (s, 1H), 6.11 (s, 1H), 5.78 (s, 1H), 4.74 (dd, $J = 13.7, 6.1$ Hz, 1H), 3.50 (m, 2H), 3.35 (s, 5H), 3.28 (d, $J = 7.7$ Hz, 1H), 2.41-1.22 (m, 26H), 0.95-0.93 (m, 9H), 0.42 (d, $J = 3.3$ Hz, 1H), 0.19 (d, $J = 3.3$ Hz, 1H); ^{13}C NMR (100 MHz, $CDCl_3$) δ_C 195.3, 171.9, 170.8, 155.2, 139.3, 139.2, 123.1, 74.5, 72.1, 58.8, 51.4, 48.7, 45.8, 39.1, 38.5, 38.4, 36.0, 34.8, 34.8, 33.7, 33.0, 31.6, 29.0, 28.5, 27.8, 27.3, 26.5, 26.0, 25.1, 23.4, 20.1, 18.3, 16.0, 9.1 ; HRESIMS m/z $[M+H]^+$ calcd for $C_{34}H_{52}NO_5$, 554.3845, found 554.3830.

Compound 105: Compound **105** (11.3 mg, 20% yield) was obtained from coronalolide (**11**) and cyclohexylamine; 1H NMR (400 MHz, $CDCl_3$) δ_H 9.40 (s, 1H), 6.49 (t, $J = 6.8$ Hz, 1H), 6.34 (s, 1H), 5.80 (s, 1H), 5.34 (d, $J = 7.4$ Hz, 1H), 4.74 (q, $J = 6.9, 6.8$ Hz, 1H), 4.12 (dd, $J = 13.6, 6.8$ Hz, 1H), 3.29 (d, $J = 7.8$ Hz, 1H), 3.74 (m, 1H), 2.43-1.10 (m, 33H), 0.95-0.93 (m, 9H), 0.41 (d, $J = 4.0$ Hz, 1H), 0.20 (d, $J = 4.0$ Hz, 1H); ^{13}C NMR (100 MHz, $CDCl_3$) δ_C 195.3, 171.1, 170.8, 155.2, 139.3, 139.2, 123.3, 74.6, 51.5, 48.7, 48.4, 45.8, 39.2, 38.4, 36.1, 34.8, 34.8, 33.8, 33.2 \times 2, 33.0, 31.6, 28.6, 27.8, 27.3, 26.6, 26.0, 25.5, 25.2, 24.9 \times 2, 23.4, 20.2, 18.3, 16.0, 9.2; HRESIMS m/z $[M+H]^+$ calcd for $C_{36}H_{54}NO_4$, 564.4053, found 564.4012.

General procedure 3: Synthesis of compounds 108-110

A solution of sootepin A (**66**) (30.0 mg, 0.06 mmol) in CH_2Cl_2 (3 mL) was treated with NEt_3 (100 μ L, 0.60 mmol) and acid chloride (0.2 mmol), then the mixture was stirred at room temperature for 30 min. After the complete reaction, the solution was evaporated under reduced pressure. The residue was then purified by column chromatography over silica gel using ethyl acetate-hexane mixture as the eluent.

Compound 108: Compound **108** (15.6 mg, 48% yield) was obtained from sootepin A (**66**) and acetyl chloride; ^1H NMR (400 MHz, CDCl_3) δ_{H} 6.33 (s, 1H), 5.73 (s, 1H), 5.45 (t, $J = 6.8$ Hz, 1H), 4.74 (dd, $J = 14.7, 7.6$ Hz, 1H), 4.45 (s, 2H), 3.69 (s, 3H), 3.23 (d, $J = 8.3$ Hz, 1H), 2.56-1.06 (m, 27H), 0.93-0.89 (m, 9H), 0.42 (d, $J = 5.1$ Hz, 1H), 0.17 (d, $J = 5.1$ Hz, 1H); ^{13}C NMR (100 MHz, CDCl_3) δ_{C} 173.5, 171.0, 170.7, 139.2, 130.4, 129.7, 123.1, 74.5, 70.4, 51.8, 51.4, 48.7, 45.7, 39.1, 38.4, 35.9, 35.7, 34.8, 33.0, 31.3, 31.0, 28.2, 27.8, 27.3, 26.6, 25.1, 24.7, 23.2, 21.0, 20.1, 18.4, 15.9, 13.9; HRESIMS m/z $[\text{M}+\text{H}^+]$ calcd for $\text{C}_{33}\text{H}_{49}\text{O}_6$, 541.3529, found 541.3553.

Compound 109: Compound **109** (25.5 mg, 73% yield) was obtained from sootepin A (**66**) and isobutyryl chloride; ^1H NMR (400 MHz, CDCl_3) δ_{H} 6.33 (s, 1H), 5.73 (s, 1H), 5.43 (t, $J = 6.5$ Hz, 1H), 4.74 (m, 1H), 4.45 (s, 2H), 3.68 (s, 3H), 3.23 (d, $J = 7.8$ Hz, 1H), 2.67-1.06 (m, 33H), 0.93-0.89 (m, 9H), 0.42 (d, $J = 4.5$ Hz, 1H), 0.17 (d, $J = 4.5$ Hz, 1H); ^{13}C NMR (100 MHz, CDCl_3) δ_{C} 177.0, 173.4, 170.7, 139.2, 130.0, 129.8, 129.8, 123.0, 74.5, 70.0, 51.8, 51.4, 48.7, 45.7, 39.1, 38.4, 35.9, 35.8, 34.8, 34.1, 33.0, 31.2, 31.0, 28.2, 27.8, 27.3, 26.6, 25.2, 24.6, 23.2, 20.1, 19.0, 18.4, 18.3, 15.9, 13.8; HRESIMS m/z $[\text{M}+\text{H}]^+$ calcd for $\text{C}_{35}\text{H}_{52}\text{O}_6$, 568.3764, found 568.3759.

Compound 110: Compound **110** (10.2 mg, 17% yield) was obtained from sootepin A (**66**) and benzoyl chloride; ^1H NMR (400 MHz, CDCl_3); 8.06 (d, $J = 7.7$ Hz, 2H), 7.45 (m, 2H), 7.38 (m, 1H), 6.34 (br s, 1H), 5.74 (br s, 1H), 5.55 (m, 1H), 4.71 (s, 2H), 3.70 (s, 3H), 3.23 (d, $J = 8.2$ Hz, 1H) 2.57-1.05 (m, 25H), 0.92 (m, 9H), 0.43 (d, $J = 4.1$ Hz, 1H), 0.18 (d, $J = 4.1$ Hz, 1H); ^{13}C NMR (100 MHz, CDCl_3) δ_{C} 173.5, 170.7, 166.5, 139.2, 133.6, 132.9, 130.2, 129.6 \times 2, 128.3 \times 2, 126.3, 123.1, 74.5, 70.7, 51.8, 51.4, 48.7, 45.7, 39.1, 38.4, 35.9, 35.7, 34.8, 33.0, 31.3, 30.9, 28.3, 27.8, 27.3, 26.6, 25.2, 24.7, 23.2, 20.1, 18.4, 15.9, 14.0; HRESIMS m/z $[\text{M}+\text{Na}]^+$ calcd for $\text{C}_{38}\text{H}_{50}\text{O}_6\text{Na}$, 625.3505, found 625.3542.

General procedure 4: Synthesis of compounds 111-118

Carboxylic acid (0.25 mmol) was dissolved in CH_2Cl_2 (2 mL). *N,N*-dimethylformamide (0.5 mL) was added into the flask while stirring. Oxalyl chloride

(85 μL , 1 mmol) was then added and stirred for 30 min at room temperature. After the complete reaction, the solution was evaporated under reduced pressure. The solution of sootepin A (**66**) (30 mg, 0.06 mmol), triethylamine (100 μL , 0.6 mmol) in CH_2Cl_2 (1 mL) was added to the prepared acid chloride. After 30 min, the reaction was quenched with 10% NaHCO_3 , and extracted with EtOAc. The combined organic layer was evaporated under reduced pressure. The residue was then purified by column chromatography over silica gel using ethyl acetate-hexane mixture as the eluent.

Compound 111: Compound **111** (20.8 mg, 56% yield) was obtained from sootepin A (**66**) and 4-fluorobenzoic acid; ^1H NMR (400 MHz, CDCl_3) ; δ_{H} 8.06 (m, 2H), 7.10 (t, $J = 8.6$ Hz, 2H), 6.33 (s, 1H), 5.73 (s, 1H), 5.53 (t, $J = 6.9$ Hz, 1H), 4.73 (dd, $J = 15.0, 7.6$ Hz, 1H), 4.69 (s, 2H), 3.68 (s, 3H), 3.23 (d, $J = 8.2$ Hz, 1H), 2.52-1.08 (m, 24H), 0.92-0.90 (m, 9H), 0.42 (d, $J = 5.2$ Hz, 1H), 0.17 (d, $J = 5.2$ Hz, 1H); ^{13}C NMR (100 MHz, CDCl_3) δ_{C} 173.5, 170.7, 167.0, 165.5, 164.5, 139.2, 132.2, 132.1, 130.5, 129.7, 123.1, 115.6, 115.4, 74.5, 70.9, 51.8, 51.4, 48.7, 45.7, 39.1, 38.4, 35.9, 35.7, 34.8, 33.0, 31.2, 31.0, 28.2, 27.8, 27.3, 26.6, 25.1, 24.7, 23.1, 20.1, 18.4, 15.9, 14.0; HRESIMS m/z $[\text{M}+\text{H}]^+$ calcd for $\text{C}_{38}\text{H}_{50}\text{FO}_6$, 621.3591, found 621.3585.

Compound 112: Compound **112** (11.1 mg, 29% yield) was obtained from sootepin A (**66**) and 4-chlorobenzoic acid; ^1H NMR (400 MHz, CDCl_3) ; δ_{H} 7.98 (d, $J = 8.3$ Hz, 2H), 7.41 (d, $J = 8.3$ Hz, 2H), 6.34 (s, 1H), 5.74 (s, 1H), 5.53 (t, $J = 6.9$ Hz, 1H), 4.75 (m, 1H), 4.70 (s, 2H), 3.69 (s, 3H), 3.23 (d, $J = 7.9$ Hz, 1H), 2.52-1.09 (m, 24H), 0.93-0.91 (m, 9H), 0.43 (d, $J = 5.1$ Hz, 1H), 0.17 (d, $J = 5.1$ Hz, 1H); ^{13}C NMR (100 MHz, CDCl_3) δ_{C} 173.5, 170.7, 165.6, 139.3, 139.2, 131.0 \times 2, 130.6, 129.6, 128.7 \times 2, 128.9, 123.1, 74.5, 71.0, 51.8, 51.4, 48.7, 45.7, 39.1, 38.4, 35.9, 35.7, 34.8, 33.0, 31.3, 31.0, 28.2, 27.8, 27.3, 26.6, 25.1, 24.7, 23.1, 20.1, 18.4, 15.9, 14.0 ; HRESIMS m/z $[\text{M}+\text{H}]^+$ calcd for $\text{C}_{38}\text{H}_{50}^{35}\text{ClO}_6$, 637.3296, found 637.3310.

Compound 113: Compound **113** (11.0 mg, 27% yield) was obtained from sootepin A (**66**) and 4-bromobenzoic acid; ^1H NMR (400 MHz, CDCl_3) ; δ_{H} 7.91 (d, $J = 8.4$ Hz, 2H), 7.58 (d, $J = 8.4$ Hz, 2H), 6.34 (s, 1H), 5.74 (s, 1H), 5.53

(t, $J = 7.0$ Hz, 1H), 4.75 (m, 1H), 4.70 (s, 2H), 3.69 (s, 3H), 3.23 (d, $J = 8.2$ Hz, 1H), 2.56-1.08 (m, 24H), 0.92-0.91 (m, 9H), 0.43 (d, $J = 5.1$ Hz, 1H), 0.17 (d, $J = 5.1$ Hz, 1H); ^{13}C NMR (100 MHz, CDCl_3) δ_{C} 173.5, 170.7, 165.7, 139.2, 131.7 \times 2, 131.1 \times 2, 130.6, 129.6, 129.4, 128.0, 123.1, 74.5, 71.0, 51.8, 51.4, 48.7, 45.7, 39.1, 38.4, 35.9, 35.7, 34.8, 33.0, 31.3, 31.0, 28.3, 27.8, 27.3, 26.6, 25.1, 24.7, 23.1, 20.1, 18.4, 15.9, 14.0 ; HRESIMS m/z $[\text{M}+\text{H}]^+$ calcd for $\text{C}_{38}\text{H}_{50}^{79}\text{BrO}_6$, 681.2791, found 681.2795.

Compound 114: Compound **114** (14.4 mg, 37% yield) was obtained from sootepin A (**66**) and 4-nitrobenzoic acid; ^1H NMR (400 MHz, CDCl_3) δ_{H} 8.28 (d, $J = 8.2$ Hz, 2H), 8.21 (d, $J = 8.2$ Hz, 2H), 6.33 (s, 1H), 5.73 (s, 1H), 5.57 (m, 1H), 4.76 (s, 2 H), 4.72 (m, 1H), 3.69 (s, 3H), 3.23 (d, $J = 7.7$ Hz, 1H), 2.52-1.22 (m, 24H), 0.93-0.92 (m, 9H), 0.42 (d, $J = 4.0$ Hz, 1H), 0.18 (d, $J = 4.0$ Hz, 1H); ^{13}C NMR (100 MHz, CDCl_3) δ_{C} 173.4, 170.7, 164.6, 150.6, 139.3, 135.8, 131.4, 130.7 \times 2, 129.2, 123.5 \times 2, 123.0, 74.5, 71.7, 51.8, 51.5, 48.7, 45.7, 39.1, 38.4, 35.9, 35.7, 34.9, 33.0, 31.3, 31.0, 28.3, 27.8, 27.3, 26.6, 25.2, 24.7, 23.3, 20.1, 18.4, 16.0, 14.0 ; HRESIMS m/z $[\text{M}+\text{H}]^+$ calcd for $\text{C}_{38}\text{H}_{50}\text{NO}_7$, 648.3536, found 648.3540.

Compound 115: Compound **115** (17.0 mg, 46% yield) was obtained from sootepin A (**66**) and 4-methylbenzoic acid; ^1H NMR (400 MHz, CDCl_3) δ_{H} 7.94 (d, $J = 8.0$ Hz, 2H), 7.23 (d, $J = 8.0$ Hz, 2H), 6.33 (d, $J = 2.1$ Hz, 1H), 5.73 (d, $J = 2.1$ Hz, 1H), 5.52 (t, $J = 6.8$ Hz, 1H), 4.74 (dd, $J = 14.7, 6.9$ Hz, 1H), 4.69 (s, 2H), 3.69 (s, 3H), 3.23 (d, $J = 8.3$ Hz, 1H), 2.56-1.08 (m, 27H), 0.92-0.90 (m, 9H), 0.42 (d, $J = 5.2$ Hz, 1H), 0.16 (d, $J = 5.2$ Hz, 1H) ; ^{13}C NMR (100 MHz, CDCl_3) δ_{C} 173.5, 170.7, 166.5, 142.7, 139.2, 130.5, 129.5 \times 2, 128.7 \times 2, 128.5, 127.1, 123.1, 74.5, 70.7, 51.8, 51.4, 48.7, 45.7, 39.1, 38.4, 35.9, 35.7, 34.8, 33.0, 31.2, 31.0, 28.2, 27.8, 27.3, 26.6, 25.1, 24.7, 23.1, 21.3, 20.1, 18.4, 15.9, 14.0 ; HRESIMS m/z $[\text{M}+\text{H}]^+$ calcd for $\text{C}_{39}\text{H}_{53}\text{O}_6$, 617.3842, found 617.3855.

Compound 116: Compound **116** (21.3 mg, 51% yield) was accomplished from sootepin A (**66**) and 4-phenoxybenzoic acid; ^1H NMR (400 MHz, CDCl_3) 8.01 (d, $J = 8.8$ Hz, 2H), 7.38 (t, $J = 7.0$ Hz, 2H), 7.18 (t, $J = 6.9$ Hz, 1H), 7.06 (d, $J = 8.3$ Hz, 2H), 6.98 (d, $J = 8.8$ Hz, 2H), 6.33 (s, 1H), 5.73 (s, 1H), 5.52 (t, $J = 6.5$ Hz, 1H), 4.74 (dd, $J = 15.0, 7.3$ Hz, 1H), 4.68 (s, 2H), 3.69 (s, 3H), 3.23 (d, $J =$

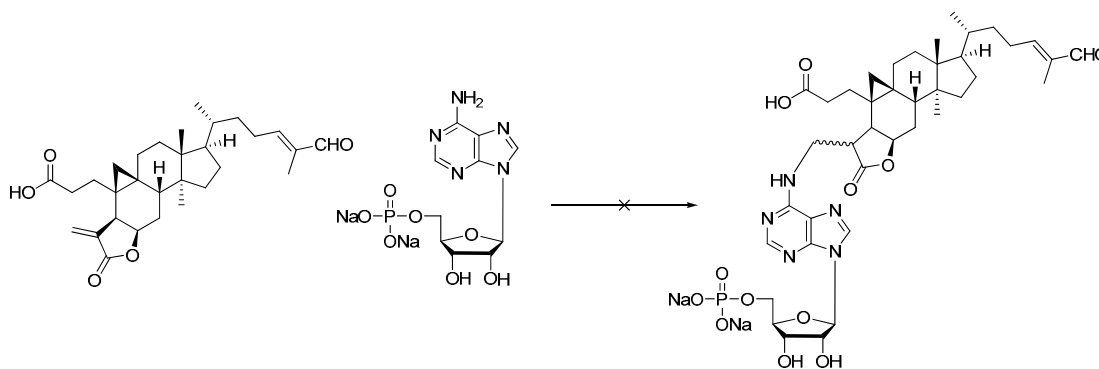
8.0 Hz, 1H), 2.52-1.08 (m, 24H), 0.92-0.90 (m, 9H), 0.42 (d, $J = 5.1$ Hz, 1H), 0.16 (d, $J = 5.1$ Hz, 1H); ^{13}C NMR (100 MHz, CDCl_3) δ_{C} 173.5, 170.7, 166.0, 161.8, 139.2, 131.7 \times 2, 130.2, 130.1, 130.0 \times 2, 129.9, 124.8, 124.5, 123.1, 120.1 \times 2, 117.3 \times 2, 74.5, 70.6, 51.9, 51.4, 48.7, 45.7, 39.1, 38.4, 35.9, 35.8, 34.8, 33.0, 31.2, 31.0, 28.2, 27.8, 27.3, 26.6, 25.1, 24.7, 23.0, 20.1, 18.4, 15.9, 14.0; HRESIMS m/z $[\text{M}+\text{H}]^+$ calcd for $\text{C}_{44}\text{H}_{55}\text{O}_7$, 695.3948, found 695.3920.

Compound 117: Compound **117** (19.9 mg, 55% yield) was accomplished from sootepin A (**66**) and isonicotinic acid; ^1H NMR (400 MHz, CDCl_3); δ_{H} 8.77 (d, $J = 3.7$ Hz, 2H), 7.85 (d, $J = 4.8$ Hz, 2H), 6.33 (br s, 1H), 5.73 (br s, 1H), 5.55 (t, $J = 6.9$ Hz, 1H), 4.74 (s, 2H), 3.68 (s, 3H), 3.23 (d, $J = 8.3$ Hz, 1H), 2.56-1.09 (m, 25H), 0.91 (m, 9H), 0.42 (d, $J = 5.2$ Hz, 1H), 0.17 (d, $J = 5.2$ Hz, 1H); ^{13}C NMR (100 MHz, CDCl_3) δ_{C} 173.5, 170.7, 164.9, 150.5 \times 2, 139.2, 137.7, 131.3 \times 2, 129.2, 123.1, 122.9, 74.5, 71.6, 51.9, 51.4, 48.7, 45.7, 39.1, 38.3, 35.9, 35.7, 34.8, 33.0, 31.2, 31.0, 28.2, 27.8, 27.3, 26.6, 25.1, 24.7, 23.2, 20.1, 18.4, 15.9, 14.0; HRESIMS m/z $[\text{M}+\text{H}]^+$ calcd for $\text{C}_{37}\text{H}_{50}\text{NO}_6$ 604.3638, found 604.3560.

Compound 118: Compound **118** (20.0 mg, 51% yield) was accomplished from sootepin A (**66**) and quinoline-2-carboxylic acid; ^1H NMR (400 MHz, CDCl_3); δ_{H} 8.30 (m, 2H), 8.16 (m, 1H), 7.88 (m, 1H), 7.78 (m, 1H), 7.64 (m, 1H), 6.33 (br s, 1H), 5.72 (br s, 1H), 5.59 (m, 1H), 4.88 (s, 2H), 4.72 (m, 1H), 3.68 (s, 3H), 3.21 (d, $J = 8.1$ Hz, 1H), 2.46-1.01 (m, 24H), 0.88 (m, 9H), 0.40 (d, $J = 5.1$ Hz, 1H), 0.15 (d, $J = 5.1$ Hz, 1H); ^{13}C NMR (100 MHz, CDCl_3) δ_{C} 173.5, 170.7, 165.2, 148.2, 147.7, 139.2, 137.2, 130.9, 130.8, 130.2, 129.4, 129.3, 128.5, 127.5, 123.1, 121.0, 74.5, 71.7, 51.8, 51.4, 48.7, 45.7, 39.1, 38.3, 35.9, 35.7, 34.8, 33.0, 31.2, 31.0, 28.2, 27.8, 27.2, 26.6, 25.1, 24.7, 23.1, 20.1, 18.4, 15.9, 14.1; HRESIMS m/z $[\text{M}+\text{H}]^+$ calcd for $\text{C}_{41}\text{H}_{52}\text{NO}_6$, 654.3795, found 654.3715.

3.4 Results and Discussion

From the chemical behavior of α -methylene- γ -butyrolactone demonstrated so far (Michael acceptors), it was the interaction of such molecules with biological structures even if an alkylation of DNA could be hypothesized. Based on the cytotoxic results of naturally occurring 3,4-*seco*-cycloartanes, it is anticipated that an exomethylene- γ -lactone moiety is required for their activity. In order to prove this fact, the addition of this group with some nucleophiles was decided to carry out. Reactions of coronalolide (**11**) and four nucleotides, guanosine, adenosine, uridine and cytidine-5'-monophosphate disodium salt hydrate were studied by ^1H NMR. No reactions could be observed both at room temperature and 40°C .



Scheme 1. Proposed reaction of coronalolide (**11**) and adenosine 5'-monophosphate disodium salt hydrate

From the literature review, Benezra and co-workers suggested that it was probably the 1,4-addition on the α -methylene exocyclic double bond of the α -methylene- γ -butyrolactone by amino acid thiol (-SH) and/or amino groups (-NH₂) of proteins (such as in cysteine and lysine) [48]. Unfortunately, ^1H -NMR spectra of both reactions between the α -methylene exocyclic moiety of coronalolide and two cysteines did not proceed as expected.

Next, the starting material was changed from coronalolide (**11**) to tubiferolide methyl ester (**41**) because we proposed that the aldehyde may react with the amine to form immine derivatives. The disappearance of the terminal alkene protons in the ^1H -NMR spectrum of reaction between tubiferolide methyl ester (**41**)

and 2-mercaptoethanol indicated that the 1,4-addition of 2-mercaptoethanol on α -methylene exocyclic double bond of (**41**) could proceed well as shown in Figure 41. Similar results were obtained by the reaction between tubiferolide methyl ester and thiophenol, pyrrolidine, and morpholine as shown in Figures 42-45, respectively. However, no reaction was observed with ethanolamine. These data supported the previous reports that the α -methylene- γ -butyrolactone prefers to react with sulfur and nitrogen nucleophiles [37, 38], although the reason why some nitrogen and sulfur nucleophiles do not work is not yet apparent.

To prove our hypothesis, that the α -methylene- γ -butyrolactone is essential to the cytotoxic activities, the adducts of tubiferolide methyl ester (**41**) and 2-mercaptoethanol and morpholine were subjected to cytotoxicity assay against five human cancer cell lines as above. Results showed that they were inactive and gave IC_{50} values more than 20 μ M. This indicated that the α -methylene- γ -butyrolactone is necessary for the cytotoxicity of this compound series as expected.

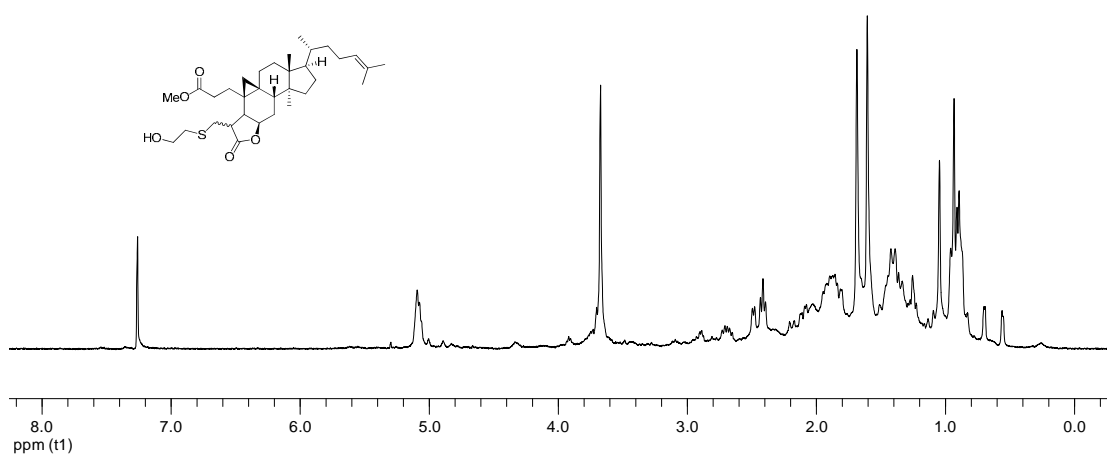


Figure 41. $^1\text{H-NMR}$ (CDCl_3) spectrum of crude reaction of tubiferolide methyl ester and 2-mercaptoethanol.

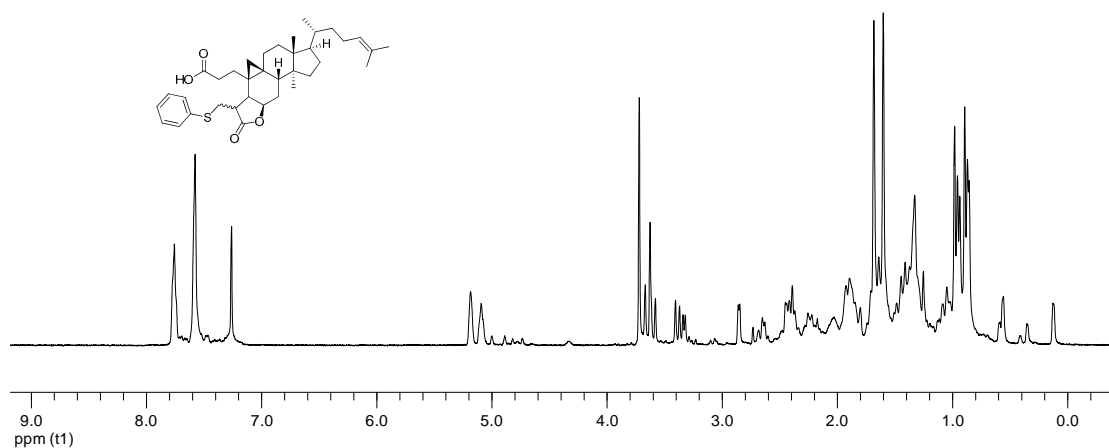


Figure 42. ¹H-NMR (CDCl₃) spectrum of crude reaction of tubiferolide methyl ester and thiophenol.

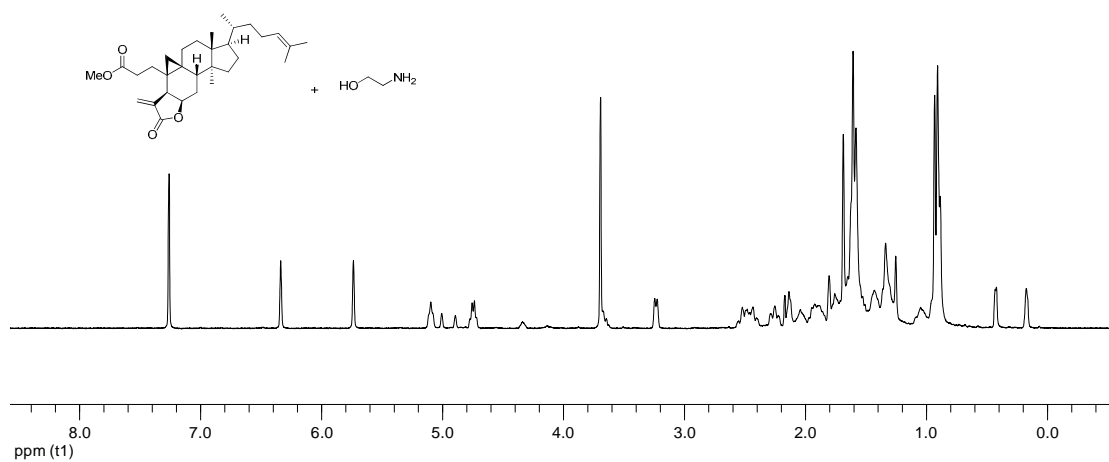


Figure 43. ¹H-NMR (CDCl₃) spectrum of crude reaction of tubiferolide methyl ester and ethanolamine.

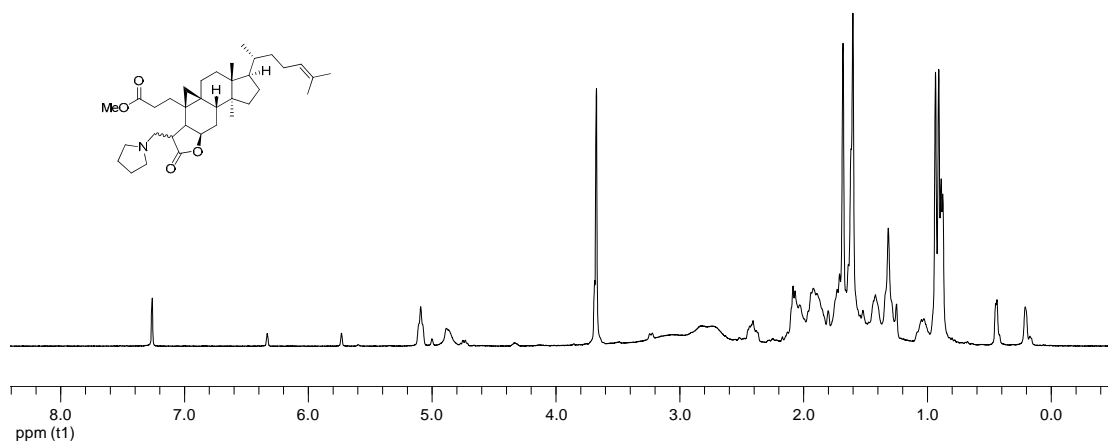


Figure 44. $^1\text{H-NMR}$ (CDCl_3) spectrum of crude reaction of tubiferolide methyl ester and pyrrolidine.

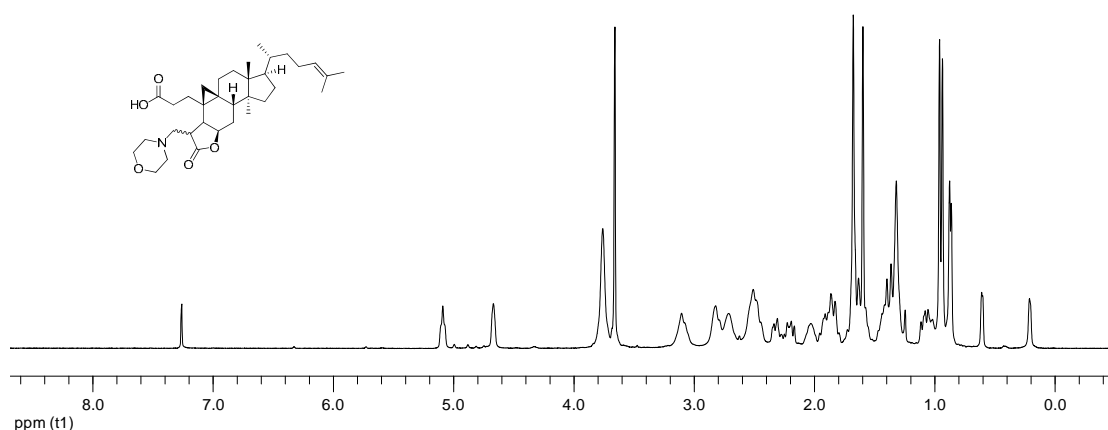


Figure 45. $^1\text{H-NMR}$ (CDCl_3) spectrum of crude reaction of tubiferolide methyl ester and morpholine

To gain more information about the structure-activity relationships of 3,4-*seco*-cycloartanes bearing an exomethylene γ -lactone, semi-synthetic derivatives of naturally occurring coronalolide (**11**) and sootepin A (**66**) were prepared. The first compound series were obtained from coronalolide (**11**) by modification of the COOH at C-1 to ester and amide functions using the combination of DCC or EDC and HOBT as the coupling agent. As shown in Figure 46, two esters and 14 amides were

synthesized. All semi-synthetic derivatives of this series were further evaluated for their cytotoxicity, compared to the parent compound **11**, and the results are presented in Table 33. Most of them showed more selectivity, particularly to CHAGO and SW-620, while the parent one exhibited broad toxicity toward all cell lines tested.

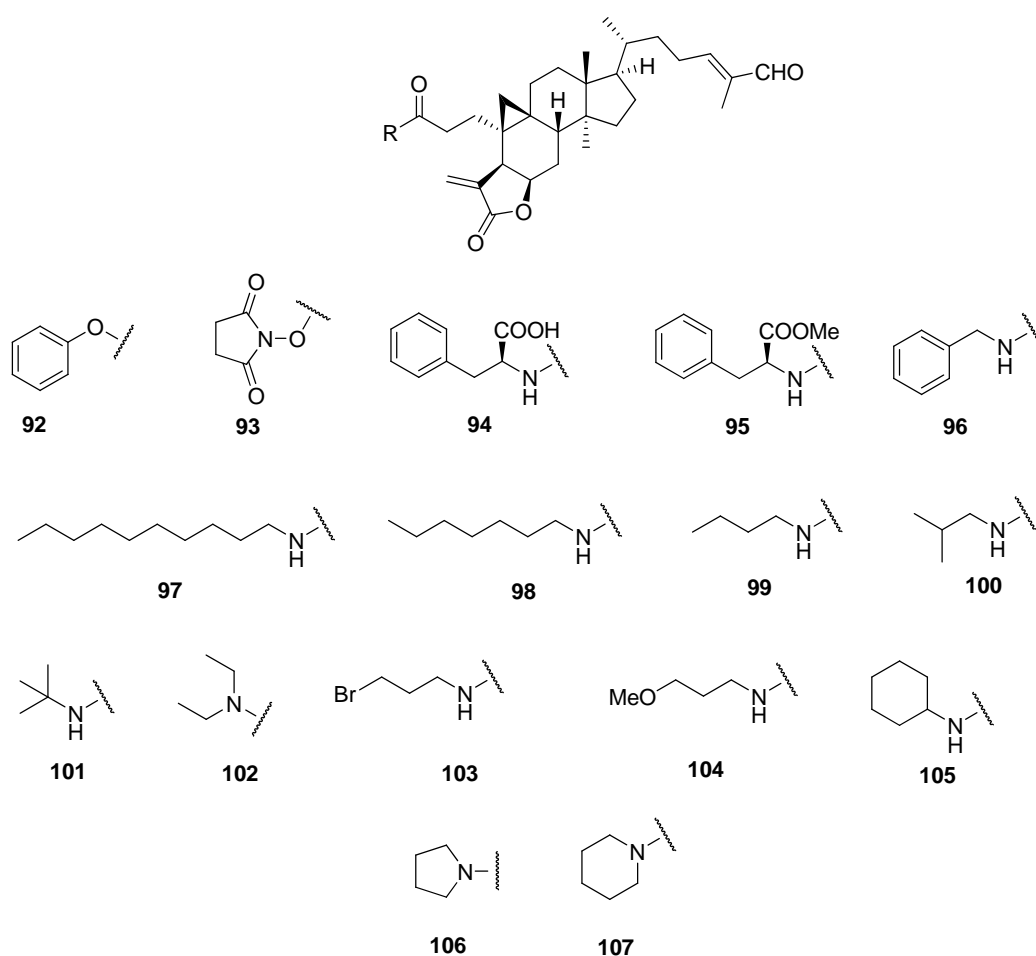


Figure 46. The ester and amide derivatives of colonarolide.

Table 33. Cytotoxic data for compounds **71**, and **157-171**.

Compound	IC ₅₀ (μM)*				
	BT474	KATO-3	CHAGO	SW-620	Hep-G2
11	13.65	12.12	11.23	10.32	13.28
92	I	I	9.65	12.21	8.21
93	I	I	I	I	I
94	I	I	7.84	10.51	9.73
95	I	I	7.55	10.05	I
96	I	16.16	10.27	12.05	10.63
97	I	I	I	I	I
98	I	I	10.71	13.40	7.52
99	I	I	10.19	11.55	I
100	I	I	8.37	10.47	I
101	I	I	10.06	10.92	I
102	I	I	12.58	12.63	11.53
103	I	I	13.42	10.37	I
104	I	I	12.64	11.07	15.75
105	I	I	7.09	12.52	I
106	I	I	15.19	9.95	16.26
107	I	14.13	14.04	11.17	I
Doxorubicin	16.41	10.02	7.32	I	6.18

*I : inactive, IC₅₀ > 20 μM

For the second series of semi-synthetic derivatives, the compounds were obtained by modification of the primary alcohol of sootepin A (**66**). Compounds **108-110** were prepared by treating **66** with the corresponding acyl chloride in the presence of triethylamine. Reactions of **66** with the corresponding acids, pretreated with oxalyl chloride in the presence of a catalytic amount of DMF to generate the acid chloride, afforded derivatives **111-118**. The structures of the modified compounds are shown in Figure 47. Also, all synthetic compounds were evaluated for their cytotoxic activity and the results are shown in Table 34. Similar to the results from coronalolide derivatives, the semi-synthetic derivatives did not display the improved activity when compared to the parent compound. However, this could be concluded that the

hydroxyl group at C-26 position of sootepin A is necessary for cytotoxicity against cancer cell lines.

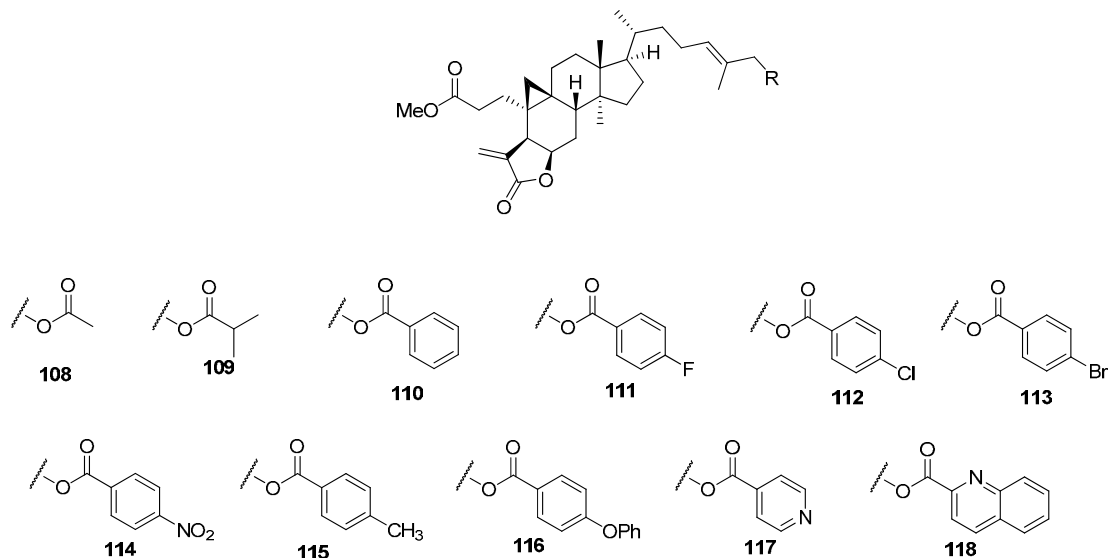


Figure 47. The ester derivatives of sootepin A.

Table 34. Cytotoxic data for compounds **66** and **108-118**.

Compound	IC ₅₀ (μM)*				
	BT474	KATO-3	CHAGO	SW-620	Hep-G2
66	11.80	4.21	7.96	3.61	5.82
108	I	I	15.05	7.84	8.91
109	I	I	14.31	4.34	7.12
110	I	I	11.99	5.08	9.65
111	I	13.69	8.75	5.82	5.62
112	I	14.45	10.18	8.13	8.46
113	I	I	I	11.02	I
114	I	I	12.98	10.81	12.69
115	I	I	11.30	12.45	14.79
116	I	I	11.83	7.47	8.76
117	I	I	11.35	12.01	11.89
118	I	I	9.54	11.18	9.79
Doxorubicin	16.41	10.02	7.32	I	6.18

*I : inactive, IC₅₀ > 20 μM

3.5 Conclusion

The chemical binding study of α -methylene- γ -butyrolactone of 3,4-*seco*-cycloartane triterpens with some nucleophiles displayed the 1,4-addition on α -methylene- γ -butyrolactone moiety selective to the sulfur than nitrogen nucleophiles. Moreover, their adducts did not show cytotoxicity at all against cancer cell lines tested, this suggested that the exomethylene γ -lactone moiety are required for cytotoxic effect of the 3,4-*seco*-cycloartanes.

In order to study the structure-activity relationships of the 3,4-*seco*-cycloartane derivatives, two ester and 14 amide derivatives of coronalolide (**11**) and 11 ester analogs of sootepin A (**66**) were synthesized and evaluated for their cytotoxic activity. All of semi-synthetic derivatives did not exhibit more potent activity than the parent compounds; however, the above data indicated the cytotoxicity of 3,4-*seco*-cycloartane triterpenes did not mainly depend on the functionality at C-3 and C-26. Additionally, it seemed that the unsaturated α -methylene- γ -butyrolactone ring skeleton plays the crucial role for cytotoxicity, and the substituents at C-3 and C-26 may affect their selectivity.

CHAPTER IV

APOPTOTIC ACTIVATION OF HUMAN LIVER CANCER, HEP-G2, INDUCED BY SOOTEPIN G

4.1 Introduction

Apoptosis, a controlled process of programmed cell death, plays an essential role in many developmental and physiological processes ranging from fetal development to adult tissue homeostasis. Amongst others, an important function of apoptosis lies in the elimination of damaged cells. For example, cells with genetic damage caused by exposure to carcinogens may be deleted by undergoing apoptosis, thereby preventing their replication and the accumulation of clones of abnormal cells [40].

Cancer is characterized by uncontrolled proliferation and reduced apoptosis. Activation of apoptotic pathways is a key mechanism by which cytotoxic drugs kill cancerous cells. Therefore, the compounds that block or suppress the growth of tumor cells by inducing apoptosis are considered to have potential as anti-cancer agents. Apoptosis pathways can generally be divided into signaling via the extrinsic (death receptors) and the intrinsic (mitochondria) pathway (Figure 48). Cross-linking of death receptors with its natural ligands (e.g. CD95L, TRAIL and TNF α) induces a sequential activation of caspase-8 and caspase-3, which cleaves target proteins leading to apoptosis. Intrinsic death stimuli (e.g. DNA-damaging agents, reactive oxygen species) directly or indirectly activate the mitochondria pathway causing the release of cytochrome c (a mitochondria protein) and the formation of the apoptosome complex consisting of cytochrome c, Apaf-1 and caspase-9. Caspase-9 is further activated at the apoptosome and in turn activates caspase-3. In the mitochondria pathway, apoptosis is largely regulated by the pro-apoptotic, such as Bax, Bak, Bid and Smac, and anti-apoptotic proteins, e.g. Bcl-2, Bcl-xl, Mcl-1 and XIAP. Overexpression of anti-apoptotic Bcl-2 family members is known to cause apoptosis

and therapy resistance in a wide range of cancers. Hence, the development of therapies by targeting these apoptosis modulators appears to be a promising approach.

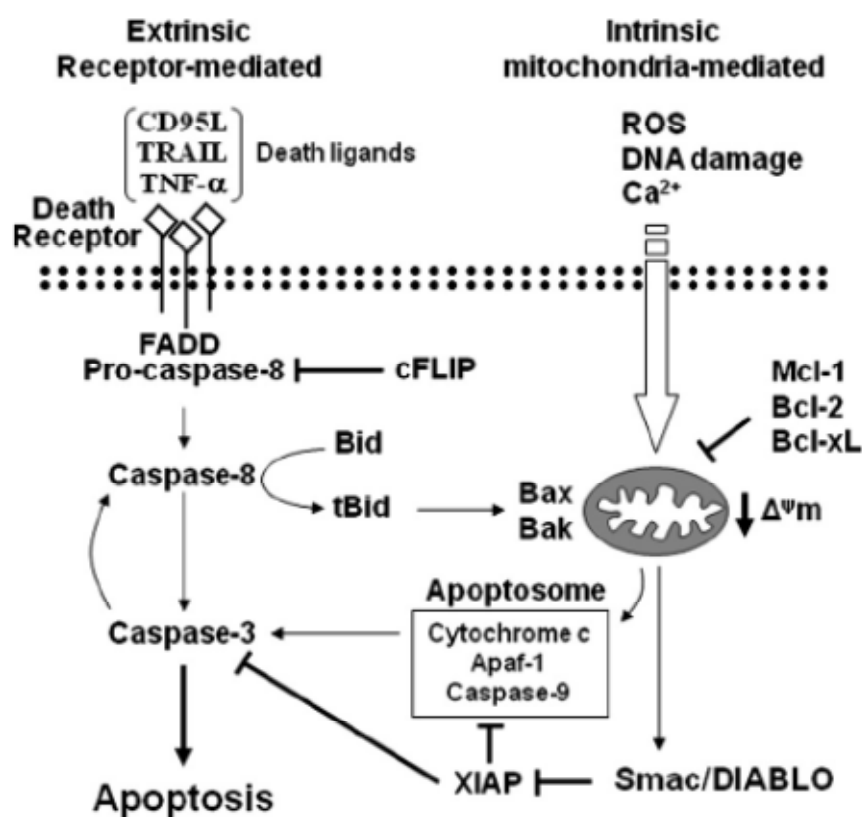


Figure 48. Extrinsic and intrinsic apoptosis pathway [72].

Based on our results in the previous chapters, sootepin G (**72**), a new 3,4-*seco*-cycloartane, isolated from *G. sootepensis* displayed the promising cytotoxicity, particularly on Hep-G2 cell lines with an IC_{50} value of 3.67 μ M, we thus decided to investigate its effect on the induction of apoptosis in this cell lines.

4.2 Literature Review

Natural products of various chemical classes can exert many beneficial effects on human health including the prevention of cancer as well as suppression of tumor growth. These chemopreventive and antitumor activities are mediated, at least to a large extent, via the modulation of cell death pathways including apoptosis in

cancer cells. There are multiple intervention points within the apoptotic machinery that have been identified to mediate the antitumor effects of natural compounds, depending on the specific agents. Natural products often exert pleiotropic effects, a feature that may prove to be especially advantageous, as distinct mechanisms of cell death evasion can be simultaneously targeted in cancer cells. Several recent studies on natural product compounds as anticancer drugs displayed in Table 35.

Table 35. Some apoptotic-inducing natural compounds used in cancer chemotherapy

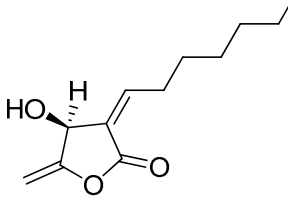
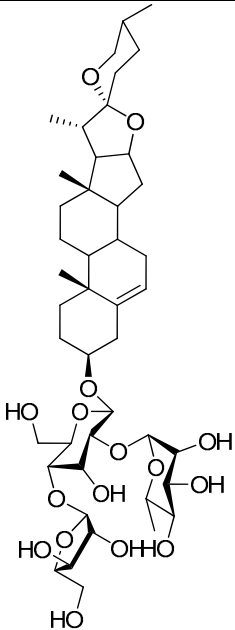
Compound	Source	Structure	Probable mechanisms	Reference
ETA	<i>Pseudomonas aeruginosa</i>		Induces cell cycle arrest and caspase-3 activation	[91, 92]
IKA	<i>Cinnamomum kotoense</i>		Block G ₀ /G ₁ cell cycle progression and also decrease the interaction of p53–MDM2	[93]
PD	<i>Paris polyphylla</i>		Acts on mitochondria and elicits dissipation of transmembrane potential ($\Delta\psi_m$), generation of ROS, and release of cytochrome c and AIF	[94]

Table 35. Some apoptotic-inducing natural compounds used in cancer chemotherapy
(Cont.)

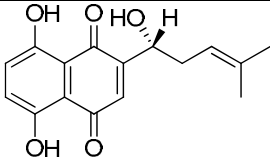
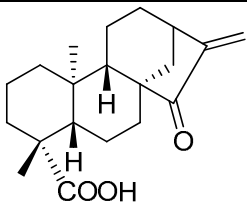
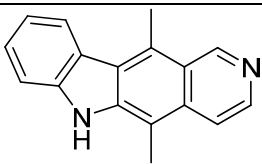
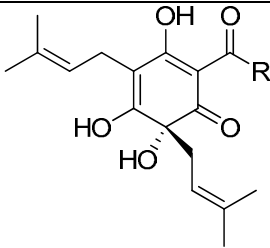
Compound	Source	Structure	Probable mechanisms	Reference
Shikonin (Human Colorectal Carcinoma Cells)	<i>Lithospermum erythrorhizon</i>		loss of mitochondrial membrane potential, reactive oxygen species (ROS) generation, cytochrome c release, and subsequent induction of pro-caspase-9 and -3 processing	[95]
EOKA	<i>Espeletia schultzei</i> ; <i>Espeletia grandiflora</i>		activates caspase-3 and caspase specific cleavage of PARP, and also induces nucleosomal DNA fragmentation as well as reduction of Bcl-2 protein level	[96]
Ellipticine	<i>Ochrosia borbonica</i> , <i>Excavatia coccinea</i>		accumulation of dephosphorylated mutant p53	[97]
Hop Bitter Acids (e. g. humulone)	<i>Humulus lupulus</i> L.		Fas activation and mitochondrial dysfunctions	[98]

Table 35. Some apoptotic-inducing natural compounds used in cancer chemotherapy
(Cont.)

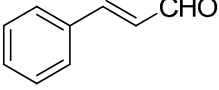
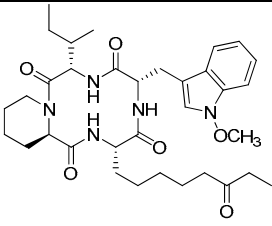
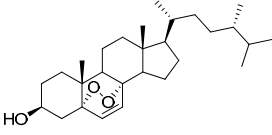
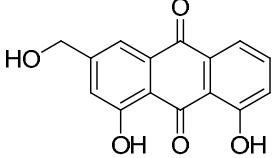
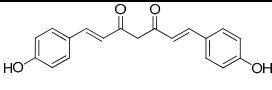
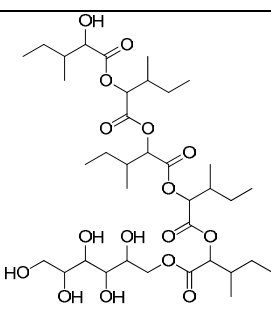
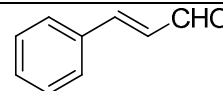
Compound	Source	Structure	Probable mechanisms	Reference
Cinnamaldehyde	<i>Cinnamomum osmophloeum</i>		loss of $\Delta\psi_m$ and release of cytochrome c into cytosol, by the imbalance of Bcl-2 family of proteins	[99]
Apicidin	<i>Fusarium</i> sp.		induces Fas and Fas-L, cytochrome c release into the cytosol, and activation of casp-9 and 3	[100]
EDS (epidioxysteroles)	<i>Meretrix lusoria</i>		induces chromatin condensation, and sub-G1 cell population	[101]
Aloe-emodin	<i>Aloe vera</i>		blocks casein kinase II activity and phosphorylation of Bid and induces Aif and cytochrome c	[102]
Curcumin	<i>Curcuma longa</i>		induces the production of ROS and downstream activation of JNK as well as activation of caspases 9, 3, and 8	[103]

Table 35. Some apoptotic-inducing natural compounds used in cancer chemotherapy (Cont.)

Compound	Source	Structure	Probable mechanisms	Reference
Hormonemate	<i>Hormonema dematioides</i>		induces caspase-3 activity	[104]
Cinnamaldehyde	<i>Cinnamomum cassia</i>		induces the ROS mediated mitochondrial permeability transition and resultant cytochrome c release	[105]

4.3 Experiments

4.3.1 Cell Culture

Human Hep-G2 cells were cultured in RPMI1640 containing 10% fetal bovine serum (FBS), 50 U/mL penicillin, 50 µg/mL streptomycin and 2mM glutamine. Cells were maintained at 37 °C in a humidified atmosphere of 5% CO₂ and 95% air.

4.3.2 Morphological analysis of apoptotic cells

Hep-G2 cells were cultured on 24-well culture plates (1 × 10⁴ cells/well), incubated for 24 h, and treated with sootepin G at a concentration of 4, 10, and 100 µM for 24, 48 and 72 h. After treatment, cells were washed with phosphate-buffered saline (PBS), fixed with 1% glutaraldehyde (1 mL) for 2 h at room temperature under dark condition, and then stained with 1mM of Hoechst 33342 (2

μL). The morphology of nuclear chromatin was defined by an imager of DNA-binding dye (PI) under a fluorescence microscope.

4.3.3 Analysis of the cell cycle

Hep-G2 cells (5×10^5) in a 6-well plate were treated with various concentrations (4-100 μM) of sootepin G for 24 and 48 h. Cells were trypsinized, resuspended in 300 μL PBS, and fixed by adding 250 μL of iced 70% ethanol. The cell pellets were collected by centrifugation, resuspended in 300 μL of PBS buffer and 3 μL of RNase A (10 mg/mL), and incubated at 37 °C for 45 min. Then, 0.75 μL of the PI solution (0.1 mg/2.5 mL) was added, and the mixture was allowed to stand at room temperature in dark condition for 30 min. The cellular DNA content was then analyzed by FC500 MCL cytometry (Beckman Coulter).

4.3.4 Western blot analysis

Western blotting was performed as described previously [32]. Cell pellets were lysed in 2 \times SDS sample buffer containing 100 mM dithiothreitol and then boiled for 5 min. A uniform amount of each sample (30 μg of protein) was resolved by SDS-PAGE (15% acrylamide). Proteins in each gel were transferred to Immobilon-P membrane. After the blots were blocked for 1 h in 3% non-fat dry milk in 0.1% Tween 20 in PBS, pH 7.4, the blots were incubated with the primary antibody overnight at 4 °C, and then with the appropriate secondary antibody for 1 h at room temperature. Signals were visualized by fluorescence emission using commercial detection kits, according to the manufacturer's instructions. Antibodies for Bcl- 2 and Bcl-xL were purchased from Cell Singaling Technology (USA).

4.4 Results and Discussion

Through a cell inhibition assay, the results showed sootepin G (**72**) induced significant cell death in Hep-G2 cells. Effect of sootepin G on the induction of apoptosis in this cell was further investigated. Staining of treated Hep-G2 cells with Hoechst 33258 resulted in differential morphological appearance, compared to non-treated cells (only DMSO). The morphological features of apoptosis (chromatin condensation and nuclear fragmentation) characterized by single intense fluorescence

or multiple strong fluorescence signals in the cell nuclei, were observed in sootepin-G treated cells, while untreated cells showed normal nuclei morphology characterized by weak intensity fluorescence with uniformly stained DNA, as shown in Figure 49.

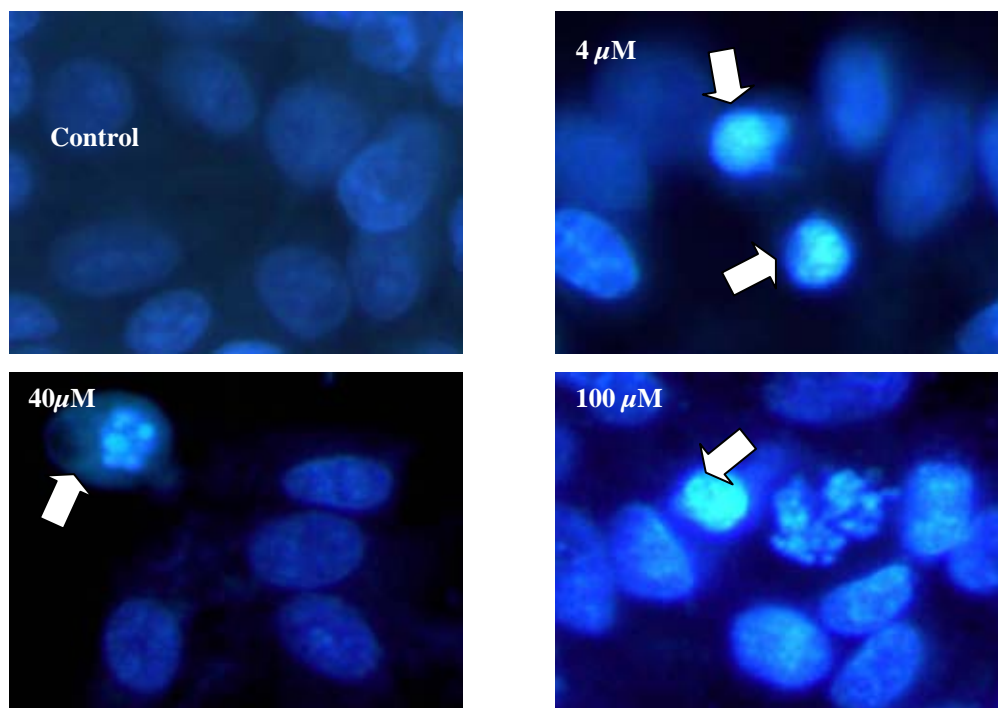
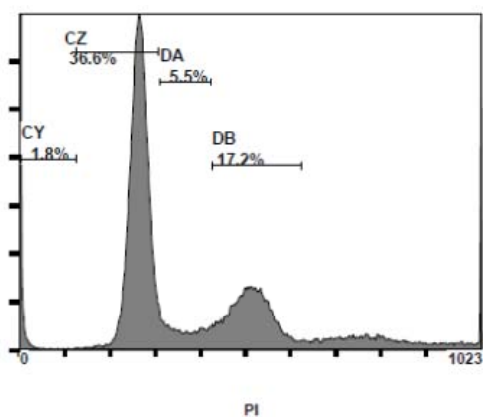


Figure 49. Cell growth inhibition activity of sootepin G after treatment with the concentration of 4, 40, and 100 μM for 48 h

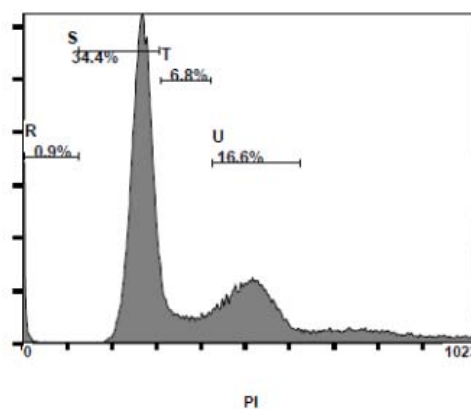
Next, to explore the underlying mechanism of sootepin-G-induced growth suppression, cell cycle analysis was performed by propidium iodide (PI) staining. In principle, PI binds to DNA by intercalating between the bases with little or no sequence preference and with a stoichiometry of one dye per 4.5 base pairs of DNA. When bound to nucleic acids, the absorption maximum for PI is 535 nm and the fluorescence emission maximum is 617 nm. Generally, PI fluorescence is detected in the FL2 channel of flow cytometer. Based on the inhibitory effects of sootepin G on Hep-G2 cell growth, the concentration of 5, 10, 20 and 40 μM of sootepin G were selected for investigating the effect of sootepin G on cell cycle progression. As shown in Figure 50, treatment of Hep-G2 cells with sootepin G at 48 h resulted in a significantly higher proportion of cells in the G1 phase at concentrations used, particularly at concentrations higher than 10 μM , 10 μM (35.3%), 20 μM (41.0) and

40 μM (44.4%), compared with control (36.6%). These data suggested that inhibition of cell proliferation in Hep-G2 by sootepin G might be associated with the induction of G1 arrest.

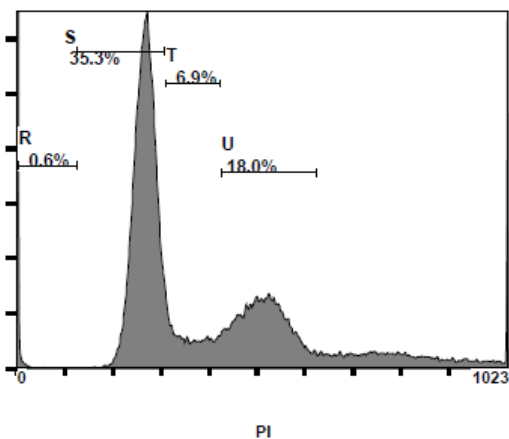
(a) control (DMSO)



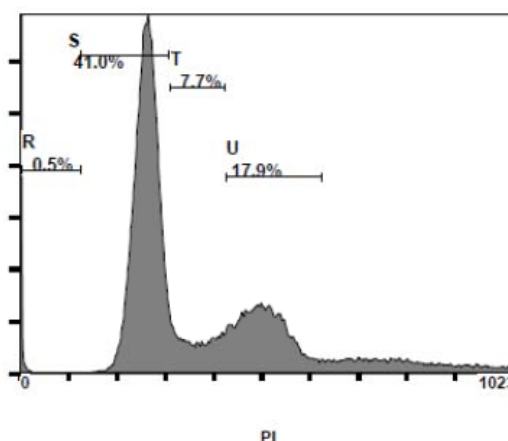
(b) 5 μM sootepin G



(c) 10 μM sootepin G



(d) 20 μM sootepin G



(e) 40 μM sootepin G

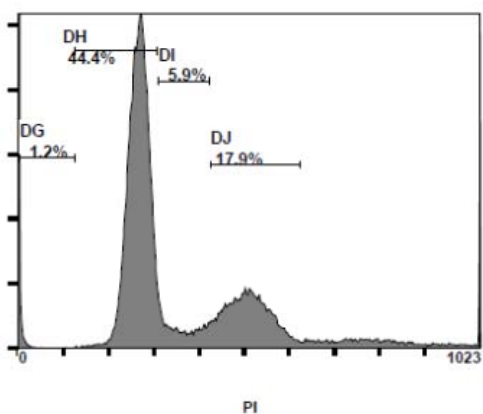


Figure 50. Sootepin G caused G1 arrest induction in Hep-G2 cells.

We next determined whether the protein levels of apoptosis-involving proteins would be altered by sootepin G. In the present study, we focused on how sootepin G is mediated by activation of intrinsic (mitochondria) pathway of apoptosis. It was thus determined the expression of Bcl-2 and Bcl-xL, anti-apoptotic proteins, after treatment 72 h with concentrations ranging from 5 to 20 μ M. Results showed that treatment with sootepin G resulted in a concentration-dependent reduction in the levels of the anti-apoptotic Bcl-2, while that of Bcl-xL was slightly decreased, as shown in Figure 51.

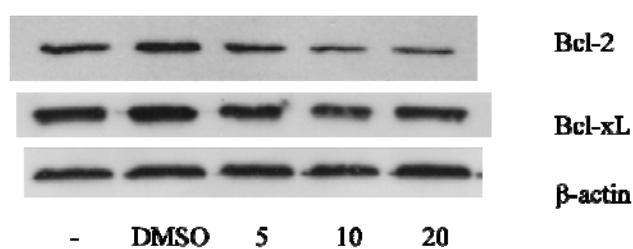


Figure 51. Effects of sootepin G on Bcl-2 and Bcl-xL expression.

4.5 Conclusion

In conclusion, sootepin G could induce G1 arrest and apoptosis in Hep-G2 cells and this might be partly mediated mainly by reduction in Bcl-2 level.

CHAPTER V

CONCLUSION

The chromatographic separation of apical buds of *G. sootepensis* led to the isolation of seven new 3,4-*seco*-cycloartane triterpenes, sootepins A-G (**66-72**), along with five known compounds; coronalolide methyl ester (**10**), tubiferolide methyl ester (**41**), coronalolide (**11**), secaubryenol (**58**), and coronalolic acid (**12**). The exudates of *G. tubifera* yielded three novel furano-3,4-*seco*-cycloartane triterpenes, gardenoins A-C (**73-75**), and a normal 3,4-*seco*-cycloartane triterpene, gardenoin D (**76**). Additionally, the apical buds of *G. obtusifolia* provided four new cycloartane triterpenes, gardenoins E-H (**77-80**), along with four known compounds; α -cycloart-24-ene-3,16,23-trione (**24**), dikamaliaratane D (**63**), dikamaliaratane C (**62**), and dikamaliaratane A (**61**). The apical buds of *G. thailandica* provided two additional new 3,4-*seco*-cycloartane triterpenoids gardenoin I and J (**81-82**). Finally, the same treatment of *G. collinsae* yielded a new dammarane-type triterpene (**83**) and its C-24 epimer (**84**). Their structures were elucidated on the basis of spectroscopic methods (1D and 2D NMR, HREIMS, and X-ray diffraction analysis).

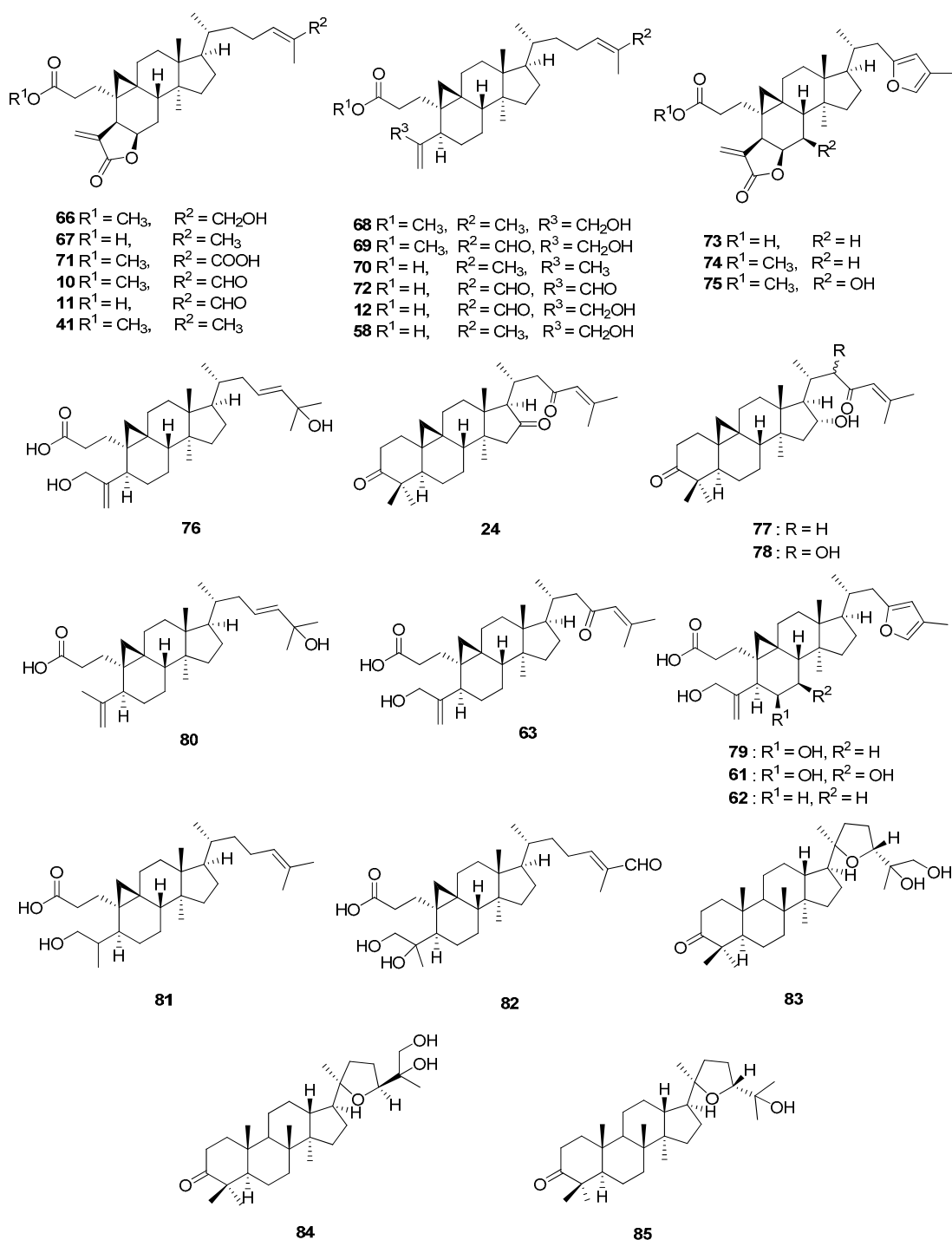


Figure 52. Isolated compounds from five *Gardenia* spp.

All isolated compounds were tested for in vitro cytotoxic activity against human breast (BT474), lung (CHAGO), liver (Hep-G2), gartric (KATO-3), and colon (SW-620) cancer cell lines. Generally, the compounds possessing an α -methylene γ -

butyrolactone moiety showed broad cytotoxicity for all cell lines tested in 5-10 micromolar range, while the compounds without an α -methylene γ -butyrolactone ring showed less cytotoxic activity.

The two ester (**92-93**) and fourteen amide derivatives (**94-107**) of coronalolide were synthesized and evaluated for the cytotoxic activity against with five human cancer cell lines. The IC₅₀ data showed the ester derivatives less cytotoxicity than amide derivatives. In addition, increasing hydrophobicity of amide derivatives were drop cytotoxicity. All amide derivatives showed the specificity with CHAGO cancer cell lines than the parent compound.

Sootepin A ester derivatives (**108-118**) were also synthesized and examined for *in vitro* cytotoxic activities against several human cancer cell lines. The parent compound sootepin A showed potent cytotoxic activity against the tested human cancer cell lines. Comparison of sootepin A to its synthetic analogues showed that all compounds, had reduced activity when compared with those sootepin A.

The chemical binding studies of α -methylene- γ -butyrolactone of 3,4-*seco*-cycloarttane triterpens with some nucleophiles suggest that the α -methylene- γ -butyrolactone can react with the sulfur than nitrogen nucleophiles. Moreover, the adduct of reaction compounds did not show the cytotoxic activity against all five human cancer cell lines. Finally, sootepin G could induce G1 arrest and apoptosis in Hep-G2 cells and this might be partly mediated mainly by reduction in Bcl-2 level.

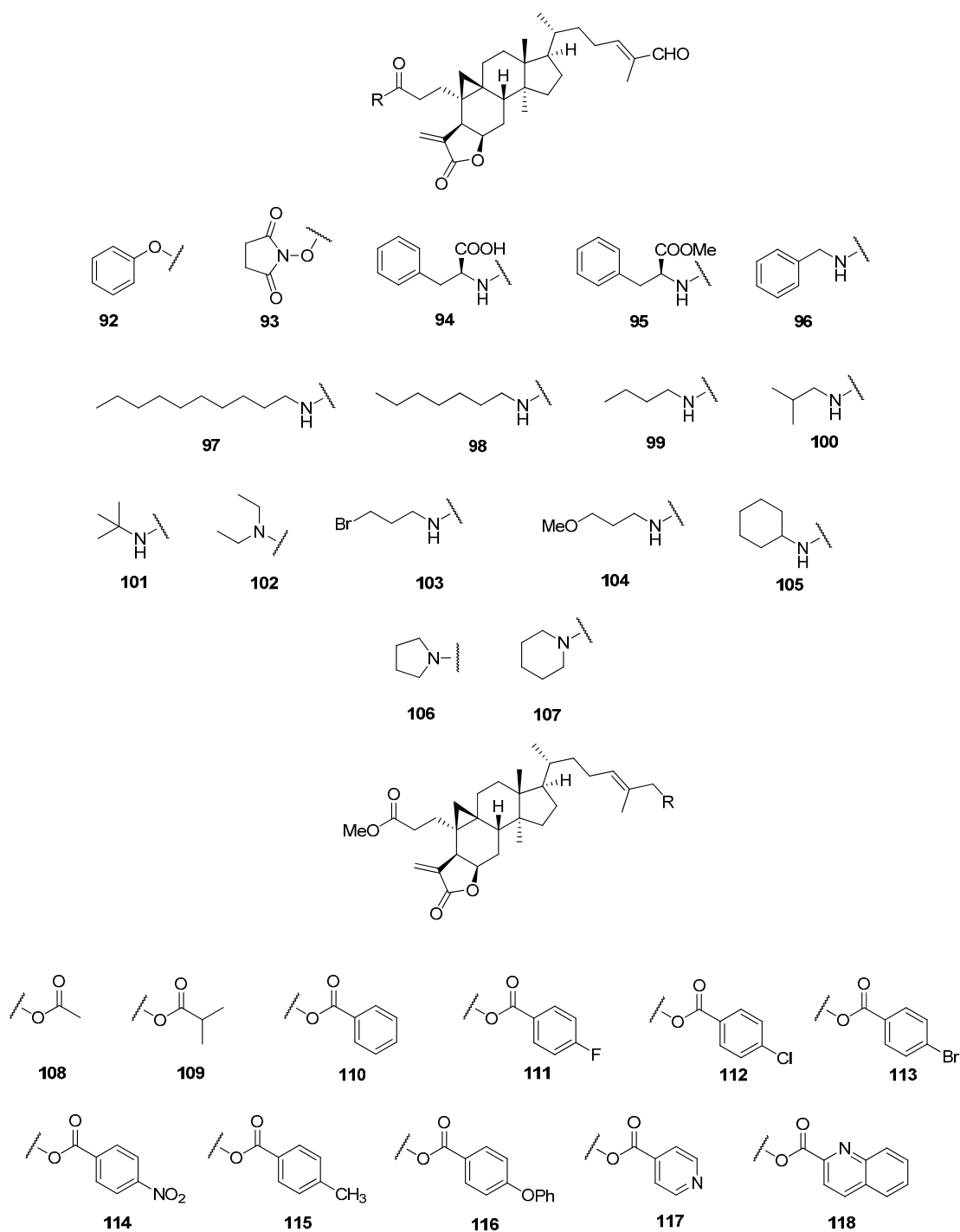


Figure 53. Ester and amide derivatives of colonarolide and sootepin A.

REFERENCES

- [1] Wagner-Dobler, I.; Beil, W.; Lang, S.; Meiners, M.; and Laatsch, H. 2002. Integrated approach to explore the potential of marine microorganisms for the production of bioactive metabolites. Advances in Biochemical Engineering/Biotechnology 74: 208-238.
- [2] Cragg, G. M.; and Newman, D. J. 2005. Plants as source of anticancer agents. Journal of Ethnopharmacology 100: 72-79.
- [3] Rowinsky, E. K.; Onetto, N.; Canetta, R. M.; and Arbuck, S. G. 1992. Taxol-the 1st of the texanes, an important new class of anti-tumor agents. Seminar in Oncology 19: 646-662.
- [4] Creemers, G. J.; Bolis, G.; Gore, M.; Scarfone, G.; Lacave, A. J.; Guastalla, J. P.; Despax, R.; Favalli, G.; Kreinberg, R.; VanBelle, S.; Hudson, I.; Verweij, J.; and Huinink, W. W. T. 1996. Topotecan, an active drug in the second-line treatment of epithelial ovarian cancer: results of a large European phase II study. Journal of Clinical Oncology 14: 3056-3061.
- [5] Bertino, J. R. 1997. Irinotecan for colorectal cancer. Seminar Oncology 24: S18-S23.
- [6] Stahelin, H. 1973. Activity of a new glycosidic lignan derivative (VP 16-213) related to podophyllotoxin in experimental tumors. European Journal of Cancer 9: 215-221.
- [7] Mehta, Kapil; Siddik, Zahid H. 2009. Drug Resistance in Cancer Cells New York: Springer.
- [8] Silva, G. L.; Gil, R. R.; Cui, B.; Chai, H.; Santisuk, T.; Srisook, E.; Reutrakul, V.; Tuchinda, P.; Sophasan, S.; Sujarit, S.; Upatham, S.; Lynn, S. M.; Farthing, J. E.; Yang, S. L.; Lewis, J. A.; O'Neill, M. J.; Farnsworth, N. R.; Cordell, G. A.; Pezzuto, J. M.; and Kinghorn, A. D. 1999. Novel Cytotoxic Ring-A *seco*-Cycloartane Triterpenes from *Gardenia coronaria* and *G. sootepensis*. Tetrahedron 53: 529-538.
- [9] Tuchinda, P.; Pompimon, W.; Reutrakul, V.; Pohmakotr, M.; Yoosook, C.; Kongyai, N.; Sophasan, S.; Sujarit, S.; Upathum, S.; and Santituk, T.

2002. Cytotoxic and anti-HIV-1 constituents of *Gardenia obtusifolia* and their modified compounds. Tetrahedron 58: 8073–8086.
- [10] Tuchinda, P.; Saiyai, A.; Pohmakotr, M.; Yoosook, C.; Kasisit, J.; Napaswat, C.; Santisuk, T.; and Reutrakul, V. 2004. Anti-HIV-1 cycloartanes from leaves and twigs of *Gardenia thailandica*. Planta Medica 70: 366–370.
- [11] Puff, C.; Chayamarit, K.; Chamchumroon, V. 2005. Rubiaceae of Thailand Bangkok: The forest Herbarium, National Park.
- [12] Wang, S. C.; Tseng, T.Y.; Huang, C. M.; and Tsai, T. H. 2004. *Gardenia* herbal active constituents: applicable separation procedures. Journal of Chromatography B 812:193–202.
- [13] Hussian, M. M.; and Sokomba E. N. 1991. Pharmacological effects of *Gardenia erubescens* in mice, rats and cats. International Journal of Pharmacognosy 29: 94-100.
- [14] Ren-Sheny, X.; and Yi-Sheng, G. 1986. Recent advances in chemical studies on the active principle from plants for fertility regulation. Pure and Applied Chemistry 58: 811-816.
- [15] Suksamran, A.; Tanachatchairatana, T.; and Kanokmedthakul, S. 2003. Antiplasmodial triterpenes from twigs of *Gardenia saxatilis*. Journal of Ethanopharmacology 88: 275-277.
- [16] Chhabra, S. C.; Mahunnah R. L. A.; and Mshiu E. N. 1991. Plants used in traditional medicine in Eastern Tanzania. V. *angiosperms* (passifloraceae to sapindaceae). Journal of Ethanopharmacology 33: 143-157.
- [17] El-Hamidi, A. 1970. Drug plants of the Sudan Republic in native medicine. Planta Medica 18: 278-280.
- [18] Gessler, M. C.; Mysuya, D. M.; Nkunya, M. H. H.; Mwasumbi, L. B.; Schar, A.; and Heinrich, M. 1995. Traditional healers in Tanzania: the treatment of malaria with plant remedies. Journal of Ethanopharmacology 48: 131-144.
- [19] Tang, W.; and Eisenbrand, G. 1992. Chinese Drug of Plant Origin Berlin: Springer–Verlag.
- [20] Xu Li. 1985. Dictionary of Chinese Materia Medica (Zhong-Yao-Da-Ci-Dian) Juangsu: Shanghai Scientific and Technological Publishers.

- [21] Harada, M.; Tenmyo, N.; Aburada, M.; and Endo, T. 1974. Pharmacological studies of *Gardeniae fructus* Yakugaku Zasshi 94: 157.
- [22] Grougnet, R.; Magiatis, P.; Mitaku, S.; Loizou, S.; Moutsatsou, P.; Terzis, A.; Cabalion, F.T.; and Michel, S. 2006. *seco*-Cycloartane triterpenes from *Gardenia aubryi*. Journal of Natural Products 69: 1711–1714.
- [23] Reutrakul, V.; Krachangchaeng, C.; Tuchinda, P.; Pohmakotr, M.; Jaipetch, T.; Yoosook, C.; Kasisit, J.; Sophasan, S.; Sujarit, K.; and Santisuk, T. 2004. Cytotoxic and anti-HIV-1 constituents from leaves and twigs of *Gardenia tubifera*. Tetrahedron 60: 1517–2152.
- [24] V-sommai, A; and Kaewduangthain, P. 2004. Wild trees in Thailand 1 Bangkok: H.N.Y. Film.
- [25] Hui-ling, L.; Hui-lan, Z.; and Si-ying, C. 1991. Pigment from the flower of *Gardenia sootepensis*. Yunnan Zhiwu Yanjiu 13: 95-96.
- [26] Vatcharin, R.; Sam-Aung, N.; Walter, C. T.; William A. B.; and Pimchit, D. 1998. A sesquiterpene from *Gardenia sootepensis*. Phytochemistry 48: 197-200.
- [27] Wang, G.; Zhao, S.; Chen, D.; Lu, Y.; and Zheng, Q. 1999. Studies on chemical constituents of fruits of *Gardenia sootepensis* Hutch. China Journal of Chinese Materia Medica 24: 38-40.
- [28] Wang, G.; Zhao, S.; and Chen, D. 1999. A Study on chemical composition of *Gardenia sootepensis* Hutch.-Quantitative determination of iridoid compounds by RP-HPLC. China Journal of Chinese Materia Medica 24: 616-618.
- [29] Kunert, O.; Sreekanth, G.; Babu, G. S.; Rao B. V.; Radhakishan, M.; Kumar, B. R.; Saf, R.; Rao A. V.; and Schühly, W. 2009. Cycloartane triterpenes from dikamali, the gum resin of *Gardenia gummifera* and *Gardenia lucida*. Chemistry and Biodiversity 6: 1185-1192.
- [30] Betacor, C.; Freire, R.; Herna´ ndez, R.; and Sua´ rez. 1983. Dammarane triterpenes of *Trevoa trinervis*: structure and absolute stereochemistry of trevoagenins A, B, and C. Journal of the Chemical Society, Perkin Transactions 1 1119–1126.

- [31] Wahlberg, I.; and Enzell, C. R. 1971. 20R,24-epsilon-2-ocotillone, triterpenoid from commercial tolibalsam. Acta Chemica Scandinavica 25: 352–355.
- [32] Anjaneyulu, V.; Babu, J. S.; Krishna, M.; and Connolly, J. D. 1993. 3-oxo-20S,24R-epoxy-dammarane-25ξ,26-diol from *Mangifera indica*. Phytochemistry 32: 469-471.
- [33] Patani, G. A.; and LaVoie, E. J. 1996. Bioisosterism: A rational approach in drug design. Chemical Reviews 96: 3147-3176.
- [34] Ghantous, A.; Muhtasib, H. G.; Vuorela, H.; Saliba, N. A.; and Darwiche, N. 2010. What made sesquiterpene lactones reach cancer clinical trials? Drug Discovery Today 15: 668-678.
- [35] Bursch, W. 2001. The autophagosomal-lysosomal compartment in programmed cell death. Cell Death & Differentiation 8: 569-581.
- [36] Schwartz, L. M.; Smith, S. W.; Jones, M. E.; and Osborne, B. A. 1993. Do all programmed cell deaths occur via apoptosis? Proceeding of the National Academy of Sciences of the United States of America 90: 980-984
- [37] Kupchan, S. M.; Fessler, D. G.; Eakin, M. A.; and Giacobbe, T. J. 1970. Reactions of alpha methylene lactone tumor inhibitors with model biological nucleophiles. Science 168: 376-378.
- [38] Dupuis, G.; Mitchell, J. C.; and Towers, G. H. N. 1974. Reaction of alantolactone, an allergenic sesquiterpene lactone, with some amino-acid-resultant loss of immunological reactivity. Canadian Journal of Biochemistry 52: 575-581.
- [39] Searle, J.; Lawson, T. A.; Abbott, P. J.; Harmon, B.; and Kerr, J. F. R. 1975. An electron-microscope study of the mode of cell death induced by cancer-chemotherapeutic agents in populations of proliferating normal and neoplastic cells. The Journal of Pathology 116: 129–138.
- [40] Hawkins, N.; Lees, J.; Hargrave, R.; O'Connor, T.; Meagher, A.; and Ward, R. 1997. Pathological and genetic correlates of apoptosis in the progression of colorectal neoplasia. Tumor Biology 18: 146-156.
- [41] A. Mohr, R.M. Zwacka, G. Jarmy, C. Buneker, H. Schrezenmeier, K. Dohner, C. Beltinger, M. Wiesneth, K.M. Debatin, K. Stahnke, Caspase-8L expression

- protects CD34+ hematopoietic progenitor cells and leukemic cells from CD95-mediated apoptosis, *Oncogene* 24 (2005) 2421–2429.
- [42] Eastman, A. 1990. Activation of programmed cell death by anticancer agents: cisplatin as a model system. *Cancer Cells* 2: 275–280.
- [43] Kaufmann, S. H.; and Earnshaw, W. C. 2000. Induction of apoptosis by cancer chemotherapy. *Experimental Cell Research* 256: 42–49.
- [44] Cheng, J. Q.; Jiang, X.; Fraser, M.; Li, M.; Dan, H. C.; Sun, M.; and Tsang, B. K. 2002. Role of X-linked inhibitor of apoptosis protein in chemoresistance in ovarian cancer: possible involvement of the phosphoinositide-3 kinase/Akt pathway. *Drug Resistance Updates* 5: 131-146.
- [45] Li, J.; Sasaki, H.; Sheng, Y. L.; Schneiderman, D.; Xiao, C. W.; Kotsuji, F.; and Tsang, B. K. 2000. Apoptosis and chemoresistance in human ovarian cancer: is Xiap a determinant? *Biological Signals and Receptors* 9: 122-130.
- [46] Reed, J. C. 2002. Apoptosis-based therapies. *Nature Reviews Drug Discovery* 1: 111–121.
- [47] Kleinsmith, L.J. 2005. *Principles of Cancer Biology* San Francisco: Benjamin Cummings.
- [48] Copper, G.M. 2000. *The cell: A molecular approach*. Sunderland: Sinauer Associates Inc.
- [49] Wyllie, A. H.; Kerr, J. F. R.; and Currie, A. R. 1980. Cell death: The significance of apoptosis. *International Review of Cytology* 68: 251-306.
- [50] Wickremasinghe, R. G.; and Hoffbrand, A. V. 1999. Biochemical and genetic control of apoptosis: Relevance to normal hematopoiesis and hematological malignancies. *Blood* 93: 3587-3560.
- [51] Ellis, H. M.; and Horvitz, H. R. 1986. Genetic control of programmed cell death in the nematode *C. elegans*. *Cell* 44: 817-829.
- [52] Metzstein, M. M.; Stanfield, G. M.; Horvitz, H. R. 1998. Genetics of programmed cell death in *C. elegans*: Past, present and future. *Trends in Genetics* 14: 410-416, 1998.

- [53] Alnemri, E. S.; Livingston, D. J.; Nicholson, D. W.; Salvesen, G.; Thornberry, N. A.; Wong, W. W.; Yuan, J. 1996. Human ICE/CED-3 protease nomenclature. Cell 87: 171.
- [54] Putcha, G. V.; Johnson, E. M. Jr. 2004. Men are but worms: Neuronal cell death in *C. elegans* and vertebrates. Cell Death & Differentiation 11: 38-48.
- [55] Korsmeyer, S. J. 1992. Chromosomal translocations in lymphoid malignancies reveal novel protooncogenes. Annual Review of Immunology 10: 785-807.
- [56] Wolf, B. B.; and Green, D. R. 1999. Suicidal tendencies: Apoptotic cell death by caspase family proteinases. The Journal of Biological Chemistry 274: 20049-20052.
- [57] Savill, J.; and Haslett, C. 1995. Granulocyte clearance by apoptosis in the resolution of inflammation. Seminars in Cell Biology 6: 385-393.
- [58] McClintock, D. S.; Santore, M. T.; Lee, V. Y.; Brunella, J.; Budinger, G. R. S.; Zong, W. X.; Thompson, C. B.; Hay, N.; and Chandel, N. S. 2002. Bcl-2 family members and functional electron transport chain regulate oxygen deprivation-induced cell death. Molecular and Cellular Biology 22: 94-104.
- [59] Steenbergen, C.; Das, S.; Su, J.; Wong, R.; Murphy, E. 2009. Cardioprotection and altered mitochondrial adenine nucleotide transport. Basic Research in Cardiology 104: 149-156.
- [60] Festjens, N.; van Gurp, M.; van Loo, G.; Saelens, X.; Vandenabeele, P. 2004. Bcl-2 family members as sentinels of cellular integrity and role of mitochondrial intermembrane space proteins in apoptotic cell death. Acta Haematologica 111: 7-27.
- [61] Kluck, R. M.; Bossy-Wetzell, E.; Green, D. R.; Newmeyer, D. D. 1997. The release of cytochrome c from mitochondria: A primary site for Bcl-2 regulation of apoptosis. Science 275: 1132-1136.
- [62] Yang, J.; Liu, X.; Bhalla, K.; Kim, C. N.; Ibrado, A. M.; Cai, J.; Peng, T. L.; Jones, D. P.; and Wang, X. 1997. Prevention of apoptosis by Bcl-2: Release of cytochrome c from mitochondria blocked. Science 275: 1129-1132.

- [63] Susnow, N.; Zeng, L.; Margineantu, D.; and Hockenbery, D. M. 2009. Bcl-2 family proteins as regulators of oxidative stress. Seminars in Cancer Biology 19: 42-49.
- [64] Tewari, M.; Quan, L. T.; O'Rourke, K.; Desnoyers, S.; Zeng, Z.; Beidler, D. R.; Poirier, G. G.; Salvesen, G. S.; and Dixit, V. M. 1995. Yama/CPP32 beta, a mammalian homolog of CED-3, is a CrmA-inhibitable protease that cleaves the death substrate poly(ADP-ribose) polymerase. Cell 81: 801-809.
- [65] Salvesen, G. S.; and Riedl, S. J. 2008. Caspase mechanisms. Advances in Experimental Medicine and Biology 615: 13-23.
- [66] Papenfuss, K.; Cordier, S. M.; Walczak, H. 2008. Death receptors as targets for anti-cancer therapy. Journal of Cellular and Molecular Medicine 12: 2566-2585.
- [67] Li P.; Nijhawan, D.; Budihardjo, I.; Srinivasula, S. M.; Ahmad, M.; Alnemri, E. S.; and Wang, X. 1997. Cytochrome c and dATP-dependent formation of Apaf-1/Caspase-9 complex initiates an apoptotic protease cascade. Cell 91: 479-498.
- [68] Yin X. M. 2006. Bid, a BH3-only multi-functional molecule, is at the cross road of life and death. Gene 369: 7-19.
- [69] Chavez-Galan, L.; Arenas-Del Angel M. C.; Zenteno, E.; Chávez, R.; and Lascurain, R. 2009. Cell death mechanisms induced by cytotoxic lymphocytes. Cellular & Molecular Immunology 6: 15-25.
- [70] Franchi, L.; Eigenbrod, T.; Munoz-Planillo, R.; Nunez, G. 2009. The inflammasome: A caspase-1-activation platform that regulates immune responses and disease pathogenesis. Nature Immunology 10: 241-247.
- [71] Lazebnik, Y. A.; Takahashi, A.; Moir, R. D.; Goldman, R. D.; Poirier, G. G.; Kaufmann, S. H.; and Earnshaw, W. C. 1995. Studies of the lamin proteinase reveal multiple parallel biochemical pathways during apoptotic execution. Proceedings of the National Academy of Sciences of the United States of America 92: 9042-9046.
- [72] Sakahira, H.; Enari, M.; and Nagata, S. 1998 Cleavage of CAD inhibitor in CAD activation and DNA degradation during apoptosis. Nature 391: 96-99.

- [73] Twig, G.; Elorza, A.; Molina, A. J.; Mohamed, H.; Wikstrom, J. D.; Walzer, G.; Stiles, L.; Haigh, S. E.; Katz, S.; Las, G.; Alroy, J.; Wu, M.; Py, B. F.; Yuan, J.; Deeney, J. T.; Corkey, B. E.; and Shirihai, O. S. 2008. Fission and selective fusion govern mitochondrial segregation and elimination by autophagy. The Embo Journal 27: 433-446.
- [74] Kondo, Y.; and Kondo, S. 2006. Autophagy and cancer therapy. Autophagy 2: 85-90.
- [75] Shi, Y. H.; Ding, Z. B.; Zhou, J.; Qiu, S. J.; and Fan, J. 2009. Prognostic significance of beclin 1-dependent apoptotic activity in hepatocellular carcinoma. Autophagy 5: 380-382.
- [76] Chen, N.; and Karantza-Wadsworth, V. 2009. Role and regulation of autophagy in cancer. Biochimica et Biophysica Acta 1793: 1516-1523.
- [77] Tsujimoto, Y.; Cossman, J.; Jaffe, E.; and Croce, C. M. 1985. Involvement of the bcl-2 gene in human follicular lymphoma. Science 228: 1440-1443.
- [78] Vaux, D. L.; Cory, S.; and Adams, J. M. 1988. Bcl-2 gene promotes haemopoietic cell survival and cooperates with c-myc to immortalize pre-B cells. Nature 335: 440-442.
- [79] McDonnell, T. J.; Deane, N.; Platt, F. M.; Nunez, G.; Jaeger, U.; McKearn, J. P.; and Korsmeyer, S. J. 1989. Bcl-2-immunoglobulin transgenic mice demonstrate extended B cell survival and follicular lymphoproliferation. Cell 57: 79-88.
- [80] Hockenbery, D.; Nunez, G.; Milliman, C.; Schreiber, R. D.; and Korsmeyer, S. J. 1990. Bcl-2 is an inner mitochondrial membrane protein that blocks programmed cell death. Nature 348: 334-336.
- [81] Strasser, A.; Harris, A. W.; Bath, M. L.; and Cory, S. 1990. Novel primitive lymphoid tumours induced in transgenic mice by cooperation between myc and bcl-2. Nature 348: 331-333.
- [82] Kerr, J. F.; Wyllie, A. H.; and Currie, A. R. 1972. Apoptosis: a basic biological phenomenon with wide-ranging implications in tissue kinetics. British Journal of Cancer 26: 239-257.
- [83] Gross, A.; McDonnell, J. M.; and Korsmeyer, S. J. 1999. Bcl-2 family members and the mitochondria in apoptosis. Genes & Development 13: 1899-1911.

- [84] Reed, J. C. 1998. Bcl-2 family proteins. Oncogene 17: 3225-3236.
- [85] Rampino, N.; Yamamoto, H.; Ionov, Y.; Li, Y.; Sawai, H.; Reed, J. C.; and Perucho, M. 1997. Somatic frameshift mutations in the BAX gene in colon cancers of the microsatellite mutator phenotype. Science 275: 967-969.
- [86] Meijerink, J. P.; Mensink, E. J.; Wang, K.; Sedlak, T. W.; Sloetjes, A. W.; de Witte, T.; Waksman, G.; and Korsmeyer, S. J. 1998. Hematopoietic malignancies demonstrate loss-of-function mutations of BAX. Blood 91: 2991-2997.
- [87] Wallace-Brodeur, R. R.; and Lowe, S. W. 1999. Clinical implications of p53 mutations. Cellular and Molecular Life Sciences 55: 64-75.
- [88] Yonish-Rouach, E.; Resnitzky, D.; Lotem, J.; Sachs, L.; Kimchi, A.; and Oren, M. 1991. Wild-type p53 induces apoptosis of myeloid leukaemic cells that is inhibited by interleukin-6. Nature 352: 345-347.
- [89] Scarlett, J.; Sheard, P.; Hughes, G.; Ledgerwood, E.; Ku, H. H.; and Murphy, M. 2000. Changes in mitochondrial membrane potential during staurosporine-induced apoptosis in Jurkat cells. FEBS Letters 475: 267-272.
- [90] Joseph, G. L. and John, A. L. 2004. A guide to drug discovery: The role of the medicinal chemist in drug discovery - then and now. Nature Reviews Drug Discovery 3; 853-862.
- [91] Christopher, E.J.; Swiatoniowski, A.; Andrew, C.; Lin, T.J. 2004. *Pseudomonas aeruginosa* exotoxin A induces human mast cell apoptosis by a caspase-8 and -3-dependent mechanism. The Journal of Biological Chemistry 279; 37201-37207.
- [92] Chang, J.H. and Kwon, H.Y. 2007. Expression of 14-3-3 δ , Cdc2 and cyclin B proteins related to exotoxin A induced apoptosis in HeLa S3 cells. International Immunopharmacology 7: 1185-1191.
- [93] Chen, C.Y.; Hsu, Y.L.; Chen, Y.Y.; Hung, J.Y.; Huang, M.S.; Kuo, P.L. 2007. Isokotomolide A, a new butanolide extracted from the leaves of *Cinnamomum kotoense*, arrests cell cycle progression and induces apoptosis through the induction of p53/p21 and the initiation of mitochondrial system in human non-small cell lung cancer A549 cells. European Journal of Pharmacology 574: 94-102.

- [94] Cheung, J.Y.N.; Ong, R.C.Y.; Suen, Y.K.; Ooi, V.; Wong, H.N.C.; Mak, T.C.W.; Fung, K.P.; Yu, B.; Kong, S.K. 2005. Polyphyllin D is a potent apoptosis inducer in drugresistant HepG2 cells. Cancer Letter 217: 203-211.
- [95] Hsu, P.C.; Huang, Y.T.; Tsai, M.L.; Wang, Y.J.; Lin, J.K.; Pan, M.H. 2004. Induction of apoptosis by shikonin through coordinative modulation of the Bcl-2 family, p27, and p53, release of cytochrome c, and sequential activation of caspases in human colorectal carcinoma cells. Journal of Agricultural and Food Chemistry 52; 6330-6337.
- [96] Yarimar, R.; Juan, R.; Francisco, A.; Alfredo, U.; Mariugenia, M.; Nardy, D.; Ivan, G.C. 2008. Cytotoxic and apoptosis-inducing effect of ent-15-oxokaur-16-en-19-oic acid, a derivative of grandiflorolic acid from *Espeletia schultzei*. Phytochemistry 69; 432-438.
- [97] Kuo, P.L.; Hsu, Y.; Chang, C.; Lin, C. 2005. The mechanism of ellipticine-induced apoptosis and cell cycle arrest in human breast MCF-7 cancer cells. Cancer Letter 223; 293-301.
- [98] Chen, W.J.; Lin, J.K. 2004. Mechanisms of cancer chemoprevention by hop bitter acids (beer aroma) through induction of apoptosis mediated by Fas and caspase cascades. Journal of Agricultural and Food Chemistry 52; 55-64.
- [99] Huang, T.C.; Fu, H.Y.; Ho, C.T.; Tan, D.; Huang, Y.T.; Pan, M.H. 2007. Induction of apoptosis by cinnamaldehyde from indigenous cinnamon *Cinnamomum osmophloeum* Kaneh through reactive oxygen species production, glutathione depletion, and caspase activation in human leukemia K562 cells. Food Chemistry 103; 434-443.
- [100] Kwon, S.H.; Ahn, S.H.; Kim, Y.K.; Bae, G.U.; Yoon, J.W.; Hong, S.; Lee, H.Y.; Lee, Y.W.; Lee, H.W.; Han, J.W. 2002. Apicidin, a histone deacetylase inhibitor, induces apoptosis and Fas/Fas ligand expression in human acute promyelocytic leukemia cells. The Journal of Biological Chemistry 277; 2073-2080.

- [101] Pan, M.H.; Huang, Y.T.; Chang, C.I.; Ho, C.T.; Pan, B.S. 2007. Apoptotic-inducing epidioxysterols identified in hard clam (*Meretrix lusoria*). Food Chemistry 102; 788-795.
- [102] Chen, S.H.; Lin, K.Y.; Chang, C.C.; Fang, C.L.; Lin, C.P. 2007. Aloe-emodin-induced apoptosis in human gastric carcinoma cells. Food and Chemical Toxicology 45: 2296-2303.
- [103] Johnson, J.J.; Mukhtar, H. 2007. Curcumin for chemoprevention of colon cancer. Cancer Letter 255; 170-181.
- [104] Filip, P.; Weber, R.W.S.; Sterner, O.; Anke, T. 2003. Hormonemate, a new cytotoxic and apoptosis-inducing compound from the endophytic fungus *Hormonema dematioides*. Identification of the producing strain, and isolation and biological properties of hormonemate. Zeitschrift für Naturforschung 58; 547-552.
- [105] Ka, H.; Park, H.J.; Jung, H.J.; Choi, J.W.; Cho, K.S.; Ha, J.; Lee, K.T. 2003. Cinnamaldehyde induces apoptosis by ROS-mediated mitochondrial permeability transition in human promyelocytic leukemia HL-60 cells. Cancer Letter 196; 143-152.
- [106] Cory, S. and Adams, J.M. 2002. The Bcl-2 family: regulators of the cellular life-or-death switch. Nature Reviews Cancer. 2; 647-656.

Appendix

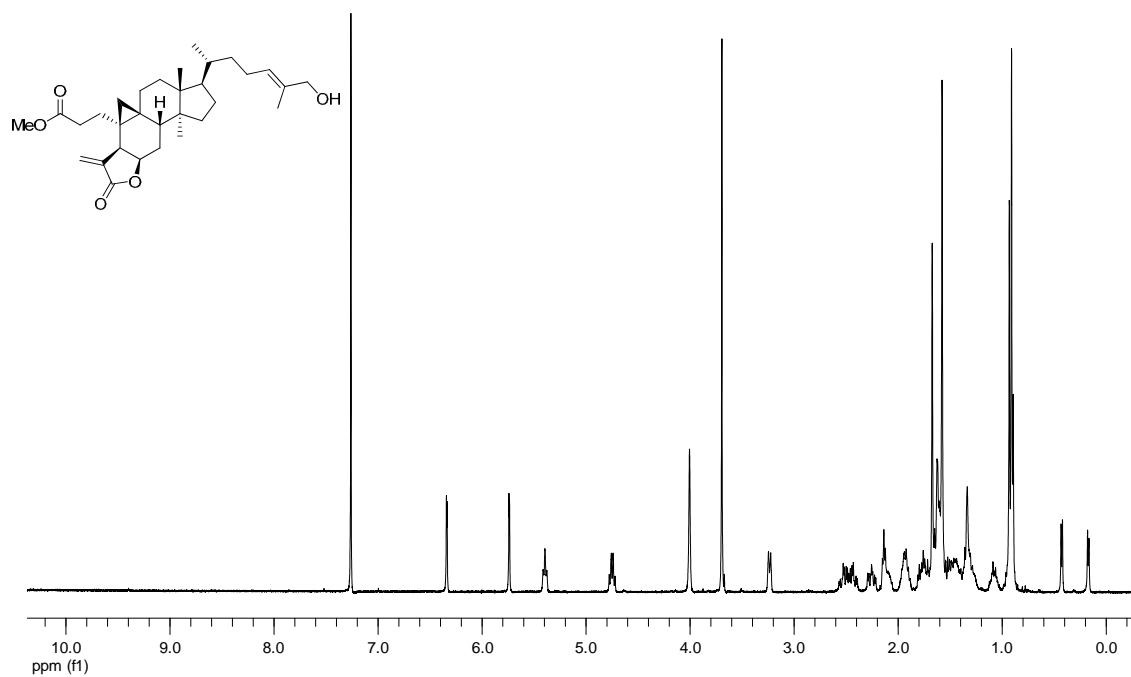


Figure 54. ¹H NMR spectrum of compound **66** (CDCl₃; 400 MHz).

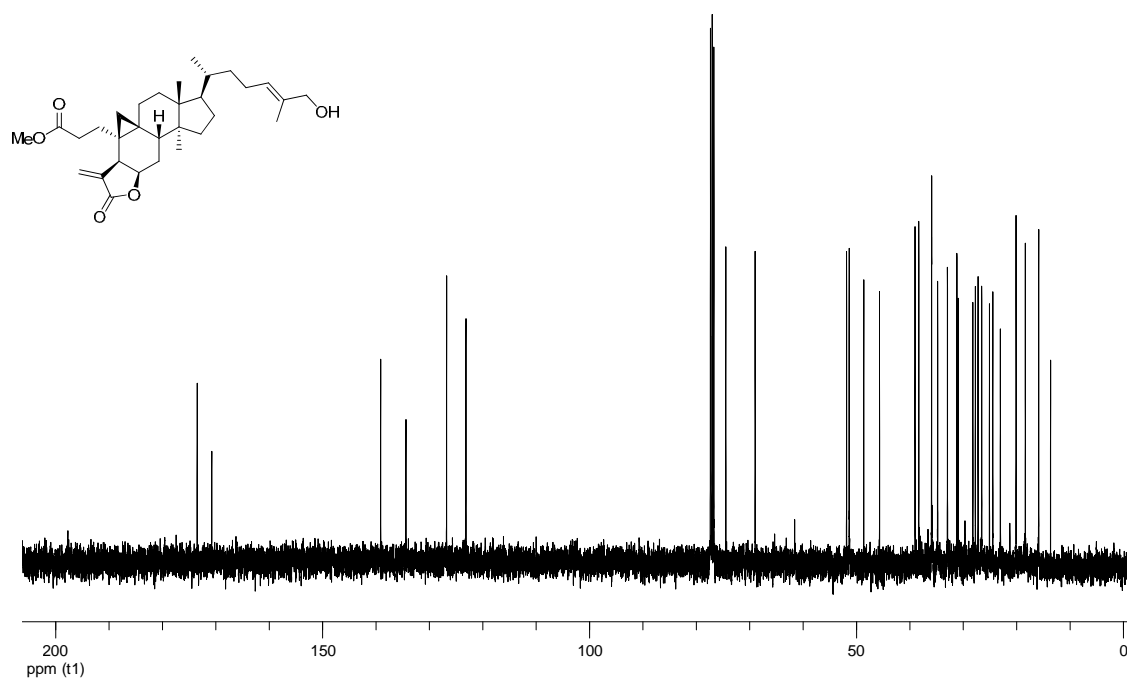


Figure 55. ¹³C NMR spectrum of compound **66** (CDCl₃; 100 MHz)

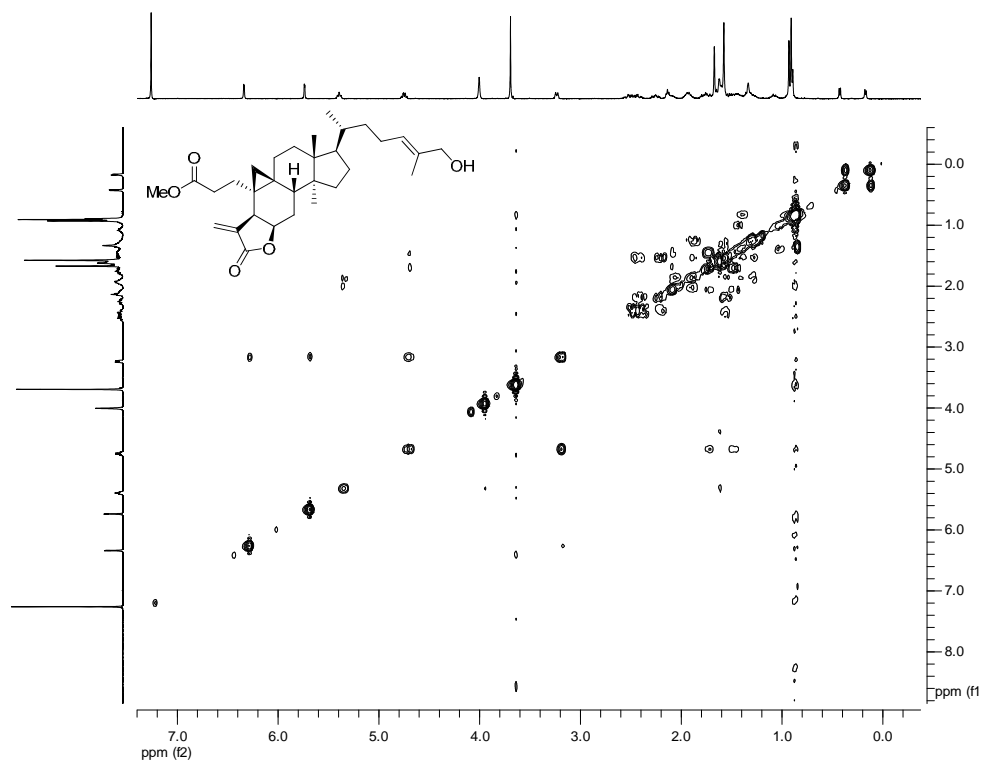


Figure 56. ^1H - ^1H COSY spectrum of compound **66** (CDCl_3 ; 400 MHz).

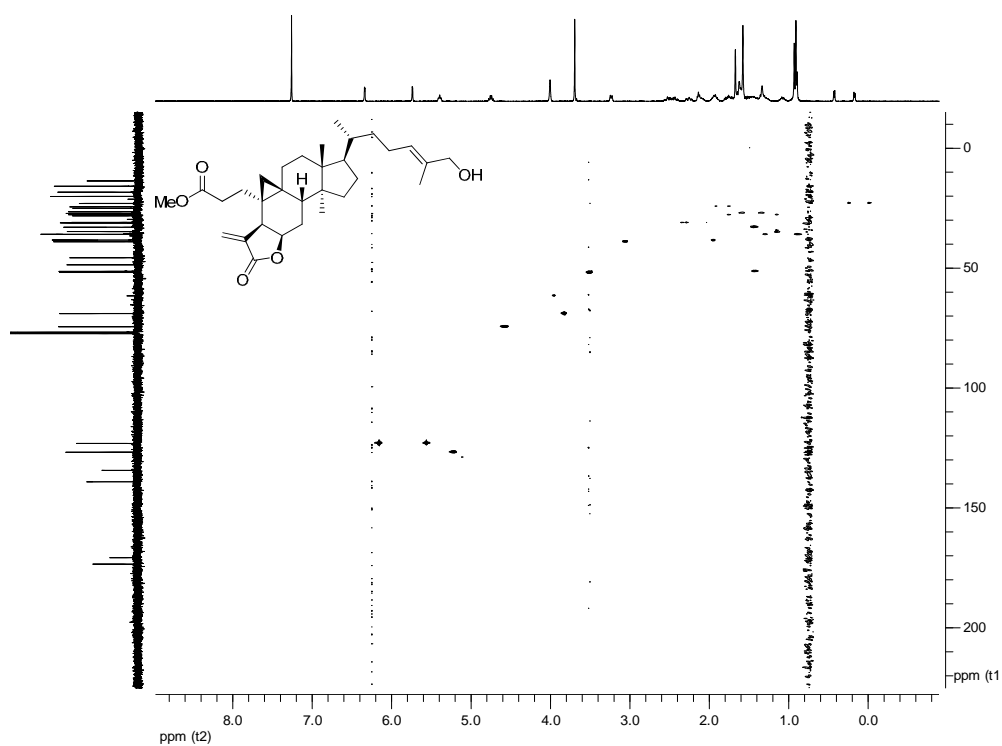


Figure 57. HSQC spectrum of compound **66** (CDCl_3 ; 400 MHz).

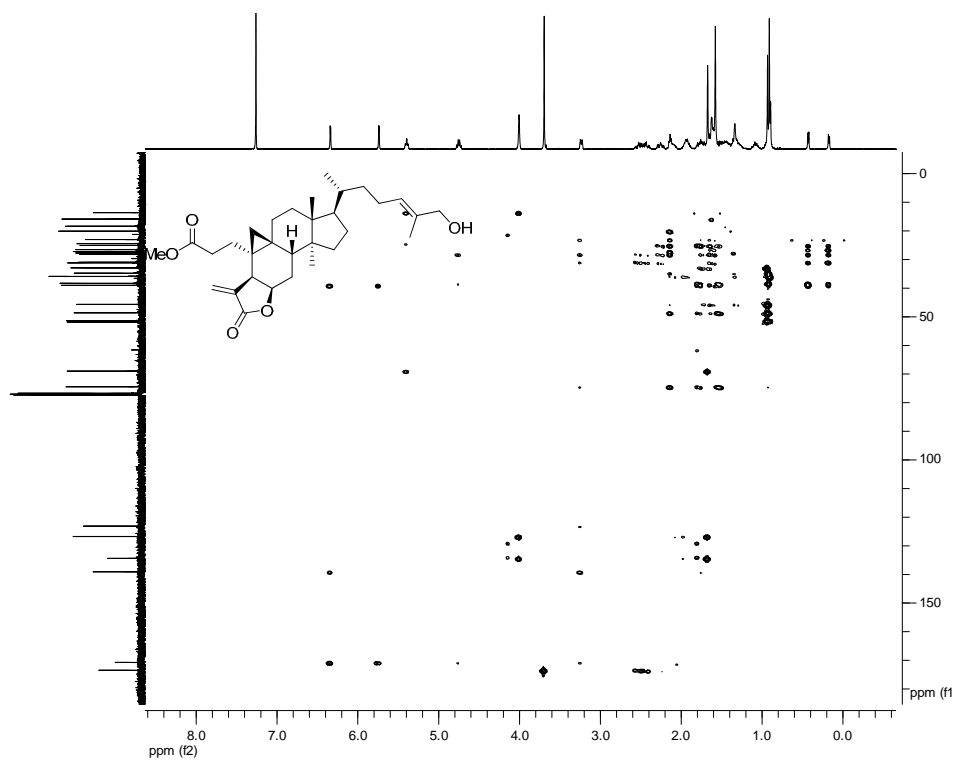


Figure 58. HMBC spectrum of compound **66** (CDCl₃; 400 MHz).

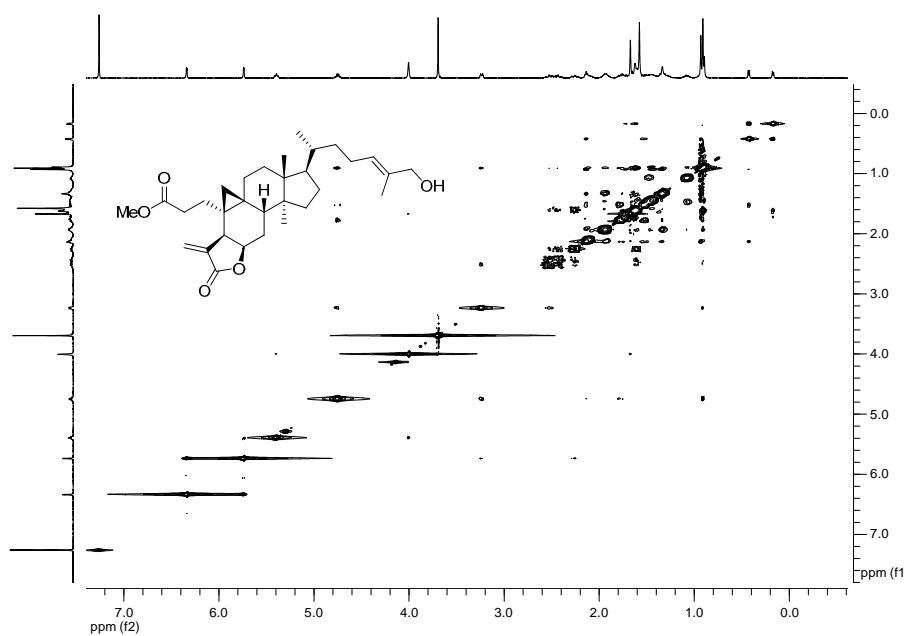


Figure 59. NOESY spectrum of compound **66** (CDCl₃; 400 MHz).

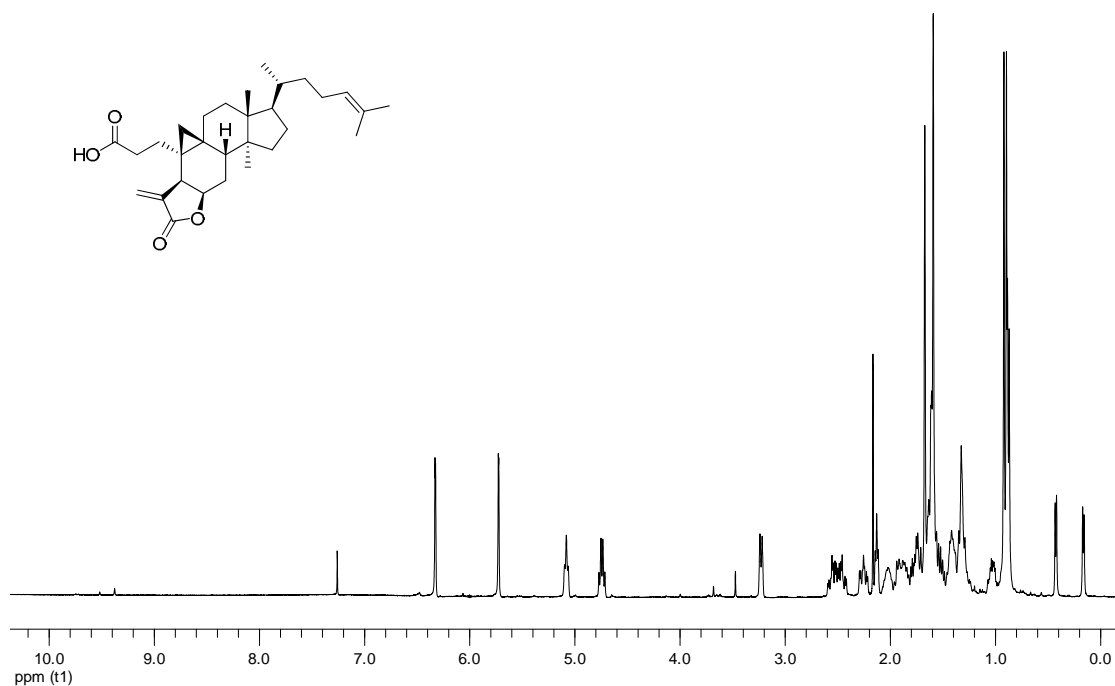


Figure 60. ¹H NMR spectrum of compound **67** (CDCl₃; 400 MHz).

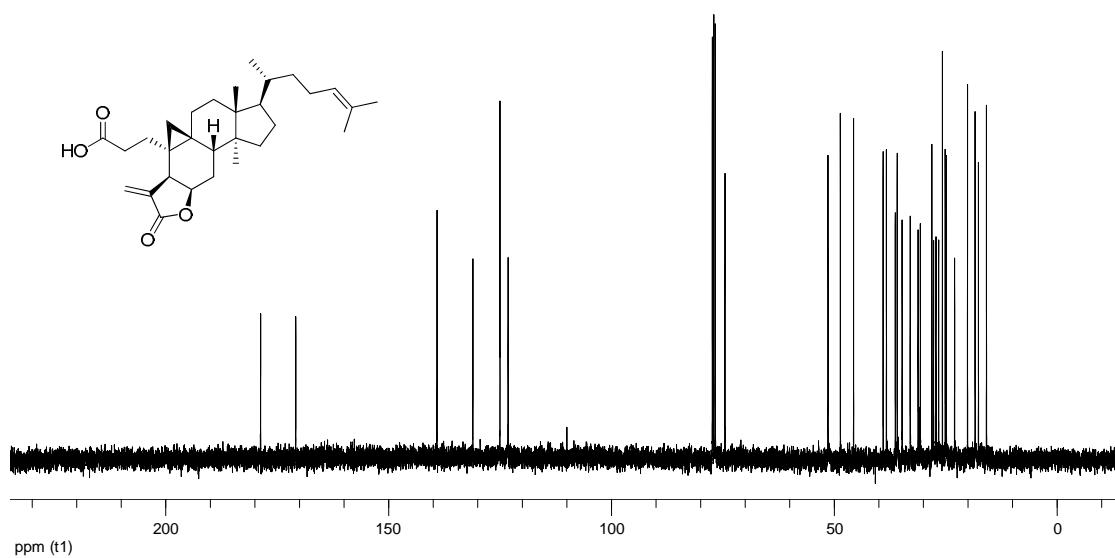


Figure 61. ¹³C NMR spectrum of compound **67** (CDCl₃; 100 MHz).

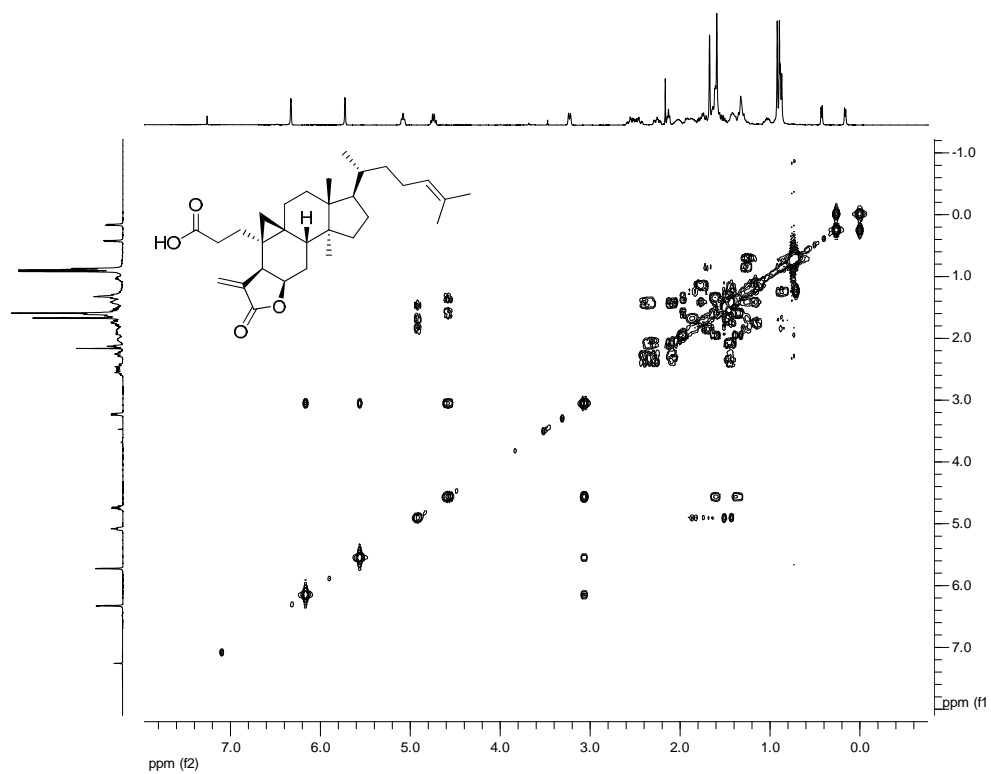


Figure 62. ^1H - ^1H COSY spectrum of compound **67** (CDCl_3 ; 400 MHz).

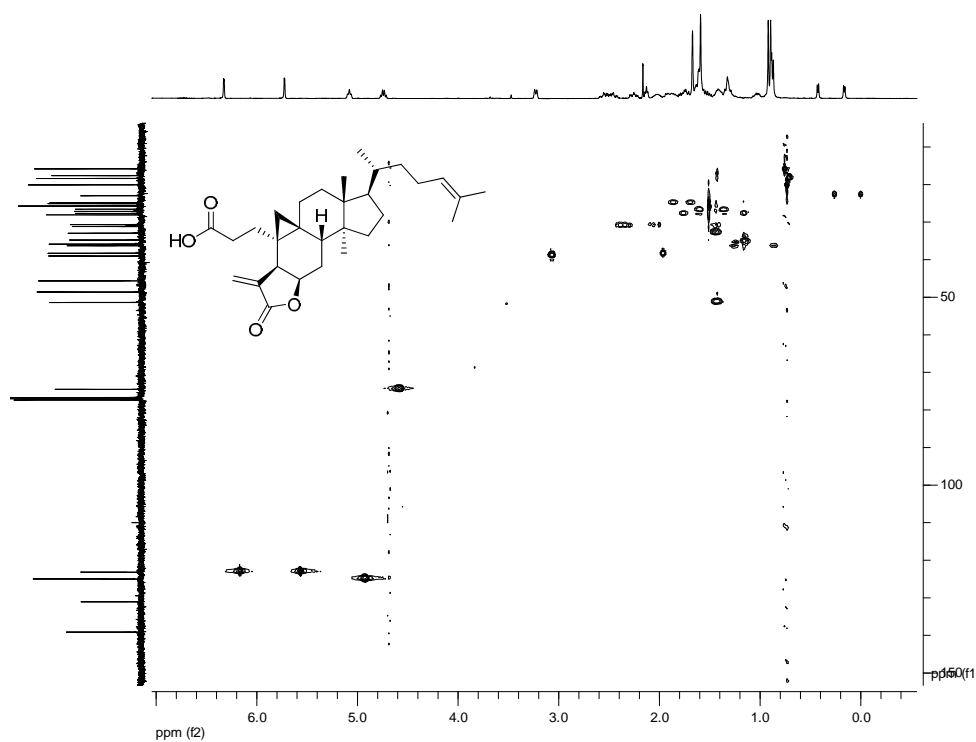


Figure 63. HSQC spectrum of compound **67** (CDCl_3 ; 400 MHz).

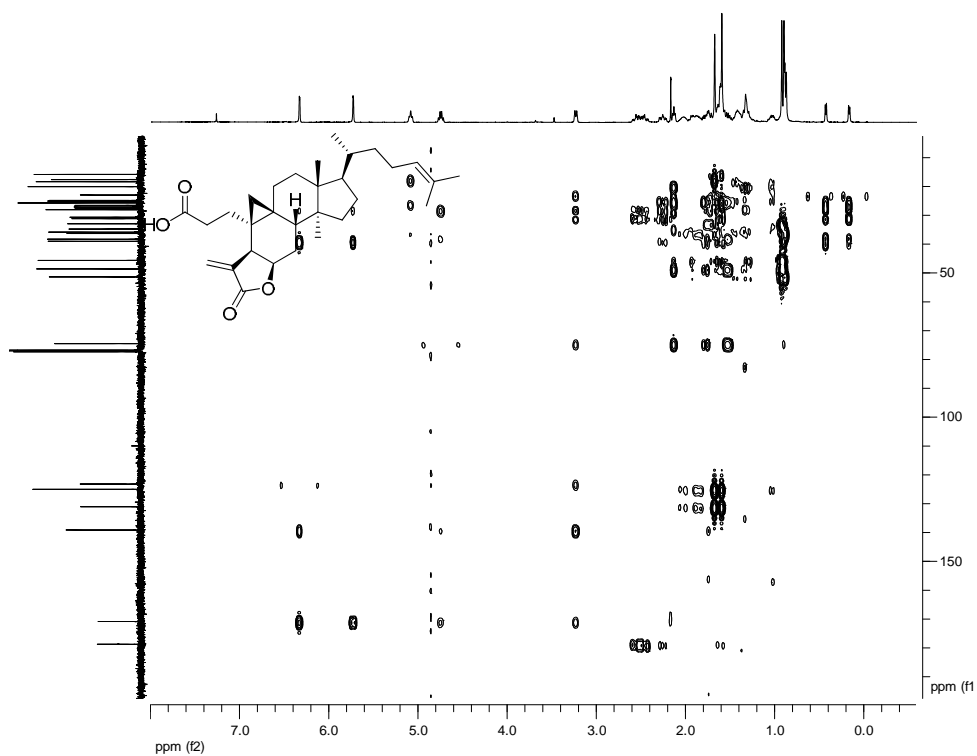


Figure 64. HMBC spectrum of compound **67** (CDCl₃; 400 MHz).

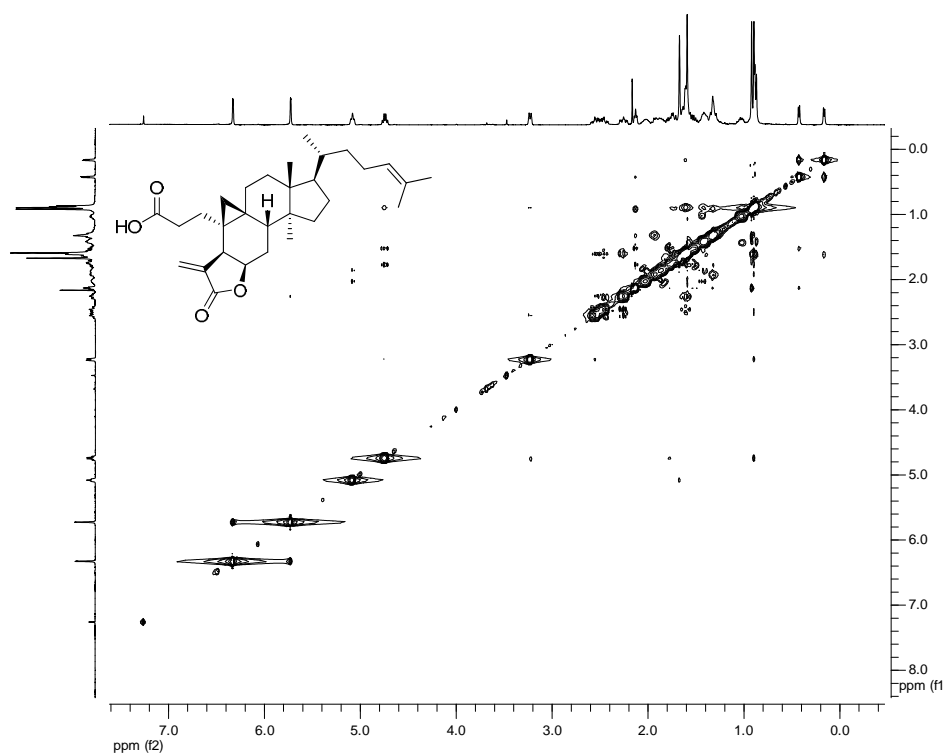


Figure 65. NOESY spectrum of compound **67** (CDCl₃; 400 MHz).

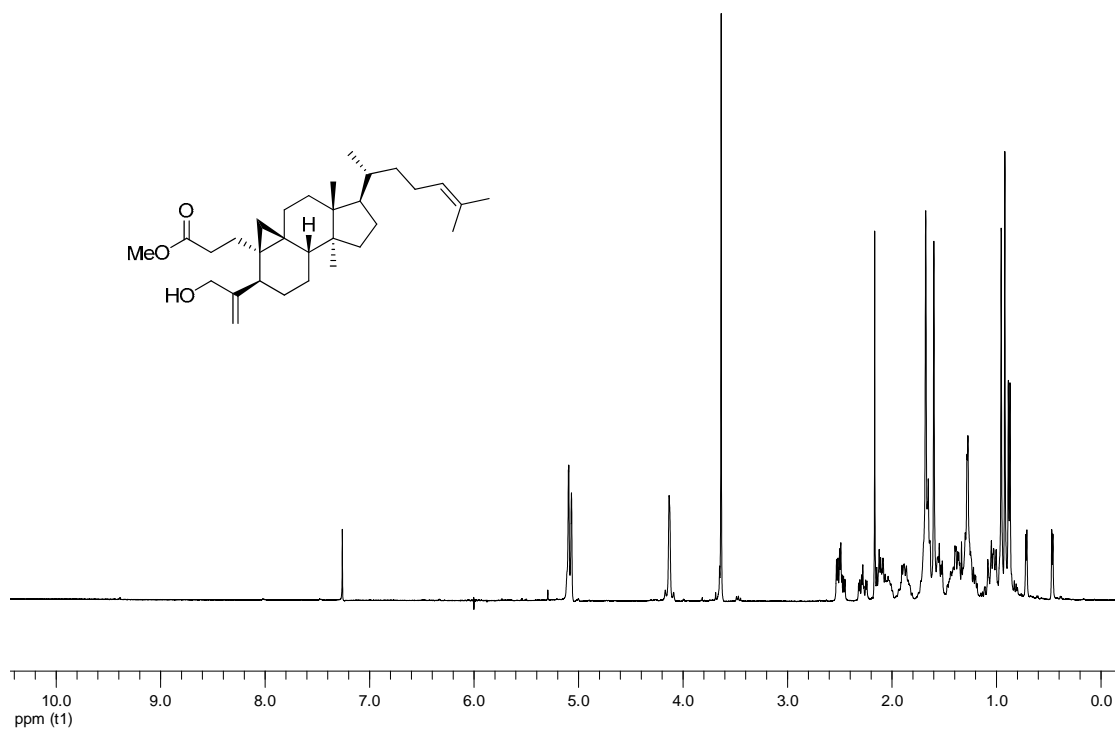


Figure 66. ^1H NMR spectrum of compound **68** (CDCl_3 ; 400 MHz).

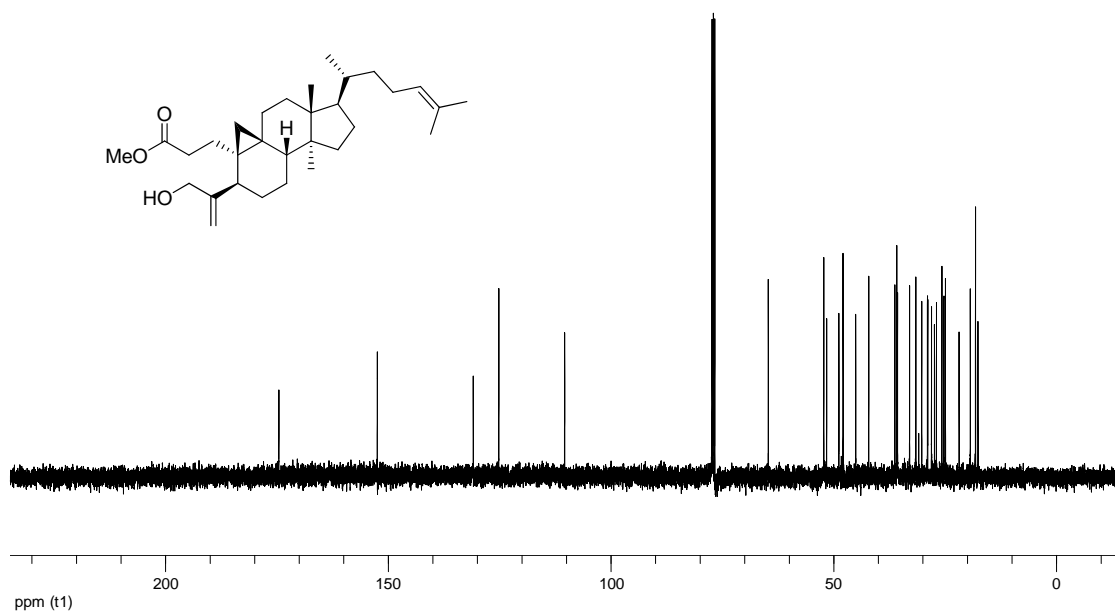


Figure 67. ^{13}C NMR spectrum of compound **68** (CDCl_3 ; 100 MHz).

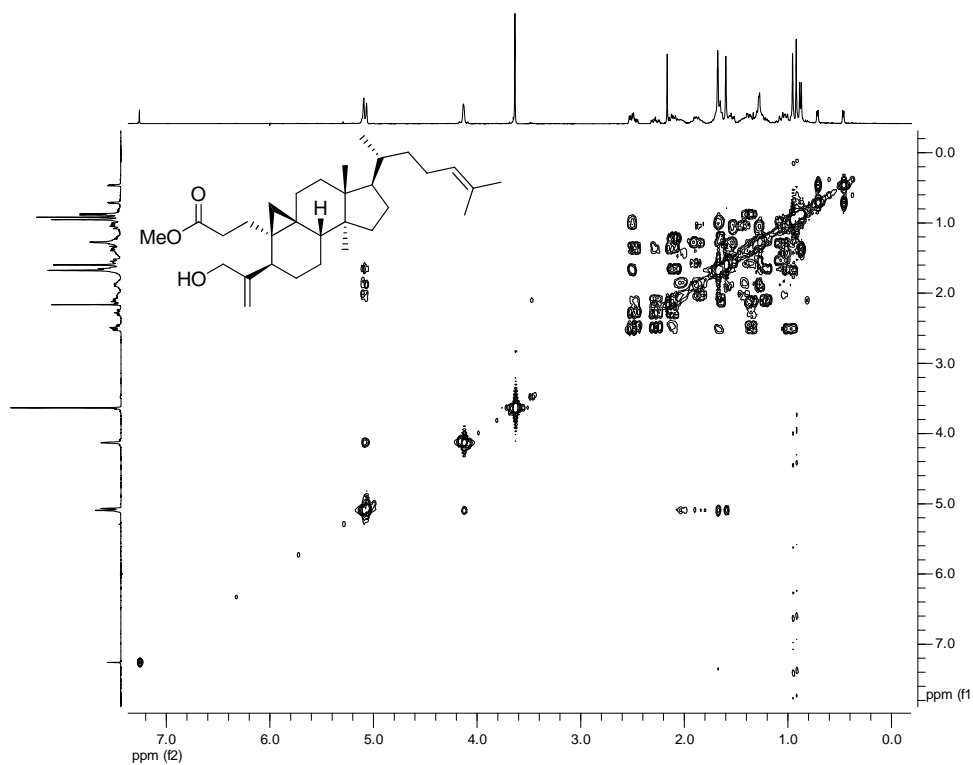


Figure 68. ^1H - ^1H COSY spectrum of compound **68** (CDCl_3 ; 400 MHz).

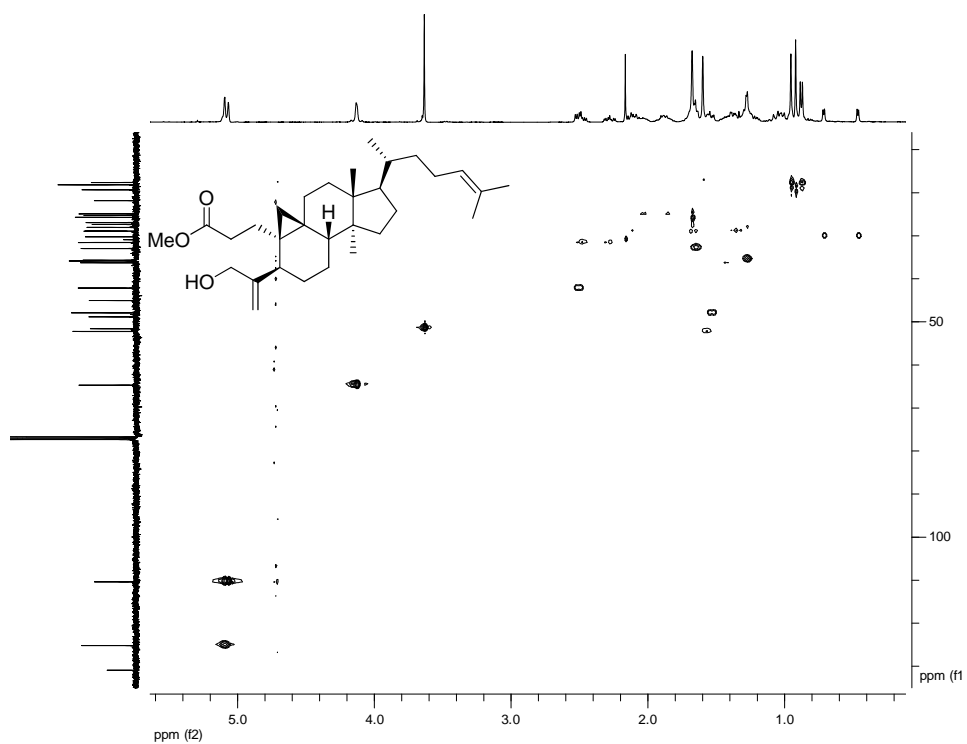


Figure 69. HSQC spectrum of compound **68** (CDCl_3 ; 400 MHz).

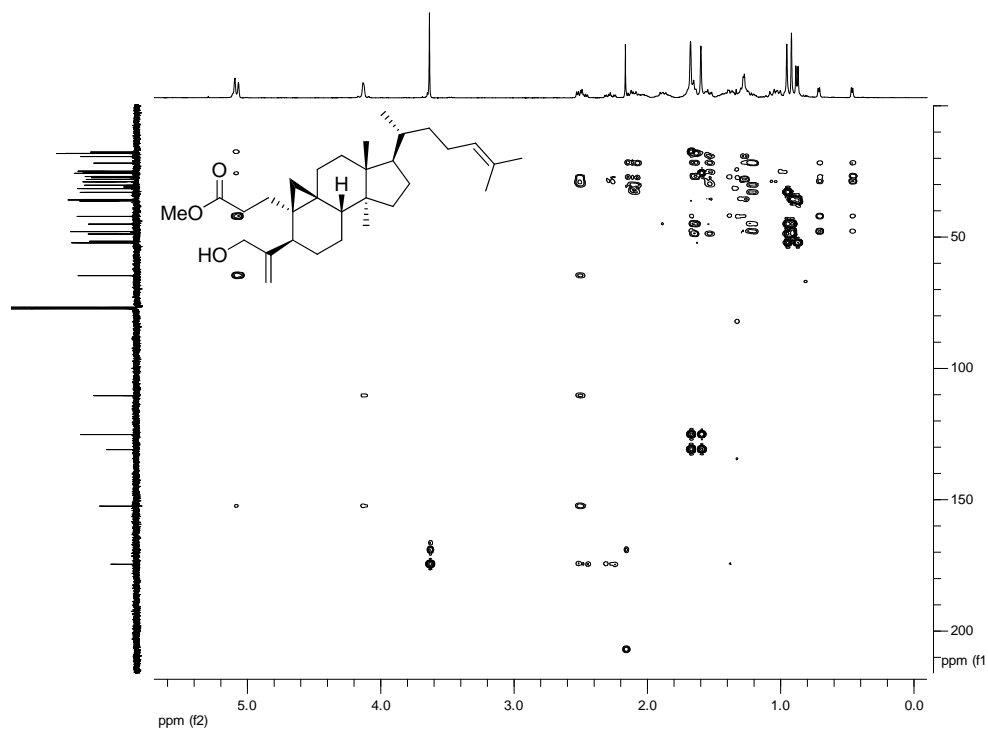


Figure 70. HMBC spectrum of compound **68** (CDCl₃; 400 MHz).

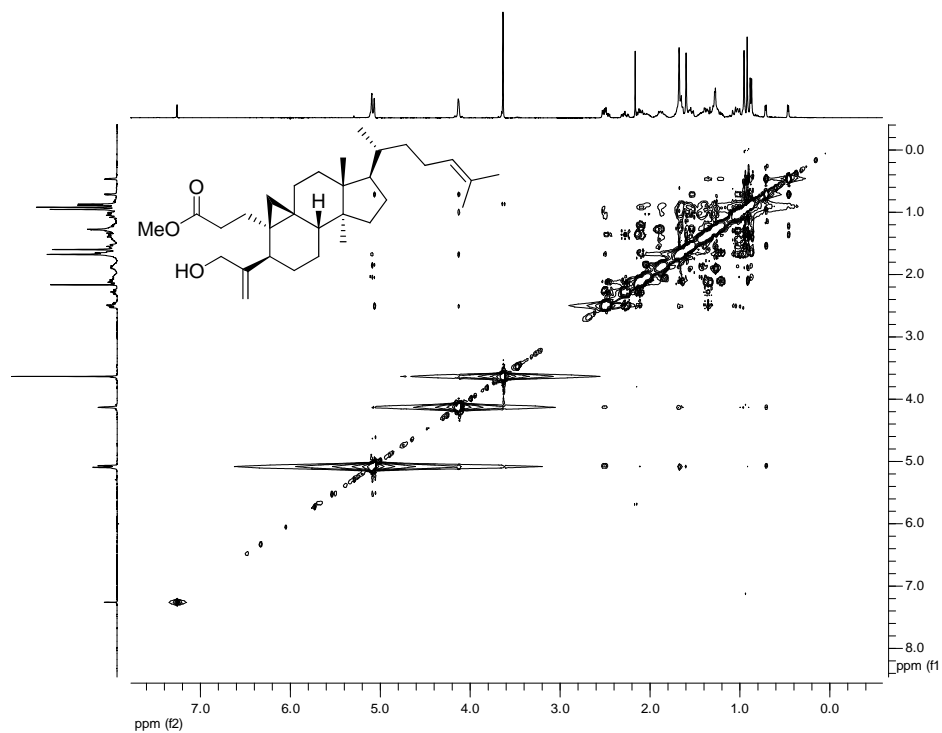


Figure 71. NOESY spectrum of compound **68** (CDCl₃; 400 MHz).

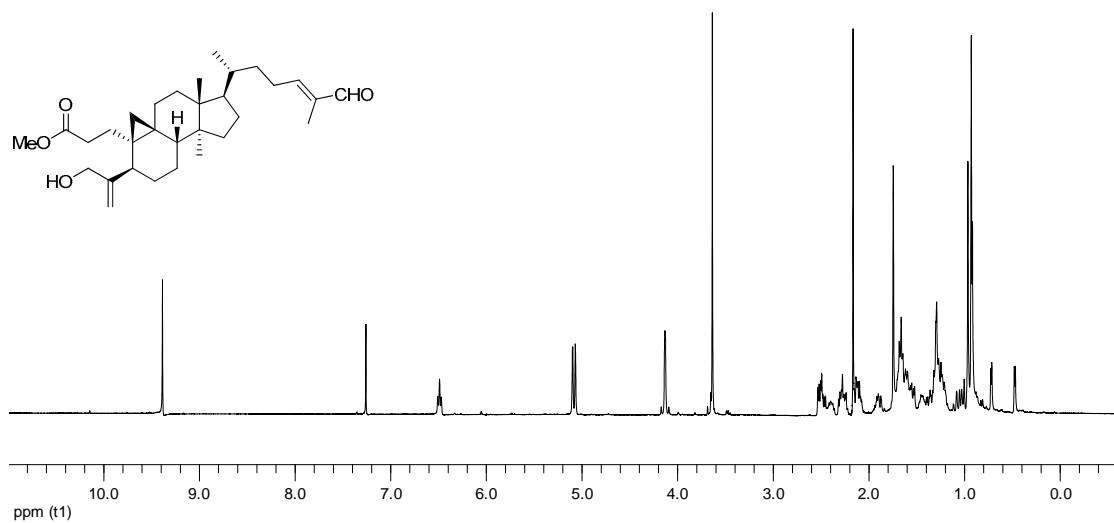


Figure 72. ^1H NMR spectrum of compound **69** (CDCl_3 ; 400 MHz).

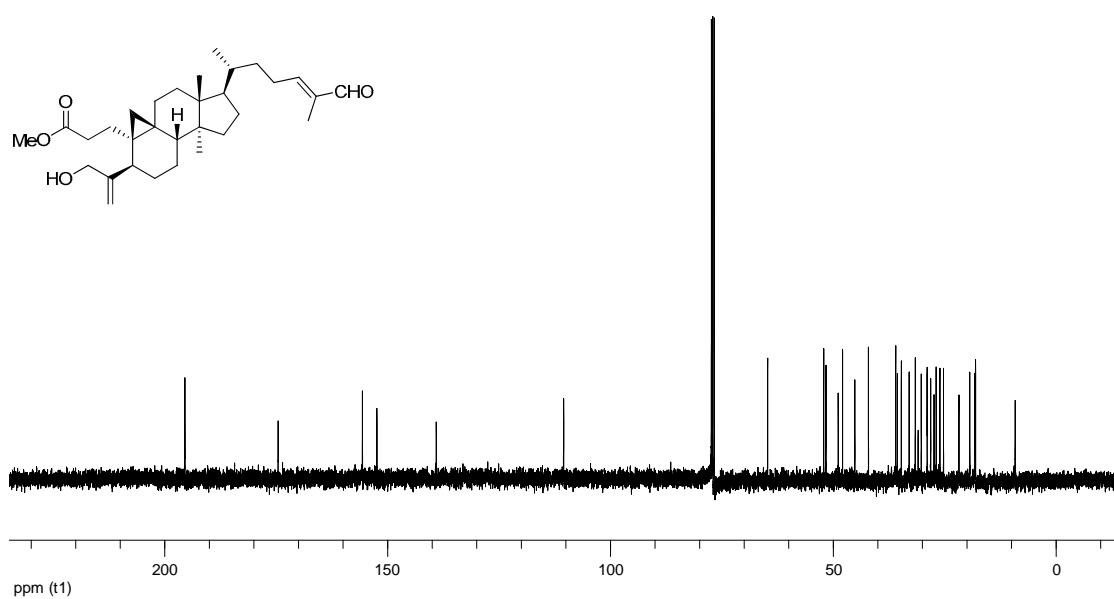


Figure 73. ^{13}C NMR spectrum of compound **69** (CDCl_3 ; 100 MHz).

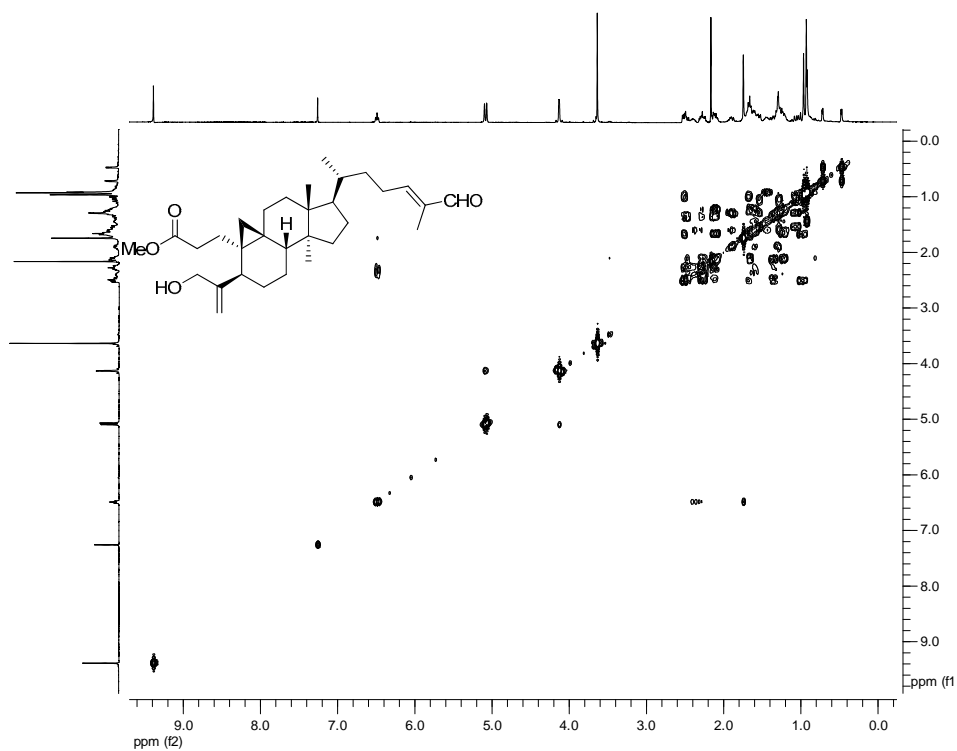


Figure 74. ^1H - ^1H COSY spectrum of compound **69** (CDCl_3 ; 400 MHz).

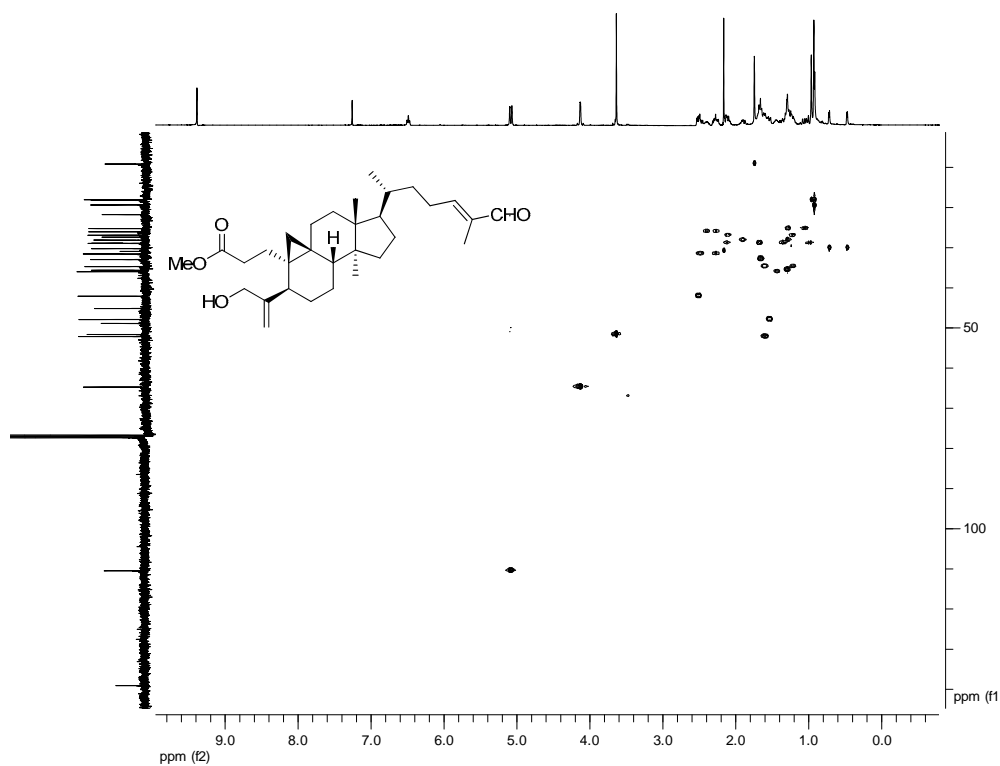


Figure 75. HSQC spectrum of compound **69** (CDCl_3 ; 400 MHz).

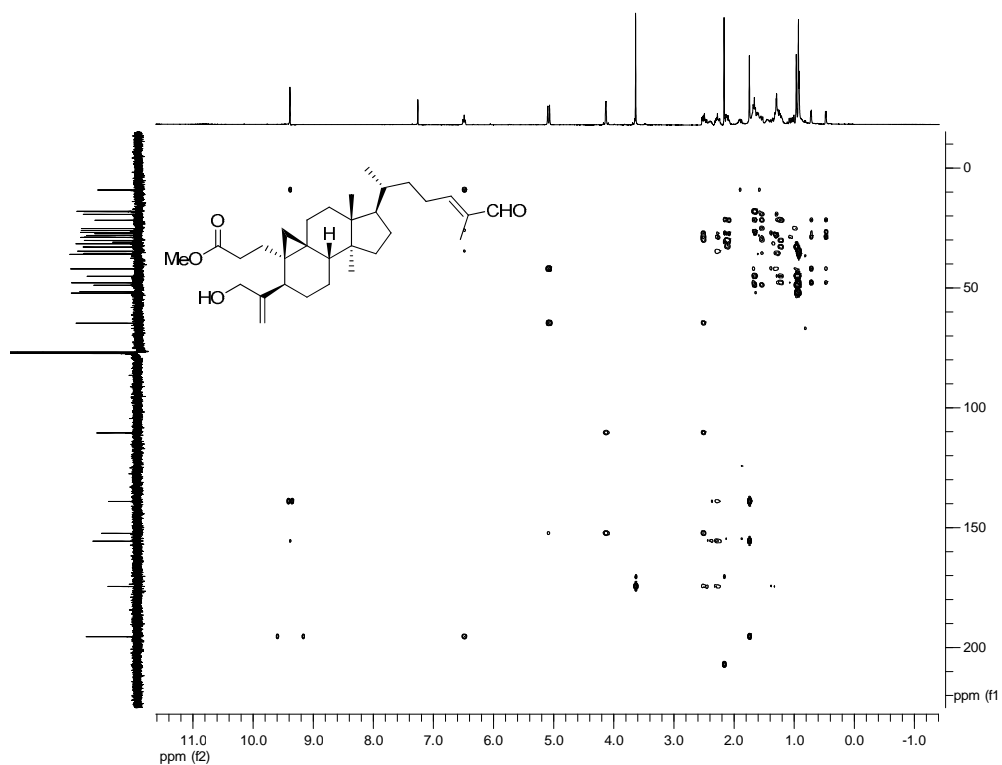


Figure 76. HMBC spectrum of compound **69** (CDCl₃; 400 MHz).

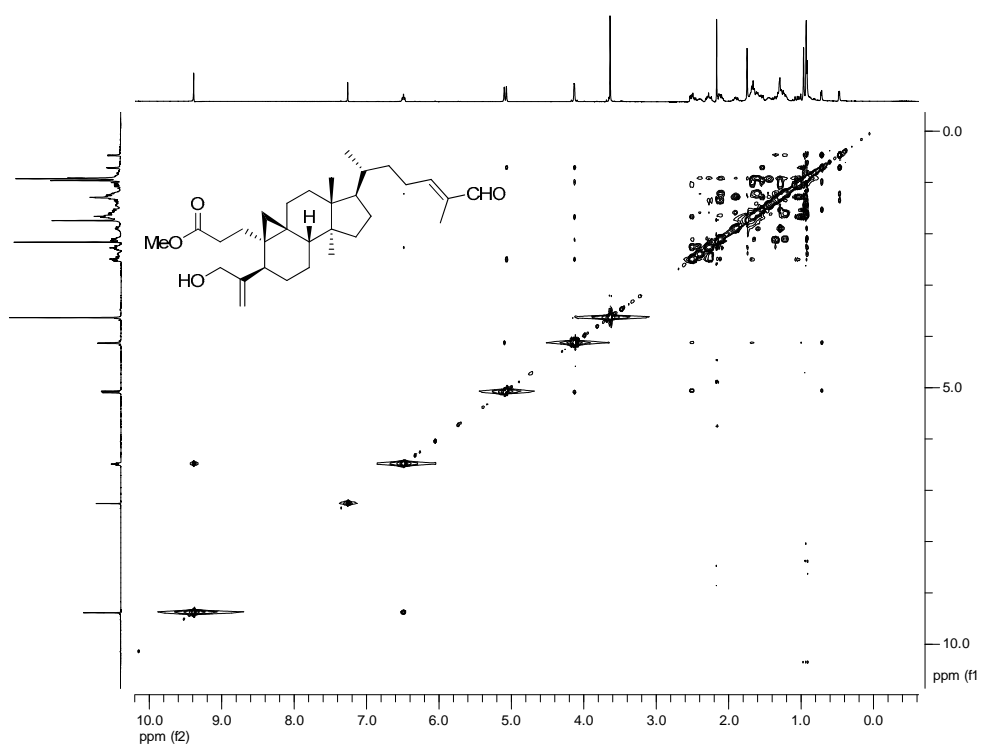


Figure 77. NOESY spectrum of compound **69** (CDCl₃; 400 MHz).

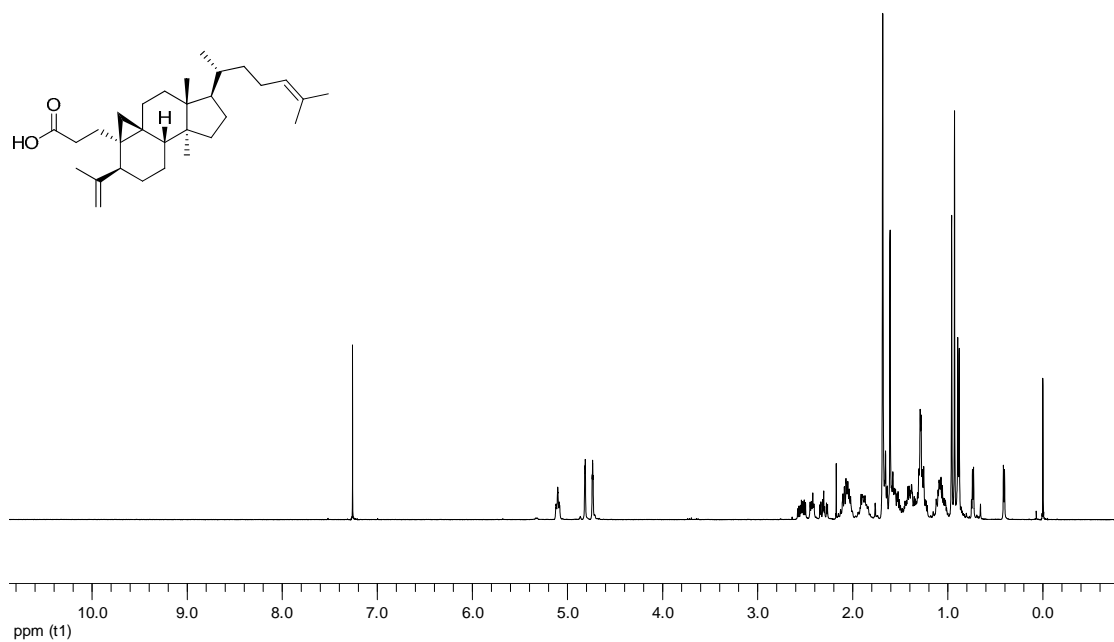


Figure 78. ¹H NMR spectrum of compound **70** (CDCl₃; 400 MHz).

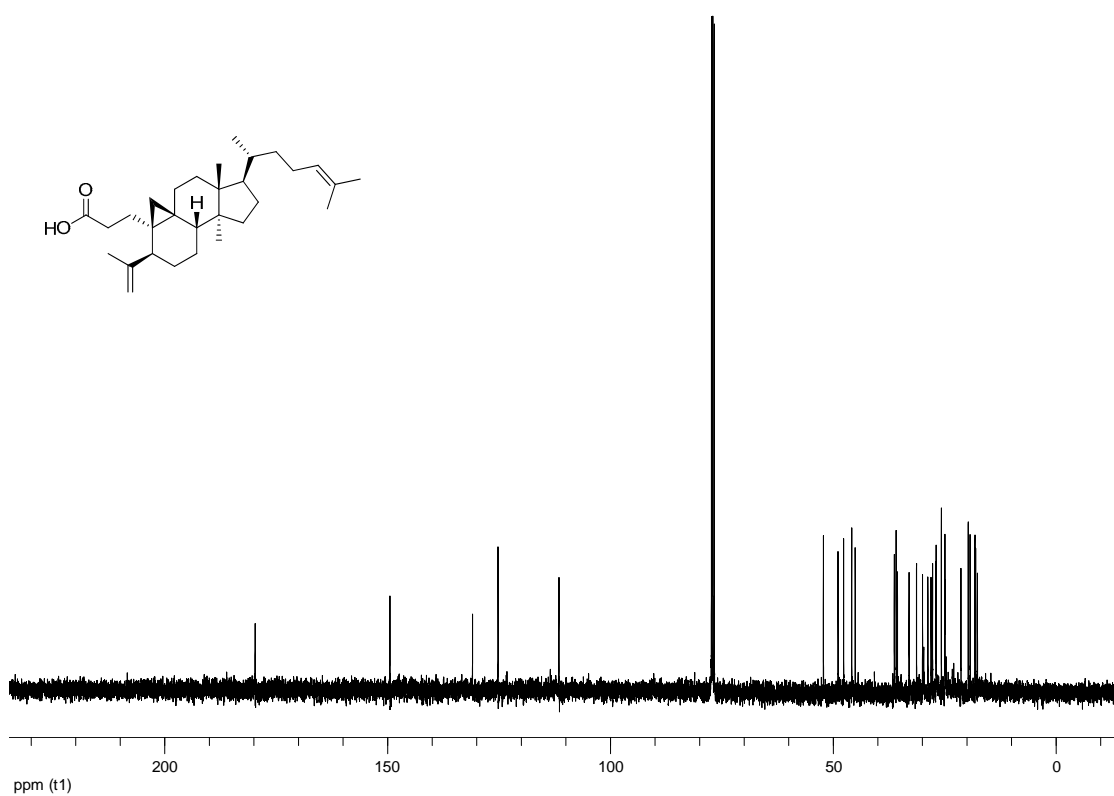


Figure 79. ¹³C NMR spectrum of compound **70** (CDCl₃; 100 MHz).

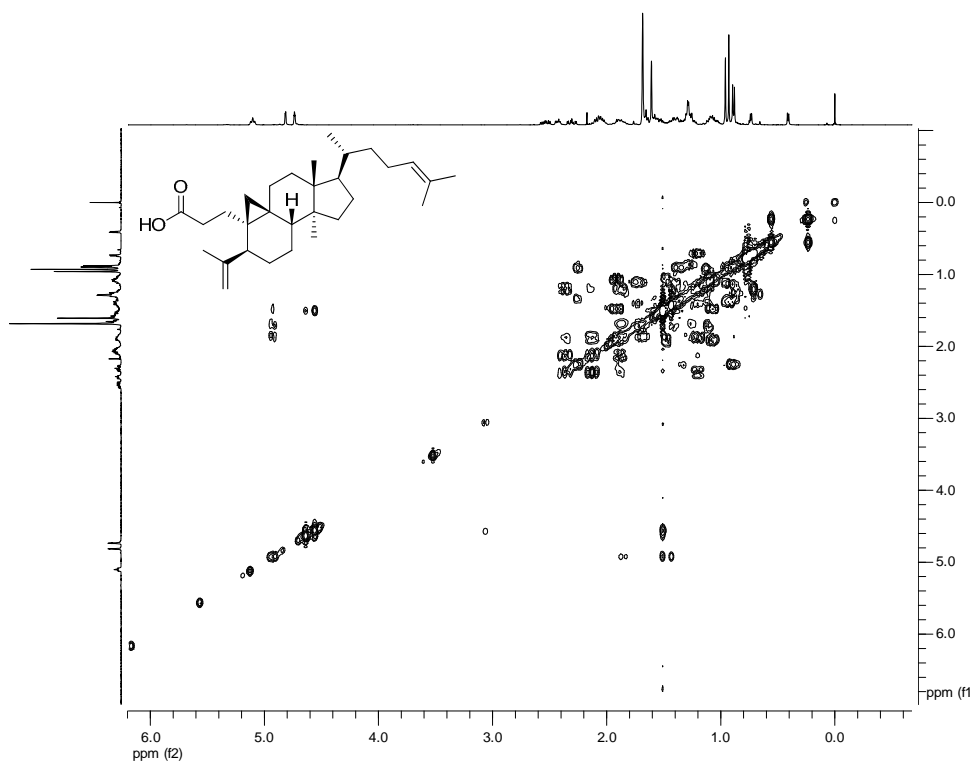


Figure 80. ^1H - ^1H COSY spectrum of compound **70** (CDCl_3 ; 400 MHz).

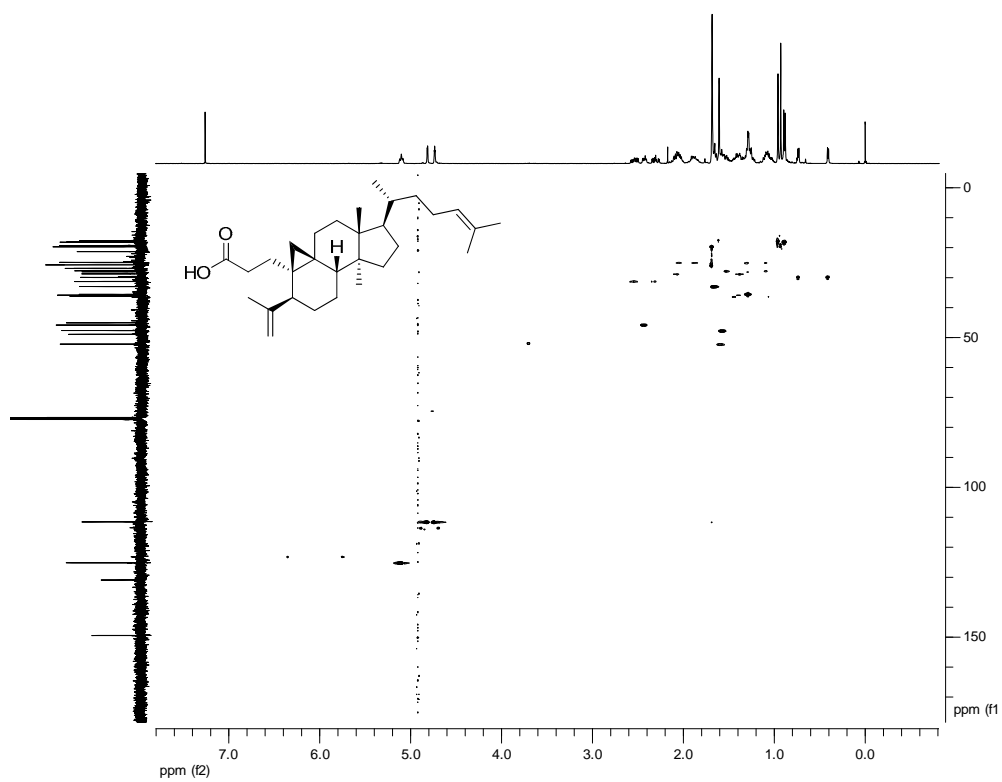


Figure 81. HSQC spectrum of compound **70** (CDCl_3 ; 400 MHz).

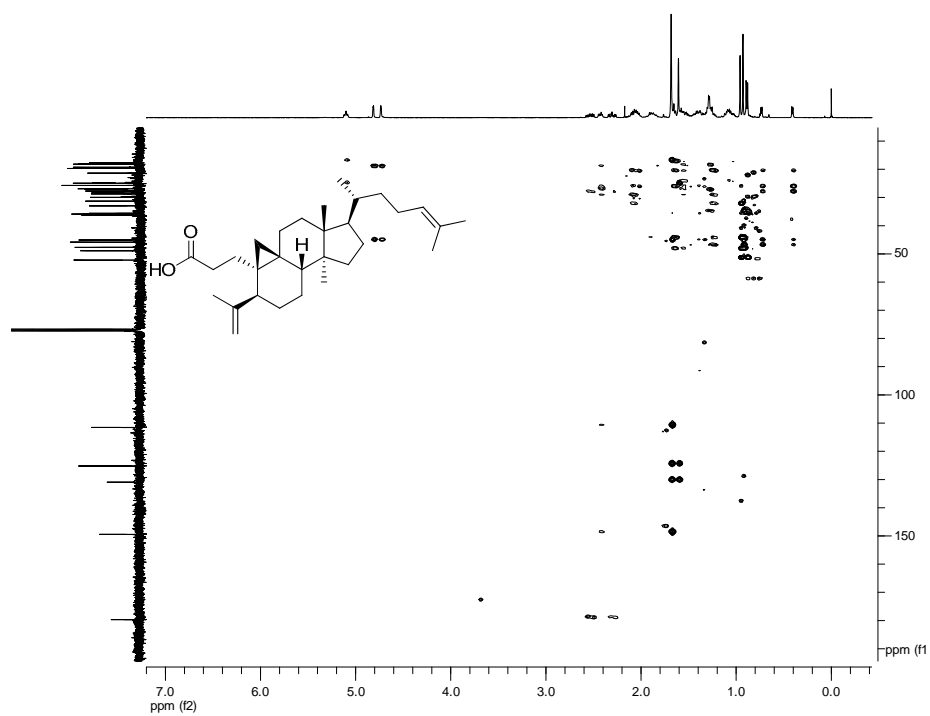


Figure 82. HMBC spectrum of compound **70** (CDCl₃; 400 MHz).

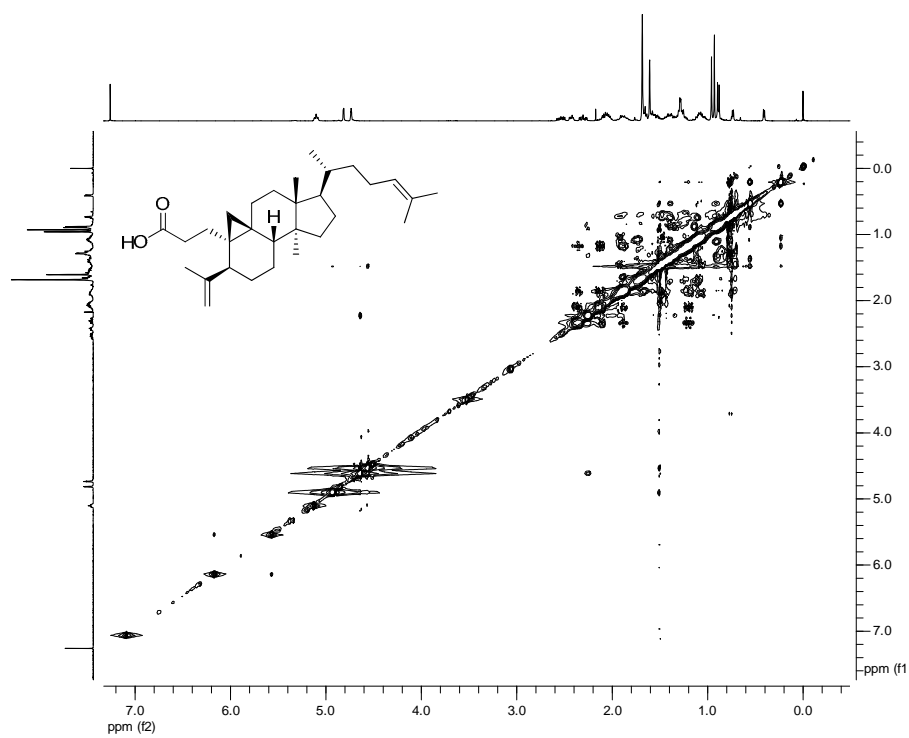


Figure 83. NOESY spectrum of compound **70** (CDCl₃; 400 MHz).

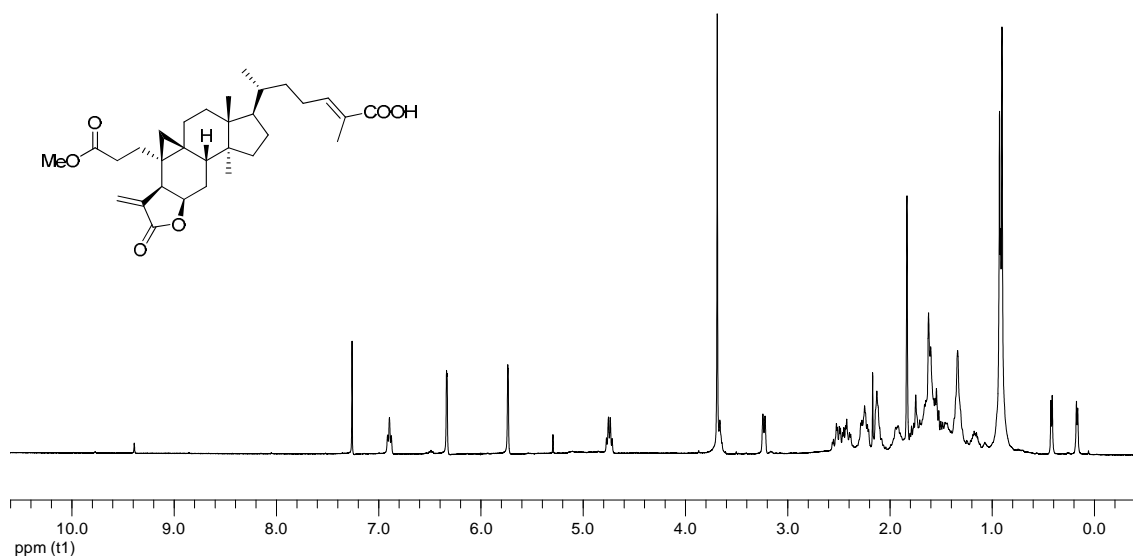


Figure 84. ¹H NMR spectrum of compound **71** (CDCl₃; 400 MHz).

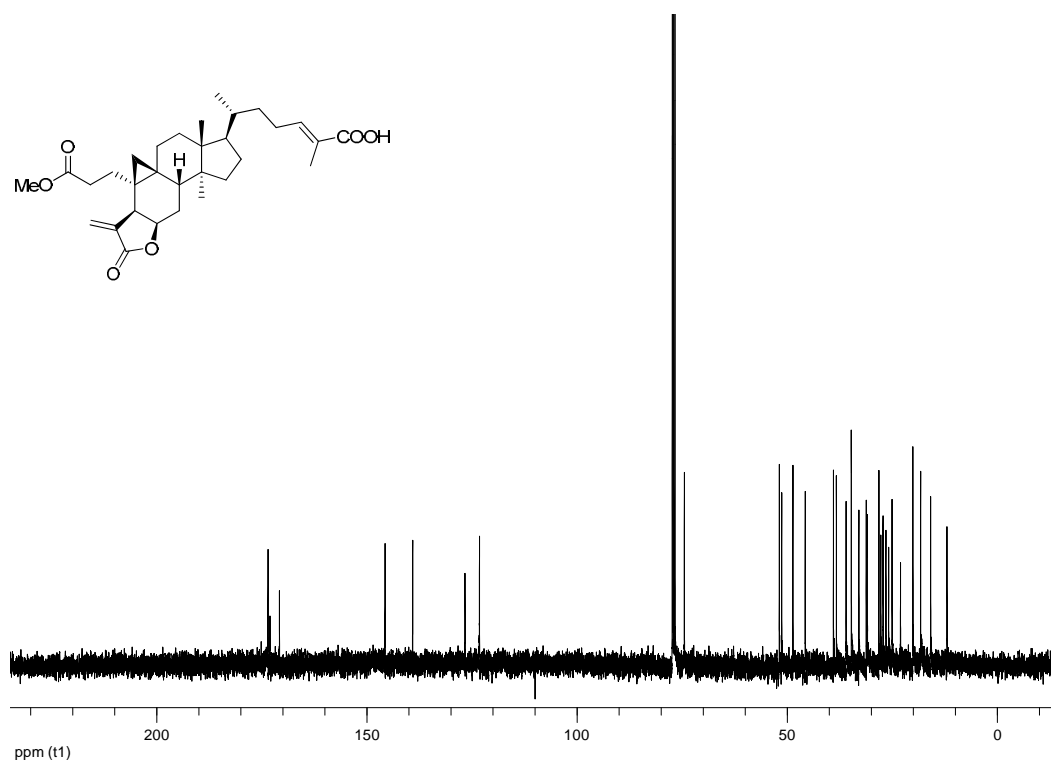


Figure 85. ¹³C NMR spectrum of compound **71** (CDCl₃; 100 MHz).

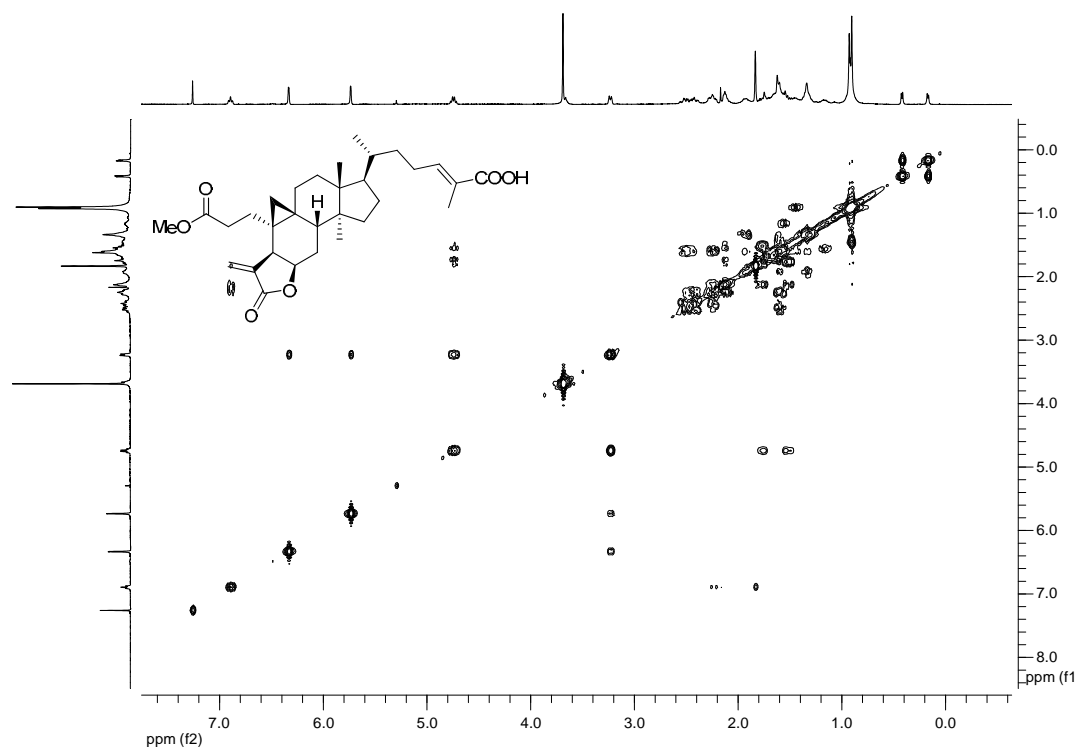


Figure 86. ^1H - ^1H COSY spectrum of compound 71 (CDCl_3 ; 400 MHz).

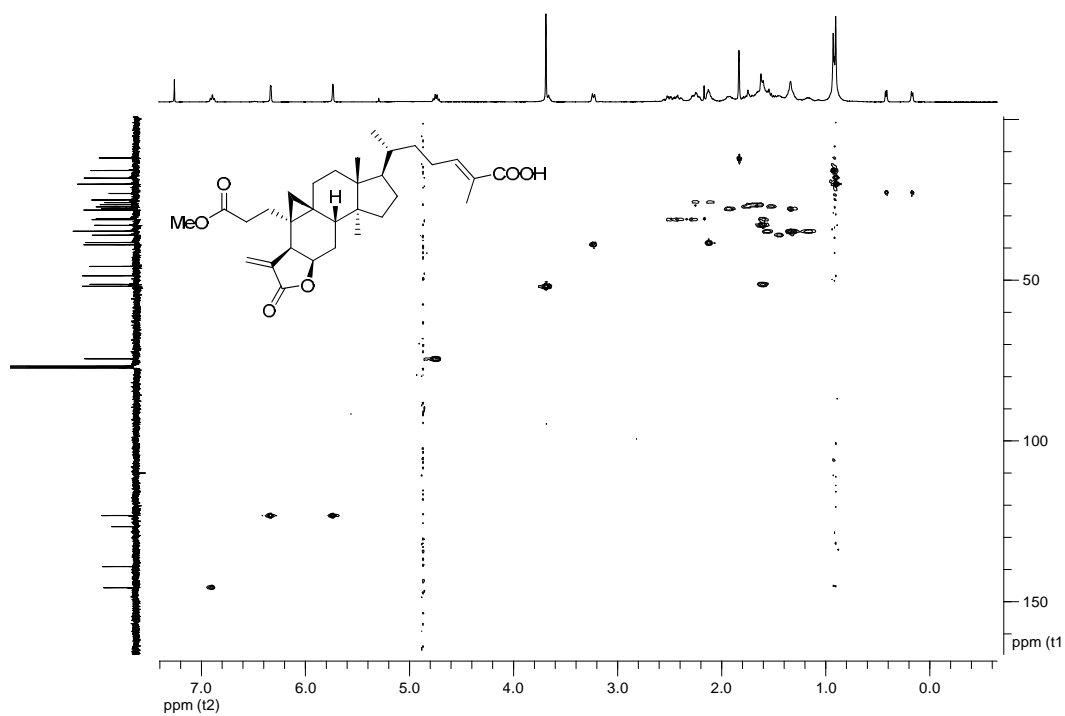


Figure 87. HSQC spectrum of compound 71 (CDCl_3 ; 400 MHz).

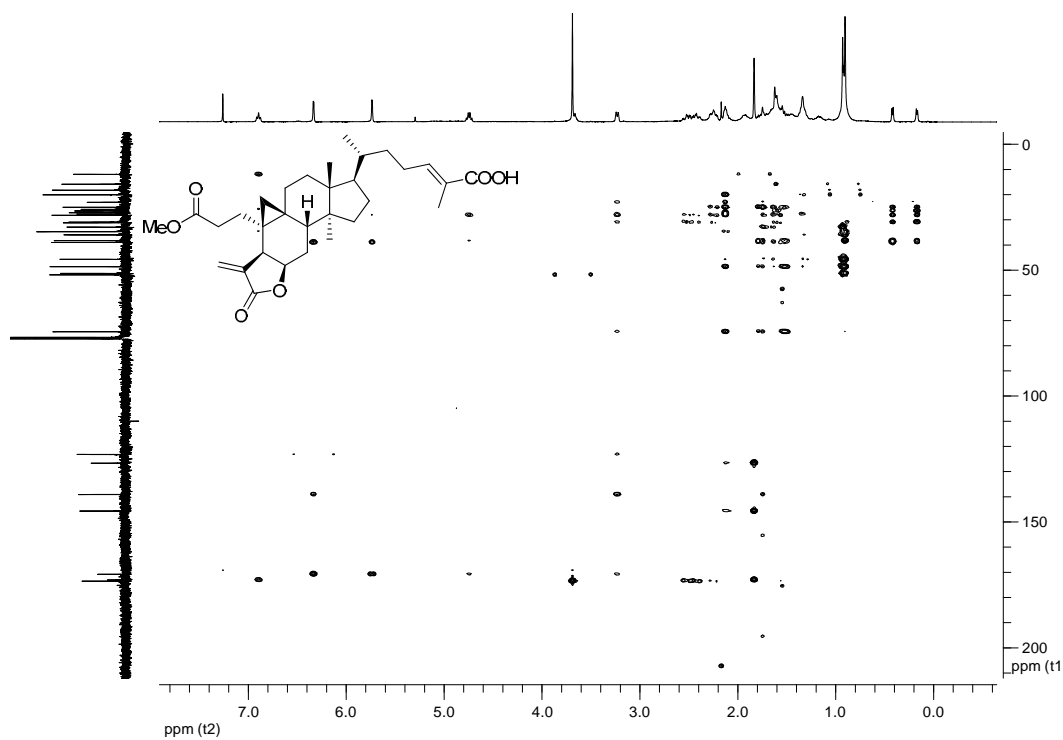


Figure 88. HMBC spectrum of compound **71** (CDCl₃; 400 MHz).

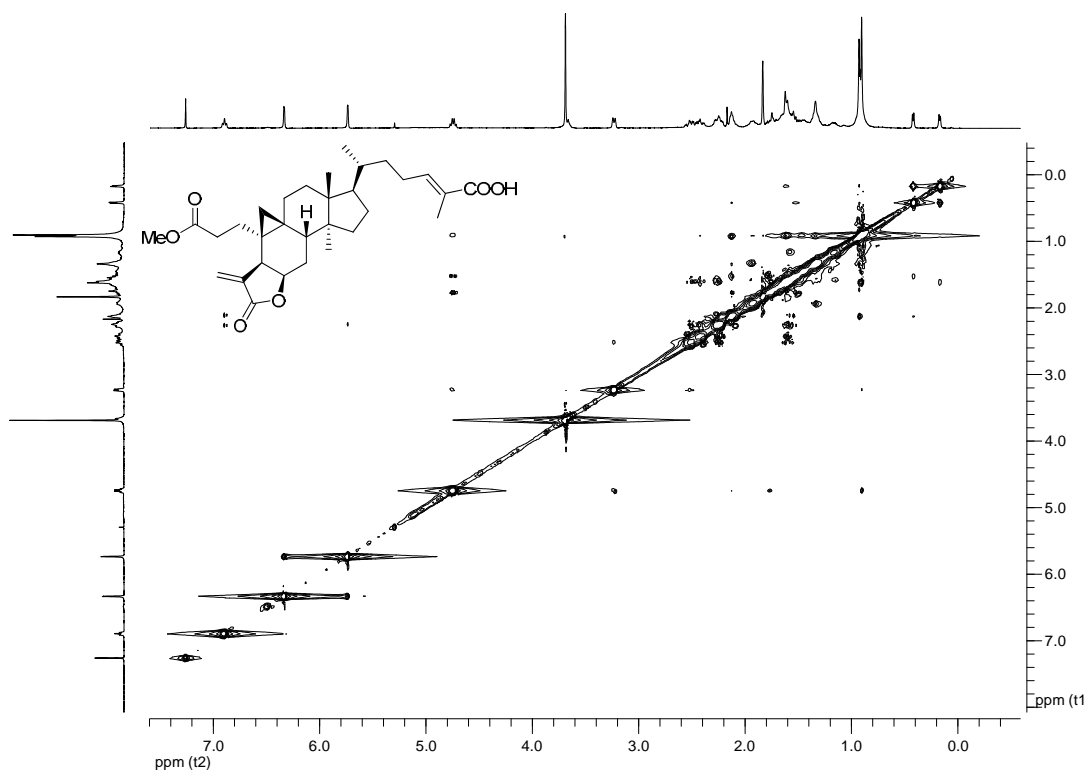


Figure 89. NOESY spectrum of compound **71** (CDCl₃; 400 MHz).

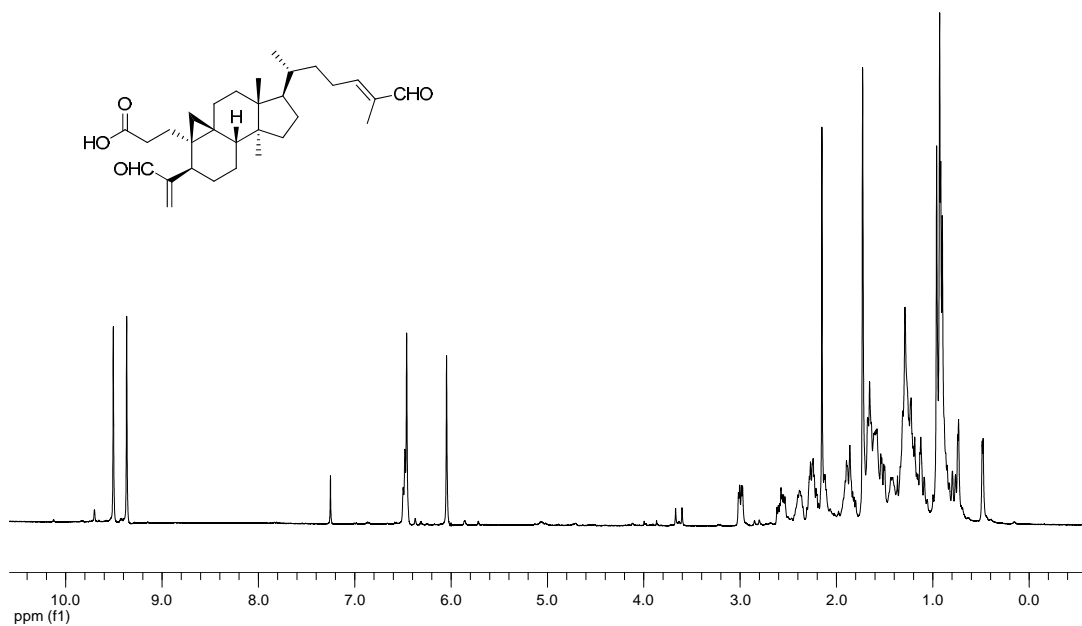


Figure 90. ^1H NMR spectrum of compound 72 (CDCl_3 ; 400 MHz).

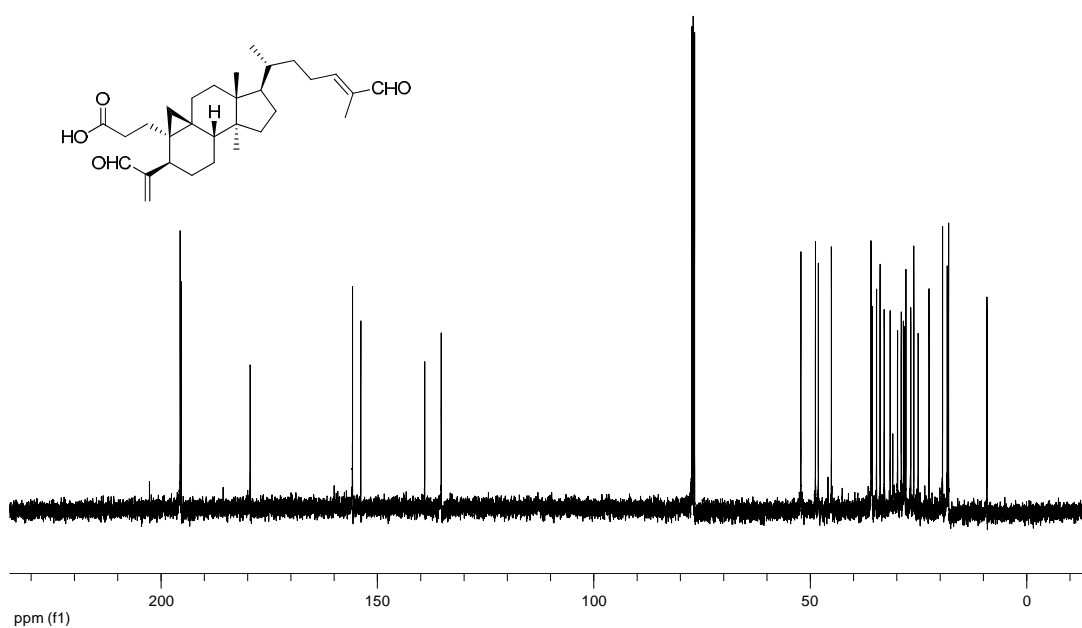


Figure 91. ^{13}C NMR spectrum of compound 72 (CDCl_3 ; 100 MHz).

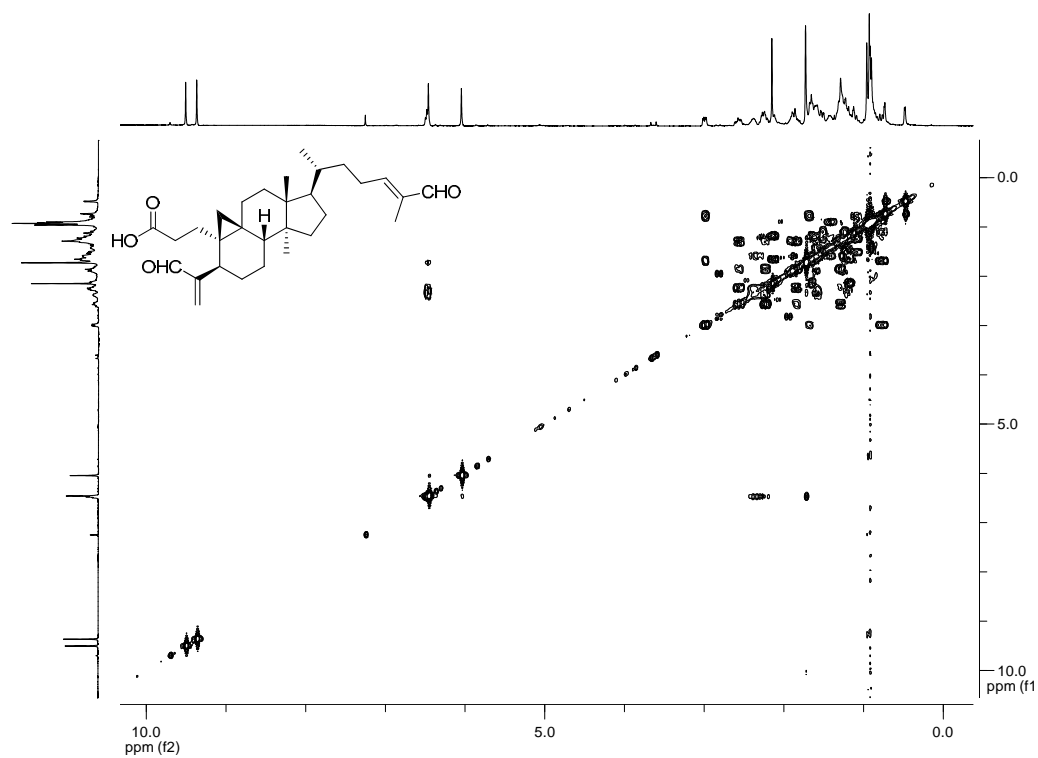


Figure 92. ^1H - ^1H COSY spectrum of compound **72** (CDCl_3 ; 400 MHz).

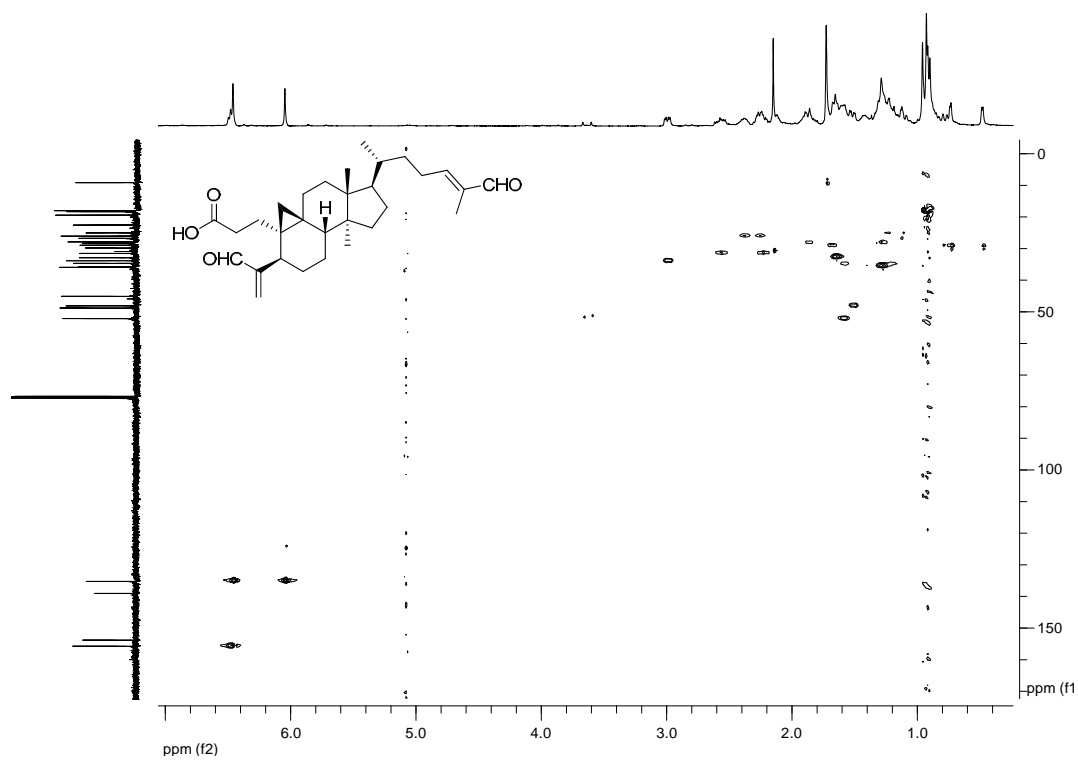


Figure 93. HSQC spectrum of compound **72** (CDCl_3 ; 400 MHz).

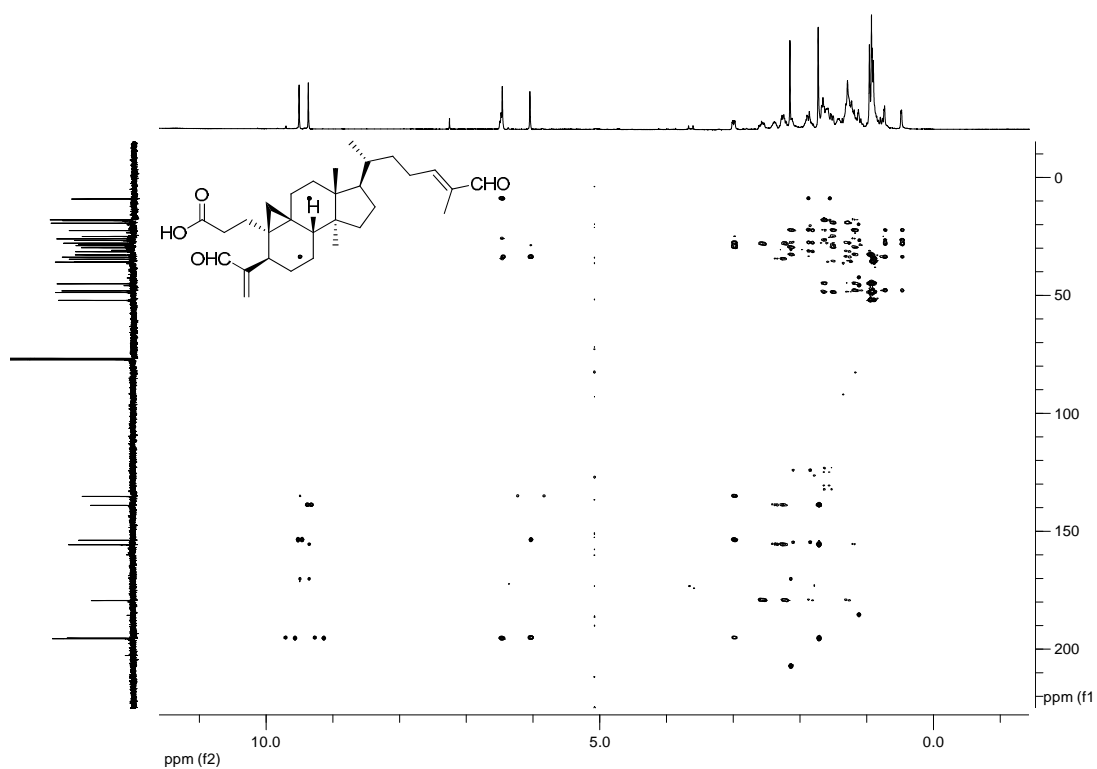


Figure 94. HMBC spectrum of compound **72** (CDCl₃; 400 MHz).

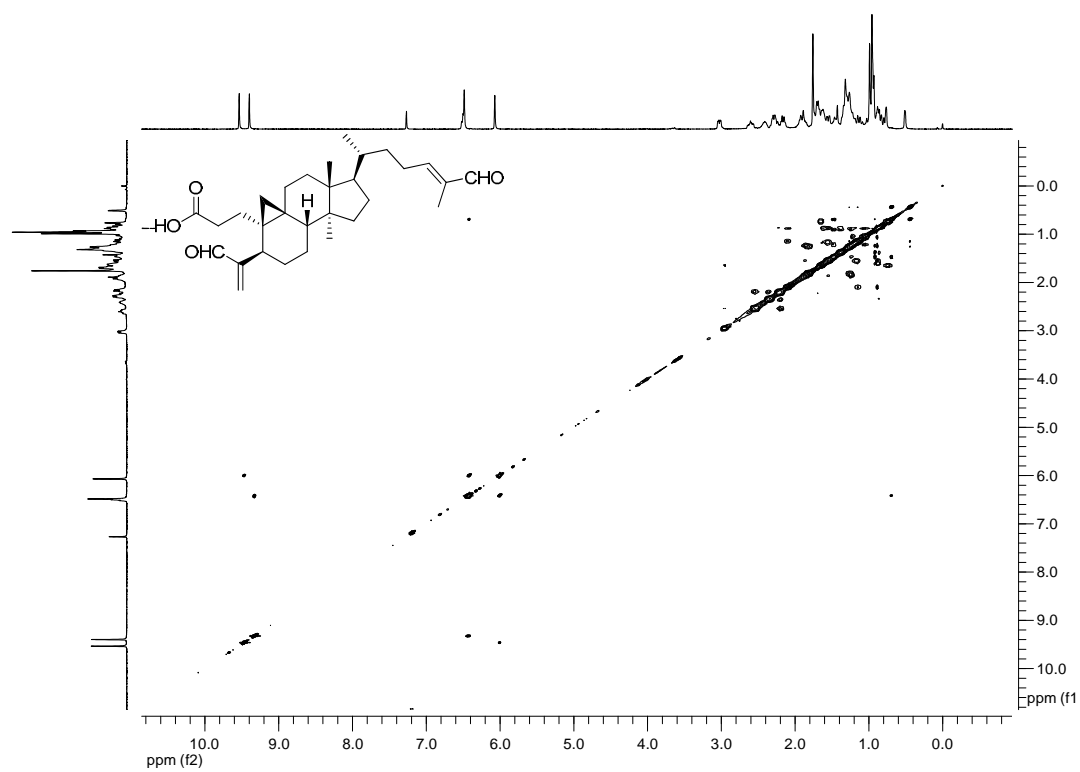


Figure 95. NOESY spectrum of compound **72** (CDCl₃; 400 MHz).

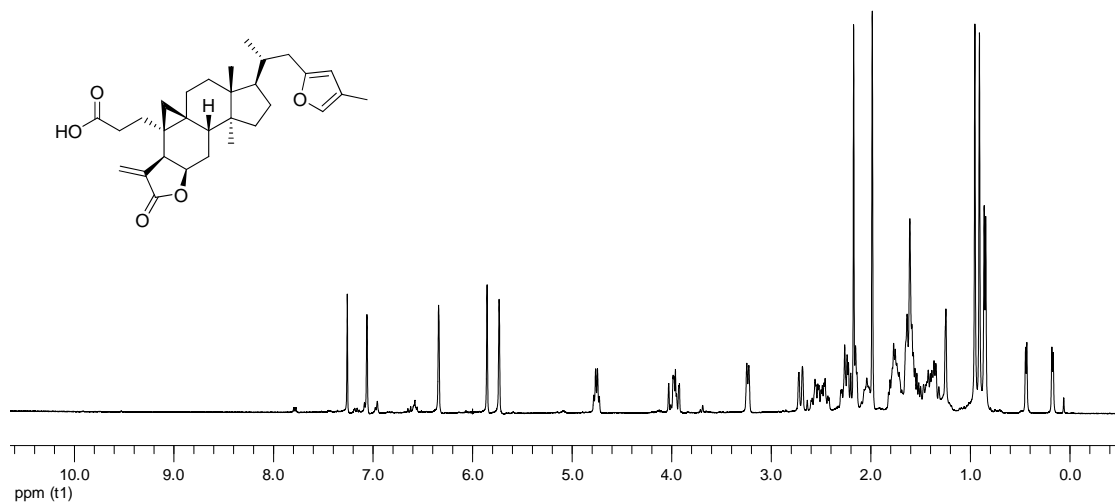


Figure 96. ¹H NMR spectrum of compound **73** (CDCl₃; 400 MHz).

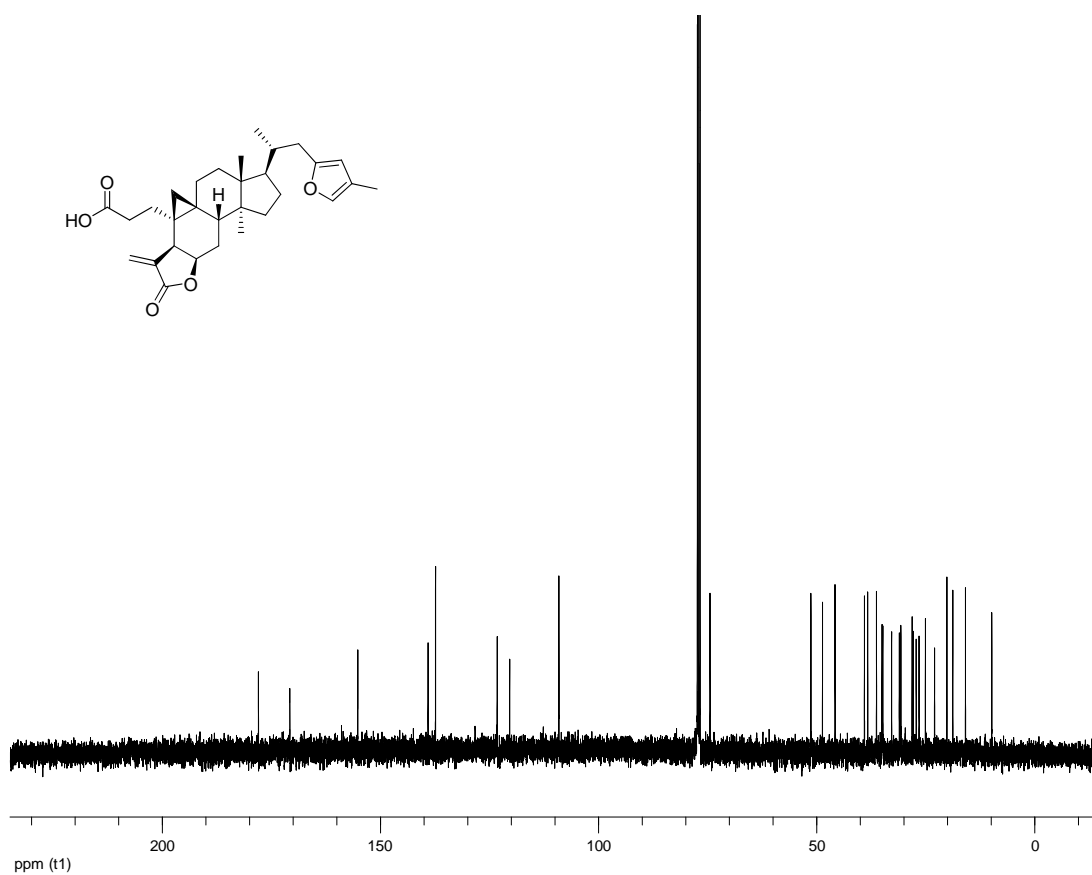


Figure 97. ¹³C NMR spectrum of compound **73** (CDCl₃; 100 MHz).

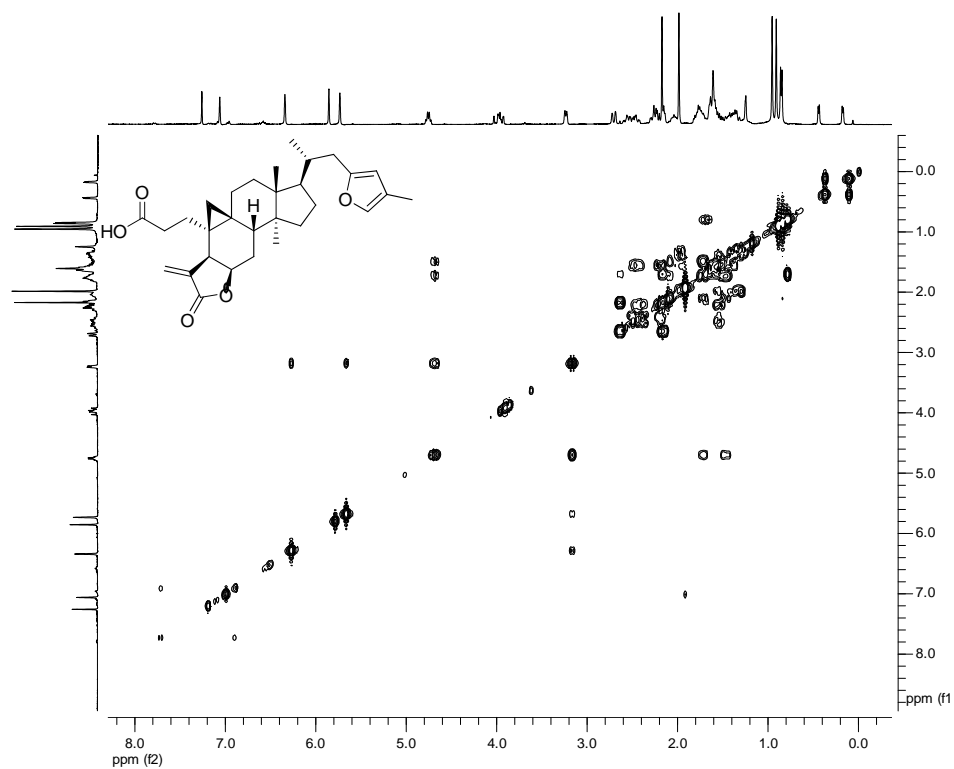


Figure 98. ^1H - ^1H COSY spectrum of compound 73 (CDCl_3 ; 400 MHz).

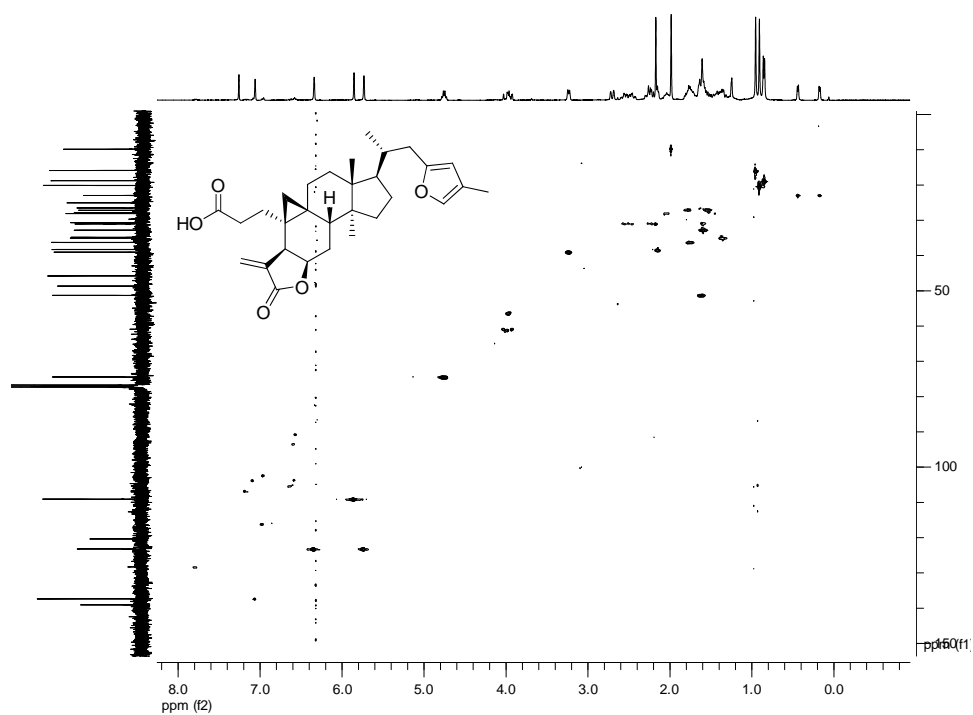


Figure 99. HSQC spectrum of compound 73 (CDCl_3 ; 400 MHz).

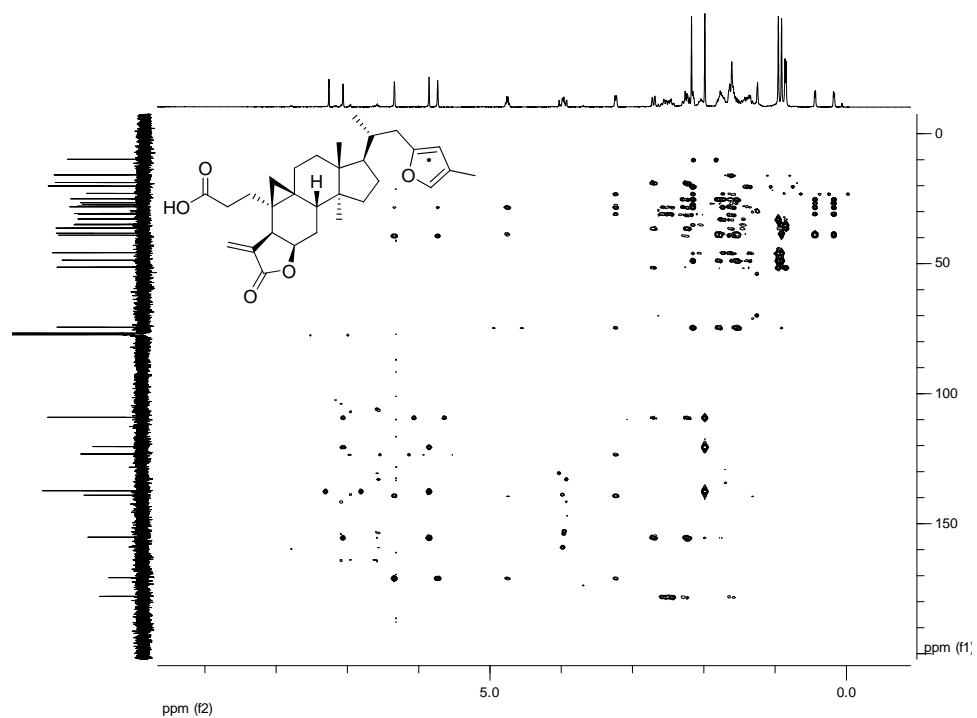


Figure 100. HMBC spectrum of compound **73** (CDCl₃; 400 MHz).

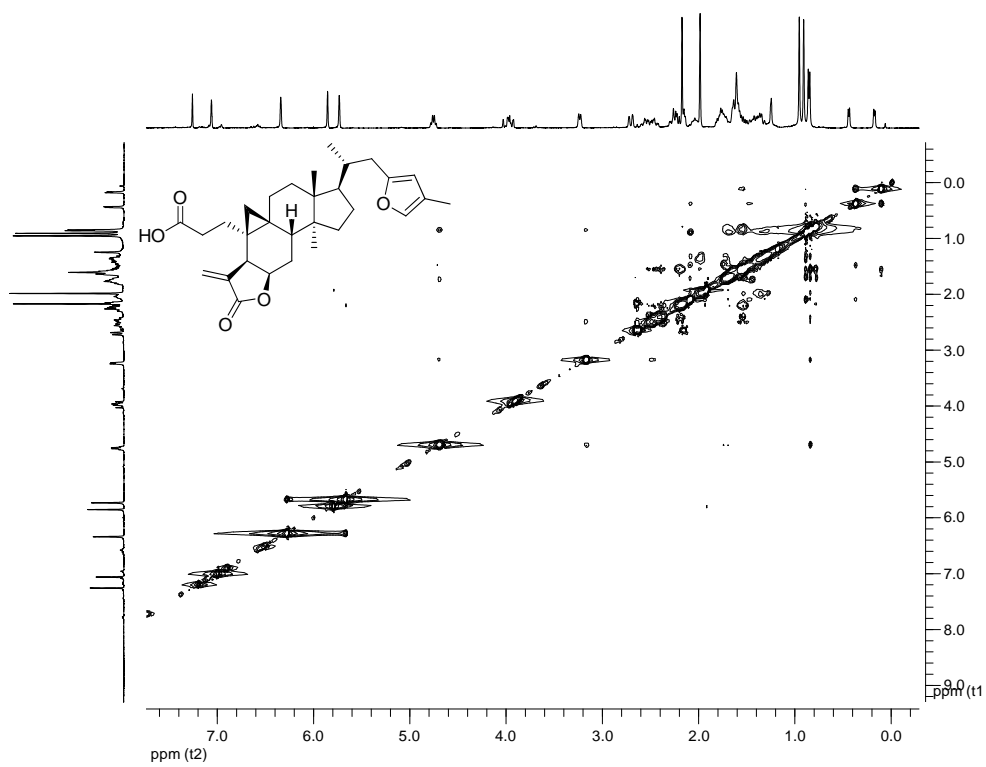


Figure 101. NOESY spectrum of compound **73** (CDCl₃; 400 MHz).

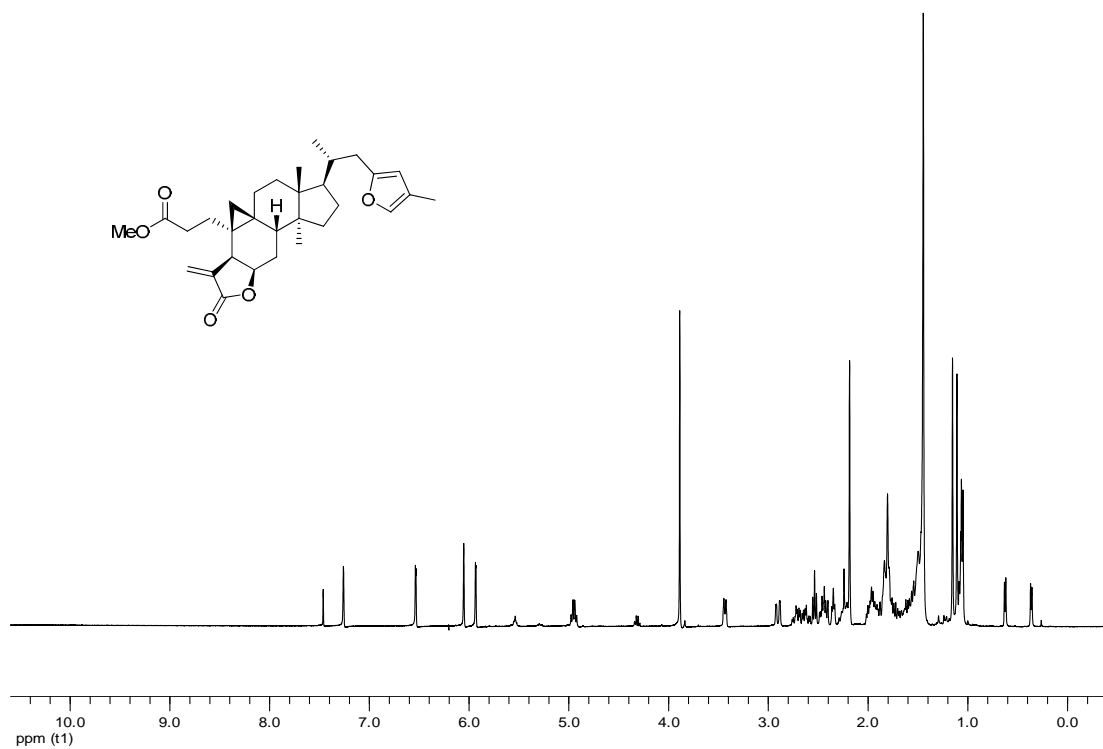


Figure 102. ¹H NMR spectrum of compound **74** (CDCl₃; 400 MHz).

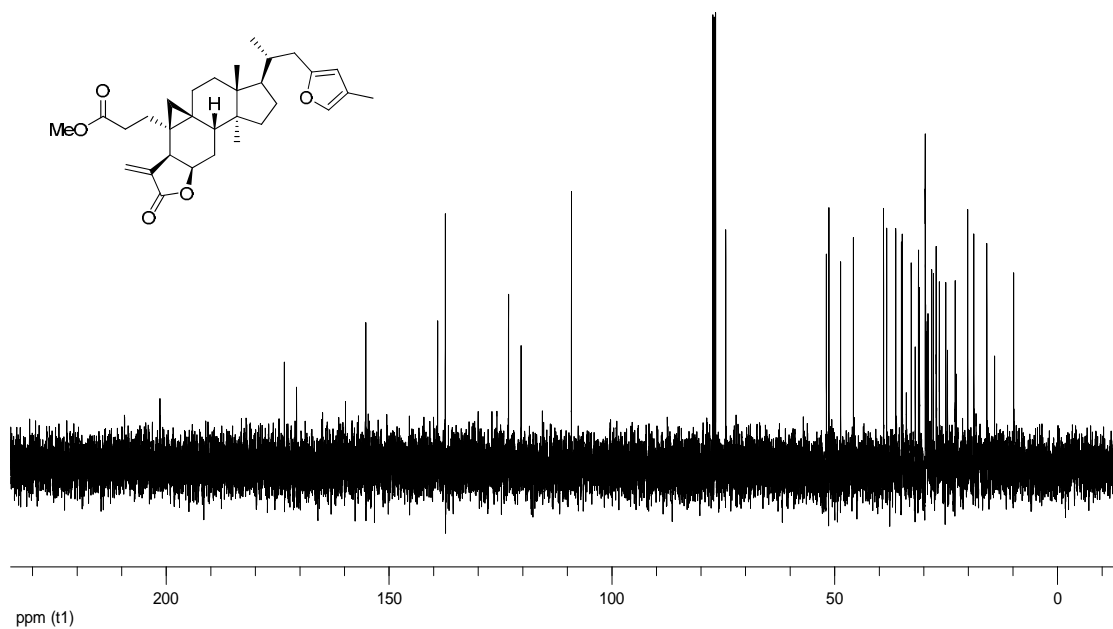


Figure 103. ¹³C NMR spectrum of compound **74** (CDCl₃; 100 MHz).

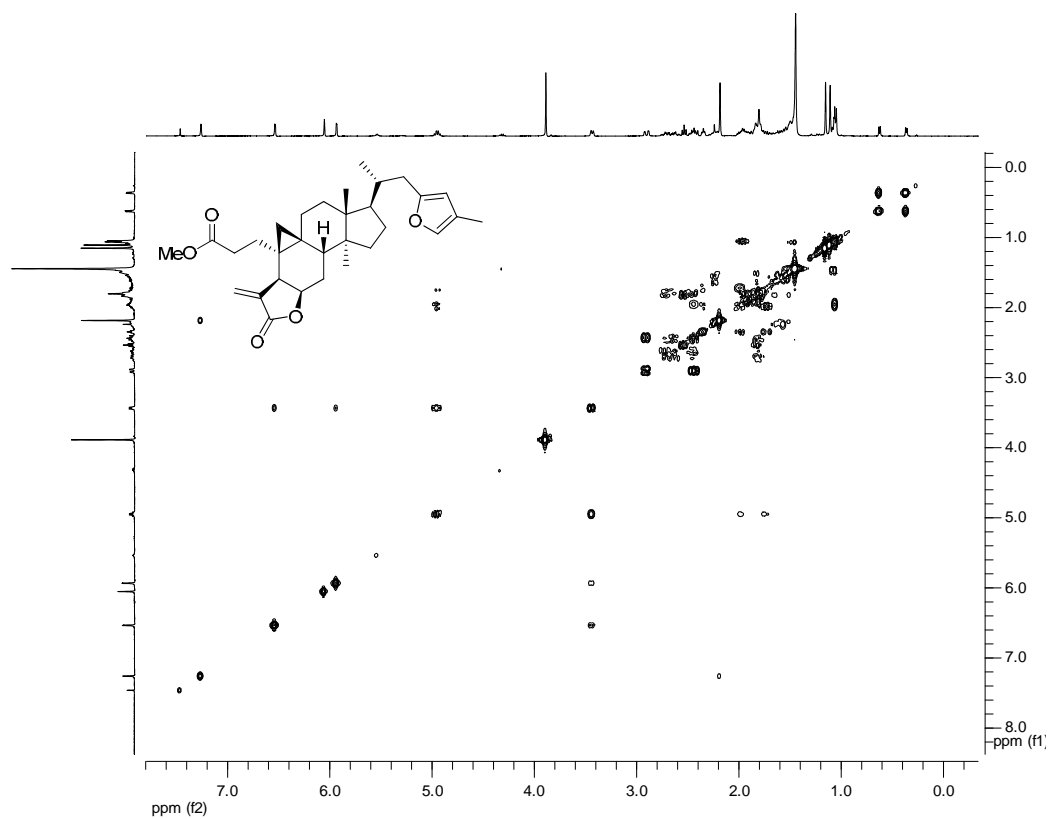


Figure 104. ^1H - ^1H COSY spectrum of compound **74** (CDCl_3 ; 400 MHz).

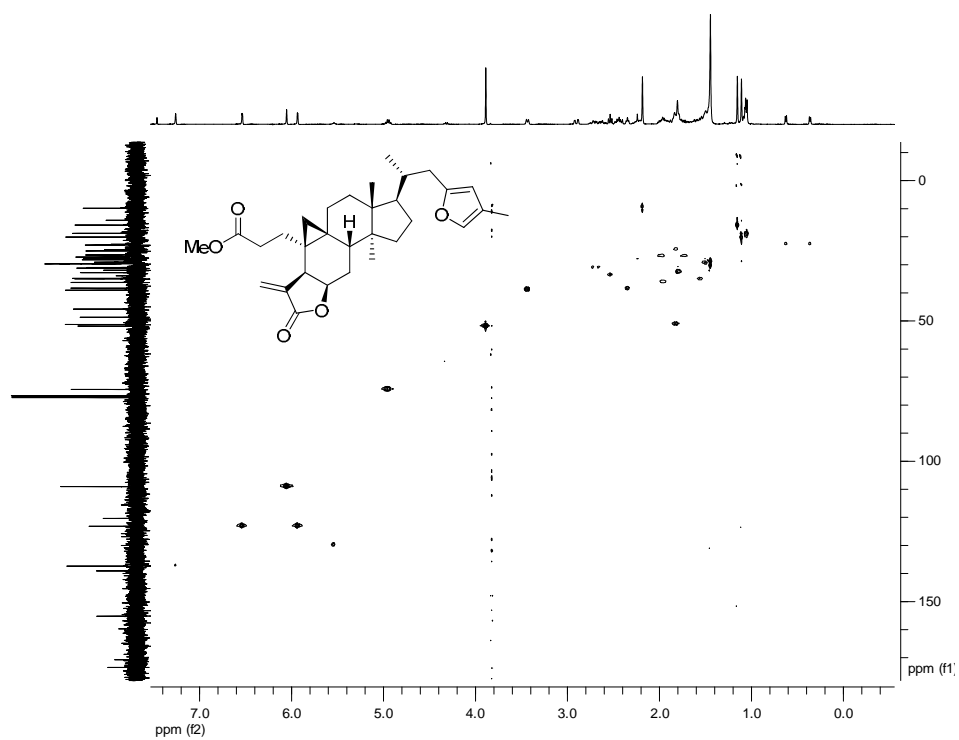


Figure 105. HSQC spectrum of compound **74** (CDCl_3 ; 400 MHz).

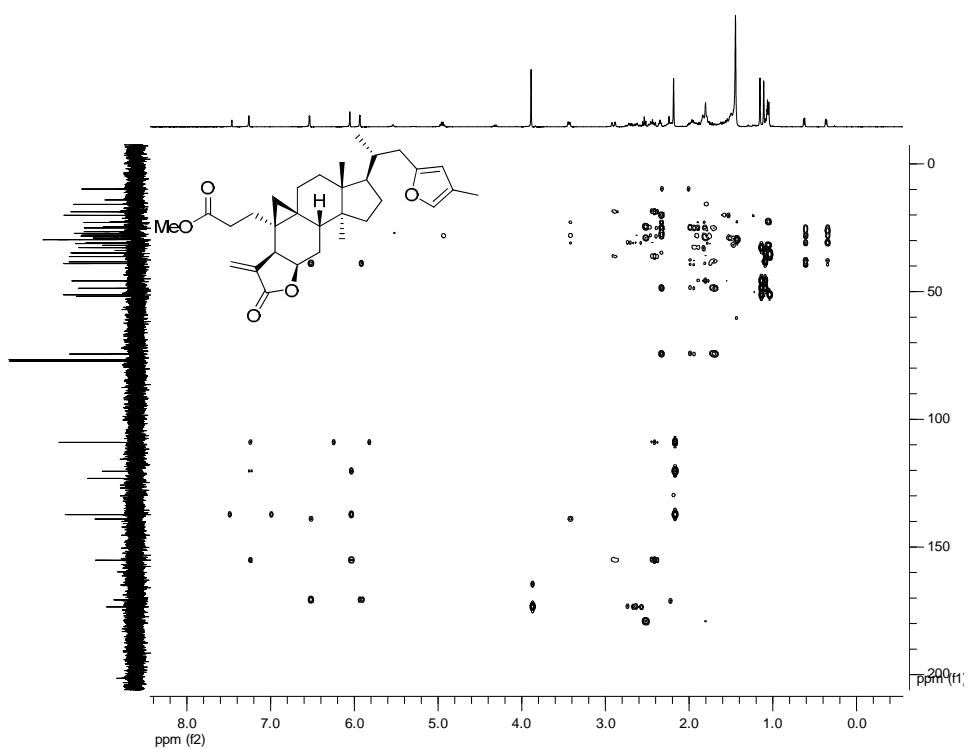


Figure 106. HMBC spectrum of compound **74** (CDCl₃; 400 MHz).

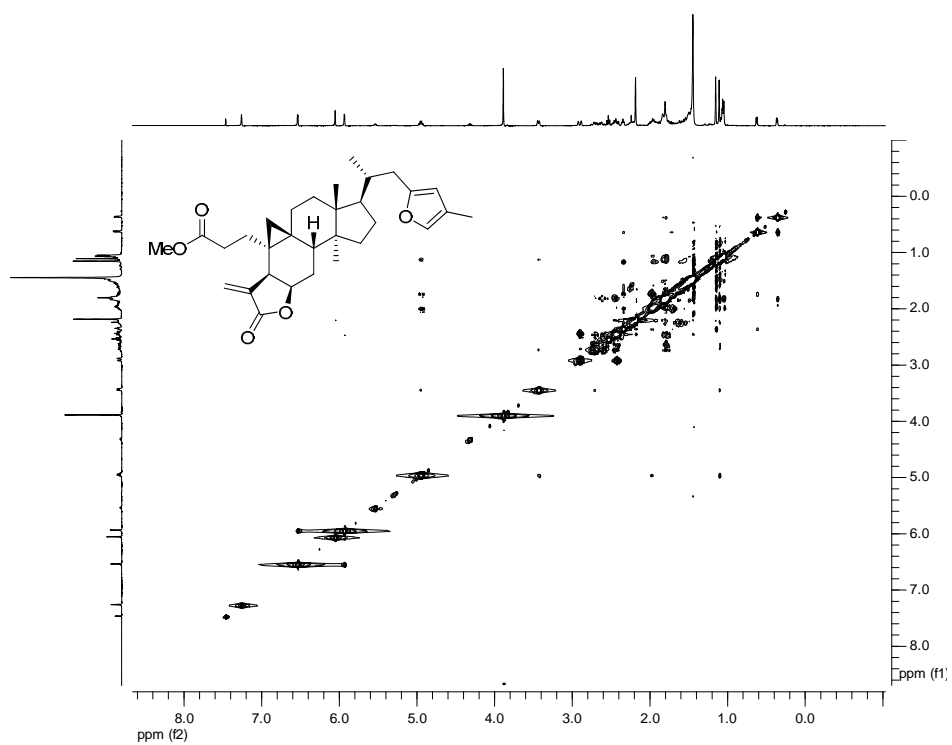


Figure 107. NOESY spectrum of compound **74** (CDCl₃; 400 MHz).

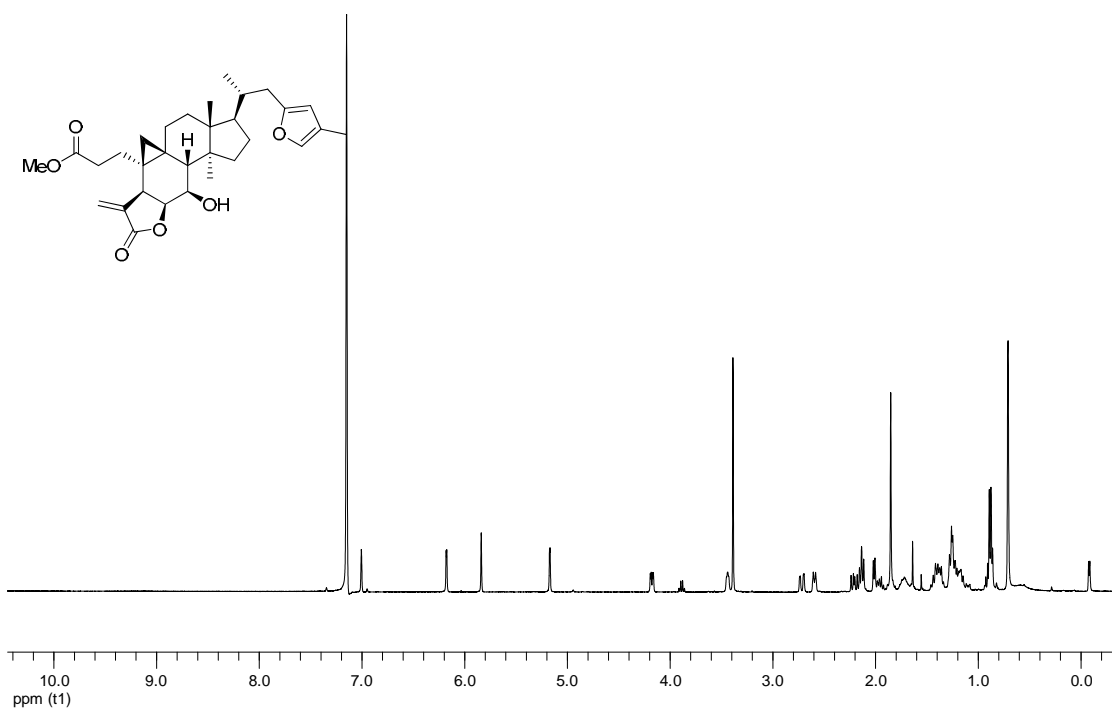


Figure 108. ¹H NMR spectrum of compound **75** (C₆D₆; 400 MHz).

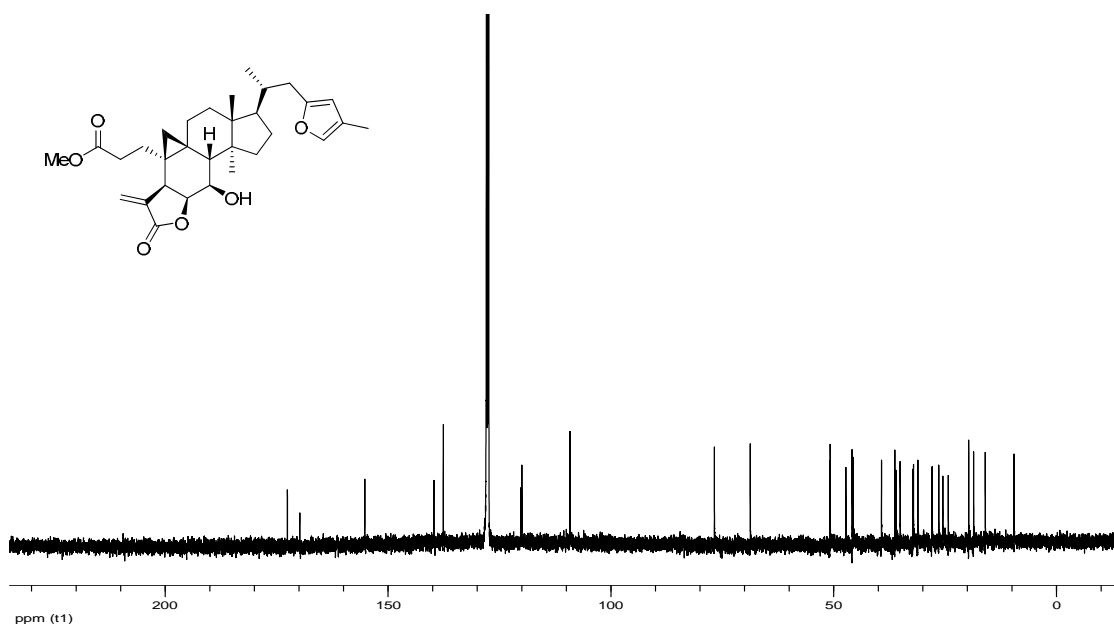


Figure 109. ¹³C NMR spectrum of compound **75** (C₆D₆; 100 MHz).

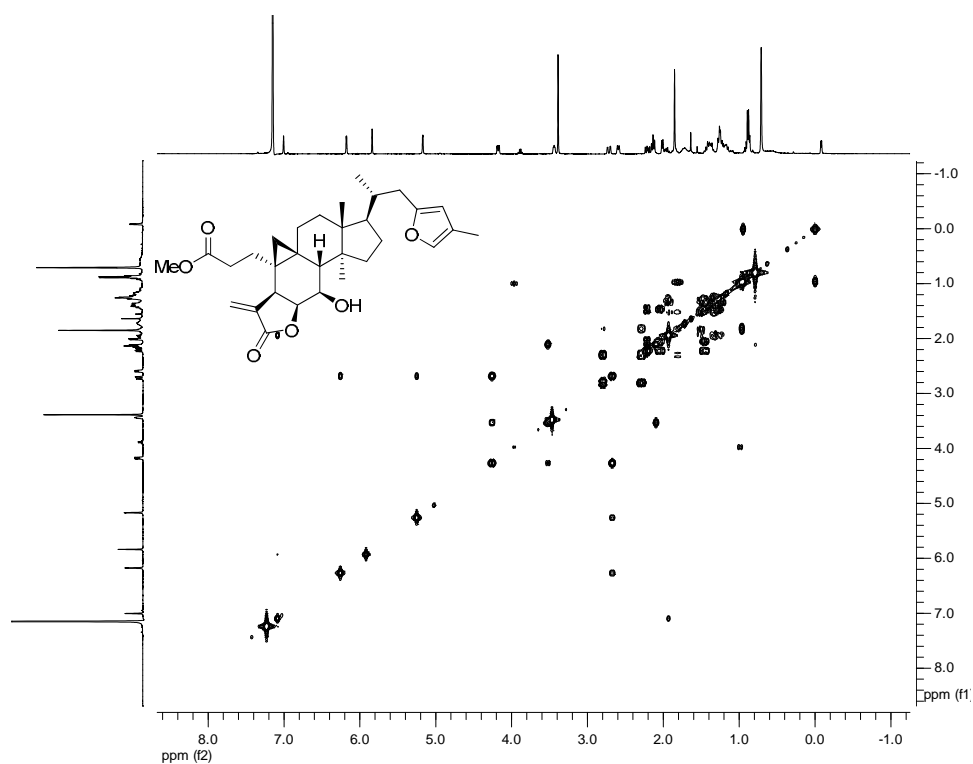


Figure 110. ^1H - ^1H COSY spectrum of compound 75 (C_6D_6 ; 400 MHz).

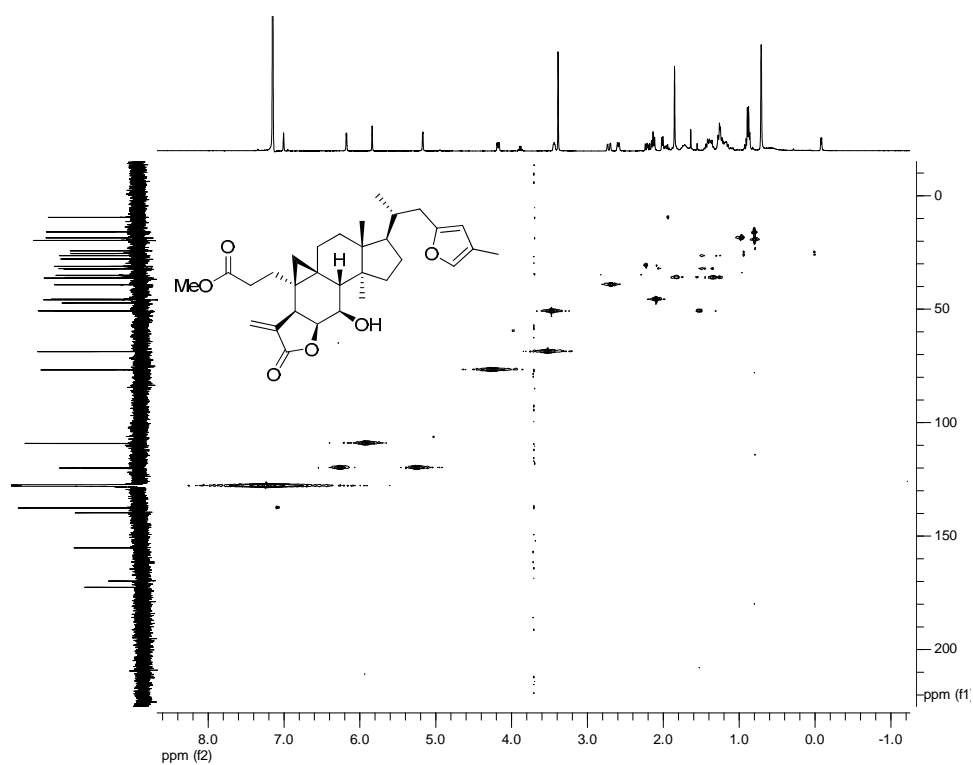


Figure 111. HSQC spectrum of compound 75 (C_6D_6 ; 400 MHz).

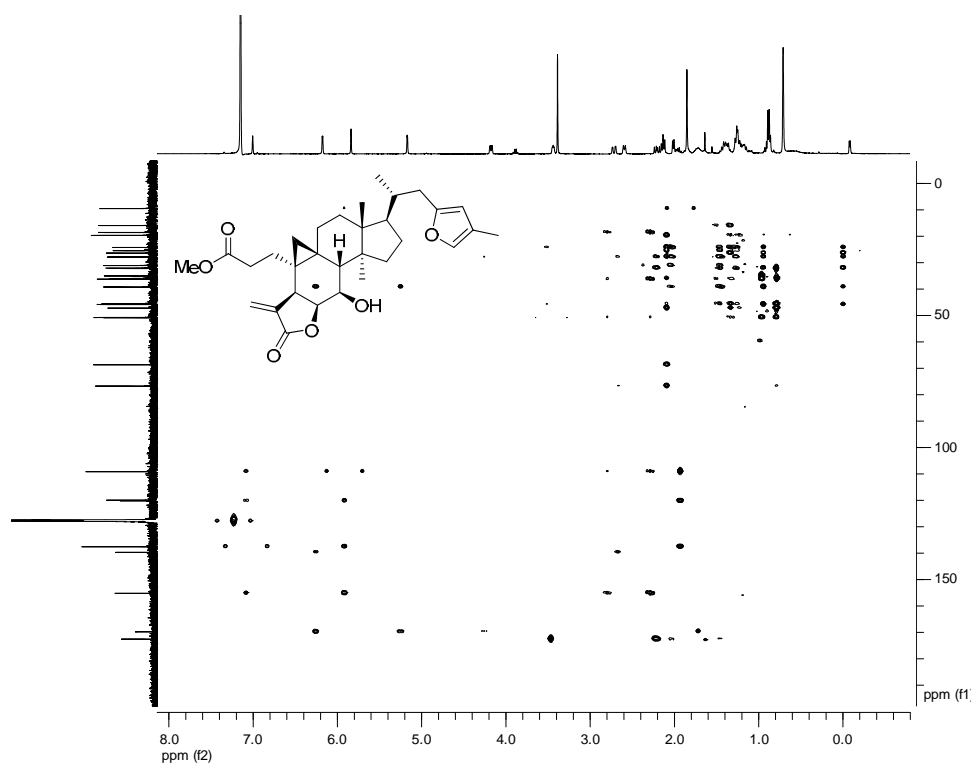


Figure 112. HMBC spectrum of compound **75** (C_6D_6 ; 400 MHz).

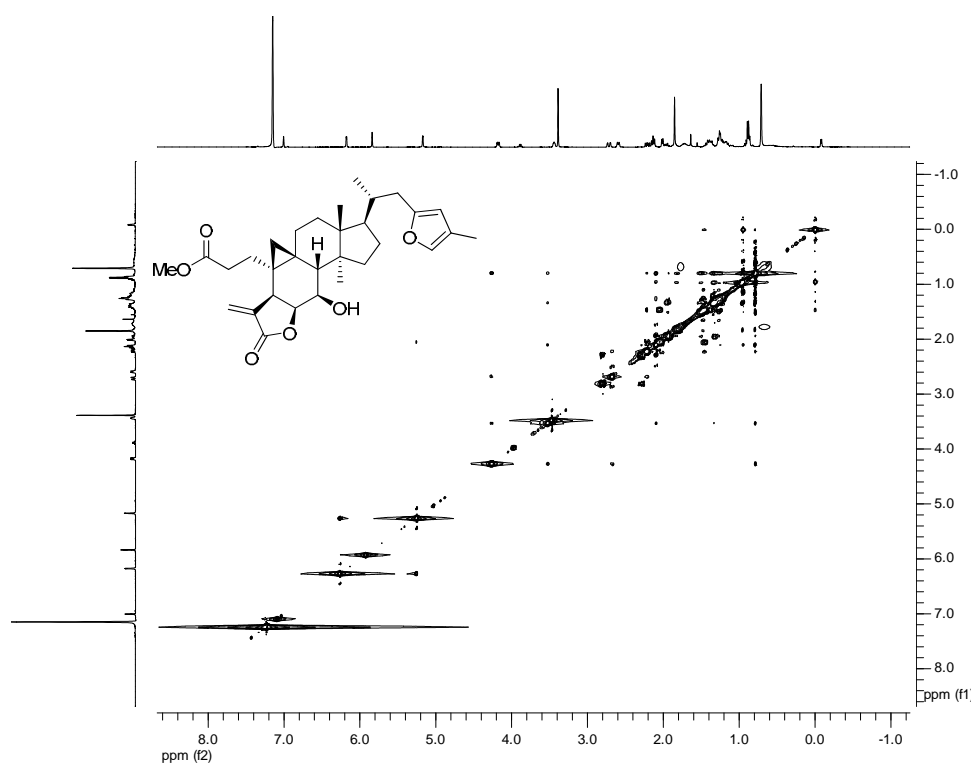


Figure 113. NOESY spectrum of compound **75** (C_6D_6 ; 400 MHz).

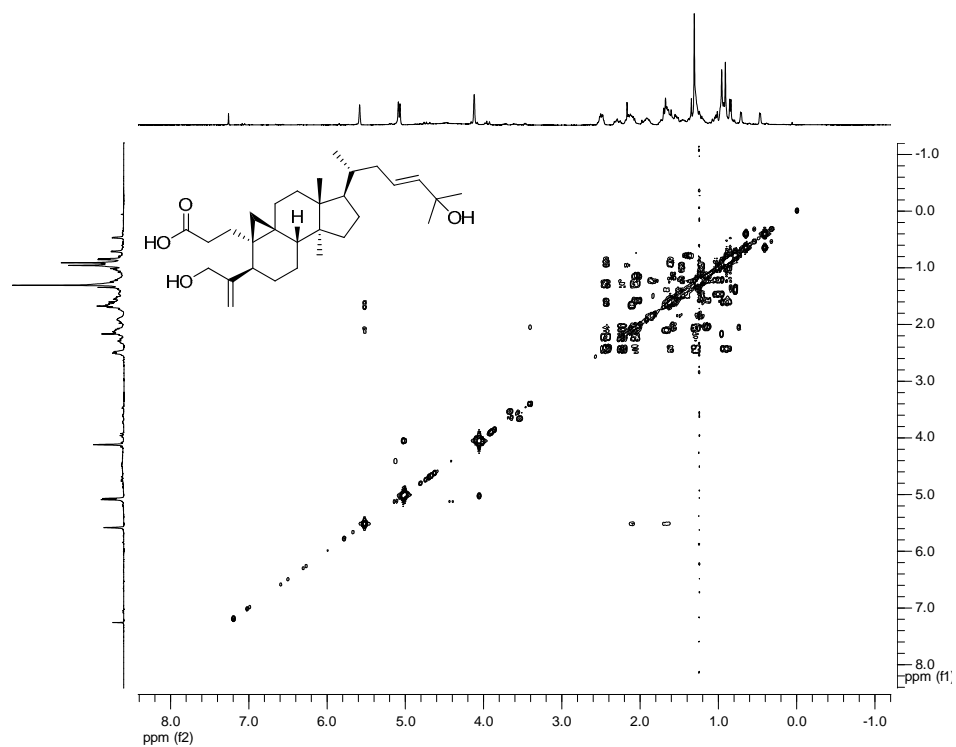


Figure 116. ^1H - ^1H COSY spectrum of compound **76** (CDCl_3 ; 400 MHz).

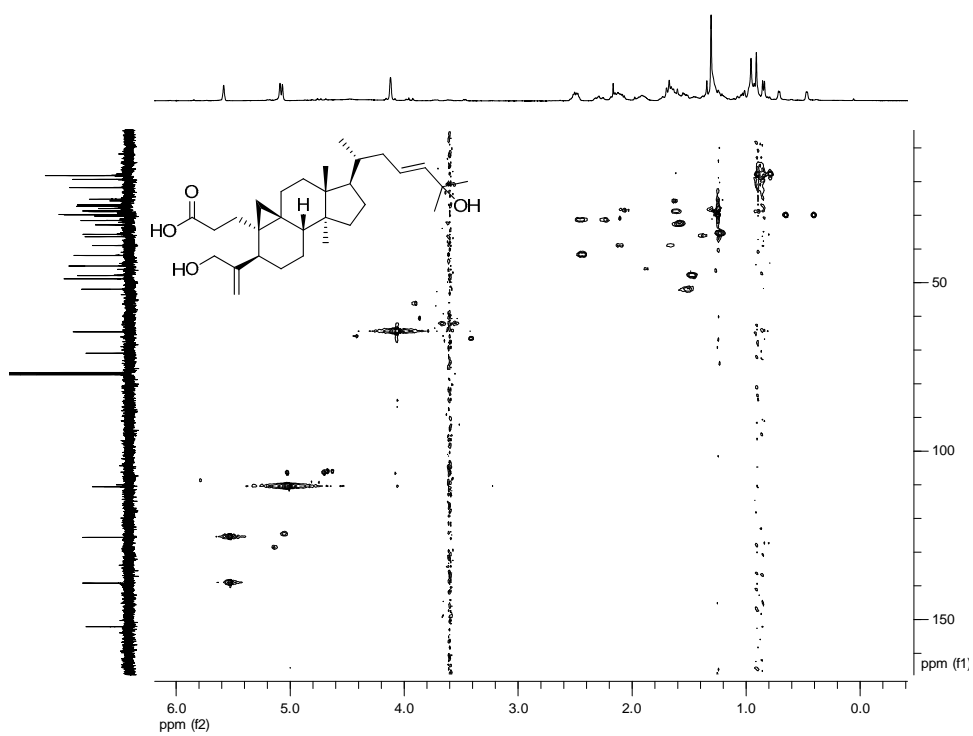


Figure 117. HSQC spectrum of compound **76** (CDCl_3 ; 400 MHz).

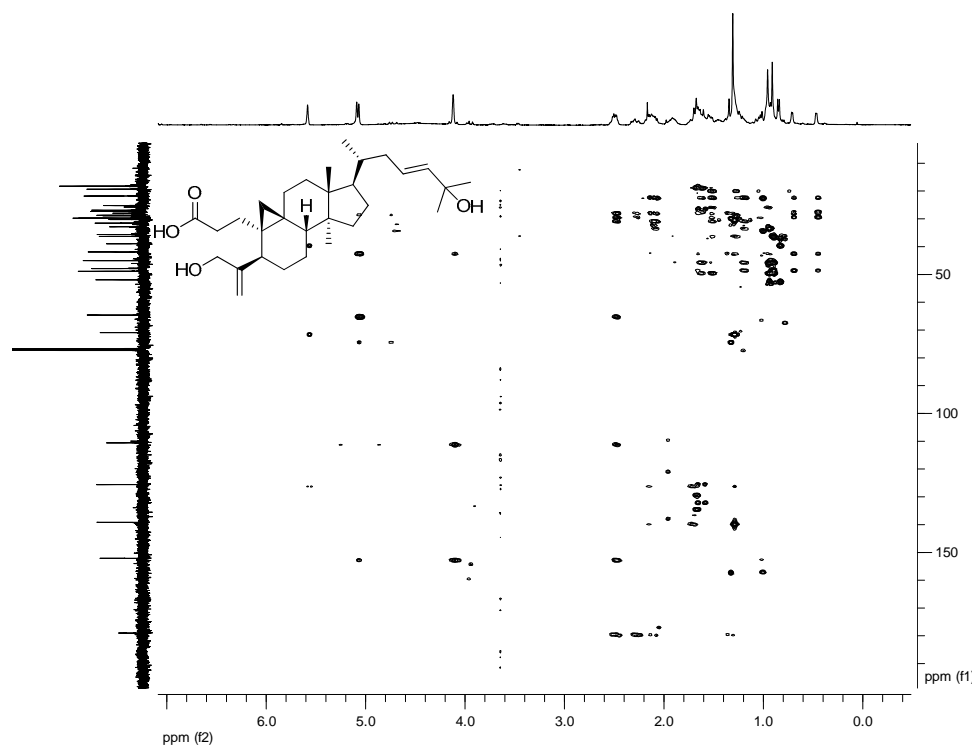


Figure 118. HMBC spectrum of compound **76** (CDCl₃; 400 MHz).

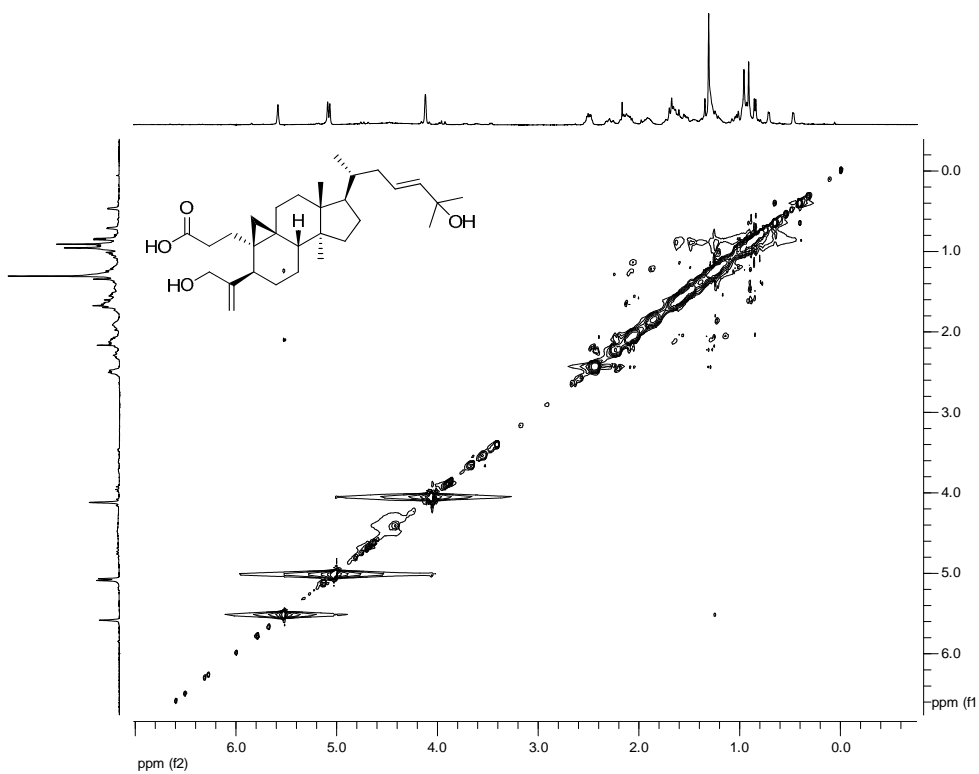


Figure 119. NOESY spectrum of compound **76** (CDCl₃; 400 MHz).

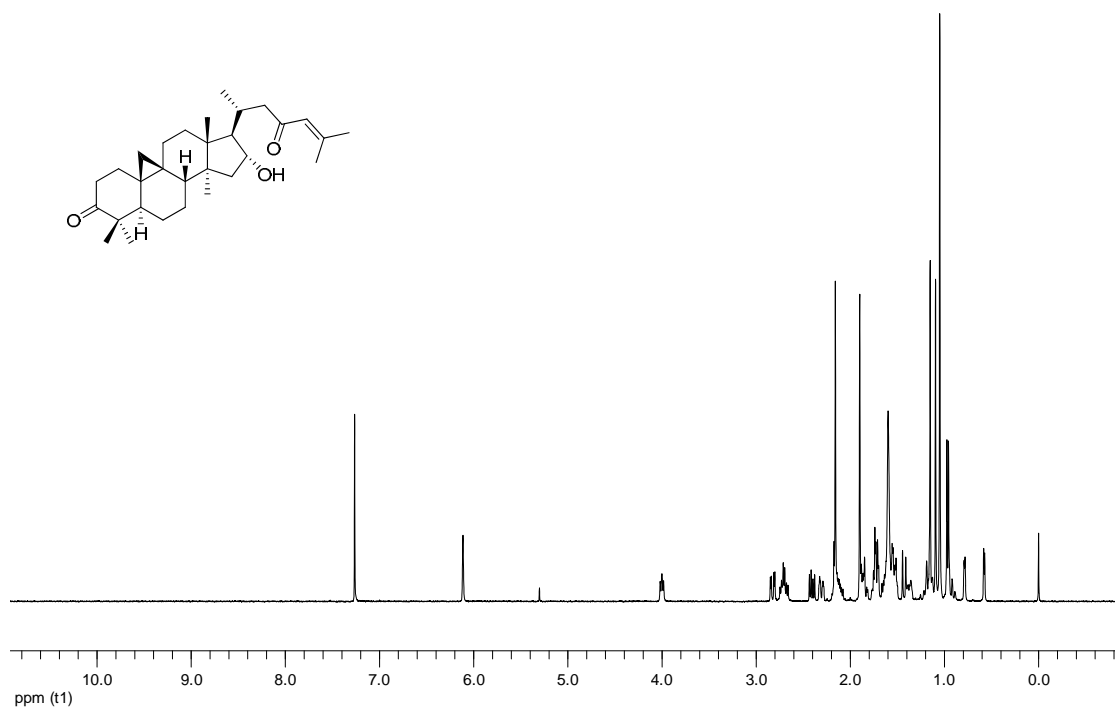


Figure 120. ¹H NMR spectrum of compound **77** (CDCl₃; 400 MHz).

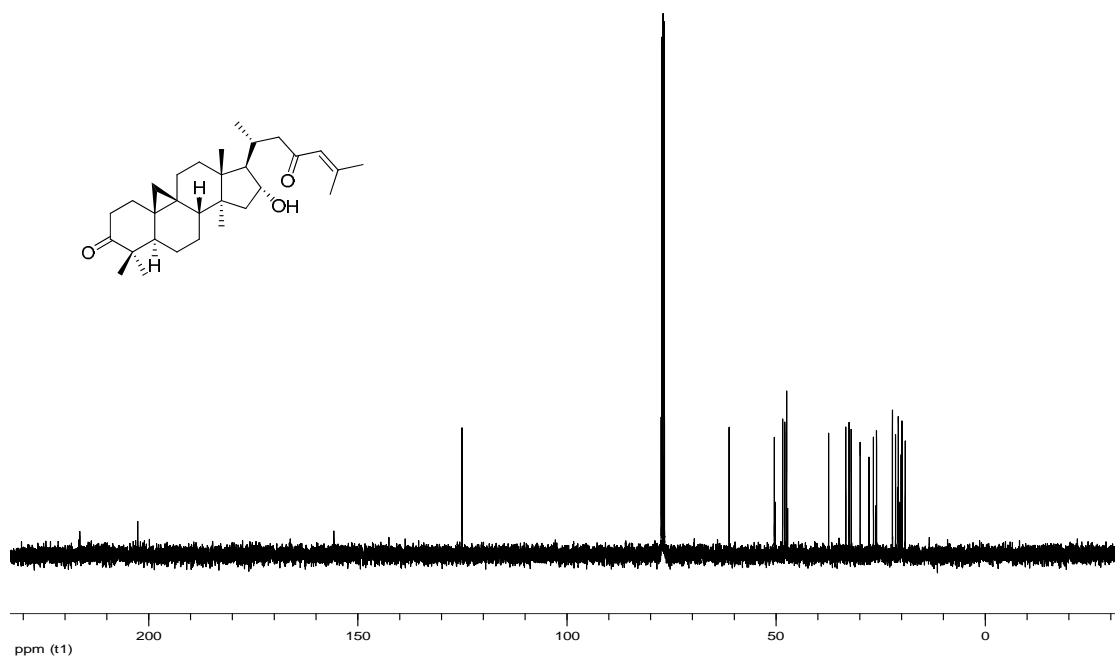


Figure 121. ¹³C NMR spectrum of compound **77** (CDCl₃; 100 MHz).

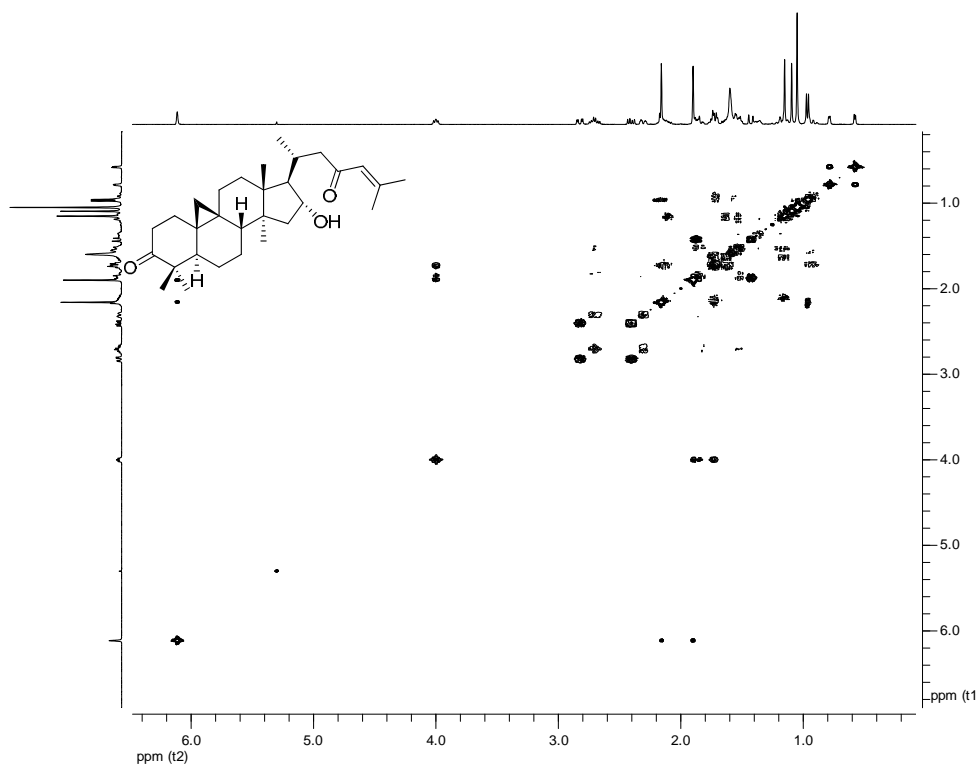


Figure 122. ^1H - ^1H COSY spectrum of compound **77** (CDCl_3 ; 400 MHz).

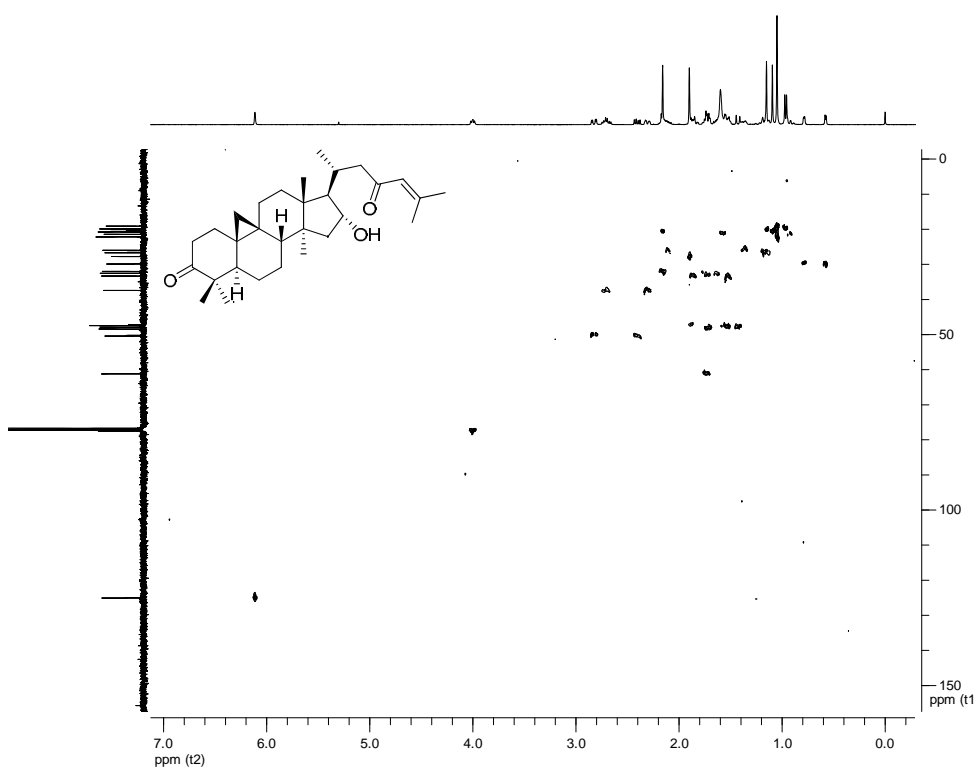


Figure 123. HSQC spectrum of compound **77** (CDCl_3 ; 400 MHz).

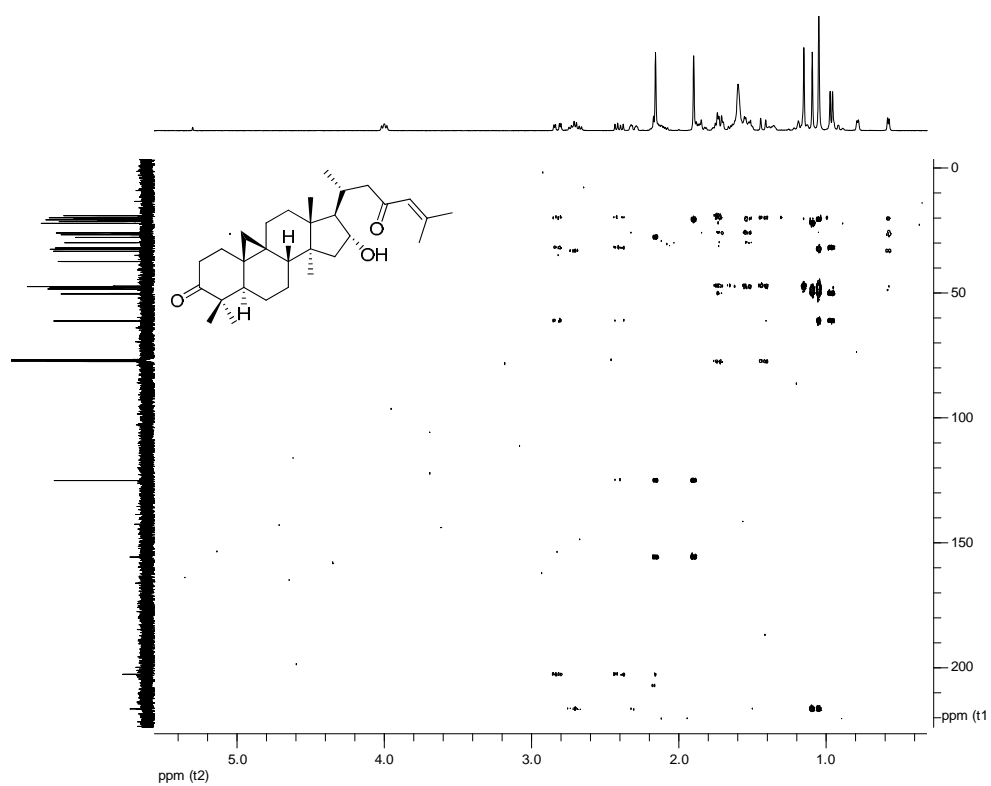


Figure 124. HMBC spectrum of compound **77** (CDCl₃; 400 MHz).

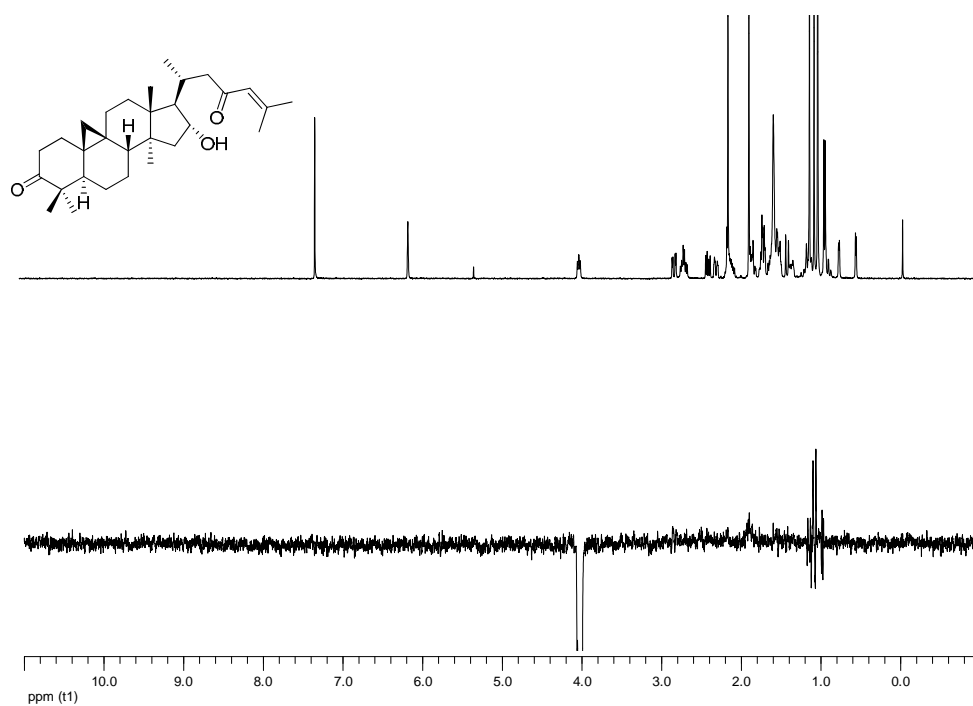


Figure 125. 1D-NOE spectrum of compound **77** (CDCl₃; 400 MHz).

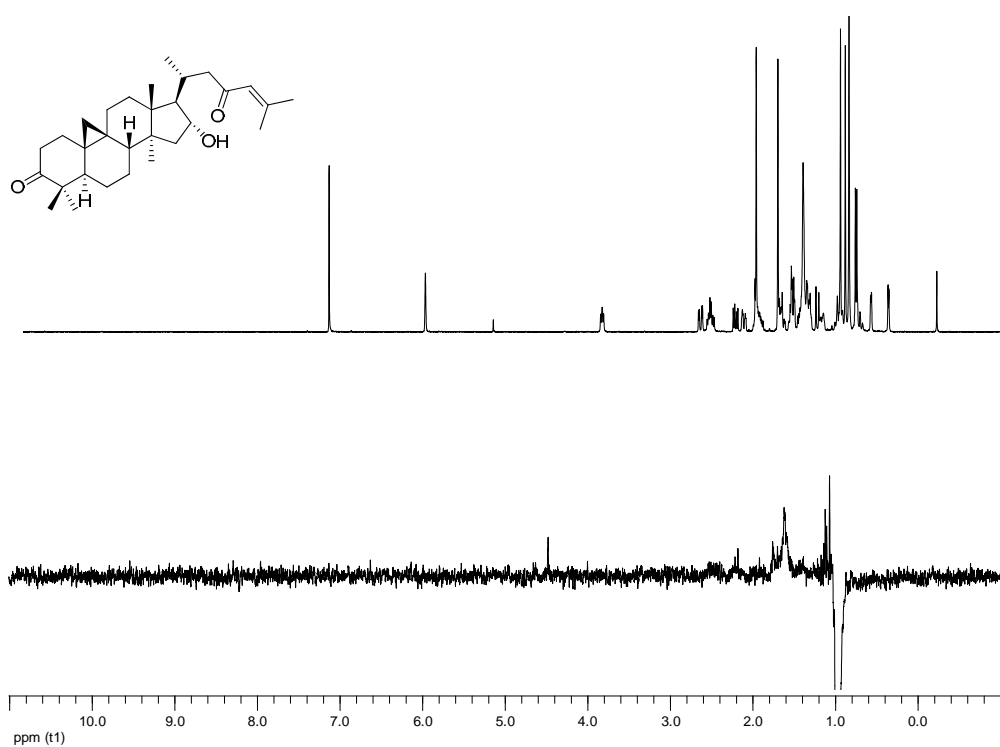


Figure 126. 1D-NOE spectrum of compound **77** (CDCl₃; 400 MHz).

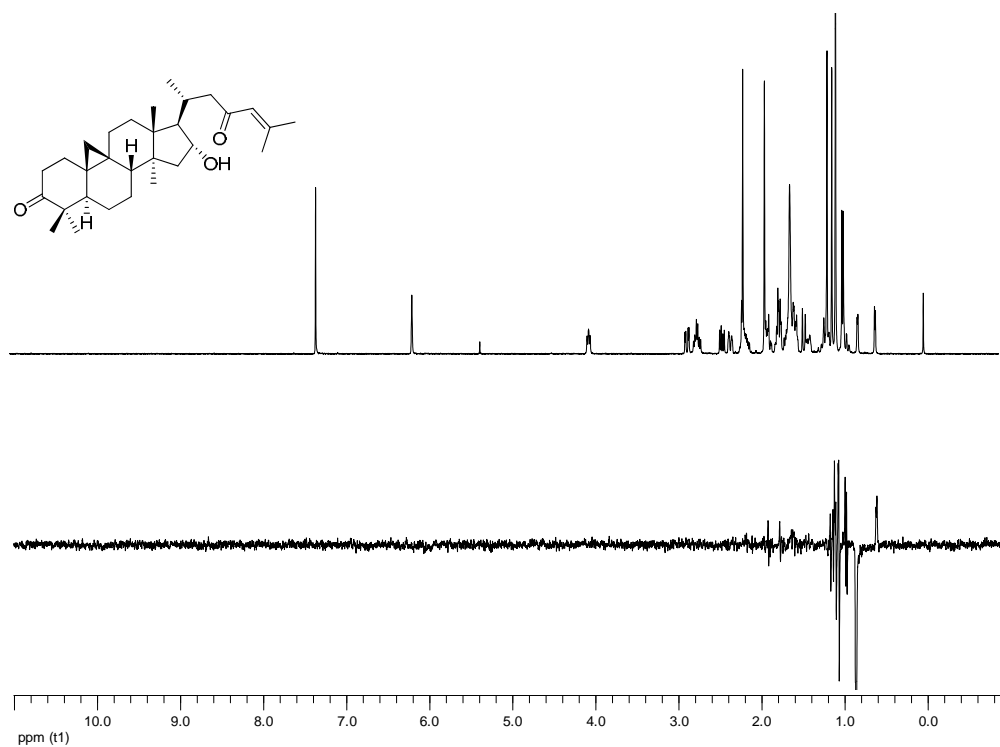


Figure 127. 1D-NOE spectrum of compound **77** (CDCl₃; 400 MHz).

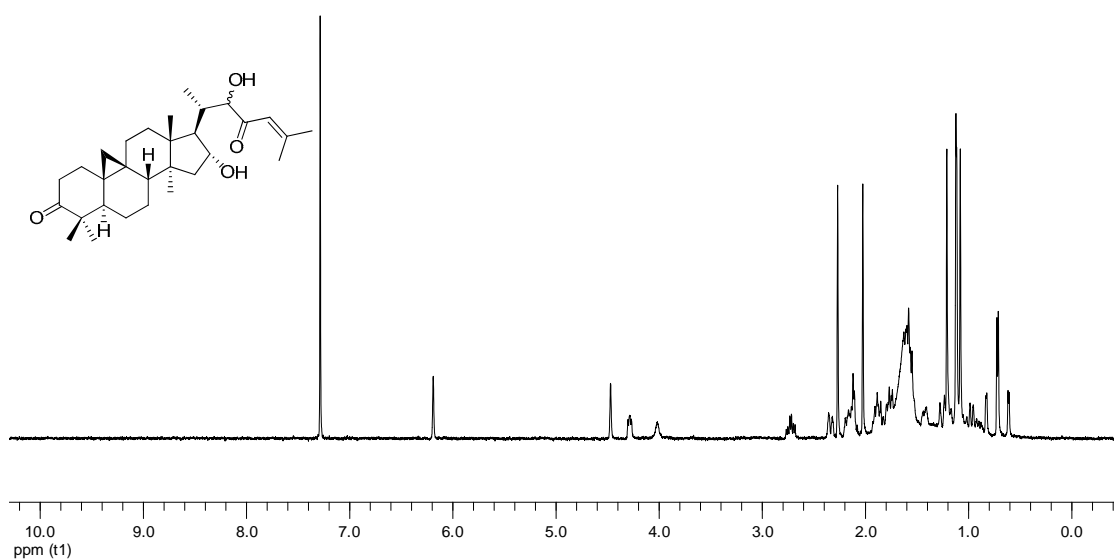


Figure 128. ^1H NMR spectrum of compound **78** (CDCl_3 ; 400 MHz).

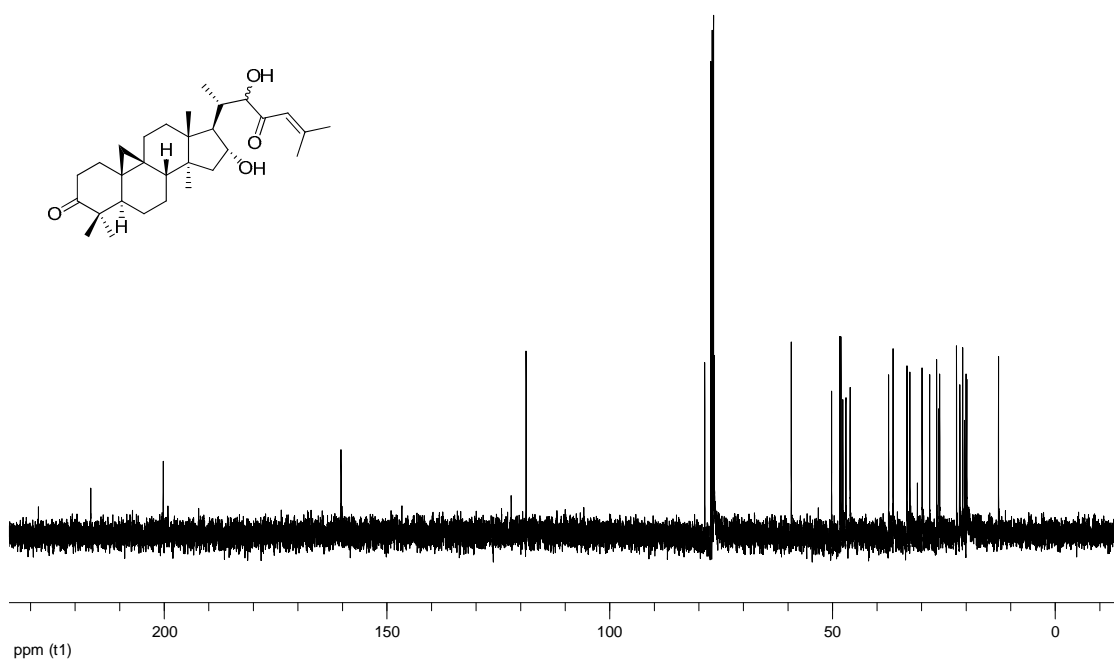


Figure 129. ^{13}C NMR spectrum of compound **78** (CDCl_3 ; 100 MHz).

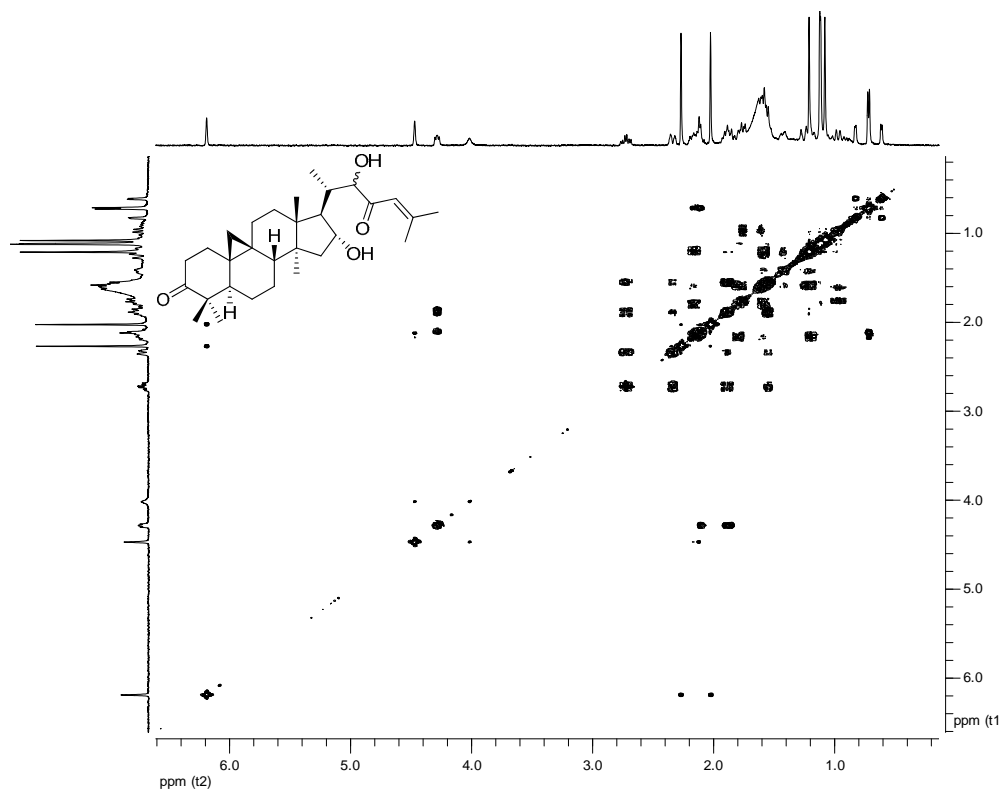


Figure 130. ^1H - ^1H COSY spectrum of compound **78** (CDCl_3 ; 400 MHz).

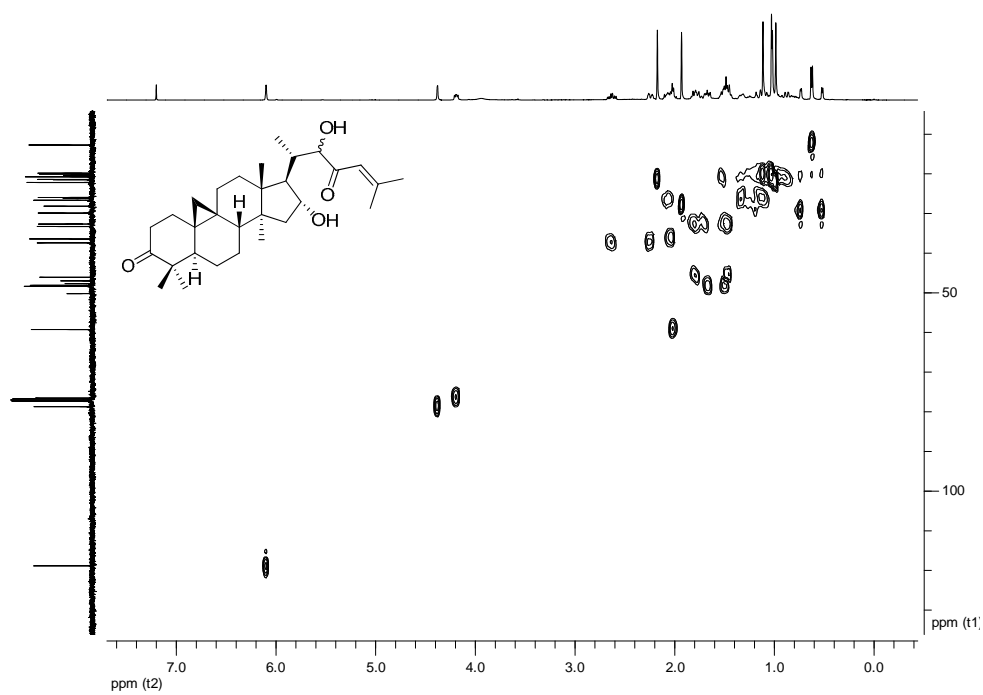


Figure 131. HSQC spectrum of compound **78** (CDCl_3 ; 400 MHz).

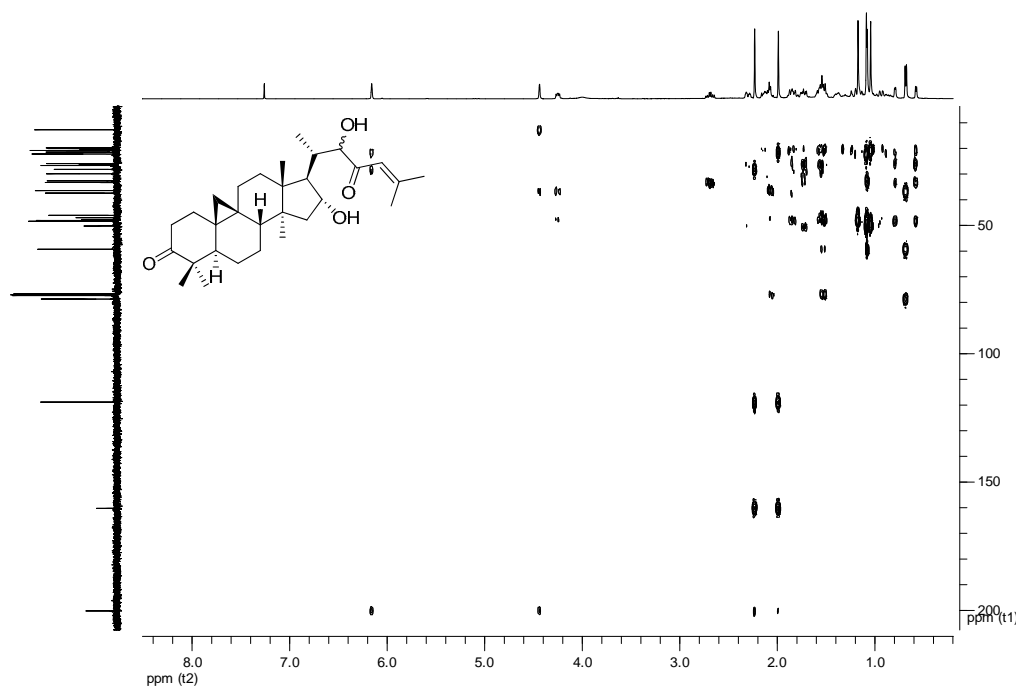


Figure 132. HMBC spectrum of compound **78** (CDCl₃; 400 MHz).

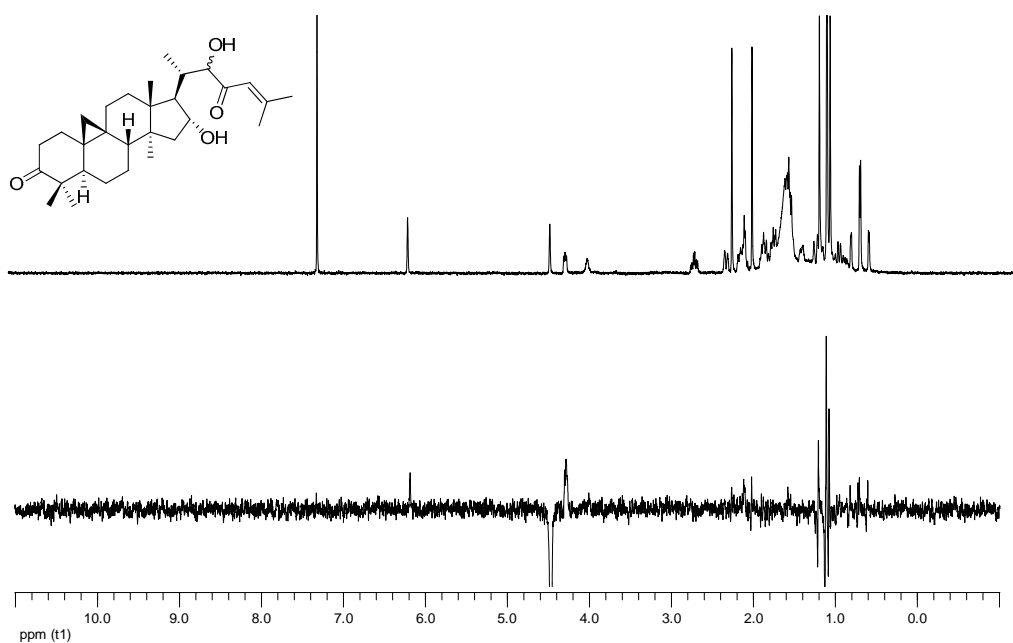


Figure 133. 1D-NOE spectrum of compound **78** (CDCl₃; 400 MHz).

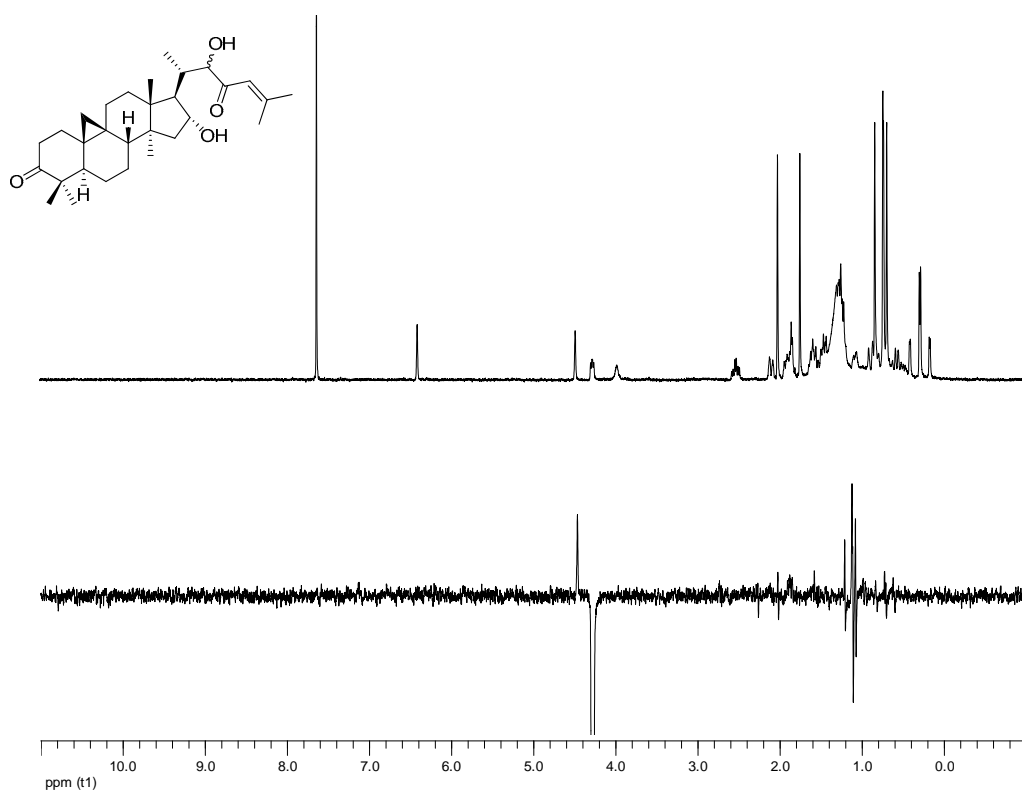


Figure 134. 1D-NOE spectrum of compound **78** (CDCl₃; 400 MHz).

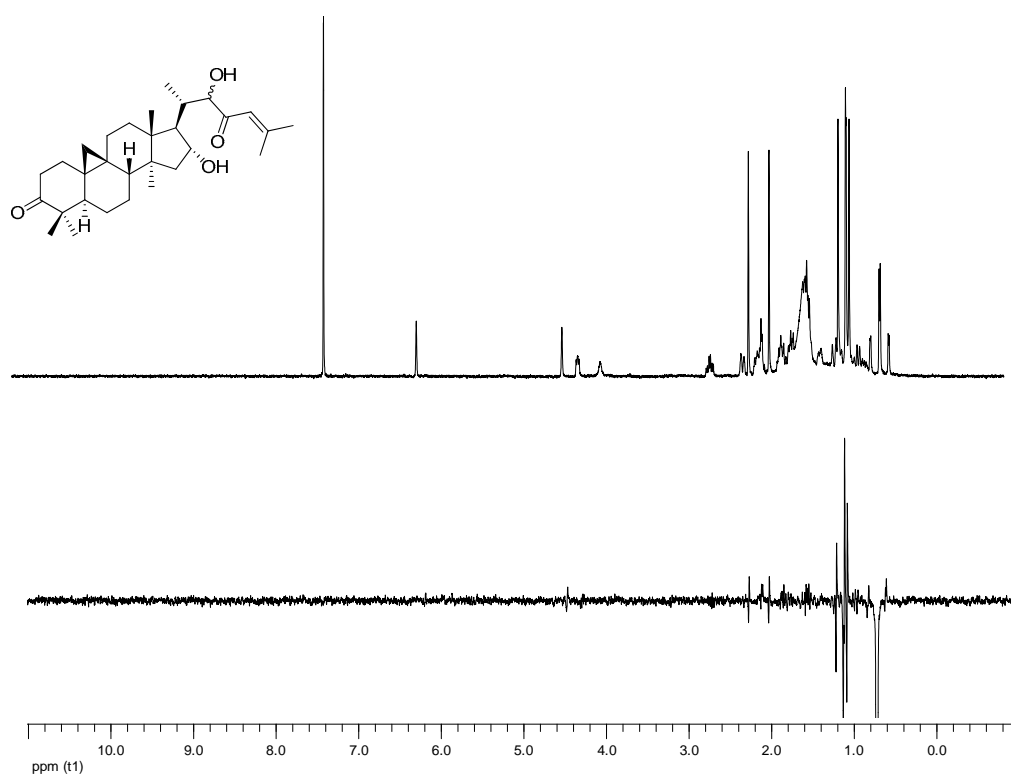


Figure 135. 1D-NOE spectrum of compound **78** (CDCl₃; 400 MHz).

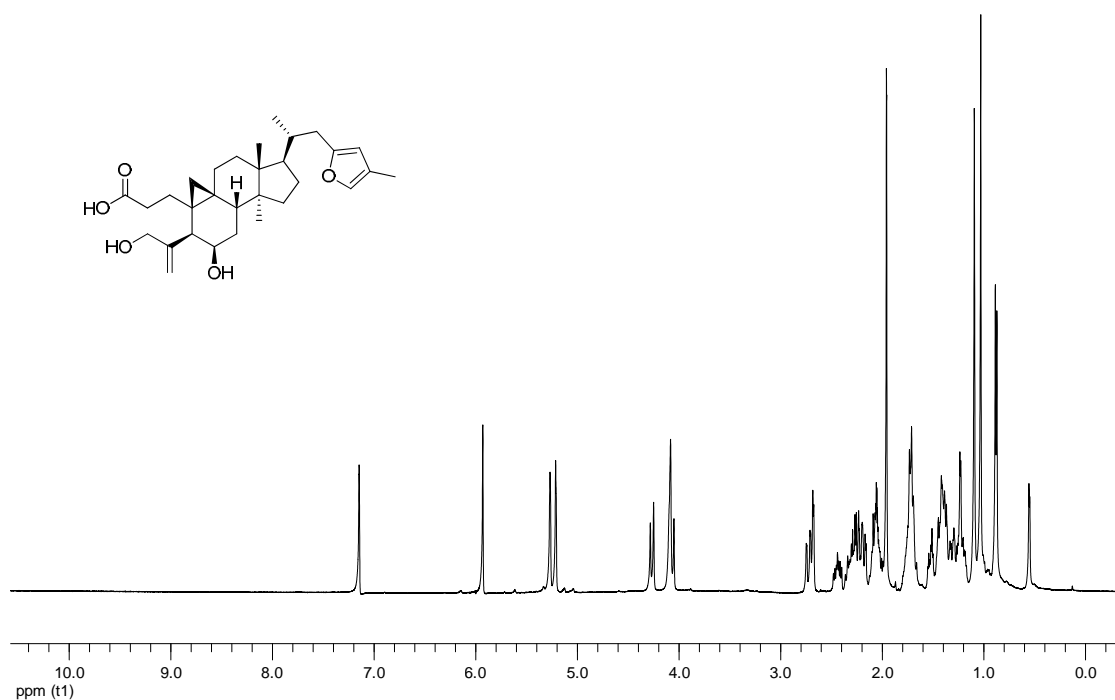


Figure 136. ¹H NMR spectrum of compound **79** (Acetone-*d*₆; 400 MHz)

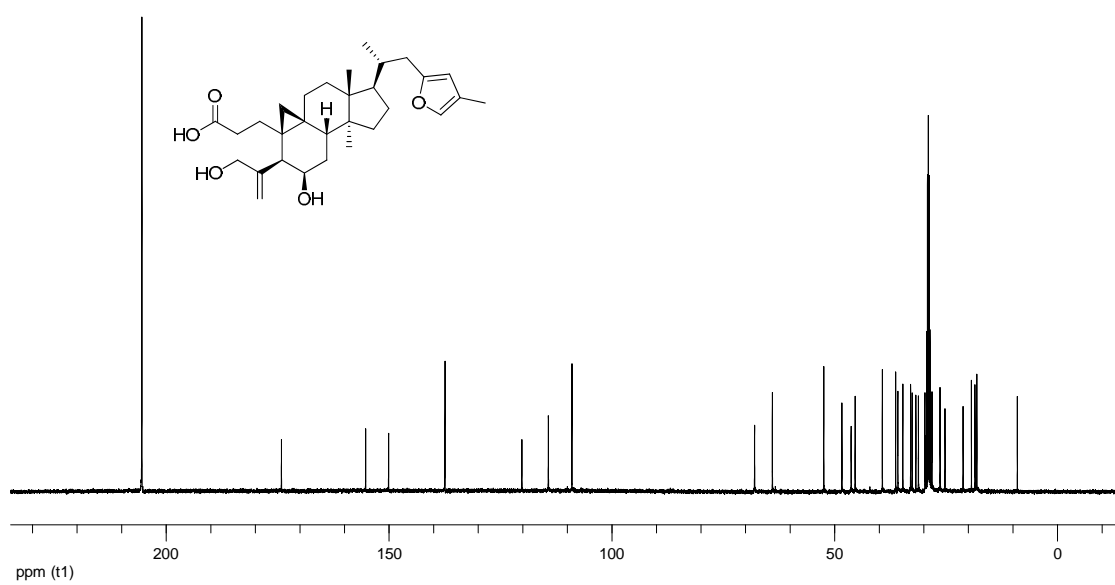


Figure 137. ¹³C NMR spectrum of compound **79** (Acetone-*d*₆; 100 MHz).

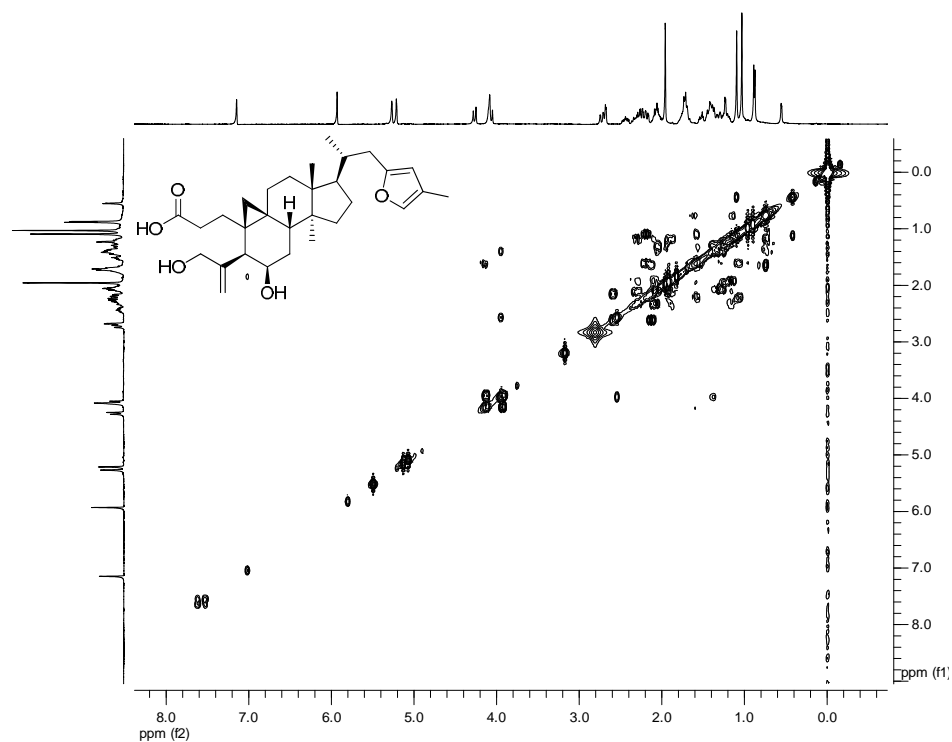


Figure 138. ^1H - ^1H COSY spectrum of compound **79** (Acetone- d_6 ; 400 MHz).

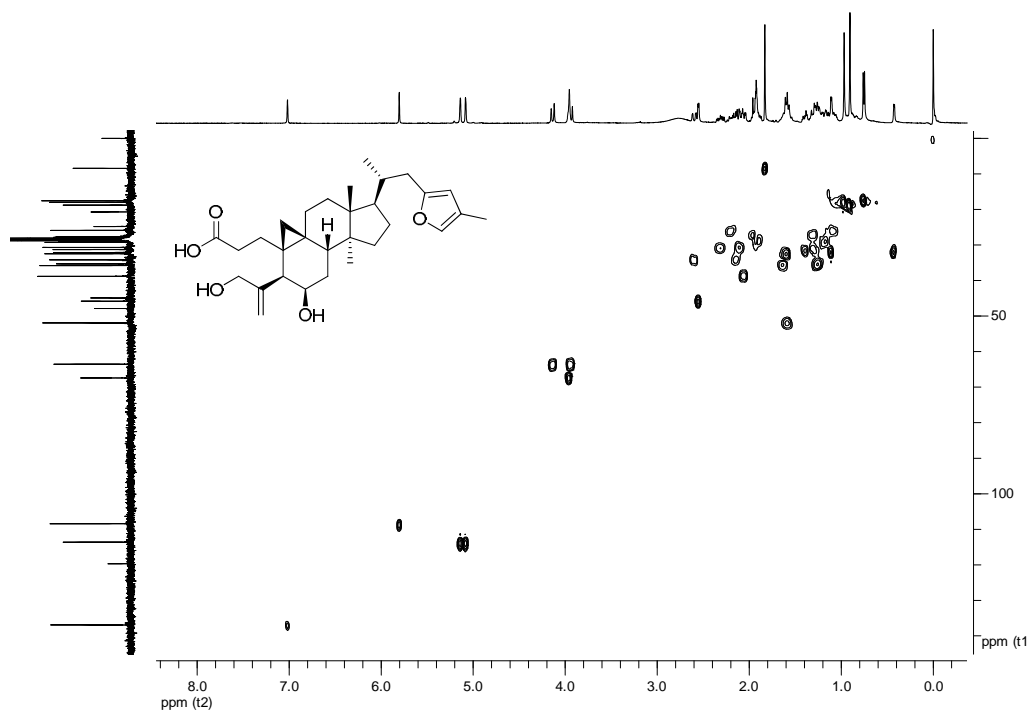


Figure 139. HSQC spectrum of compound **79** (Acetone- d_6 ; 400 MHz).

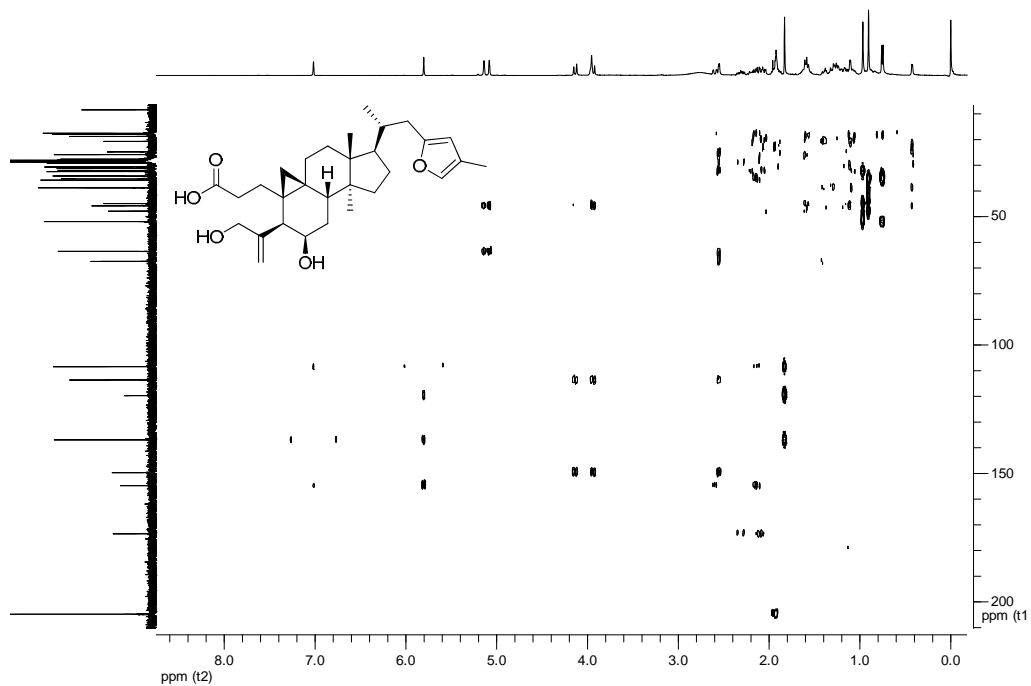


Figure 140. HMBC spectrum of compound **79** (Acetone-*d*₆; 400 MHz).

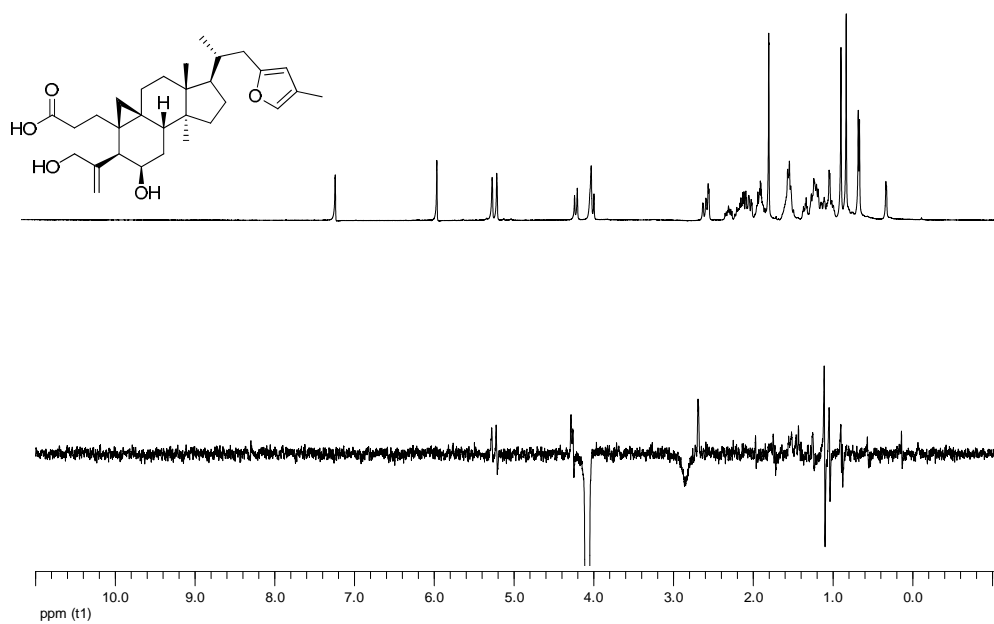


Figure 141. 1D-NOE spectrum of compound **79** (Acetone-*d*₆; 400 MHz).

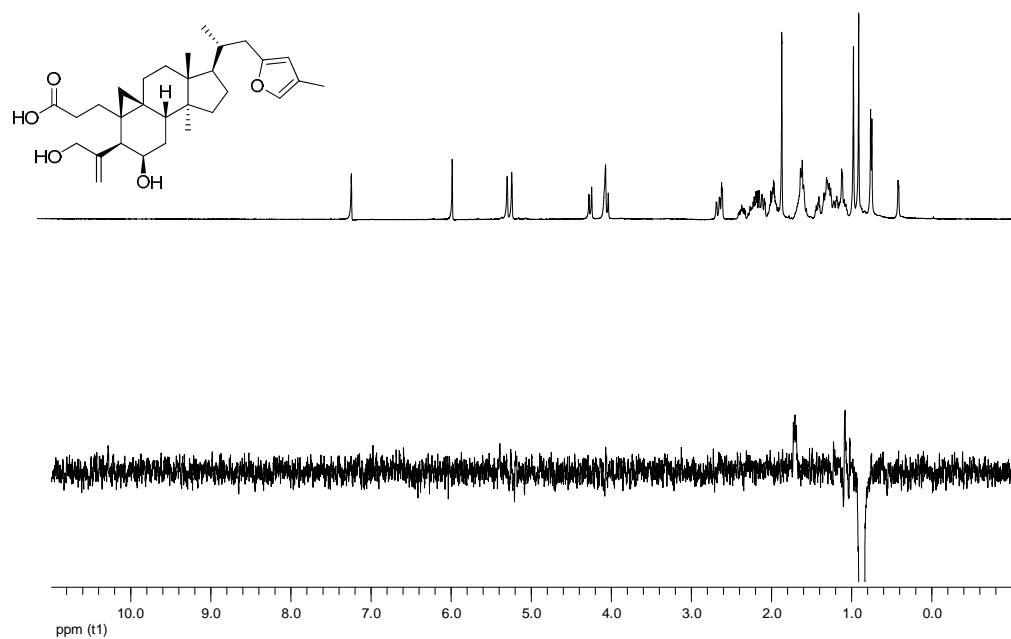


Figure 142. 1D-NOE spectrum of compound **79** (Acetone- d_6 ; 400 MHz).

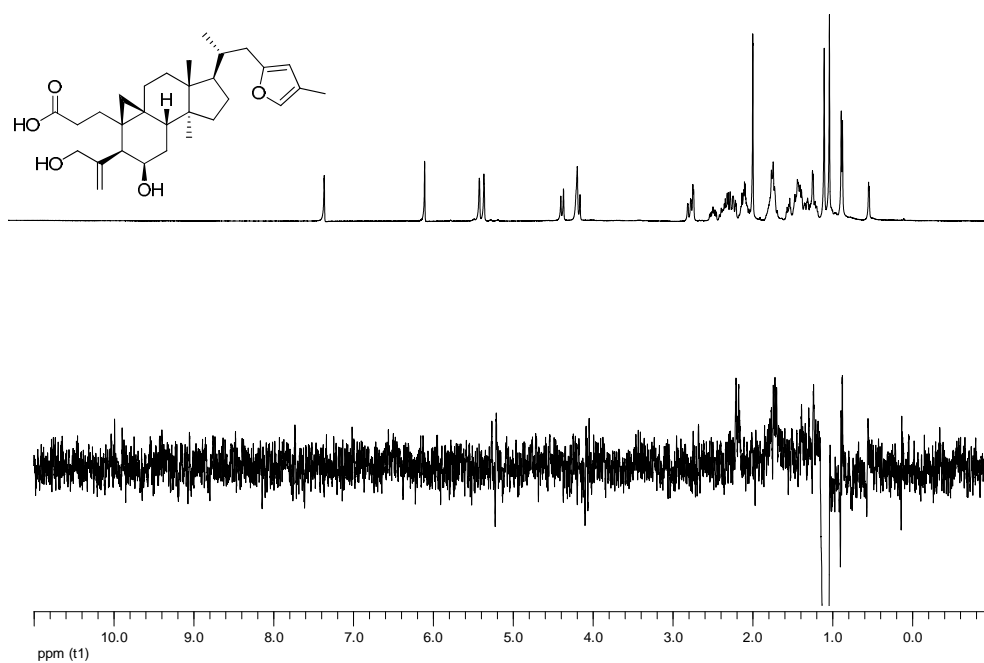


Figure 143. 1D-NOE spectrum of compound **79** (Acetone- d_6 ; 400 MHz).

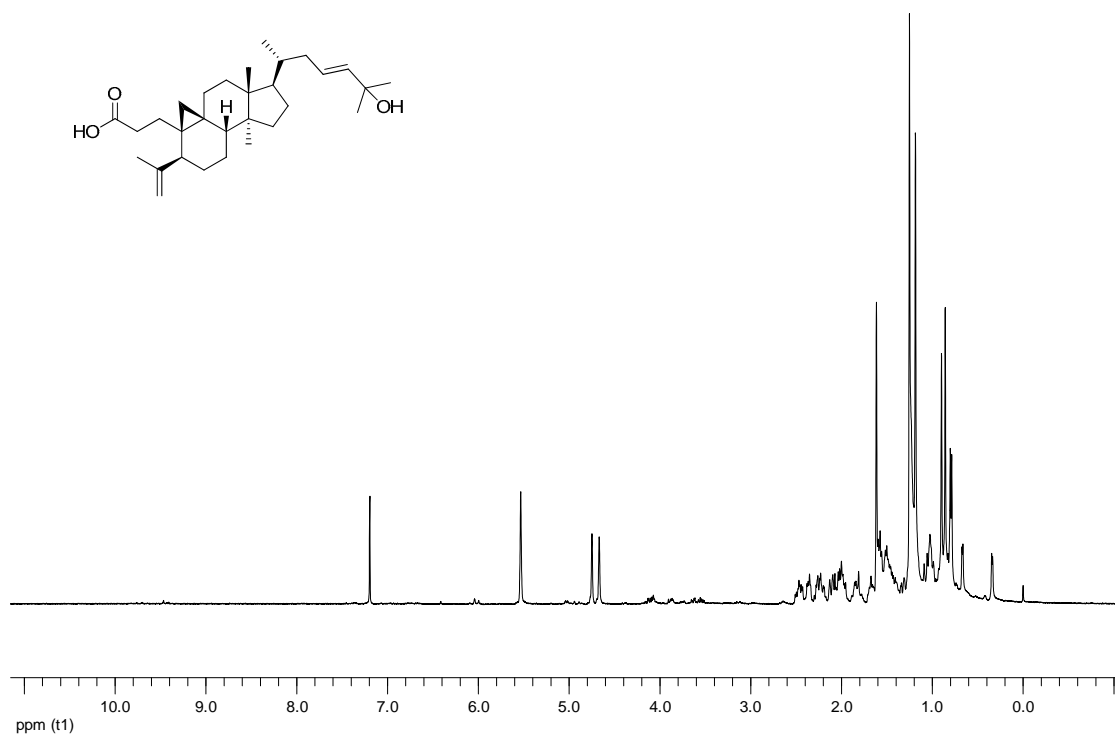


Figure 144. ¹H NMR spectrum of compound **80** (CDCl₃; 400 MHz).

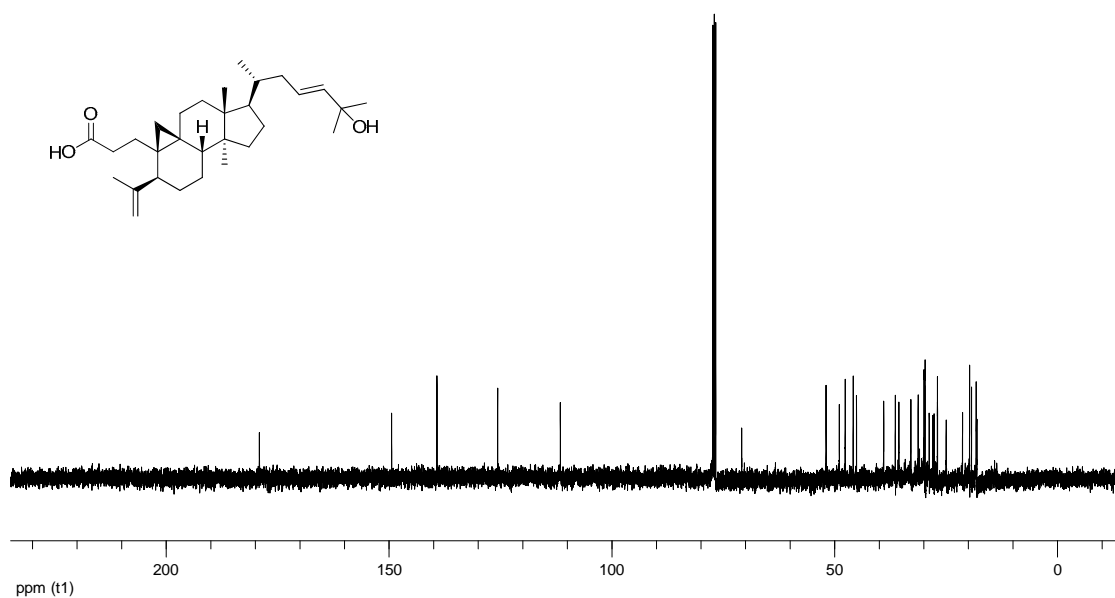


Figure 145. ¹³C NMR spectrum of compound **80** (CDCl₃; 100 MHz).

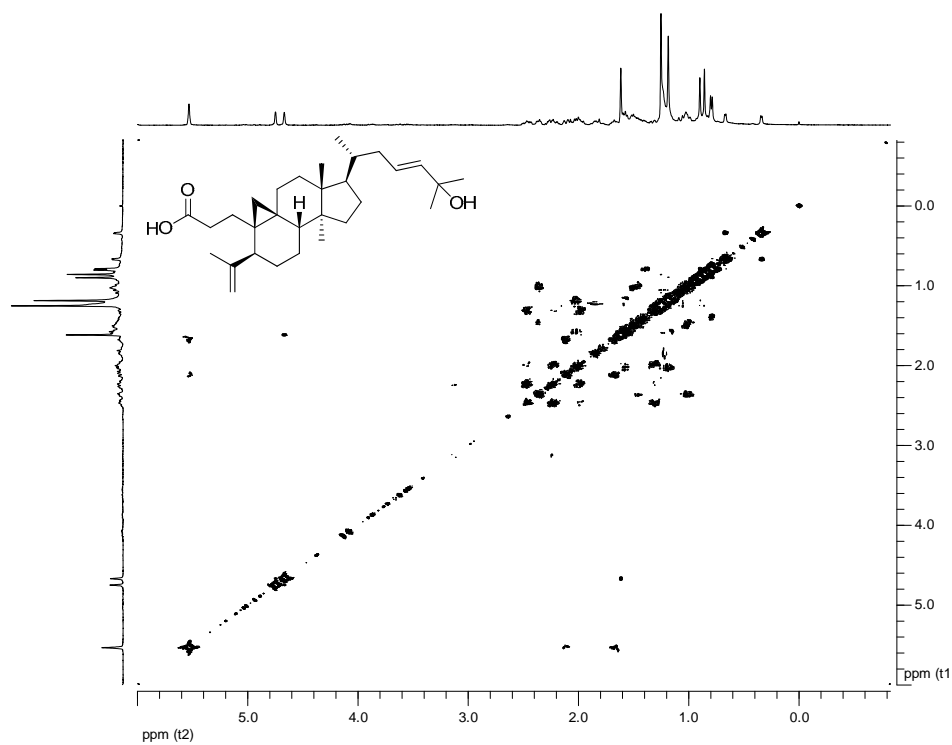


Figure 146. ^1H - ^1H COSY spectrum of compound **80** (CDCl_3 ; 400 MHz).

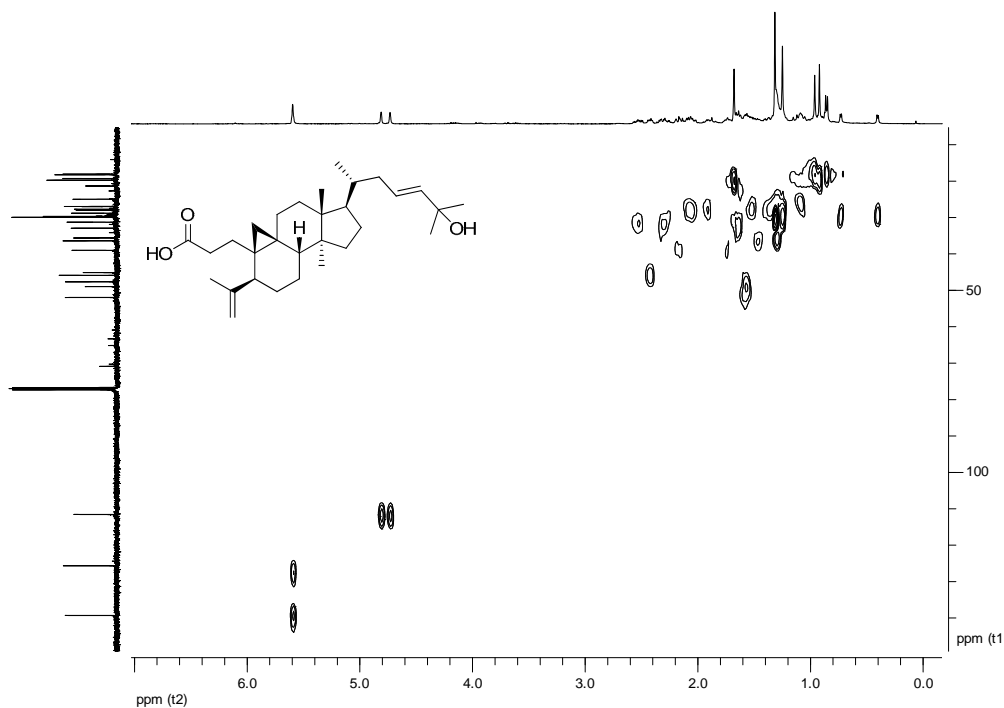


Figure 147. HSQC spectrum of compound **80** (CDCl_3 ; 400 MHz).

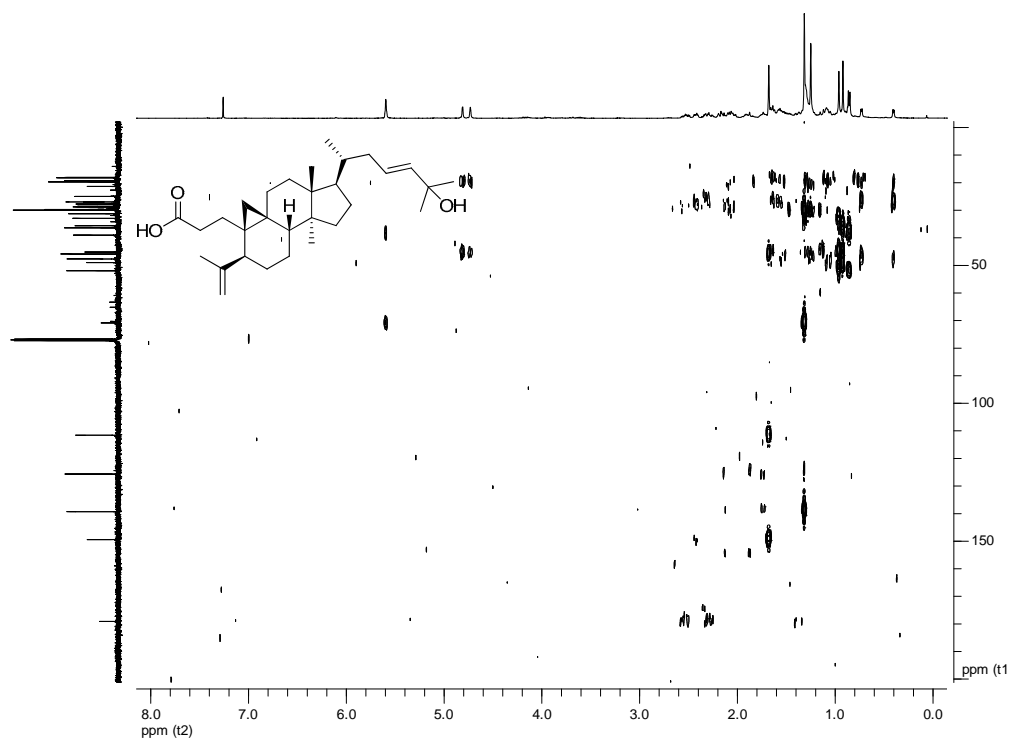


Figure 148. HMBC spectrum of compound **80** (CDCl₃; 400 MHz).

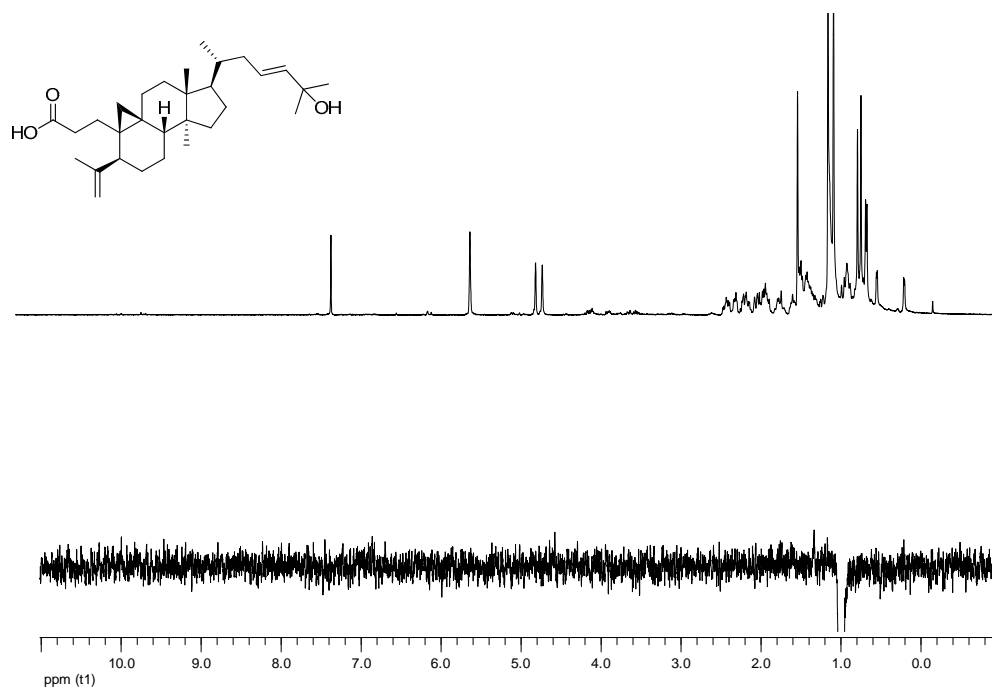


Figure 149. 1D-NOE spectrum of compound **80** (CDCl₃; 400 MHz).

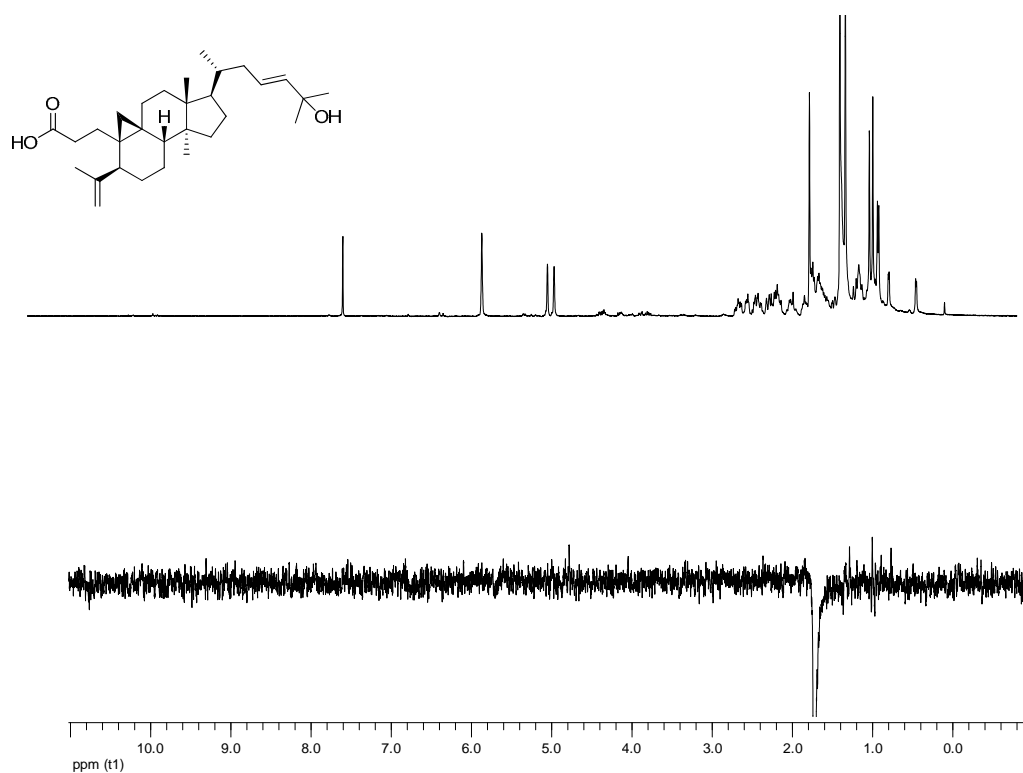


Figure 150. 1D-NOE spectrum of compound **80** (CDCl₃; 400 MHz).

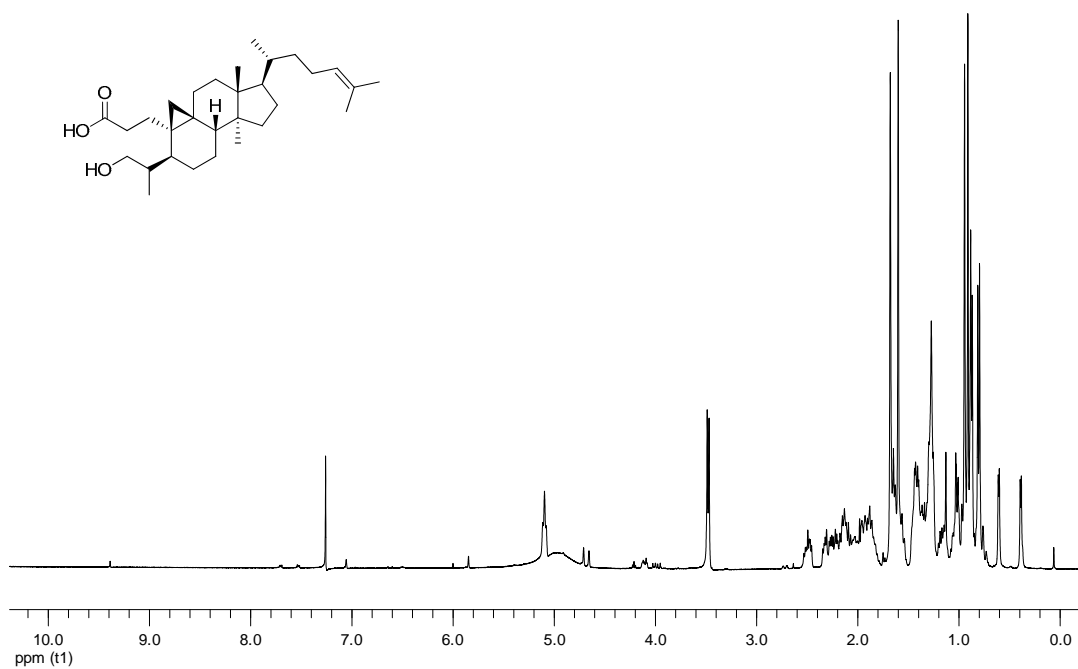


Figure 151. ¹H NMR spectrum of compound **81** (CDCl₃; 400 MHz).

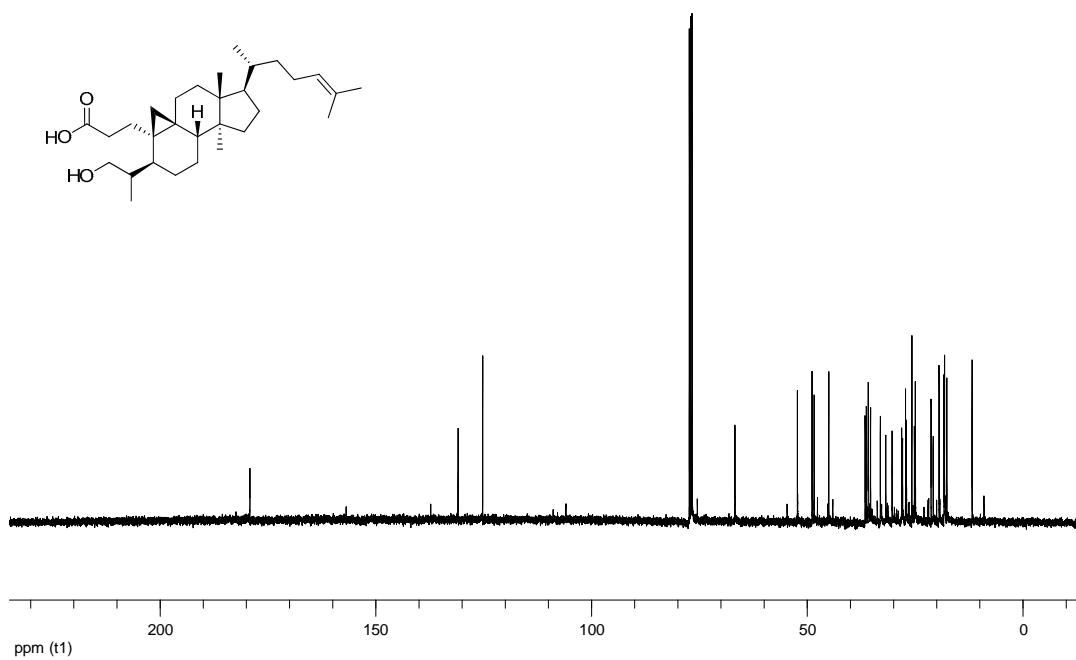


Figure 152. ^{13}C NMR spectrum of compound **81** (CDCl_3 ; 100 MHz).

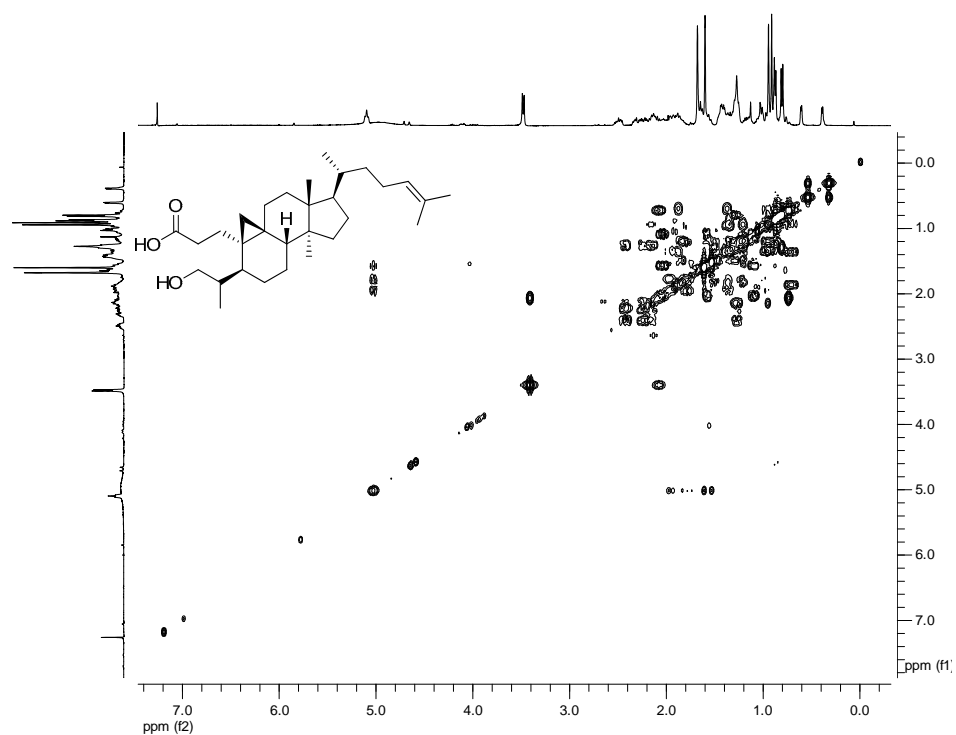


Figure 153. ^1H - ^1H COSY spectrum of compound **81** (CDCl_3 ; 400 MHz).

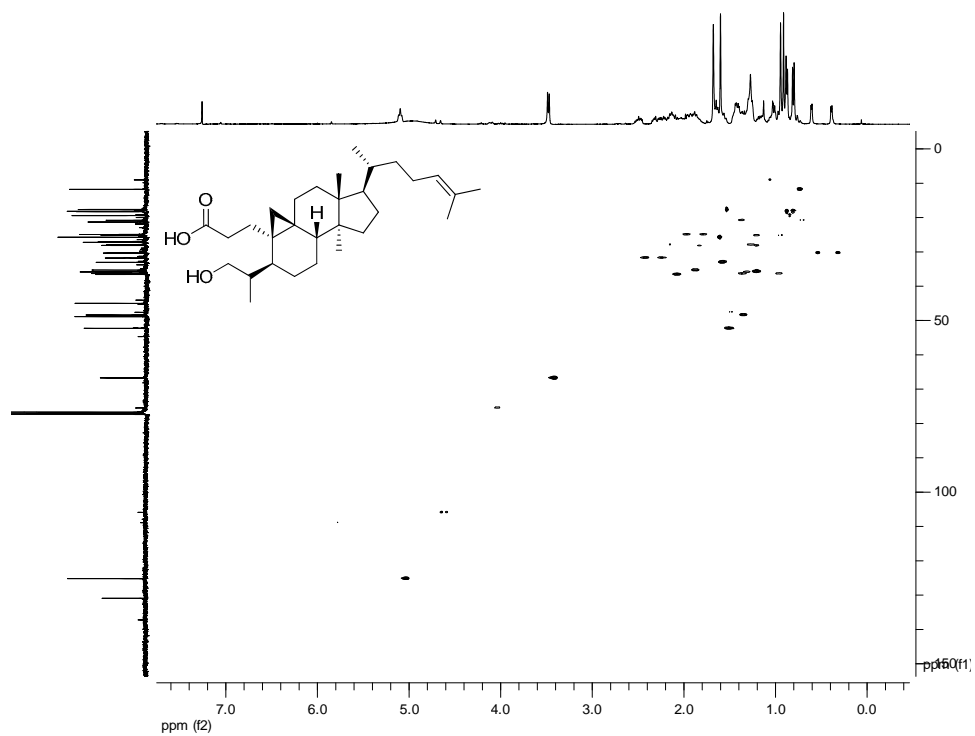


Figure 154. HSQC spectrum of compound **81** (CDCl₃; 400 MHz).

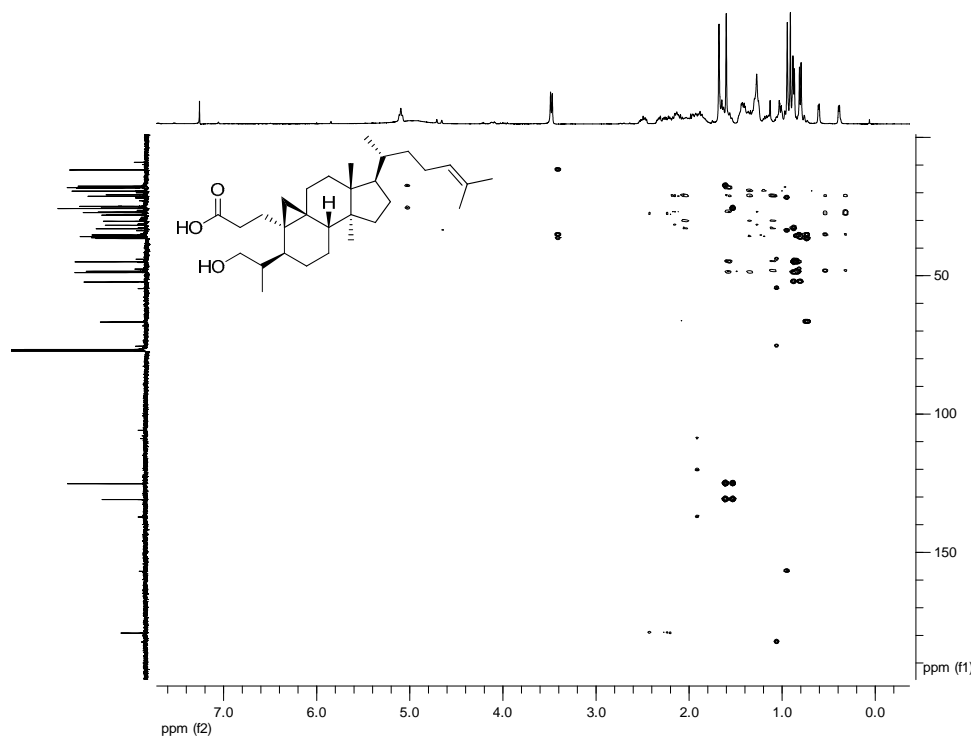


Figure 155. HMBC spectrum of compound **81** (CDCl₃; 400 MHz).

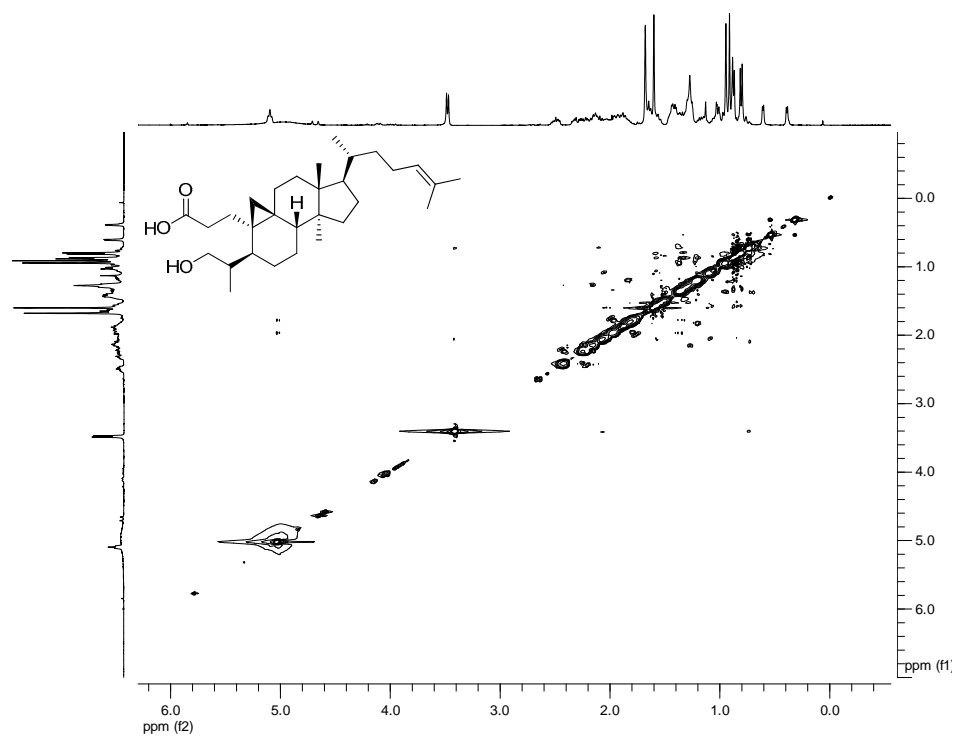


Figure 156. NOESY spectrum of compound **81** (CDCl₃; 400 MHz).

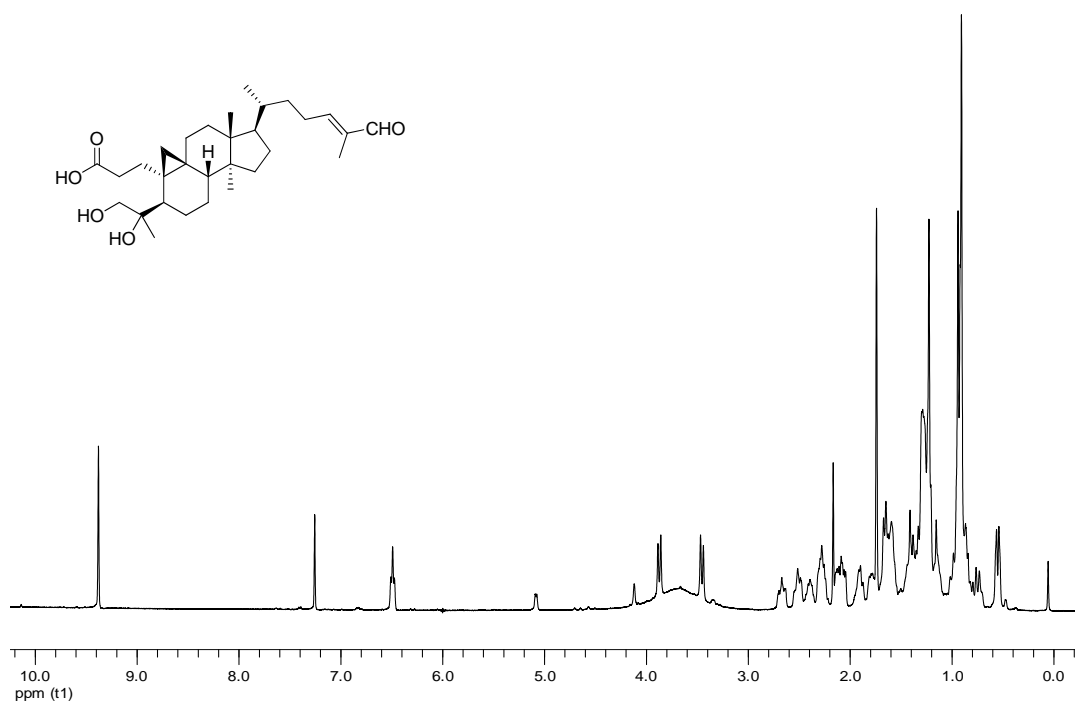


Figure 157. ¹H NMR spectrum of compound **82** (CDCl₃; 400 MHz).

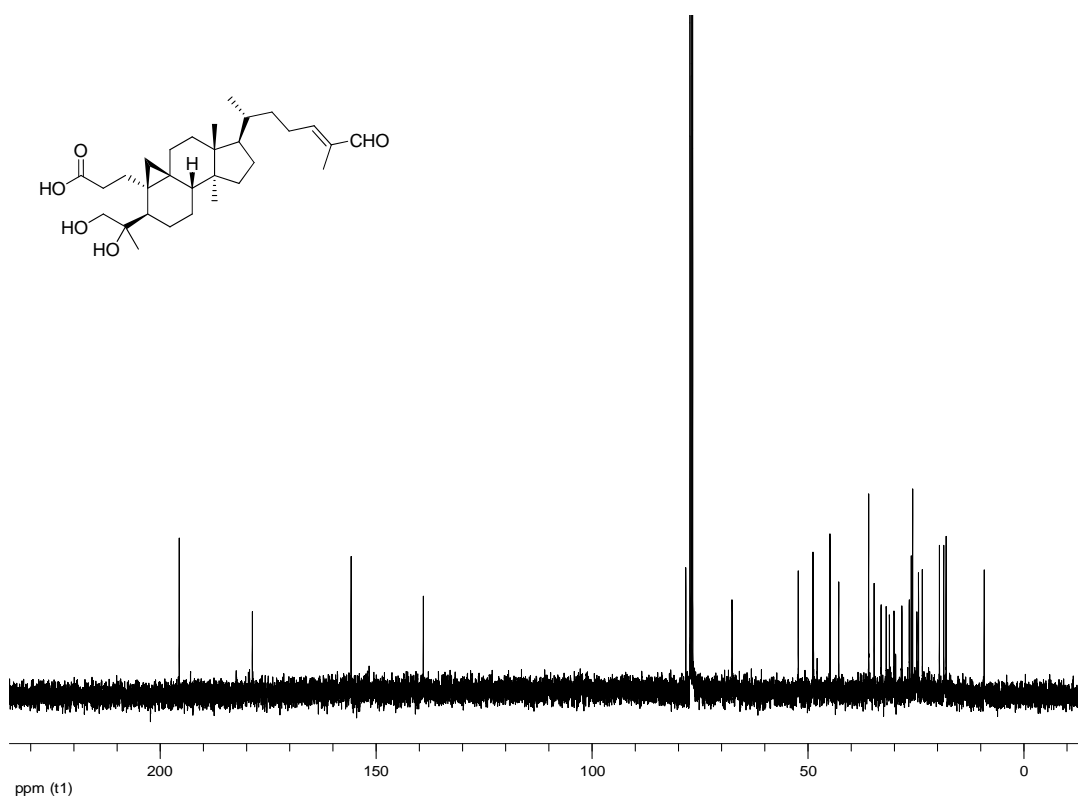


Figure 158. ^{13}C NMR spectrum of compound **82** (CDCl_3 ; 100 MHz).

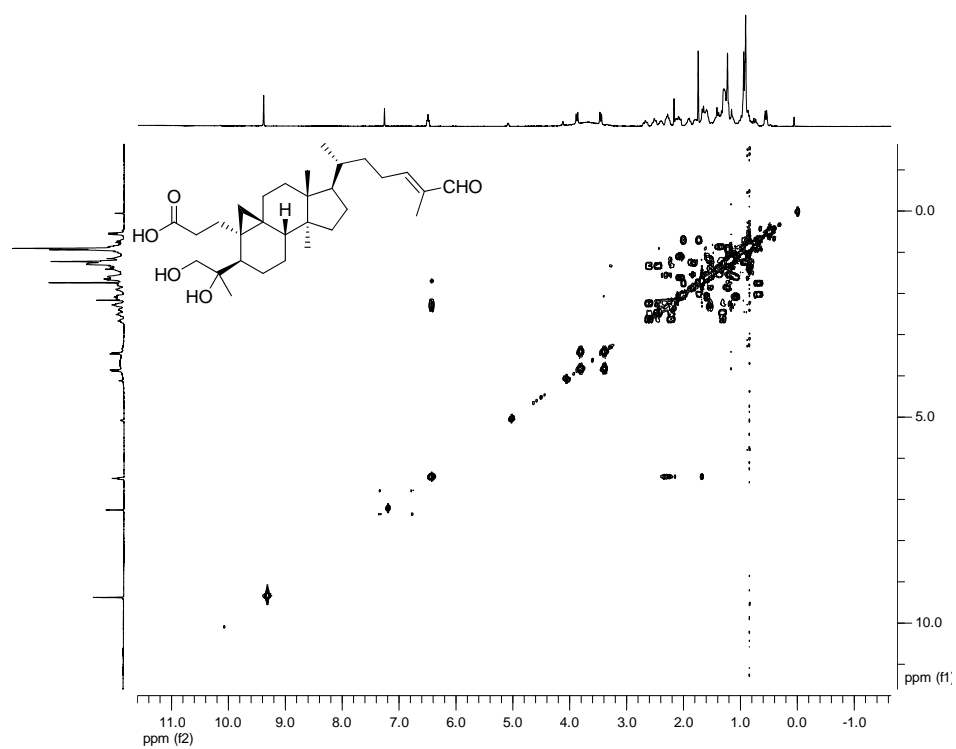


Figure 159. ^1H - ^1H COSY spectrum of compound **82** (CDCl_3 ; 400 MHz).

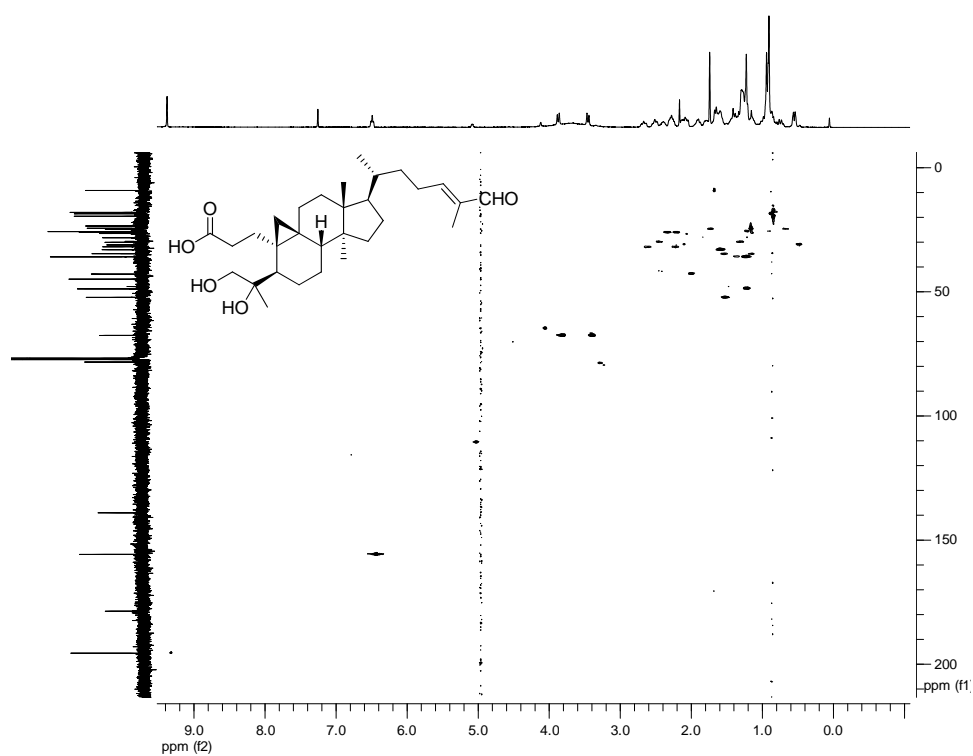


Figure 160. HSQC spectrum of compound **82** (CDCl₃; 400 MHz).

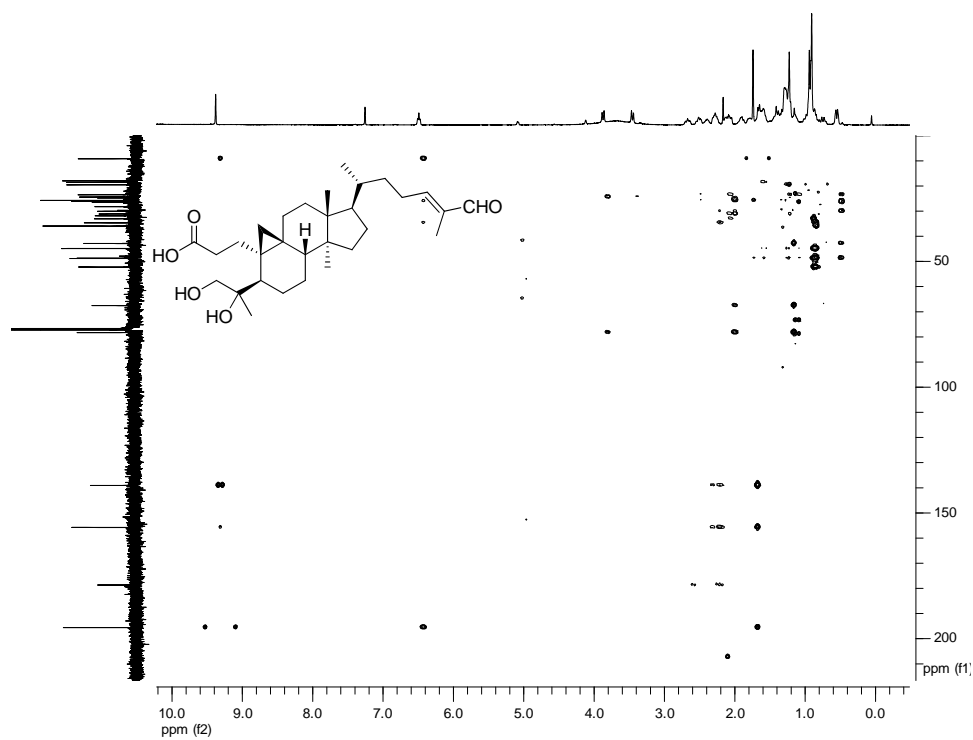


Figure 161. HMBC spectrum of compound **82** (CDCl₃; 400 MHz).

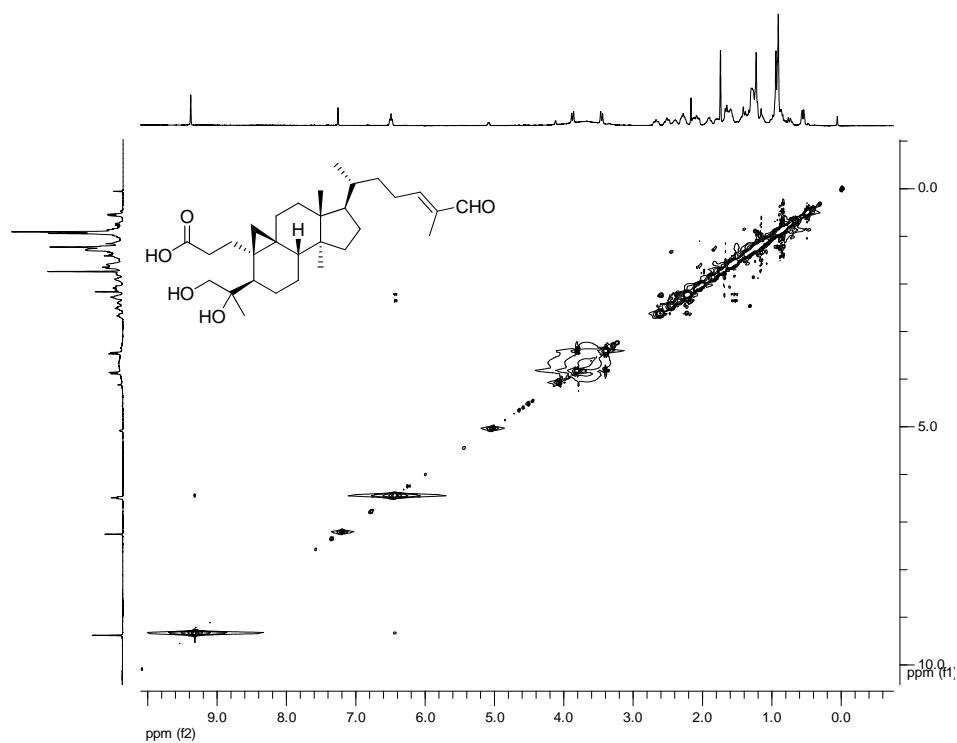


Figure 162. NOESY spectrum of compound **82** (CDCl₃; 400 MHz).

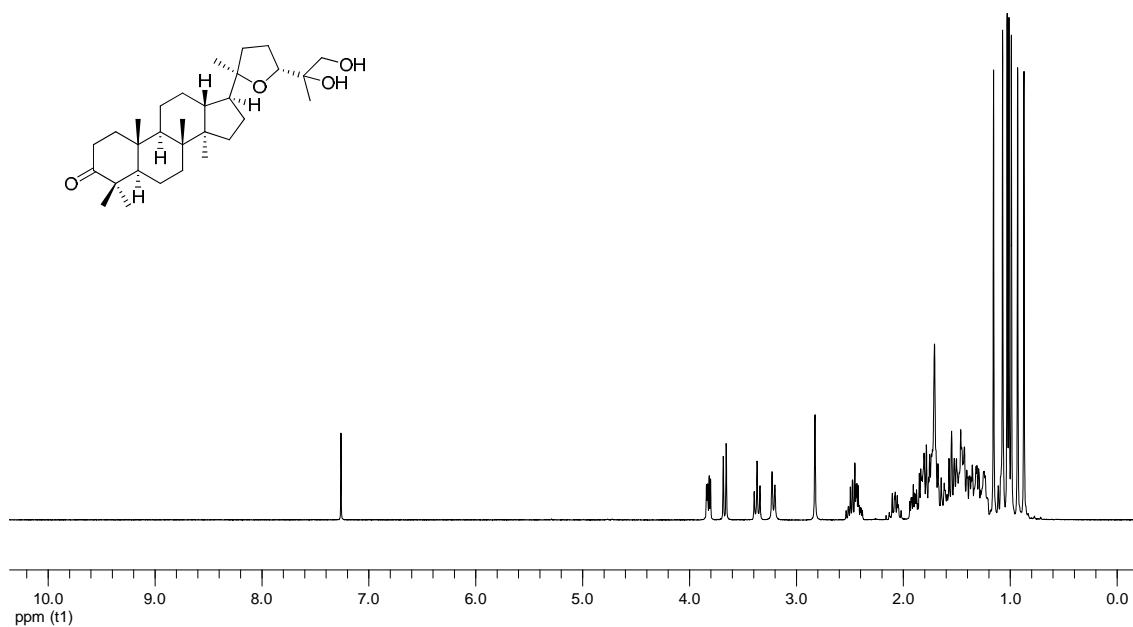


Figure 163. ¹H NMR spectrum of compound **83** (CDCl₃; 400 MHz).

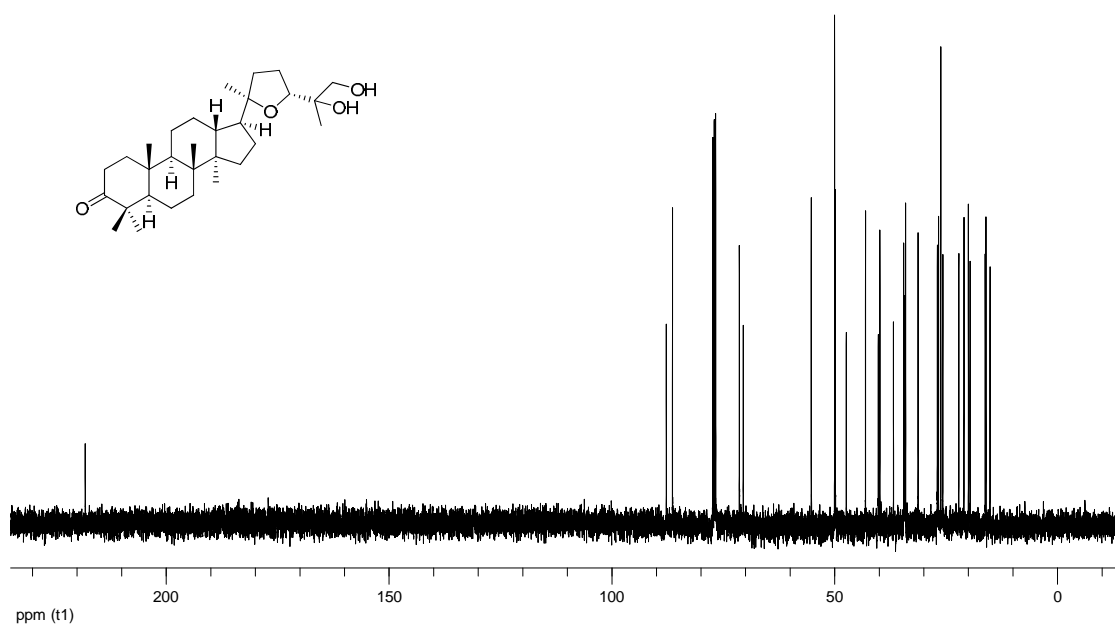


Figure 164. ^{13}C NMR spectrum of compound 83 (CDCl_3 ; 100 MHz).

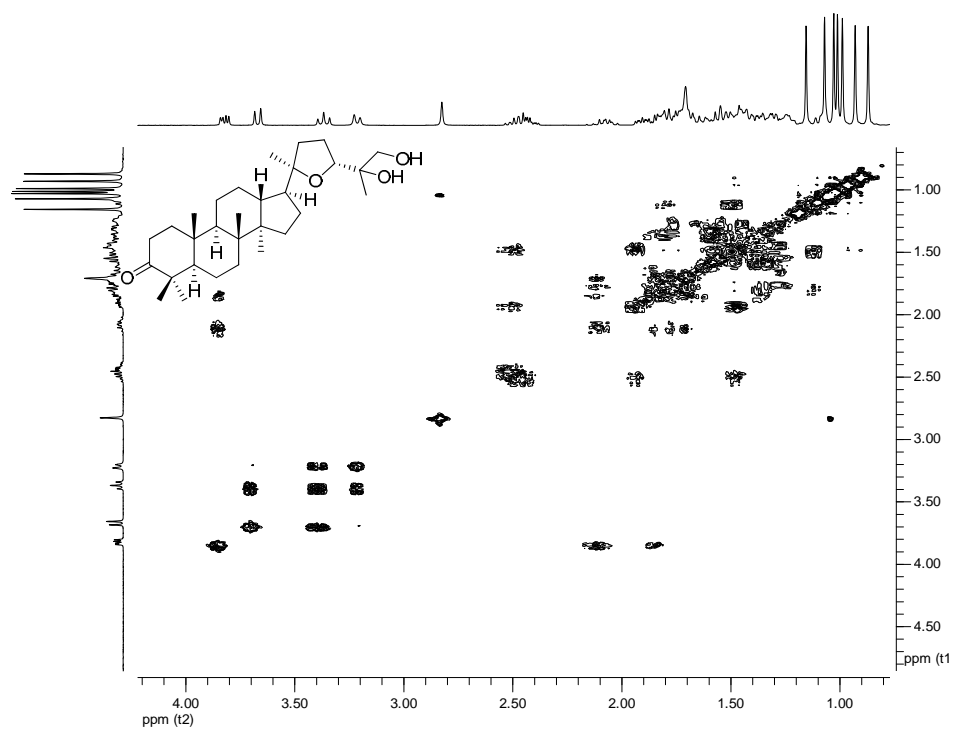


Figure 165. ^1H - ^1H COSY spectrum of compound 83 (CDCl_3 ; 400 MHz).

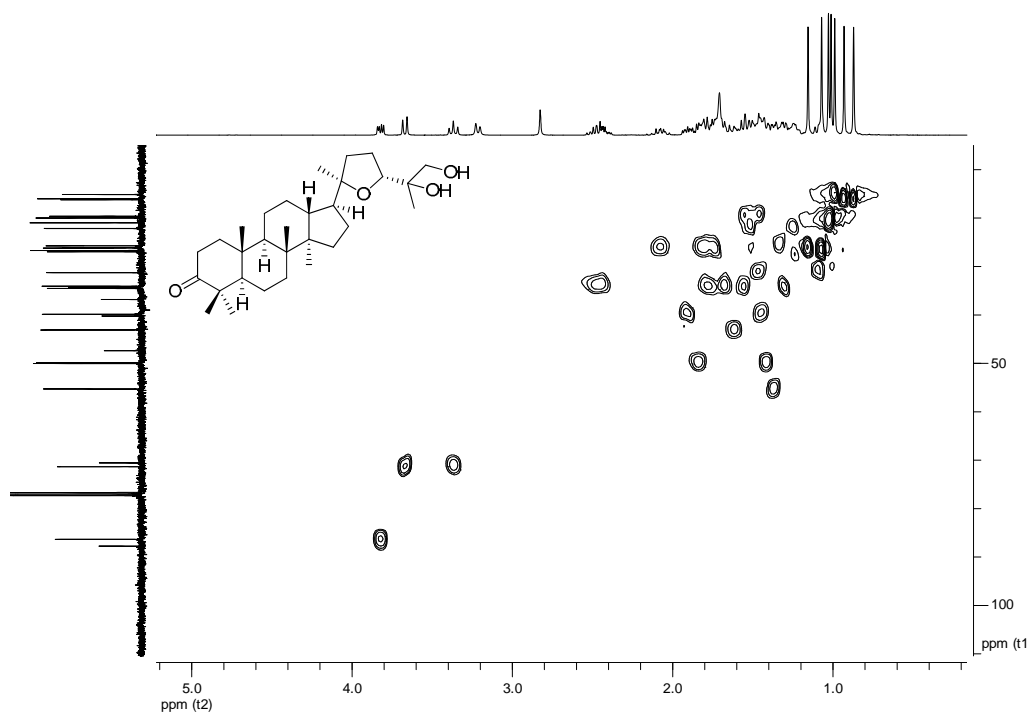


Figure 166. HSQC spectrum of compound **83** (CDCl₃; 400 MHz).

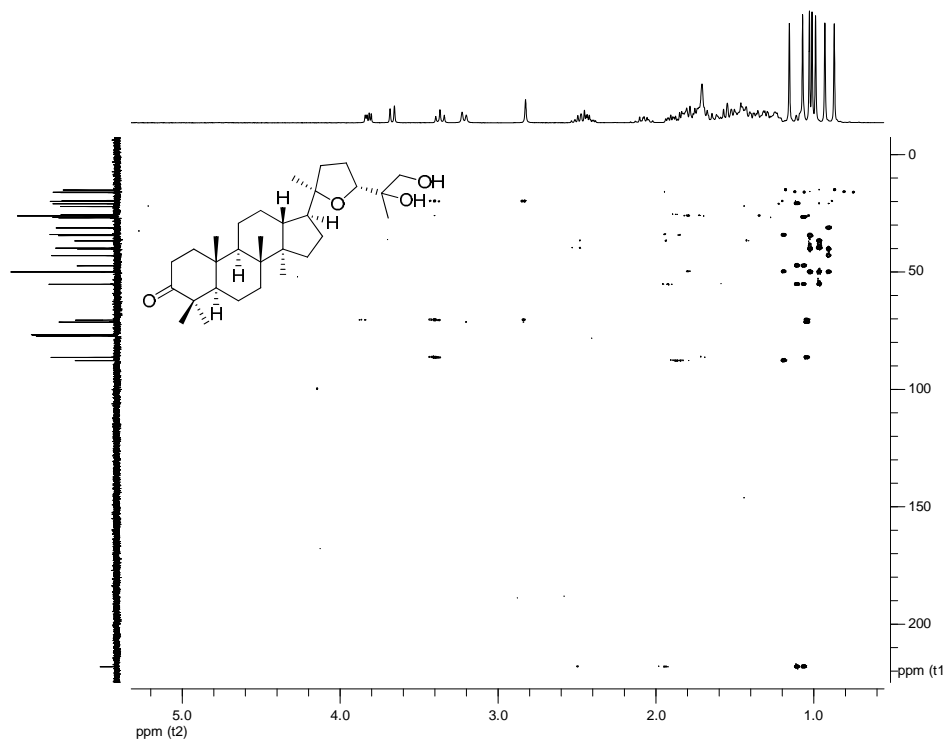


Figure 167. HMBC spectrum of compound **83** (CDCl₃; 400 MHz).

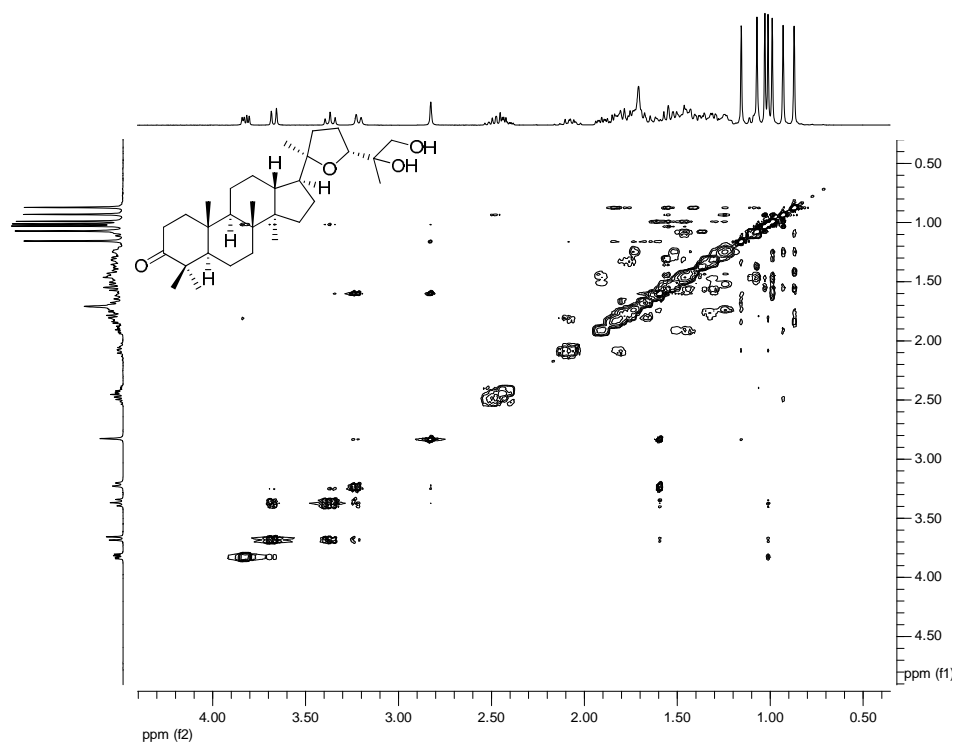


Figure 168. NOESY spectrum of compound **83** (CDCl₃; 400 MHz).

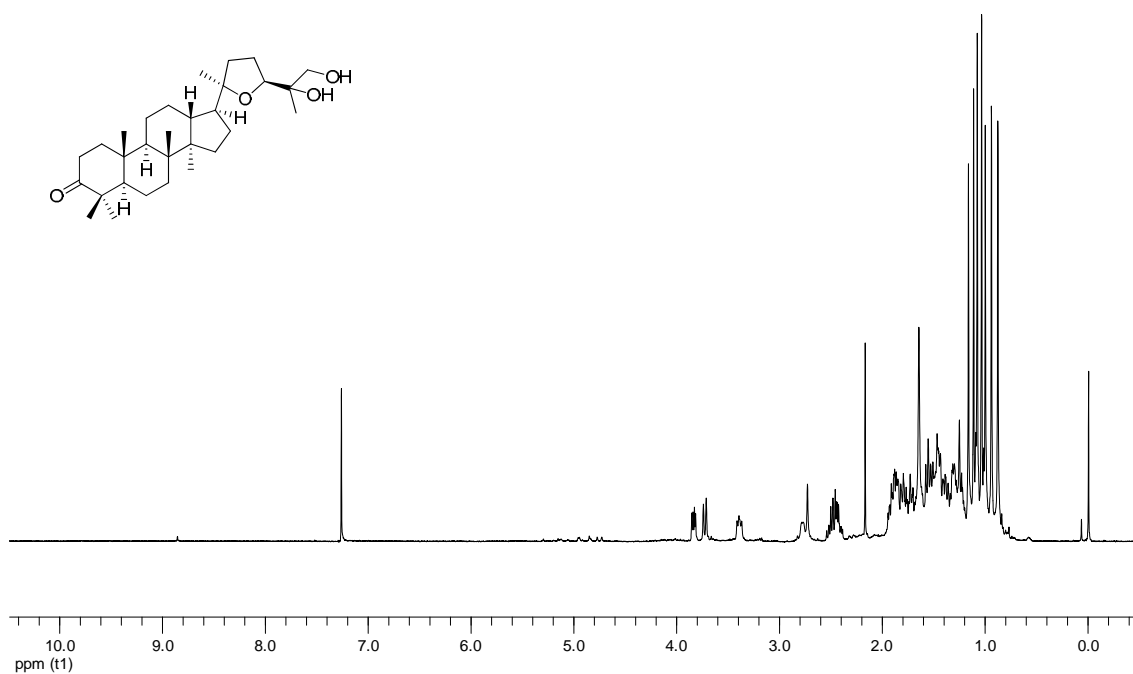


Figure 169. ¹H NMR spectrum of compound **84** (CDCl₃; 400 MHz).

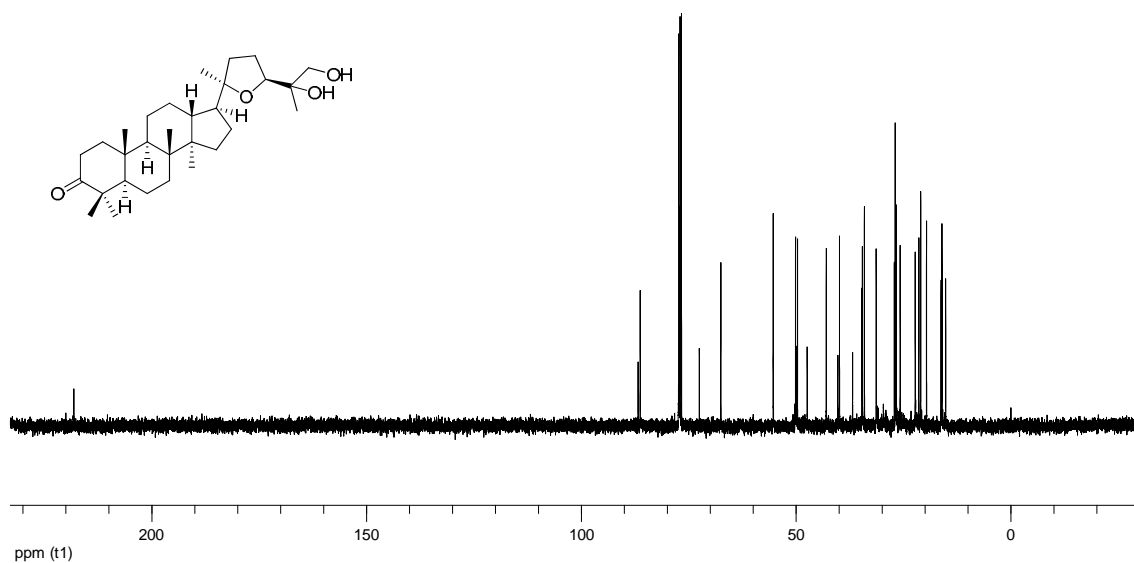


Figure 170. ^{13}C NMR spectrum of compound **84** (CDCl_3 ; 100 MHz).

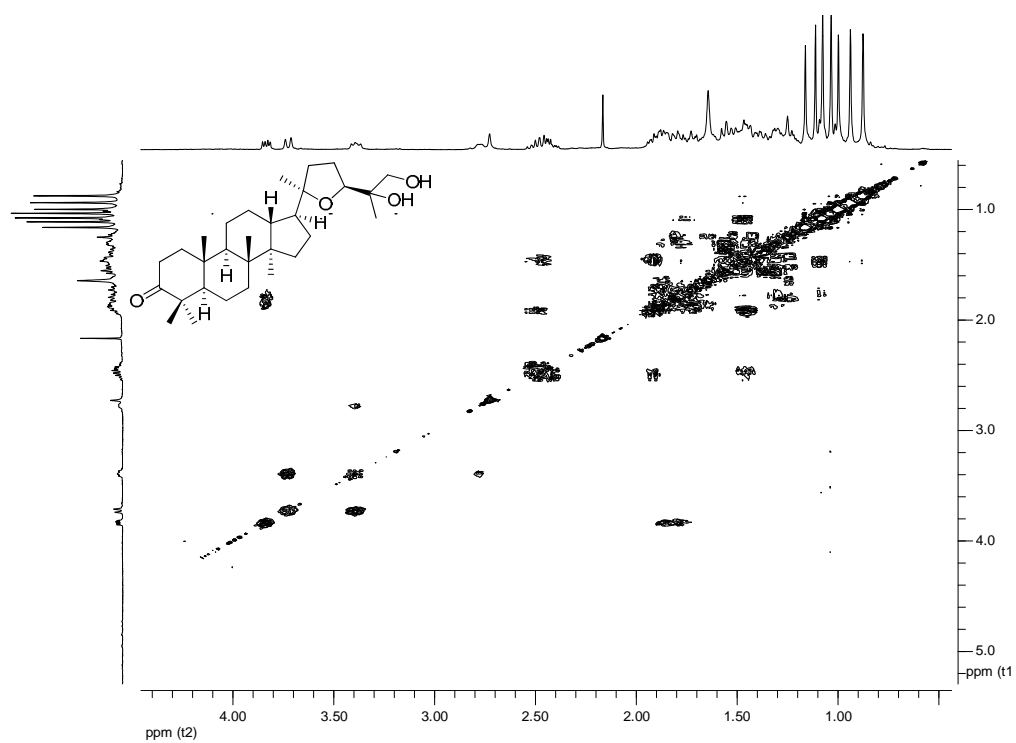


Figure 171. ^1H - ^1H COSY spectrum of compound **84** (CDCl_3 ; 400 MHz).

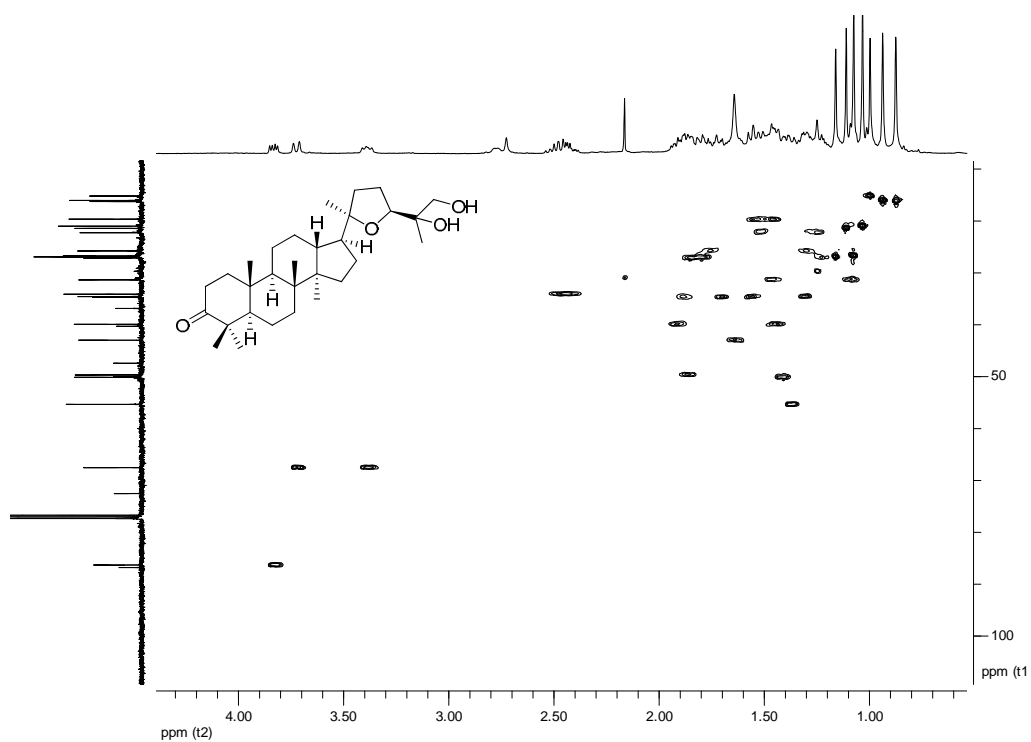


Figure 172. HSQC spectrum of compound **84** (CDCl₃; 400 MHz).

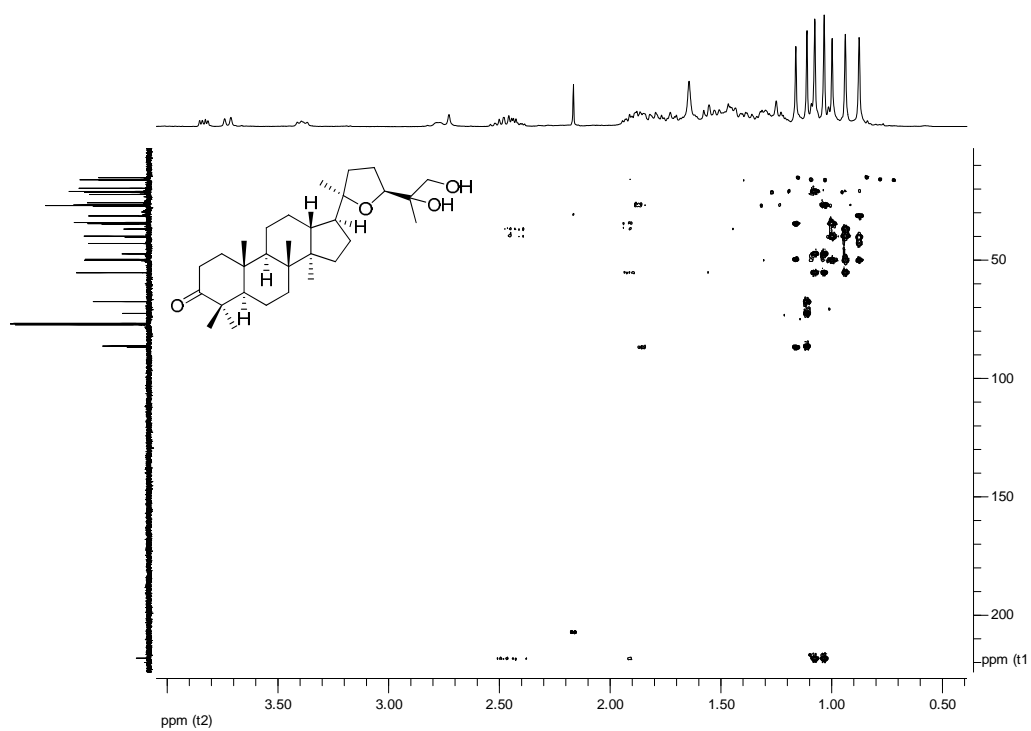


Figure 173. HMBC spectrum of compound **84** (CDCl₃; 400 MHz).

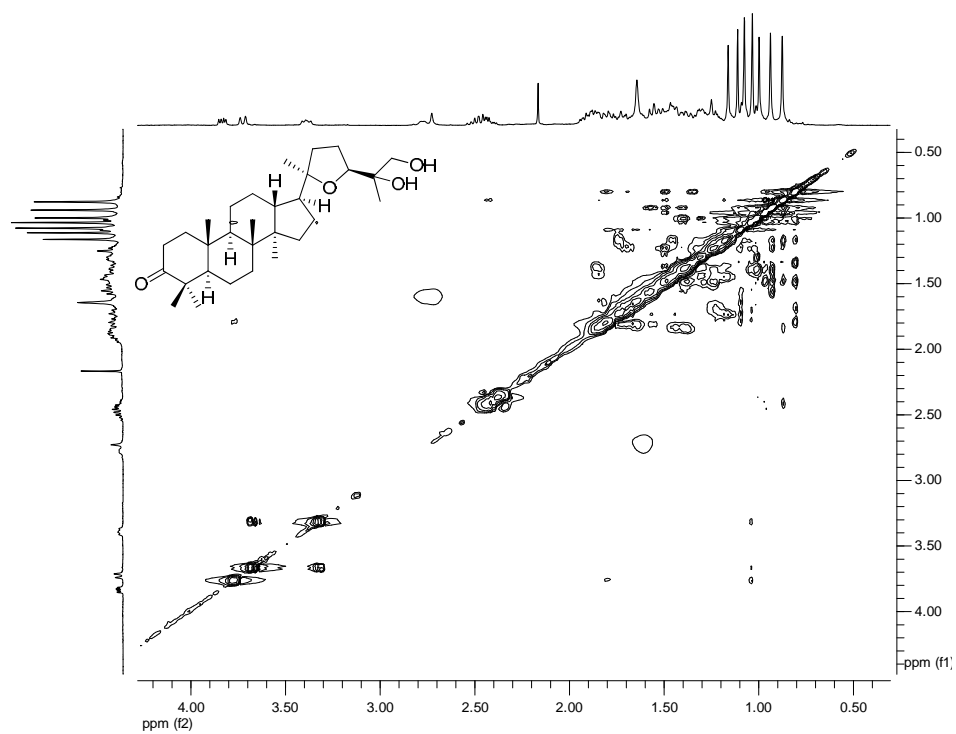


Figure 174. NOESY spectrum of compound **84** (CDCl₃; 400 MHz).

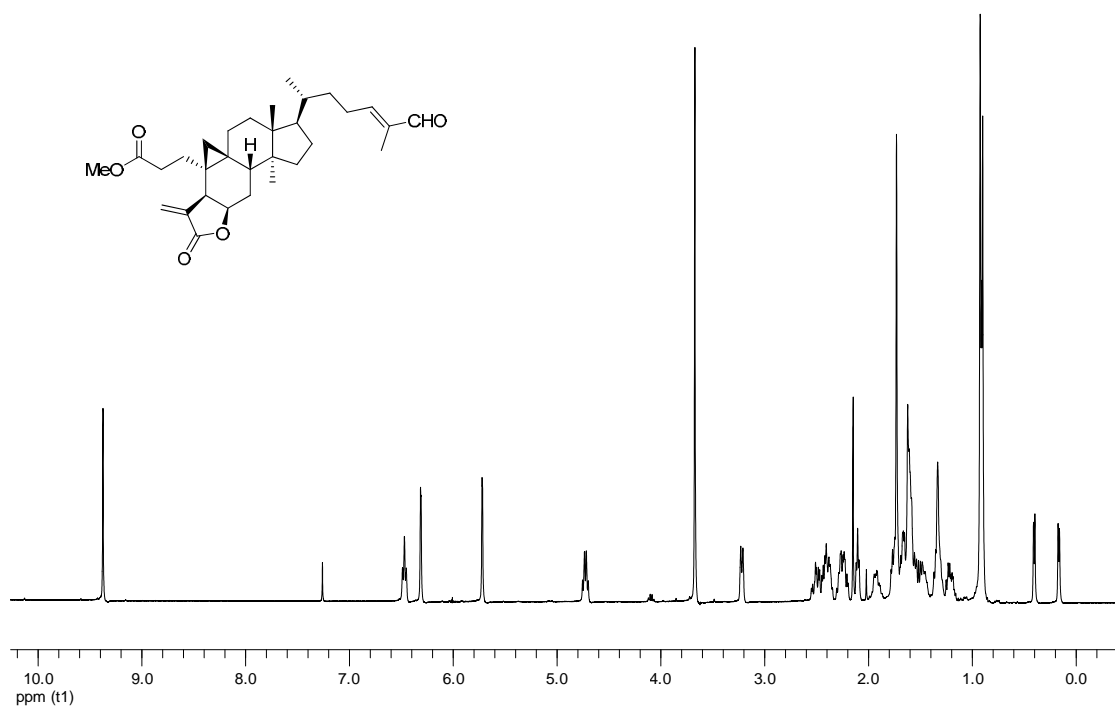


Figure 175. ¹H NMR spectrum of compound **10** (CDCl₃; 400 MHz).

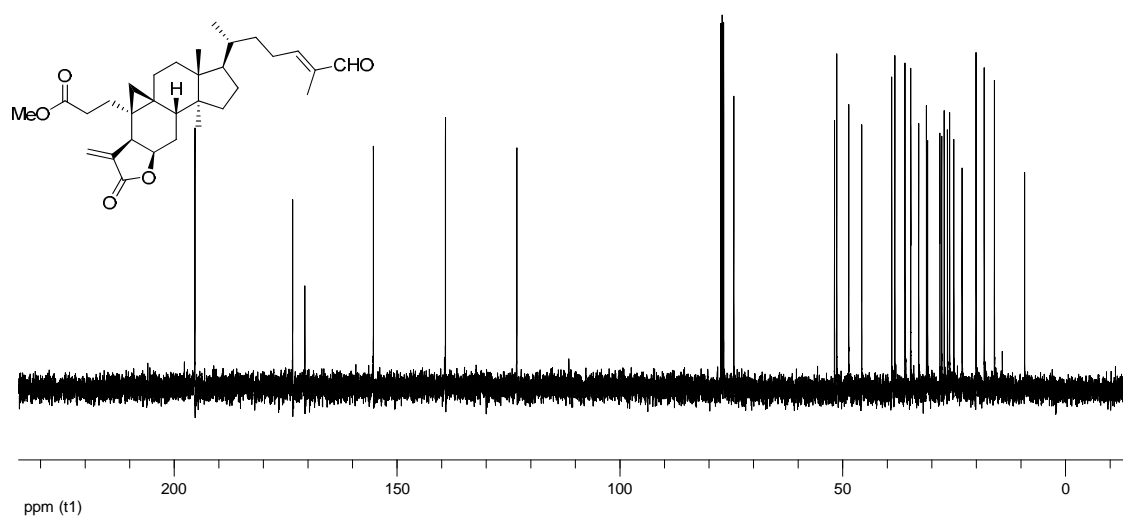


Figure 176. ^{13}C NMR spectrum of compound **10** (CDCl_3 ; 100 MHz).

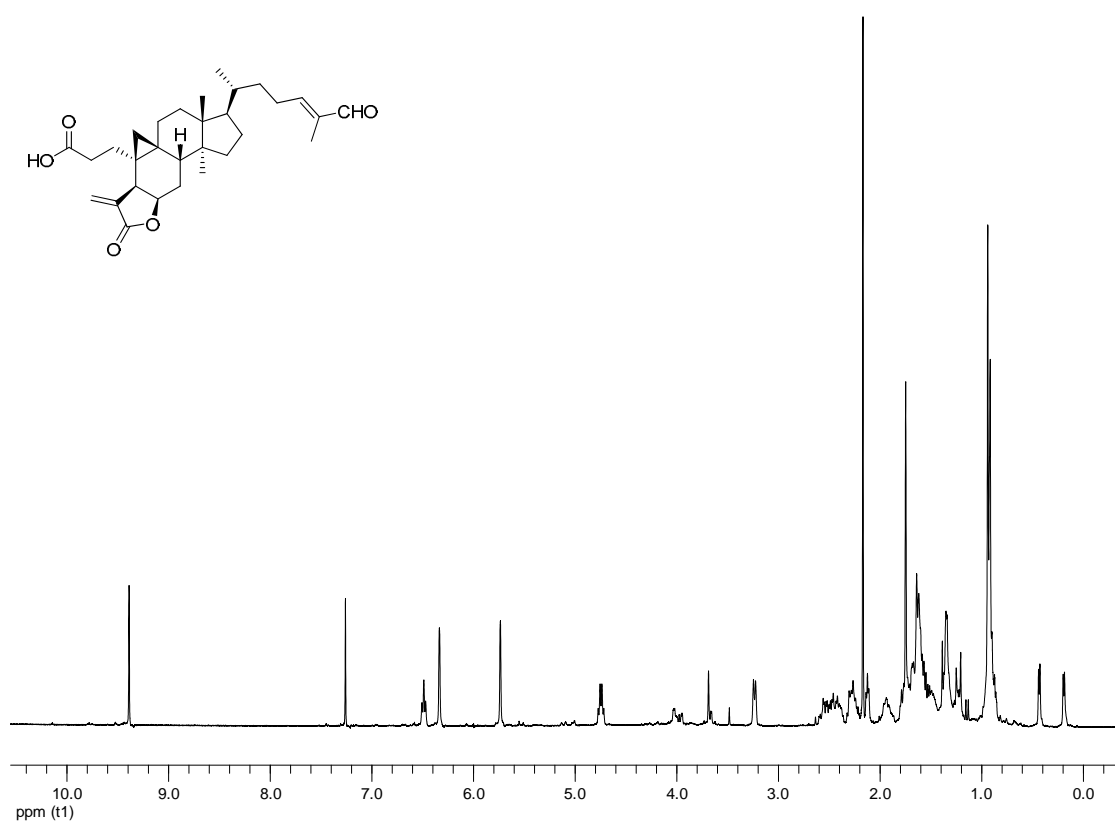


Figure 177. ^1H NMR spectrum of compound **11** (CDCl_3 ; 400 MHz).

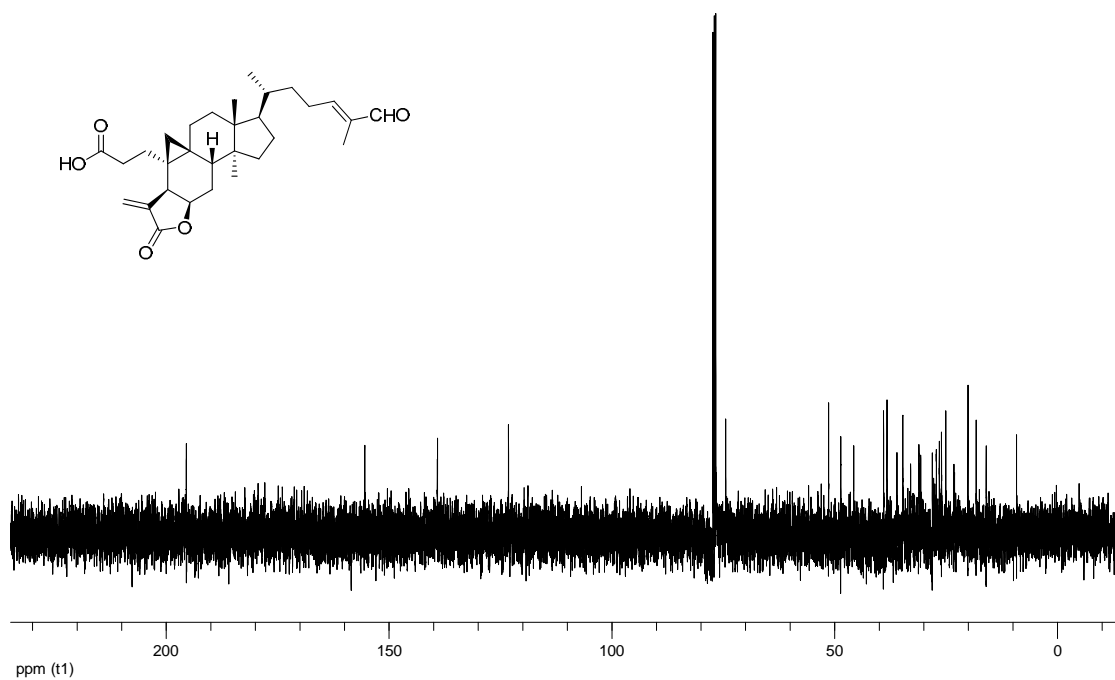


Figure 178. ^{13}C NMR spectrum of compound **11** (CDCl_3 ; 100 MHz).

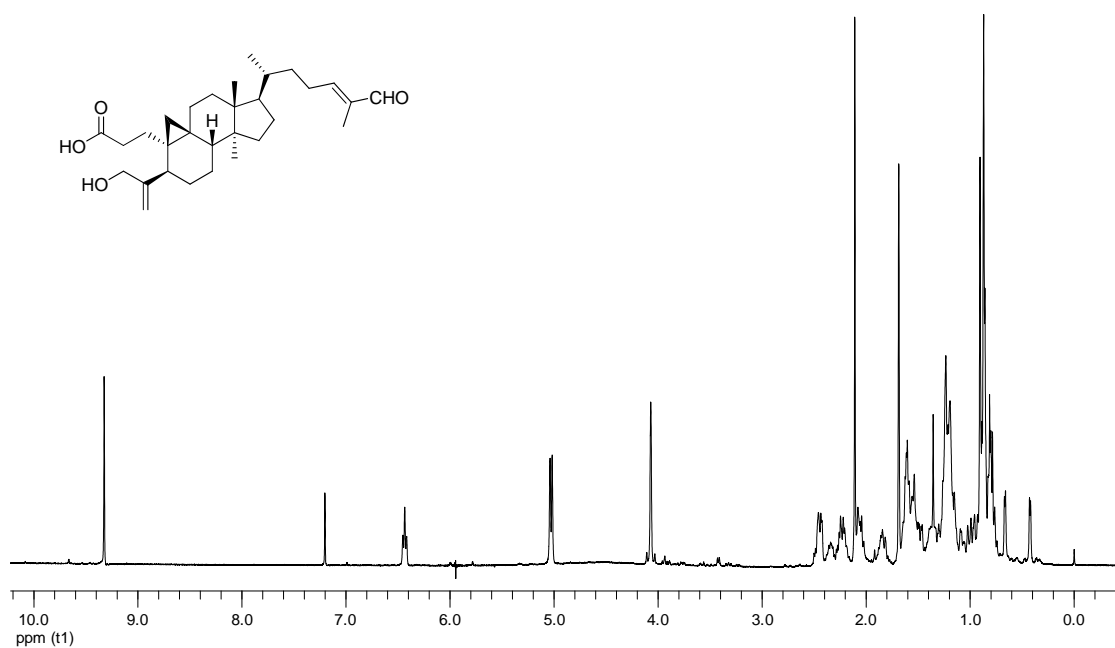


Figure 179. ^1H NMR spectrum of compound **12** (CDCl_3 ; 400 MHz).

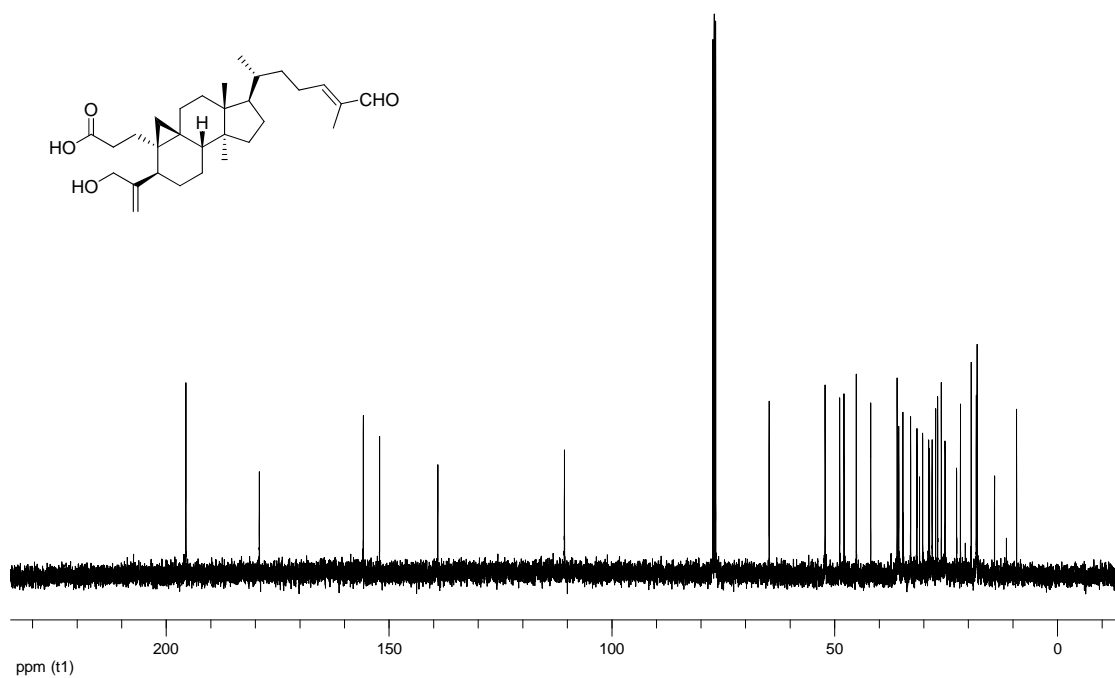


Figure 180. ¹³C NMR spectrum of compound **12** (CDCl₃; 100 MHz).

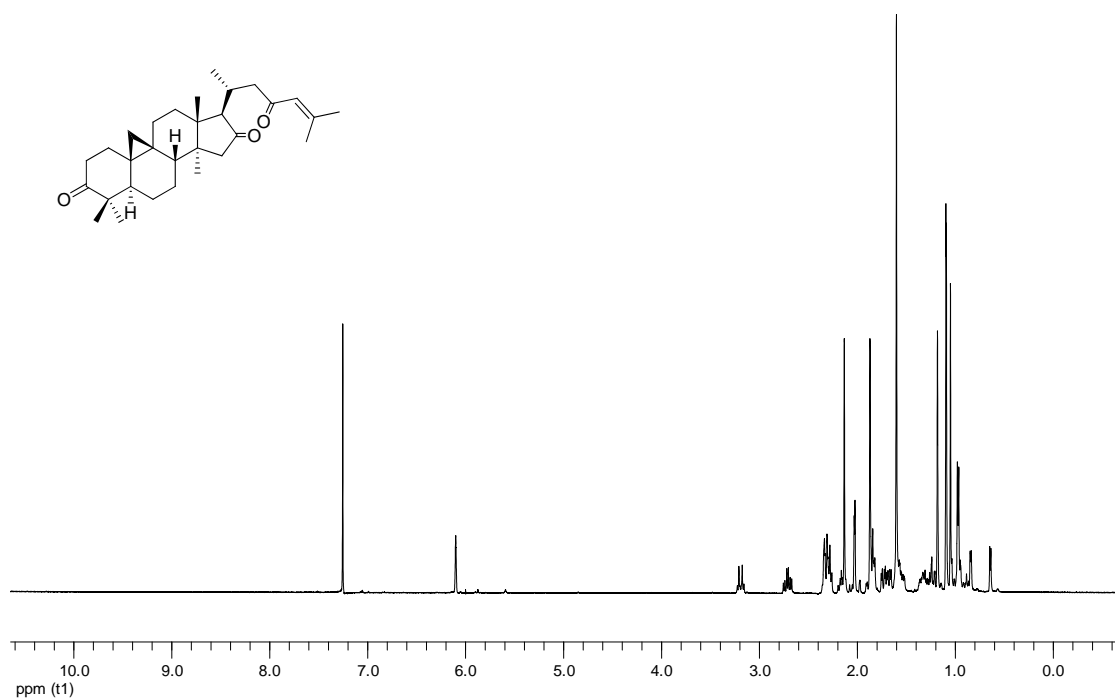


Figure 181. ¹H NMR spectrum of compound **24** (CDCl₃; 400 MHz).

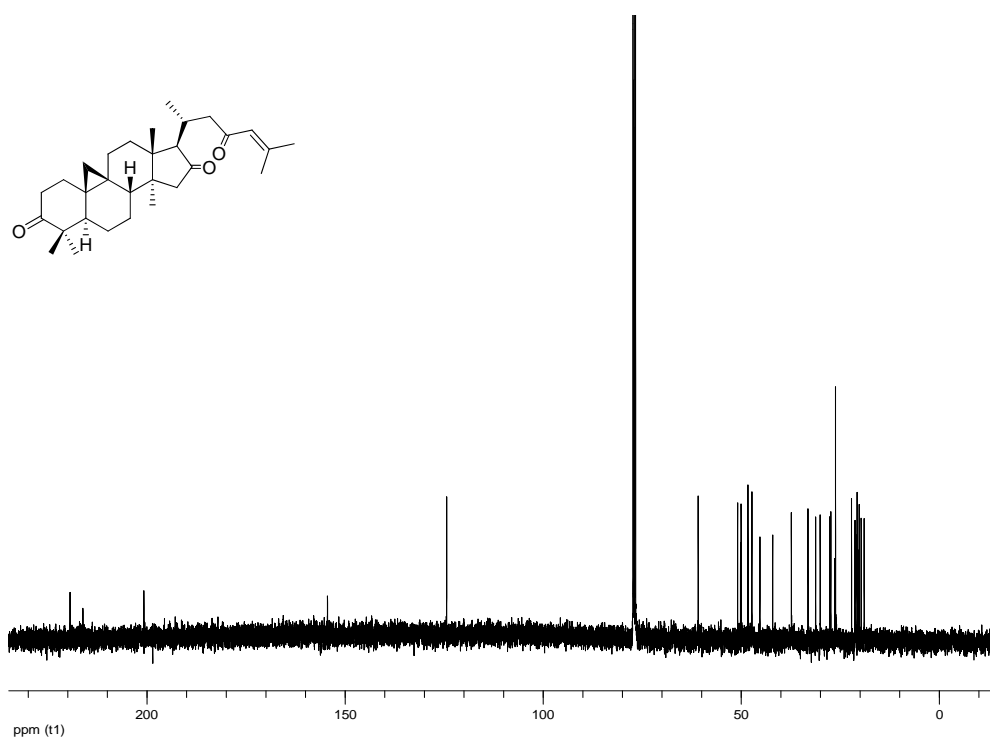


Figure 182. ¹³C NMR spectrum of compound **24** (CDCl₃; 100 MHz).

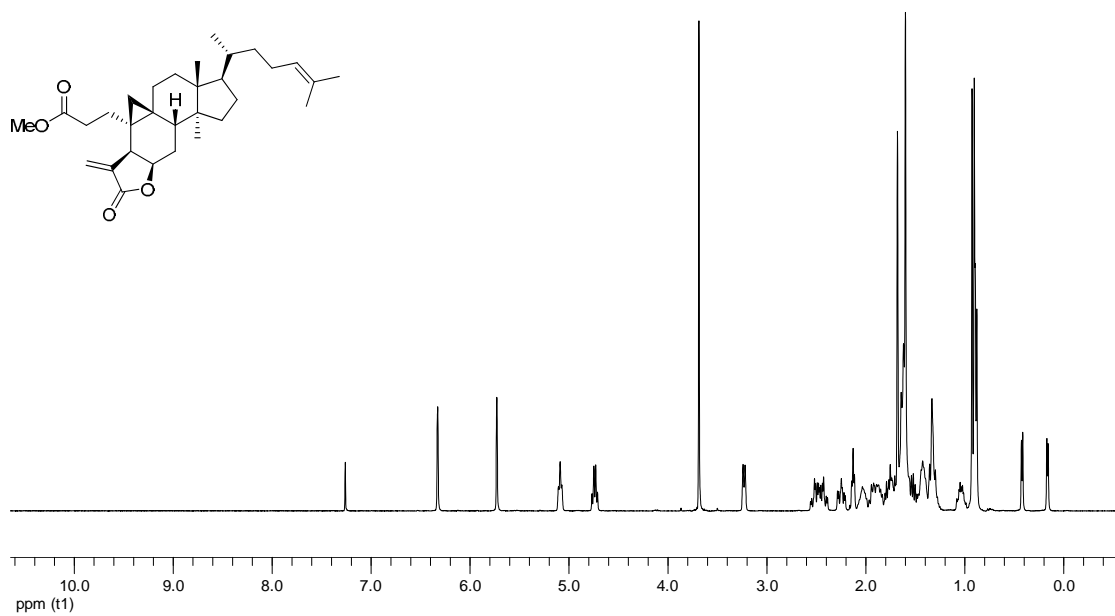


Figure 183. ¹H NMR spectrum of compound **41** (CDCl₃; 400 MHz).

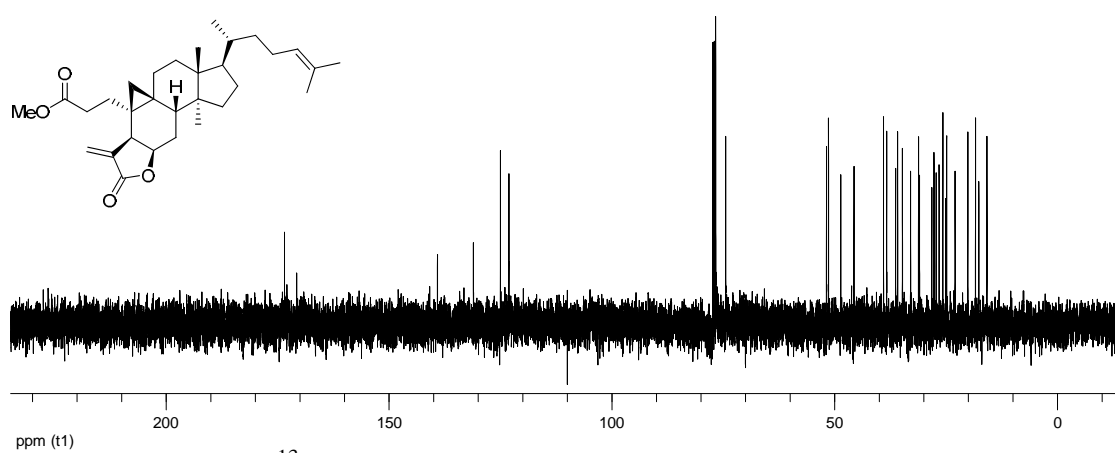


Figure 184. ^{13}C NMR spectrum of compound **41** (CDCl_3 ; 100 MHz).

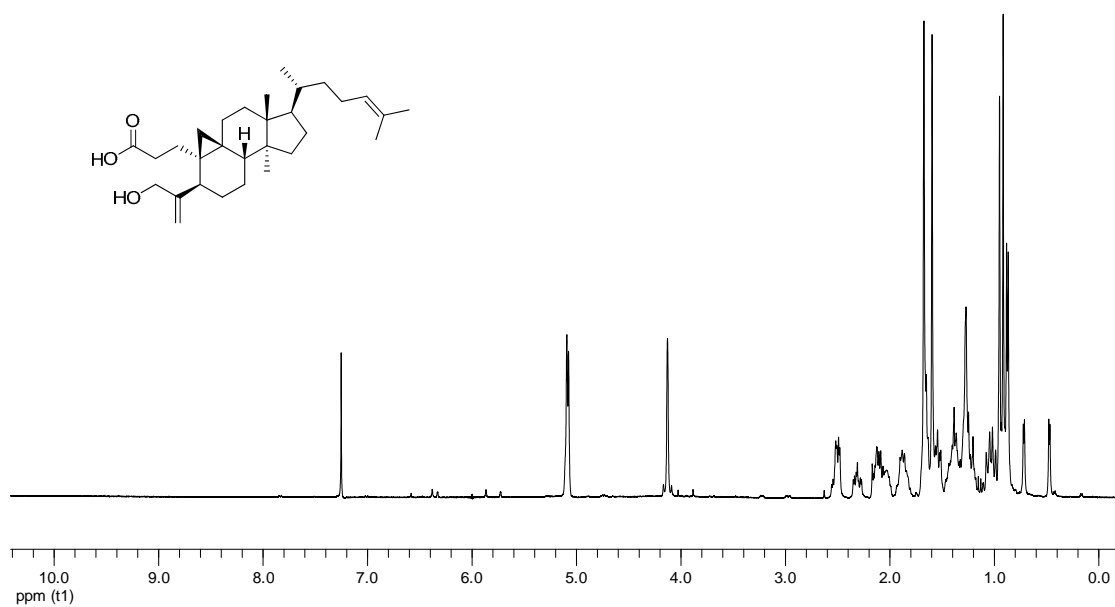


Figure 185. ^1H NMR spectrum of compound **58** (CDCl_3 ; 400 MHz).

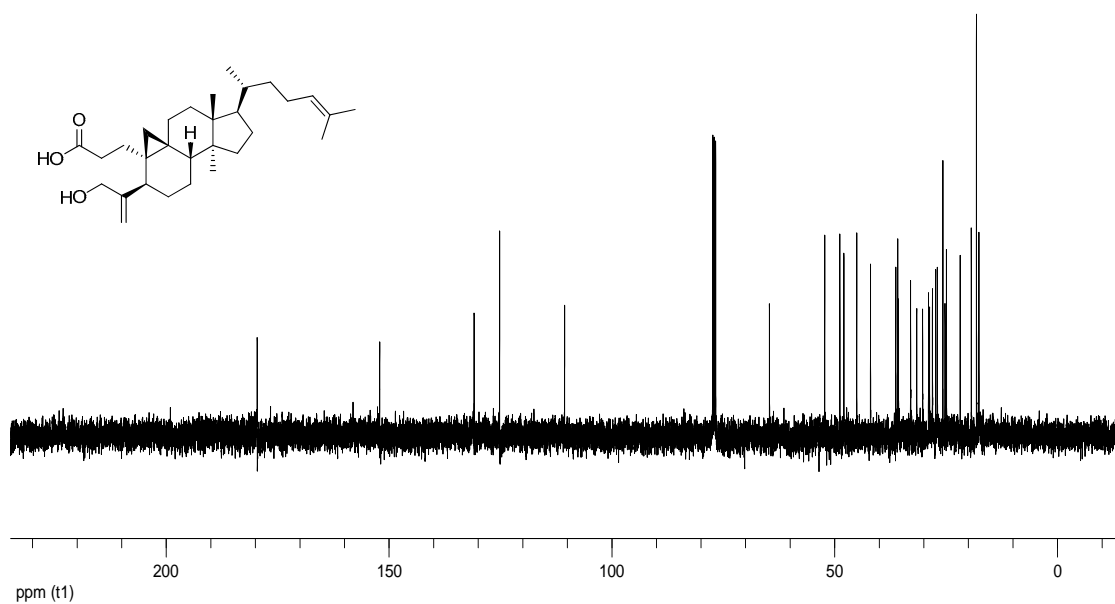


Figure 186. ^{13}C NMR spectrum of compound **58** (CDCl_3 ; 100 MHz).

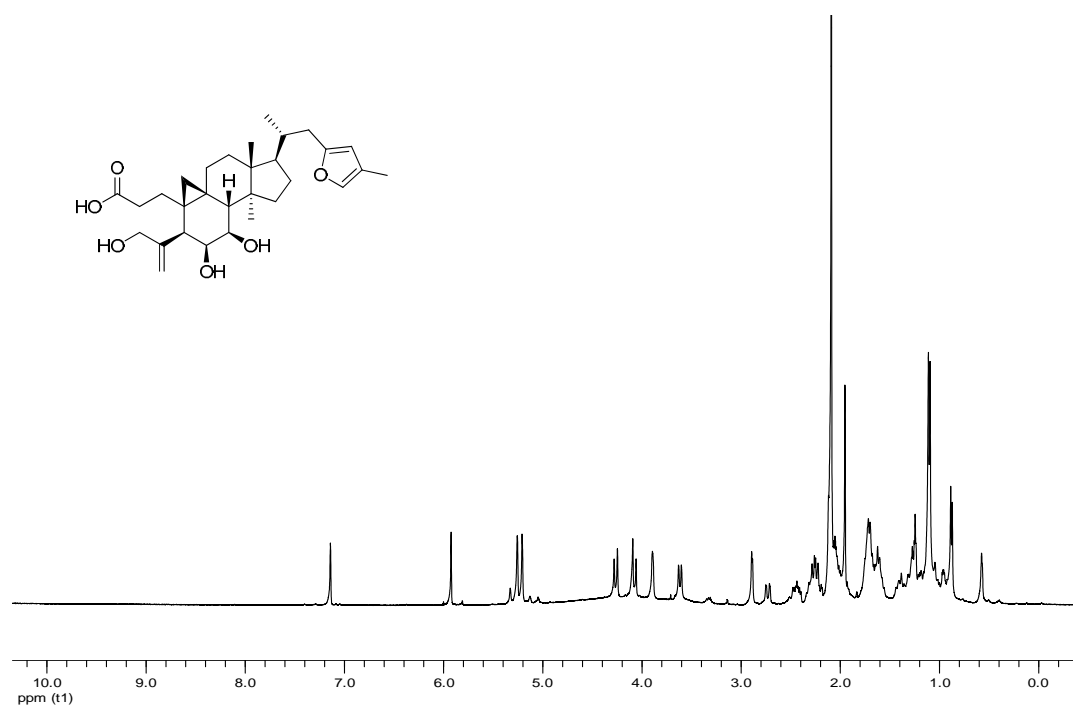


Figure 187. ^1H NMR spectrum of compound **61** ($\text{Acetone-}d_6$; 400 MHz).

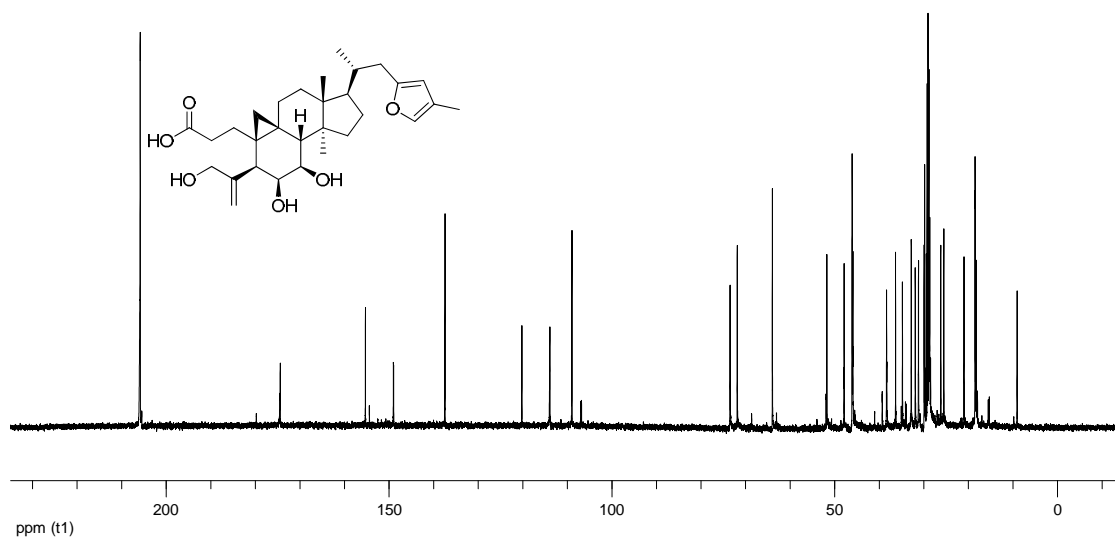


Figure 188. ^{13}C NMR spectrum of compound **61** (Acetone- d_6 ; 100 MHz).

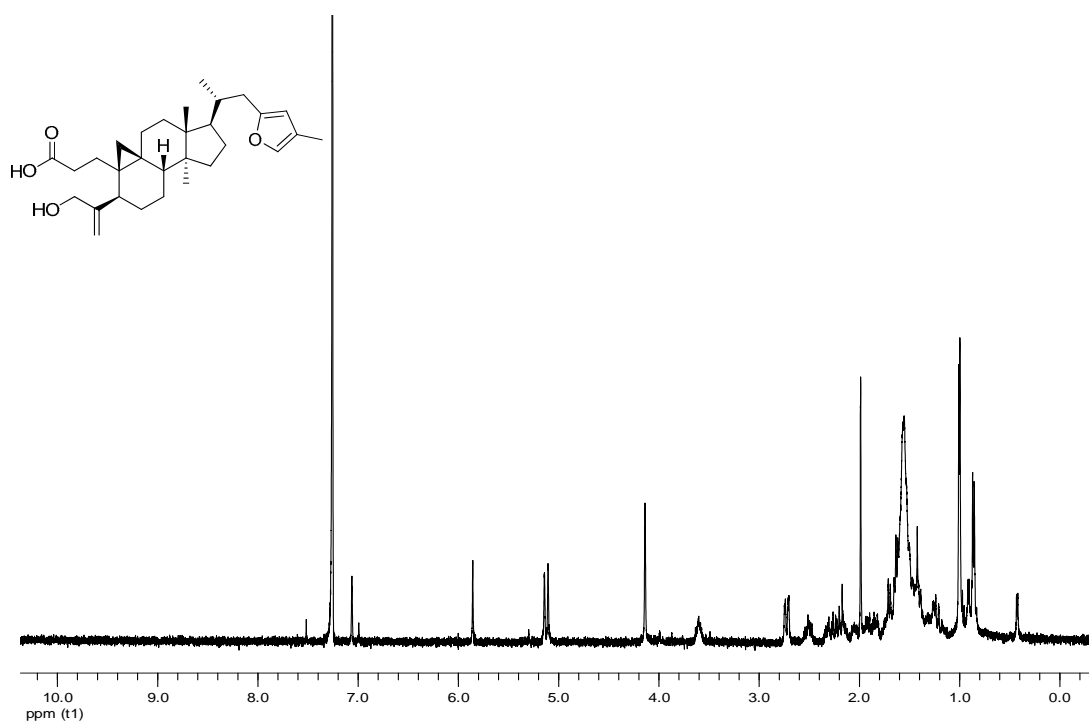


Figure 189. ^1H NMR spectrum of compound **62** (CDCl_3 ; 400 MHz).

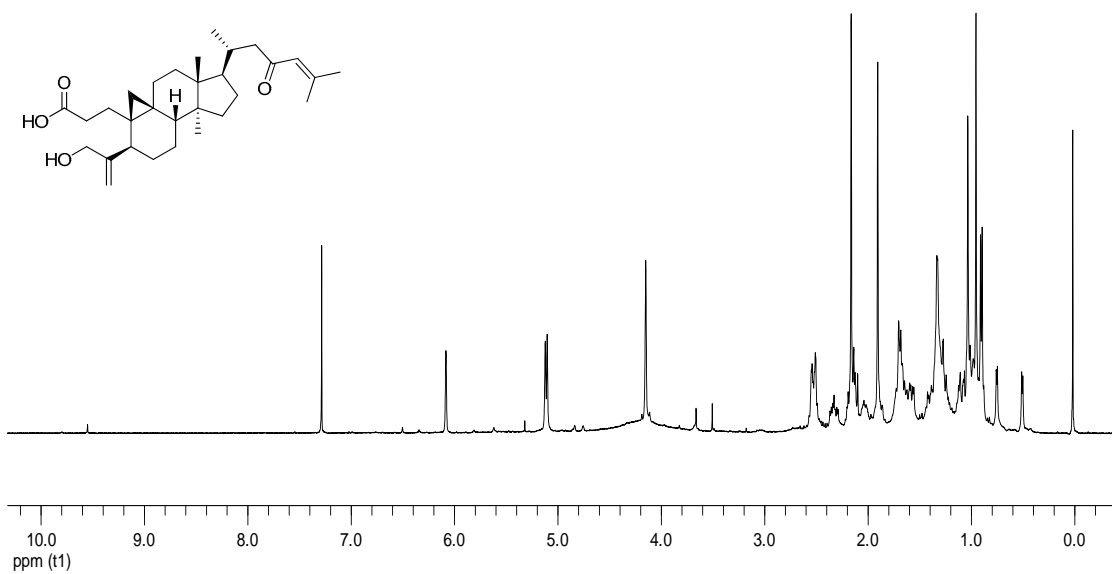


Figure 190. ^1H NMR spectrum of compound **63** (CDCl_3 ; 400 MHz).

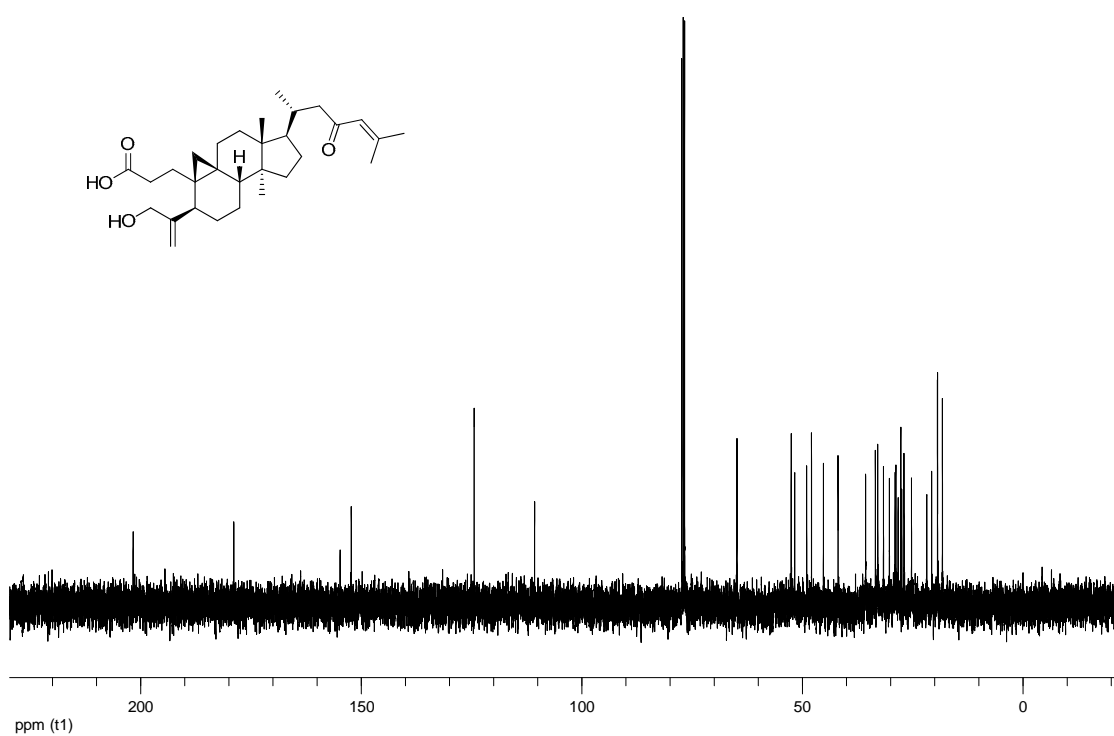


Figure 191. ^{13}C NMR spectrum of compound **63** (CDCl_3 ; 100 MHz).

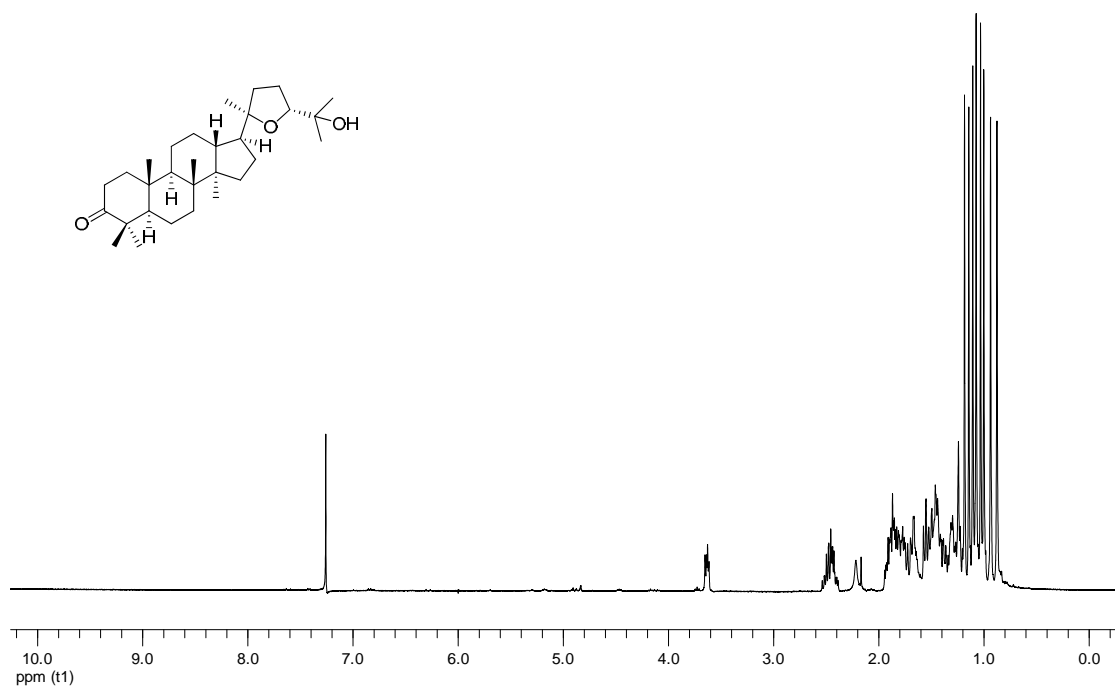


Figure 192. ¹H NMR spectrum of compound **85** (CDCl₃; 400 MHz).

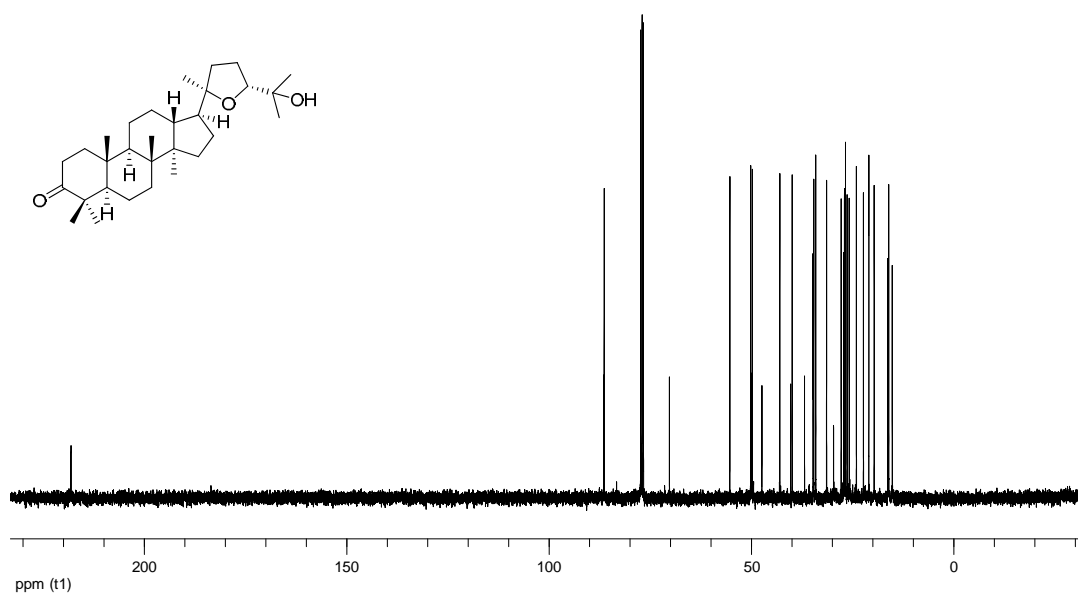


Figure 193. ¹³C NMR spectrum of compound **85** (CDCl₃; 100 MHz).

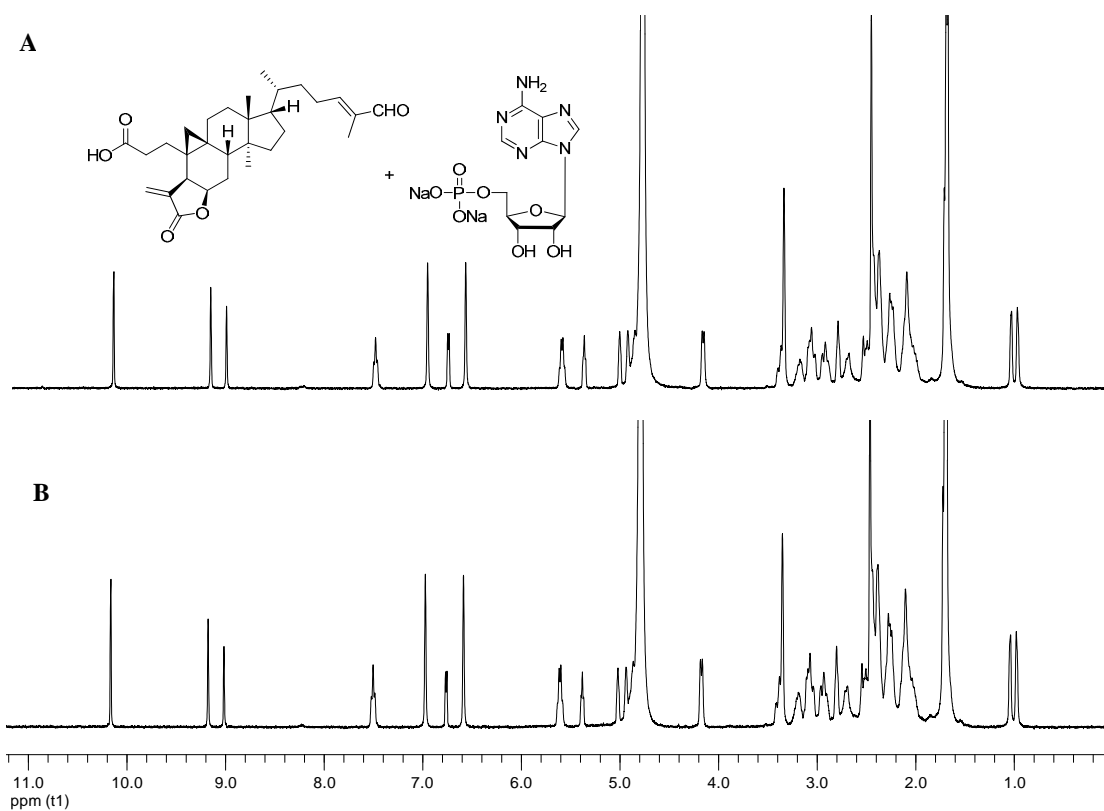


Figure 194. ¹H-NMR spectrum of reaction of coronalolide and adenosine 5'-monophosphate disodium salt hydrate in DMSO-*d*₆:D₂O (5:1); **A**) at room temperature (24 h.), **B**) at 40°C (72 h).

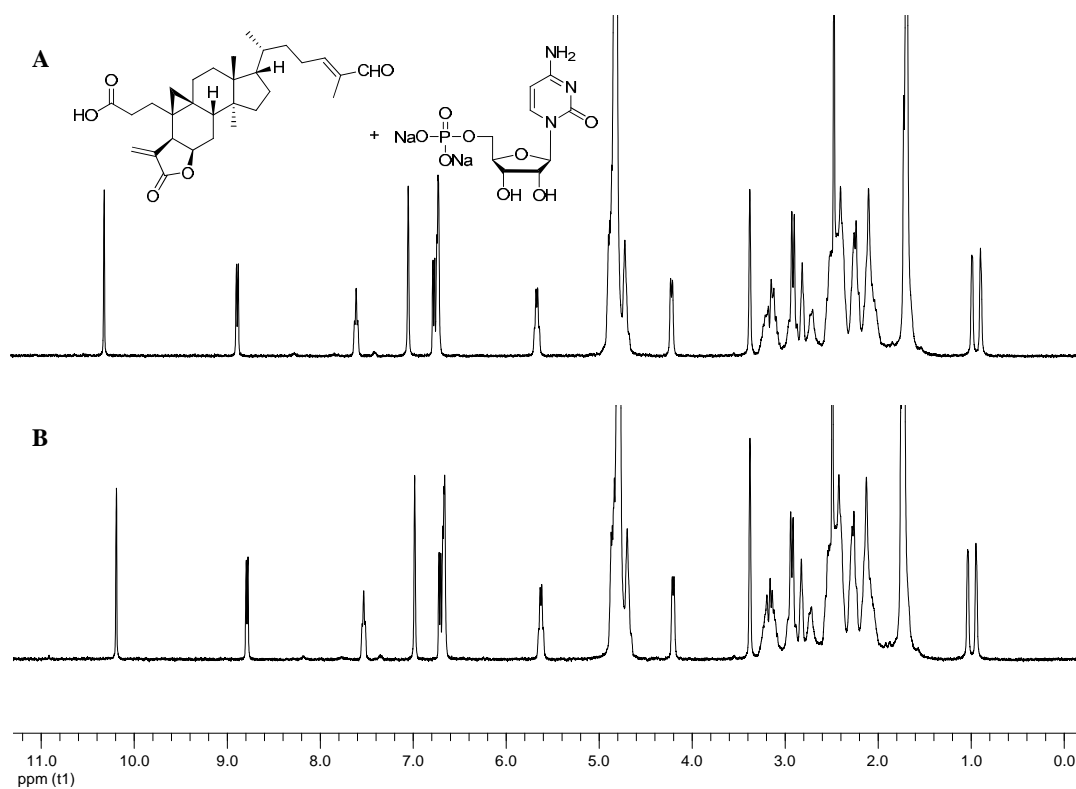


Figure 195. $^1\text{H-NMR}$ spectrum of reaction of coronalolide and cytidine 5'-monophosphate disodium salt hydrate in $\text{DMSO-}d_6\text{:D}_2\text{O}$ (5:1); **A**) at room temperature (24 h.), **B**) at 40°C (72 h).

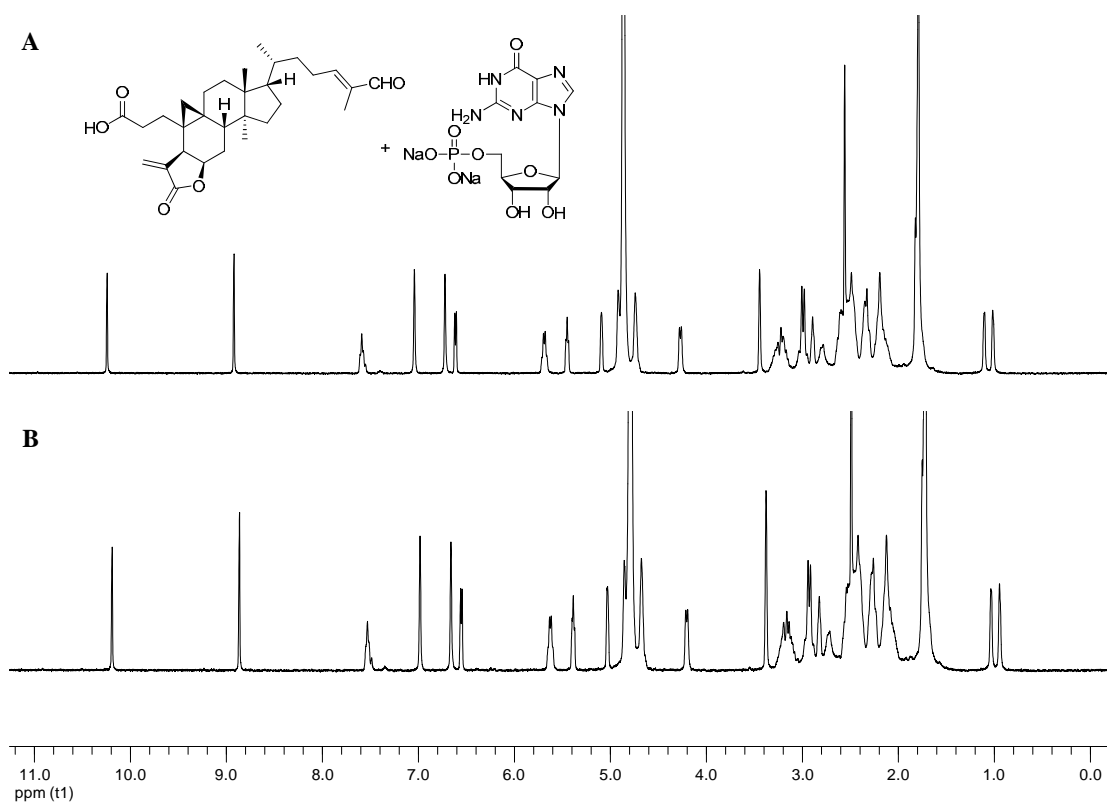


Figure 196. $^1\text{H-NMR}$ spectrum of reaction of coronalolide and guanosine 5'-monophosphate disodium salt hydrate in $\text{DMSO-}d_6\text{:D}_2\text{O}$ (5:1); **A**) at room temperature (24 h.), **B**) at 40°C (72 h).

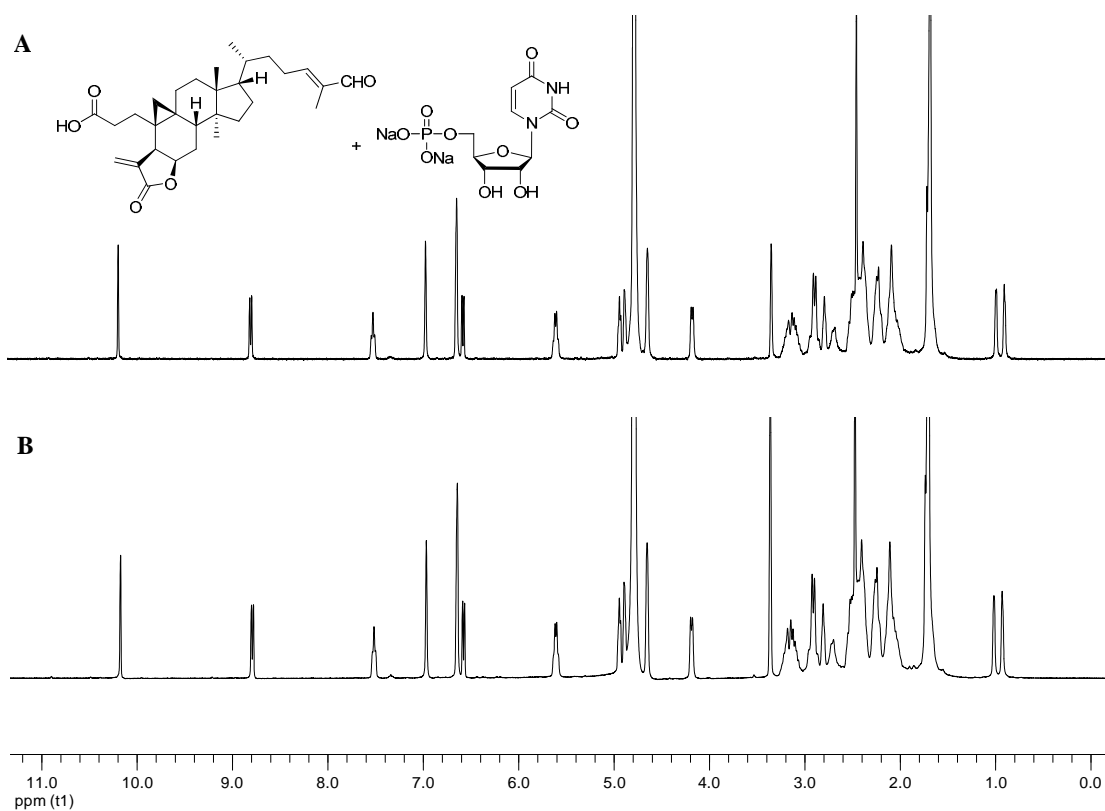


Figure 197. $^1\text{H-NMR}$ spectrum of reaction of coronalolide and uridine 5'-monophosphate disodium salt hydrate in $\text{DMSO-}d_6\text{:D}_2\text{O}$ (5:1); **A**) at room temperature (24 h.), **B**) at 40°C (72 h).

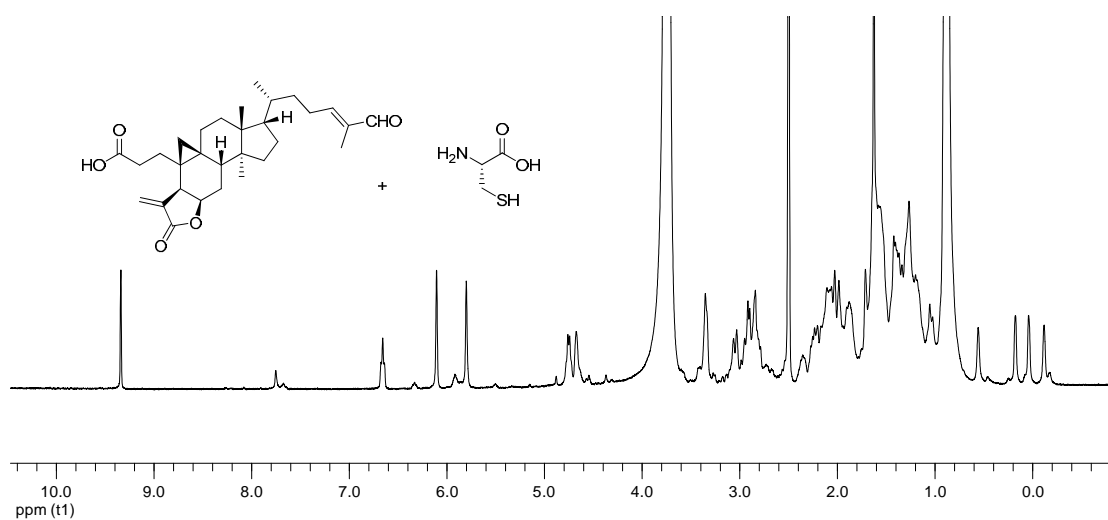


Figure 198. $^1\text{H-NMR}$ ($\text{DMSO-}d_6$) spectrum of reaction of coronalolide and cysteine at room temperature (72 h.).

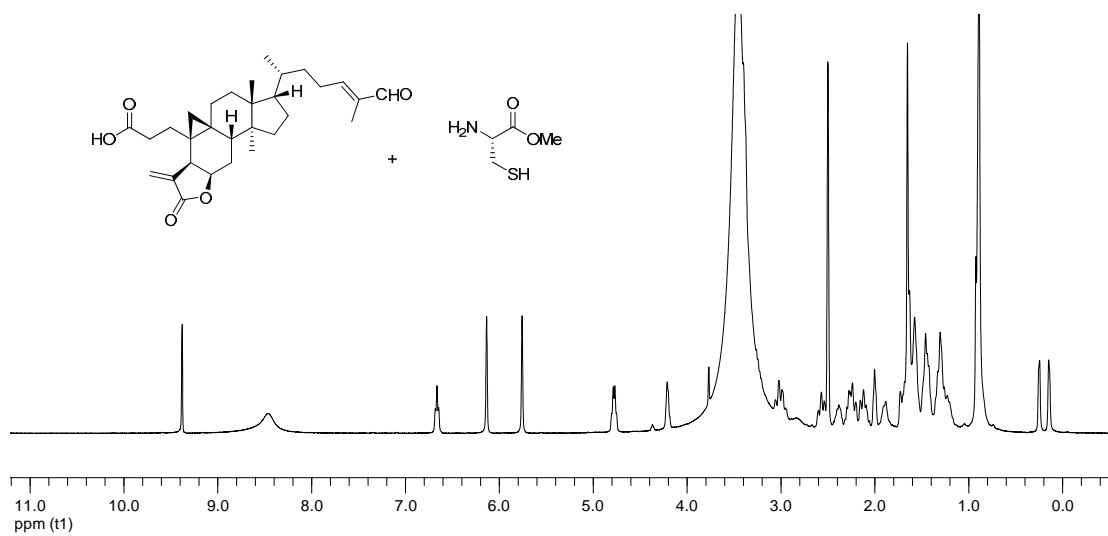


Figure 199. ¹H-NMR (DMSO-*d*₆) spectrum of reaction of coronalolide and cysteine methyl ester HCl at room temperature (72 h.).



Figure 200. *Gardenia sootepensis* (Rubiaceae)



Figure 201. *Gardenia tubifera* (Rubiaceae)

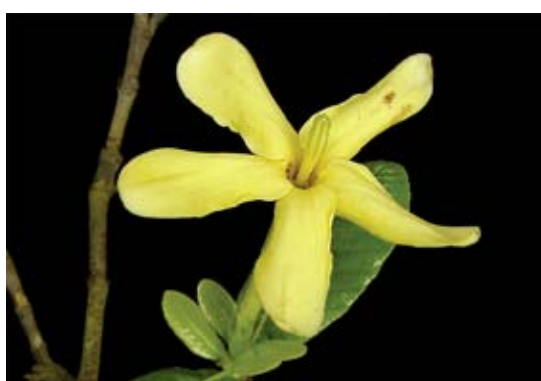


Figure 202. *Gardenia obtusifolia* (Rubiaceae)



Figure 203. *Gardenia thailandica* (Rubiaceae)

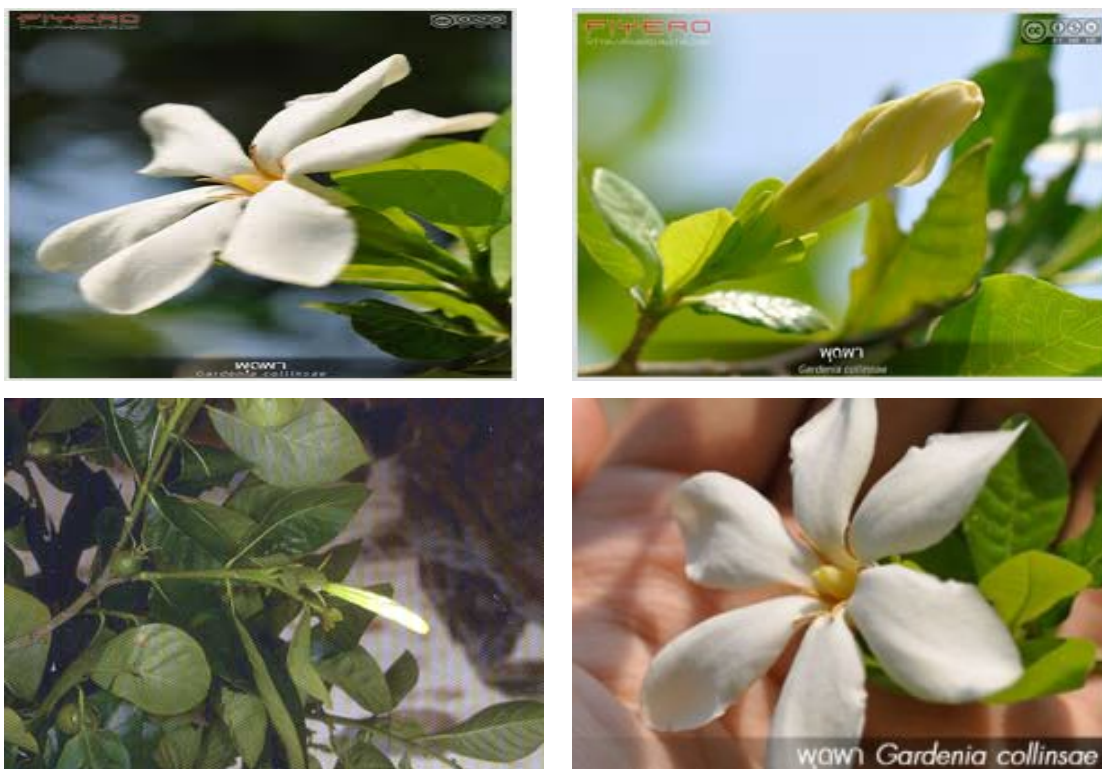


Figure 204. *Gardenia collinsae* (Rubiaceae)

VITA

Mr.Thanesuan Nuanyai was born on June 26, 1982 in Bangkok, Thailand. He graduated with Bachelor's Degree of Science in Chemistry from Faculty of Science, Rajamangala Institute of Technology, in 2004.

His present address is 385/2 Soi Ruampatthana 33, Phahonyothin Rd. Anusawari, Bang Khen, Bangkok, Thailand, 10220, Tel: +668-1444-9908.

Publications

- Nuanyai, T.; Sappapan, R.; Teerawatananon, T.; Muangsin, N.; and Pudhom, K. 2009. Cytotoxic 3,4-*seco*-Cycloartane Triterpenes from *Gardenia sootepensis*. Journal of Natural Product 72: 1161–1164.
- Nuanyai, T.; Chokpaiboon, S.; Vilaivan, T.; and Pudhom, K. 2010. Cytotoxic 3,4-*seco*-Cycloartane Triterpenes from the Exudate of *Gardenia tubifera*. Journal of Natural Product 73: 51-54.
- Nuanyai, T.; Sappapan, R.; Vilaivan, T.; and Pudhom, K. 2010. Gardenoins E—H, Cycloartane Triterpenes from the Apical Buds of *Gardenia obtusifolia*. Chemical and Pharmaceutical Bulletin 59: 385-387.
- Nuanyai, T.; Sappapan, R.; Vilaivan, T. and Pudhom, K. 2011. Cycloartane triterpenes from the exudate of *Gardenia thailandica*. Phytochemistry Letters 4: 26-29 .
- Nuanyai, T.; Sappapan, R.; Vilaivan, T. and Pudhom, K. 2011. Dammarane triterpenes from the apical buds of *Gardenia collinsae*. Phytochemistry Letters 4: 183-186.